Facultad de Ciencias
Departamento de Química Orgánica

Towards a combinatorial approach to supramolecular catalysis using hydrogen bonding driven substrate activation and anchoring

Director:
Pr. Dr. Javier de Mendoza Sans

Memoria que presenta
Frédéric Ratel
Para optar al grado de Doctor en Ciencias Químicas

Madrid, febrero de 2009

A ma famille…

Acknowledgements

The entire work presented herein would not have been possible without the help, support and advice of some people I would like to acknowledge. In the first place, I would like to thank Pr. Javier de Mendoza for welcoming me so well in his enthusiastic group and sharing all his scientific knowledge with his students. These years spent in the group helped me growing, not only as a scientist, but also as a person. This stay in the laboratory would not have been so pleasant and productive without the constant help and advice of my co-workers of Madrid and Tarragona. That's why I would like to thank Pilar Prados, Hitos, Curra, Ruth, José and Marieta (the UAM team) for making my arrival in Spain and in the group as pleasant as possible. I also would like to thank Margot and Enrique for their total disponibility during the first months of our arrival at Tarragona (I will never forget the first months setting up the lab). I then need to acknowledge deeply my co-workers of the daily routine at the laboratory, the ones that shared most of my disgusts and joices, the ones that created such a nice working atmosphere, the ones that sometimes had to bear my bad temper; without them my stay would not have been the same: Ruth, Pascal, Eric, Jesús, Gerald, Elisa, Caterina, Vera, Alla, Augustin, Pilar, Simona, Julián and Aritz.

D'altra banda, i pel que fa a la vida extra-laboral, la meva estància a Tarragona ha sigut inolvidable gràcies a molta gent que vull també agrair en aquest moment. En primer lloc, vull agrair als membres de la banda Txipi Aité a la qual pertanyia, per introduir-me a la cultura catalana i acompanyar-me en els meus primers passos a Tarragona. Han sigut 3 anys

de convivència que mai oblidaré, gràcies doncs a Roger, Aitana, Marcel, Jesús, Gerard, Quimet i Riberita. La meva immersió a la societat tarragonina es va completar rapidament per la meva inclusió al consell de caps de l'Agrupament Escolta i Guia Alverna de Tarragona, del qual vull agrair tots els membres per a donar-me l'oportunitat de desenvolupar-me personalment amb ells i pels bons moments passats junts: Marc, les Marias, LuisJa, Txus, Llivia, Ramon, Blanca, Sergi, les Aris, Mar, Gemma, Núria, Alba, Arcadi, Marta, Dani, Toni, Rat, Albert, Joan, Olga... (segur que em deixo algu). Voldria finalment agrair especialment a la meva companyia, Marta, per haver sempre estat aquí, tant en els bons moments com en els moments més dificils, per fer-me tocar els peus a terra i per haver-me donat el suport necessari per a dur a terme la tesí. Sense tu, tot haguès estat diferent.

En dernier lieu, je voudrais tout spécialement remercier ma famille pour avoir accepté sans conditions les sacrifices imposés par la distance, l'éloignement et ma petite disponibilité, et ce, tout au long de mon cursus universitaire. Eux aussi ont su, malgré les nombreux kilomètres nous séparant, me donner le courage nécessaire pour afronter les difficultés.

Projects CTQ 2005-08948, Consolider Ingenio 2010 CSD 2006-003 and the ICIQ foundation are acknowledged for financial support.

Merci à tous!

List of abbreviations

[α]: optical rotation
Å: ångstrom
Ac: acetyl
acac: acetylacetonate
ADP: adenosine diphosphate
Ar: aromatic
Arg: arginine
Asp: asparagine
atm: atmosphere (pressure unit)
ATP: adenosine triphosphate
Boc: tert-butoxycarbonyl
Bz: benzoyl
cal: calory
Cbz: carbobenzyloxy
CDI: carbonyldiimidazole
COD: cyclooctadiene
COSY: correlation spectroscopy
DABCO: 1,4-diazabicyclo[2.2.2] octane
DCM: dichloromethane
DDQ: 2,3-dichloro-5,6-dicyanobenzoquinone
DIPEA: diisopropylethylamine
DMAP: 4-dimethylaminopyridine
DMF: *N*,*N*-dimethylformamide
DMSO: dimethylsulfoxide
DNA: desoxyribonucleic acid
dtcb: *trans*-2-[3-(4-*tert*-butylphenyl)-2-methyl-2-propenylidene] malononitrile
ee: enantiomeric excess
eq.: equivalent
ESI: electrospray ionization
Et: ethyl
FAB: fast atom bombardment
g: gram
GC: gas chromatography
Glu: glutamate
h: hour
HPLC: high performance liquid chromatography
HR-MS: high resolution mass spectrometry
Hz: hertz
i-Bu: isobutyl
i-Pr: isopropyl
IR: infrared spectroscopy
ITC: isothermal titration calorimetry
J: coupling constant

K: equilibrium constant
K: Kelvin
L: liter
λ: wavelength
M.p.: melting point
m: meter
M: mole per liter
MALDI-TOF: matrix assisted laser direct ionization- time of flight
Me: methyl
min: minute
mol: mole
MS: mass spectrometry
N: normality
NBS. N-bromosuccinimide
n-Bu: butyl
NMM: *N*-methylmorpholine
NMR: nuclear magnetic resonance
NOESY: nuclear overhauser enhancement spectroscopy
°C: degree celsius
Ph: phenyl
ppm: part per million
Pr: propyl
psi: pounds per square inch
Pybop: benzotriazol-1-yl-oxytripyrrolidinophosphonium hexafluorophosphate
RNA: ribonucleic acid
RT: room temperature
Ser: serine
SNase: staphylococcus aureus nuclease
TBA: tetrabutylammonium
TBDMS: *tert*-butyldimethylsilyl
TBDPS: *tert*-butyldiphenylsilyl
TCDI: thiocarbonyldiimidazole
TDO: taddolate
Tf: trifluoromethanesulfonyl
TFA: trifluoroacetic acid
THF: tetrahydrofurane
TLC: thin layer chromatography
TMS: trimethylsilyl
TOF: Turnover frequency
TON: Turnover number
Ts: *p*-toluenesulfonyl
UV-Vis: ultra violet-visible spectroscopy

Chapter 1

Supramolecular approaches to catalysis

1.1 General introduction 1

1.2 Space confined supramolecular catalysis 4

  1.2.1 Covalent macrocyclic catalysts 4

  1.2.2 Self-assembled nanoreactors 13

  1.2.3 Active site encapsulation 23

1.3 Self-assembly as a tool for ligand construction 27

1.4 Objectives 33

Chapter 2

Influence of the acidity of guanidinium cations on binding and catalysis

2.1 Introduction 41

  2.1.1 The guanidinium group 41

  2.1.2 Anion binding *vs*. transprotonation 44

  2.1.3 Guanidinium cations as organocatalysts 48

2.2 Synthesis of model guanidinium cations 50

  2.2.1 Bicyclic chiral guanidinium cation **1** 50

  2.2.2 Chiral benzoguanidinium cation **2** 52

  2.2.3 Dibenzoguanidinium cation **3** 55

2.3 Binding studies 56

  2.3.1 ^{1}H NMR experiments 56

  2.3.2 Isothermal titration calorimetry (ITC) 58

2.4 Catalysis 64

  2.4.1 General 64

  2.4.2 Catalysis experiments 67

2.5 Conclusions 73

2.6 Experimental part 73

Chapter 3

Functionalized metalloporphyrins as cooperative catalysts

3.1 Introduction 89

3.2 Results and discussion 98

3.2.1 Synthesis of functionalized porphyrins **14aH-14cH** 98

3.2.2 Metallation of porphyrin derivatives **14aH-14cH** 102

3.2.3 Metal screening experiments 106

3.2.3.1 Zinc (II) porphyrins 107

3.2.3.2 Nickel (II) porphyrins 109

3.2.3.3 Magnesium (II) porphyrins 109

3.2.3.4 Tin (IV) porphyrins 111

3.2.4 Cooperativity studies 113

3.3 Conclusions 116

3.4 Experimental part 117

Chapter 4

Functionalized ligands for substrate binding in catalysis

4.1 Introduction 137

4.2 Synthesis of ligands 146

4.2.1 Synthesis of chiral ligands (L2) 146

4.2.2 Synthesis of functionalized ligands (L1) 148

4.2.2.1 Synthesis of **20a-c** 148

4.2.2.2 Synthetic studies for **21a-e** 150

4.2.2.3 Synthetic studies for **22a-c** 160

4.2.2.4 Towards the preparation of **23a-b** 162

4.2.2.5 Synthesis of **24a-d** 165

4.3 Mixing up the ligands libraries with metals 168

4.3.1 Monodentate functionalized ligands 168

4.3.1.1 Complexation studies for **20a-c** 168

4.3.1.2 Complexation studies for **21a-b** 172

4.3.1.3 Complexation studies for **21c** 182

4.3.2 Bidentate functionalized ligands **24a-d** 185

4.4 Catalysis experiments (preliminary results) 192

4.4.1 Monodentate ligands 192

4.4.2 Bidentate ligands 194

4.5 Conclusions 204

4.6 Experimental part 204

Summary 267

Introducción general y resultados 271

CHAPTER 1

SUPRAMOLECULAR APPROACHES TO CATALYSIS

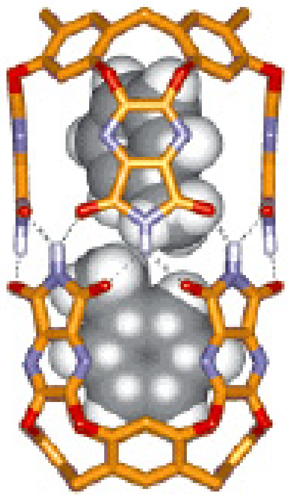

1. Supramolecular approaches to catalysis.

1.1 General introduction.

Supramolecular chemistry[1] is nowadays one of the most interdisciplinary areas of chemistry since it strongly overlaps with different sciences, such as physics and biology among others.[2] Applications of supramolecular chemistry in synthetic organic chemistry, and more particularly in catalysis, are constantly rising (Fig. 1.1). Interactions involved in supramolecular chemistry are indeed found in most enzymatic systems at the biological level. The amazing efficiency of enzymes as chemical reactors in terms of conversion, regioselectivity and enantioselectivity led the chemical community to design systems able to mimic their activity, according to the principles of molecular recognition and self-assembly. This rising interest for supramolecular catalysis, especially in the new century, is reflected by the number of publications concerning this topic over the past four decades, as shown in figure 1. Enzymes are indeed the best catalysts so far since they perform chemical transformations in a very selective way at physiological pH and in water, which makes them the most sustainable catalysts ever.

---

[1] Term introduced by Jean-Marie Lehn *Science* **1985**, *227*, 849.

[2] a) Self-assembled nanostructures are widely used in new materials sciences due to their physical properties: Zhang, J. Z.; Wang, Z.-L.; Liu, J.; Chen, S.; Liu, G.-Y. S*elf-Assembled Nanostructured Materials* **2003,** Kluwer Academic/Plenum Publisher: New York. b) Supramolecular chemistry is involved in the structure of biological systems: Quinkert, G.; Wallmeier, H.; Windhab, N.; Reichert, D. *Chemical Biology* **2007**, *1*, 3.

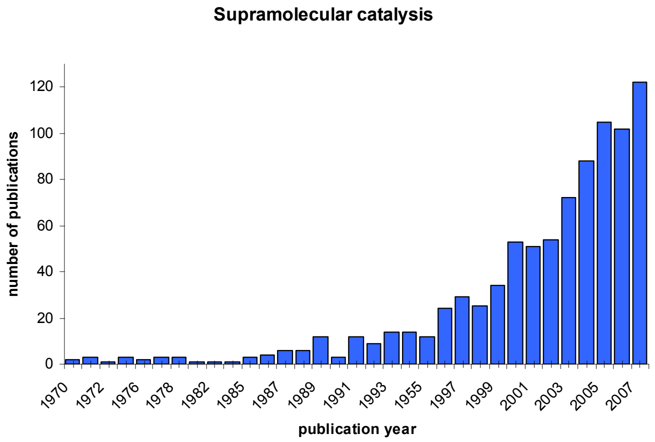

Fig. 1.1: Scientific publications in supramolecular catalysis over time.

Enzymes' conformation is maintained at physiological conditions by supramolecular interactions, such as π-stacking, hydrophobic forces and hydrogen bonds. In the active site, cooperativity between the participating groups leads to the observed efficiency. Enzymes form a more stable complex with the transition state of a reaction than with the substrate thanks to additional binding interactions.[3] Enzymes are also known for enabling a full delivery of the reaction product, due to its lower affinity with the binding site. Substrate conformation and motion in the active site are also fixed thanks to well placed interactions: substrate is desolvated and placed in a microenvironment that favors the reaction.[4] Enzymes therefore represent a key inspiration for chemists in the design of supramolecular catalytic systems (artificial enzymes).[5] Supramolecular approaches to catalysis therefore represent a powerful way to translate these principles to usual chemical systems, for which molecular recognition and cooperativity might give rise to new selectivity in well designed systems. Currently, three main strategies are employed for the elaboration of supramolecular catalysts:

---

[3] Pauling, L. *Chem. Eng. News* **1946**, *24*, 1375.

[4] a) Dewar, M. S. J.; Storch, D. M. *Proc. Nat. Ac. Sci. U. S. A.* **1985**, *82*, 2225. b) Zhang, X.; Houk, K. N. *Acc. Chem. Res.* **2005**, *38*, 379. c) Gao, J.; Ma, S.; Major, D. T.; Nam, K.; Pu, J.; Truhlar, D. G. *Chem. Rev.* **2006**, *106*, 3188.

1) Transition state analogue-selection approach: construction of a system able to recognize a structure analog to the one of the transition state of the target reaction (catalytic antibodies,[6] molecularly imprinted polymers,[7] bioimprinting…)
2) Catalytic activity-selection approach: use of combinatorial synthetic tools and high-throughput screening methods for the selection of the best catalyst from a prepared library (combinatorial chemistry of polymers[8] and peptides,[9] directed evolution of artificial enzymes).[10]

---

[5] For examples, see: a) Kirby, A. J. *Angew. Chem. Int. Ed. Engl.* **1996**, *35*, 707. b) Sanders, J. K. M. *Chem. Eur. J.* **1998**, *4*, 1378. c) Motherwell, W. B., Bingham, M. J., Six, Y. *Tetrahedron* **2001**, *57*, 4663.

[6] a) Tramontano, A.; Janda, K. D.; Lerner, R. A. *Science* **1986**, *234*, 1566. b) Pollack, S. J.; Jacobs, J. W.; Schultz, P. G. *Science* **1986**, *234*, 1570. c) Li, T.; Janda, K. D.; Ashley, J. A.; Lerner, R. A. *Science* **1994**, *264*, 1289. d) Li, T.; Janda, K. D.; Lerner, R. A. *Nature* **1996**, *379*, 326.

[7] a) Wulff, G. *Angew. Chem. Int. Ed. Engl.* **1995**, *34*, 1812. b) Takeuchi, T.; Matsuji, J. *Acta Polymer* **1996**, *47*, 471. c) Cormack, P. A. G.; Mosbach, K. *Reac. and Func. Polymers* **1999**, *41*, 115. d) Whitcombe, M. J.; Alexander. C.; Vulfson, E. N. *Synlett* **2000**, 911. e) Liu, X.-C.; Mosbach, K. *Macromol. Rapad. Commun.* **1997**, *18*, 609.

[8] a) Menger, F. M.; Eliseev, A. V.; Mingulin, V. A. *J. Org. Chem.* **1995**, *60*, 6666.

3) Rational design approach: use of supramolecular interactions for substrate recognition (functionalized cavities for catalysis or catalyst encapsulation, self-assembled micelles and polymersomes[11], biomacromolecular assemblies, capsids, dendrimeric catalysts…).

Some relevant examples of the rational design approach will be briefly presented in the next section (biomacromolecular assemblies, micelles, dendrimers and polymersomes will not be treated here). Emphasis will be laid on examples involving cavities (covalent and non-covalent), encapsulated active sites and self-assembled ligands.

1.2 Space confined supramolecular catalysis.

1.2.1 Covalent macrocyclic catalysts.

Since 1987, some synthetic macrocycles and covalent systems have been reported as potential supramolecular catalysts by the groups of Cram

---

b) Menger, F. M.; West, C. A.; Ding, J. *J. Chem. Soc., Chem. Commun.* **1997**, 633.

[9] a) Kuntz, K. W.; Snapper, M. L.; Hoveyda, A. H. *Current Opinion in Chemical Biology* **1999**, *3*, 313. b) Jandeleit, B.; Schaefer, D. J.; Powers, T. S.; Turner, H. W.; Weinberg, W. H. *Angew. Chem. Int. Ed.* **1999**, *38*, 2494.

[10] For some reviews, see: a) Reetz, M. T. *Tetrahedron* **2002**, *58*, 6595. b) Reetz, M. T. *Advances in catalysis* **2006**, *49*, 1.

[11] For a complete review on self-assembled macromolecular nanoreactors: Vriezema, D. M.; Aragonès, M. C.; Elemans, J. A. A. W.; Cornelissen, J. J. L. M.; Rowan, A. E.; Nolte, R. J. M. *Chem. Rev.* **2005**, *105*, 1445.

and Lehn (Nobel Prize laureates for their pioneering work in supramolecular chemistry). Lehn *et al.* indeed reported functionalized cryptands able to catalyze the aminolysis of ATP to ADP. The substrate was first recognized by the catalyst thanks to electrostatic and H-bonding interactions and then hydrolyzed due to functionalization at an appropriate position of the cryptand.[12] At neutral pH, the catalyst is partially protonated, thus permitting both substrate recognition (coulombic interactions with ammonium groups) and catalysis (free amines). A 500-fold rate acceleration was obtained in presence of the catalyst. Addition of an aromatic residue to the free amine afforded some additional π-stacking interactions, resulting in improved selectivity for ATP (Fig. 1.2).[12c] This is an early example of catalysis assisted by substrate recognition.

Cyclodextrins, the cyclic oligomers of glucose with a conical shape and hydrophobic interiors, were also used as potential catalysts in water.[13] Their use as catalysts in selective ester hydrolysis,[14] enzyme mimics

---

[12] Phosphoryl transfer reactions: a) Hosseini, M. W.; Lehn, J.-M. *J. Am. Chem. Soc.* **1987**, *109*, 537. ATP hydrolysis: b) Hosseini, M. W.; Lehn, J.-M.; Jones, K. C.; Plute, K. E.; Mertes, K. B.; Mertes, M. P. *J. Am. Chem. Soc.* **1989**, *111*, 6330. c) Hosseini, M. W.; Blacker, A. J.; Lehn, J.-M. *J. Am. Chem. Soc.* **1990**, *112*, 3896. Additional examples of catalysis mediated by cryptands: d) Cram, D. J. *Angew. Chem. Int. Ed. Engl.* **1988**, *27*, 1009. e) Pedersen, C. J. *Angew. Chem. Int. Ed. Engl.* **1988**, *27*, 1021. f) Cacciapaglia, R.; Di Stefano, S., Kelderman, E.; Mandolini, L. *Angew. Chem. Int. Ed.* **1999**, *38*, 348.

[13] For reviews, see: a) Breslow, R.; Dong, S. D. *Chem. Rev.* **1998**, *98*, 1997. b) Takahashi, K. *Chem. Rev.* **1998**, *98*, 2013.

[14] a) Breslow, R.; Schmuck, C. *J. Am. Chem. Soc.* **1996**, *118*, 6601. b) Zhang, B. L.; Breslow, R. *J. Am. Chem. Soc.* **1997**, *119*, 1676. c) Liu, S.; Luo, Z.; Hamilton, A. D.

(ribonuclease A),[13a, 15] Diels-Alder reactions,[16] or intramolecular aldol reactions[17] is well documented. Many other examples can be found, where cyclodextrins were functionalized with ligand-transition metal complexes for catalysis of various processes: ester hydrolysis,[18] a tryptophan synthase mimic,[19] oxidation reactions (metalloporphyrin based systems)[20] and phosphodiester hydrolysis.[21]

Angew. Chem. Int. Ed. Engl. **1997**, *36*, 2678. d) Barr, L.; Easton, C. J.; Lee, K.; Lincoln, S. F.; Simpson, J. S. *Tetrahedron Lett.* **2002**, *42*, 7797.

[15] Breslow, R.; Anslyn, E. *J. Am. Chem. Soc.* **1989**, *111*, 8931.

[16] a) Rideout, D. C.; Breslow, R. *J. Am. Chem. Soc.* **1980**, *102*, 7817. b) Schneider, H.-J.; Sangwan, N. K. *J. Chem. Soc., Chem. Commun.* **1986**, 1787. c) Schneider, H.-J.; Sangwan, N. K. *Angew. Chem., Int. Ed. Engl.* **1987**, *26*, 896. d) Breslow, R.; Guo, T. *J. Am. Chem. Soc.* **1988**, *110*, 5613.

[17] a) Desper, J. M.; Breslow, R. *J. Am. Chem. Soc.* **1994**, *116*, 12081 b) Breslow, R.; Desper, J.; Huang, Y. *Tetrahedron Lett.* **1996**, *37*, 2541.

[18] Breslow, R. Enzyme Models Related to Inclusion Compounds in *Inclusion Compounds*; Atwood, J. L., Davies, J. E., Eds.; Academic Press: Orlando, FL, 1984; Vol. 3, pp 473-508.

[19] Weiner, W.; Winkler, J.; Zimmerman, S. C.; Czarnik, A.W.; Breslow, R. *J. Am. Chem. Soc.* **1985**, *107*, 4093.

[20] a) Kuroda, Y.; Hiroshige, T.; Sera, T.; Shiroiwa, Y.; Tanaka, H.; Ogoshi, H. *J. Am. Chem. Soc.* **1989**, *111*, 1912. b) Kuroda, Y.; Hiroshige, T.; Sera, T.; Ogoshi, H. *Carbohydr. Res.* **1989**, *192*, 347. c) Kuroda, Y.; Hiroshige, T.; Ogoshi, H. *J. Chem. Soc., Chem. Commun.* **1990**, 1594. d) Kuroda, Y.; Egawa, Y.; Seshimo, H.; Ogoshi, H. *Chem. Lett.* **1994**, 2361. e) Breslow, R.; Huang, Y.; Zhang, X.; Yang, J. *Proc. Natl. Acad. Sci. U.S.A.* **1997**, *94*, 11156.

[21] a) Breslow, R.; Zhang, B. *J. Am. Chem. Soc.* **1992**, *114*, 5882. b) Breslow, R.; Zhang, B. *J. Am. Chem. Soc.* **1994**, *116*, 7893. c) Zhang, B.; Breslow, R. *J. Am. Chem. Soc.* **1997**, *119*, 1676.

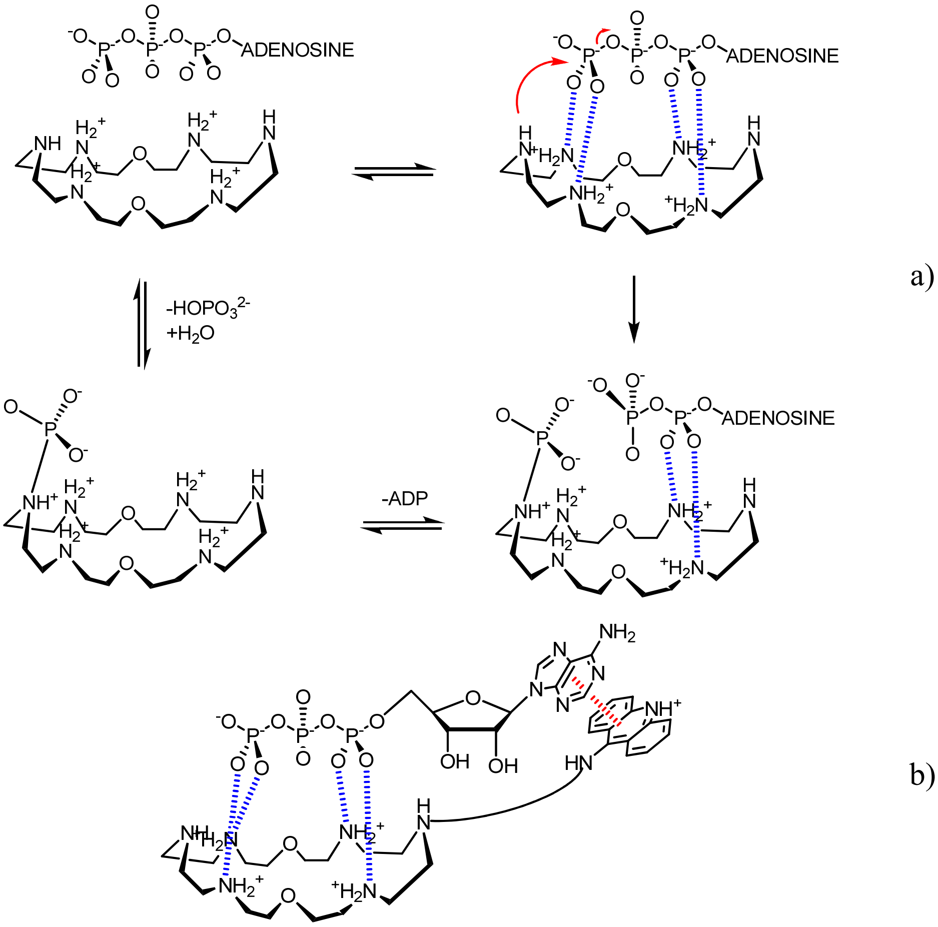

Fig. 1.2: a) Proposed catalytic cycle for the action of the polyamine cryptand prepared by Lehn *et al.* for the hydrolysis of ATP to ADP.[11c]
b) Modified catalyst and its interaction with the substrate.

Breslow *et al.* showed that a stilbene disubstituted steroid derivative could be selectively oxidized at the 6-CH_2 position of the steroid skeleton, thanks to adequate positioning of the metal oxide with respect to the steroid skeleton (stilbene encapsulation leads to the observed regioselectivity, see

Fig. 1.3).[22]

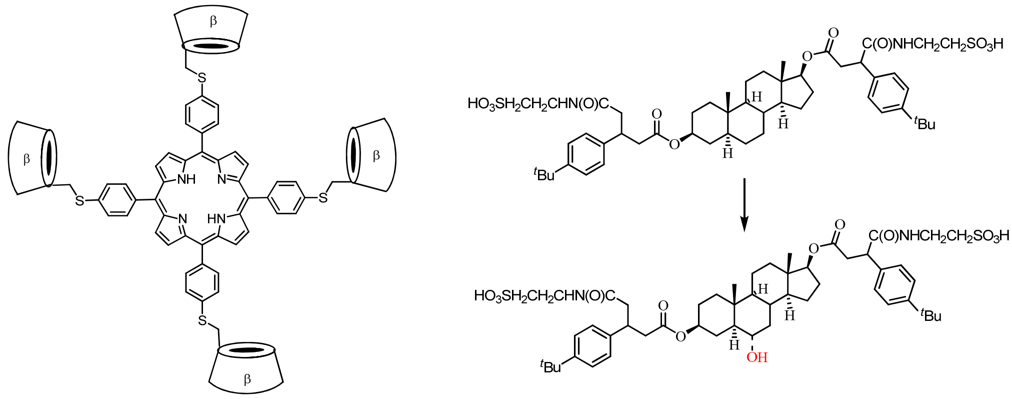

Fig. 1.3: Regioselective oxidation of steroid skeleton catalyzed by a metalloporphyrin-cyclodextrin conjugate.

Similarly, the family of cucurbiturils corresponds to the cyclic penta- to decamers of glycoluril and therefore present close characteristics to cyclodextrins (polar exterior and hydrophobic interior).[23] High electronic density found at cucurbiturils' portal renders them good receptors for organic cations. This lead Mock *et al.* to develop a catalytic procedure for 1,3-dipolar cycloadditions of azidoammonium to ammoniumalkynes.[24]

---

[22] Breslow, R.; Zhang, X.; Xu, R.; Maletic, M.; Merger, R. *J. Am. Chem. Soc.* **1996**, *118*, 11678.

[23] For recent reviews on cucurbiturils, see: a) Kim, K. *Chem. Soc. Rev.* **2002**, *31*, 96. b) Lagona, J.; Mukhopadhyay, P.; Chakrabarti, S.; Isaacs, L. *Angew. Chem. Int. Ed.* **2005**, *44*, 4844. c) Kim, K.; Selvapalam, N.; Ko, Y. H.; Park, K. M.; Kim, D.; Kim, J. *Chem. Soc. Rev.* **2007**, *36*, 267.

[24] Mock, W. L.; Irra, T. A.; Wepsiec, J. P.; Manimaran, T. L. *J. Org. Chem.* **1983**, *48*, 3619.

Inclusion of both reaction substrates in a close to straight line in cucurbit[6]uril gave rise to the exclusive formation of the 1,4 adduct and reaction occurred 55,000 times faster than in absence of the catalyst (Fig. 1.4).[25] Steinke *et al.* took then benefit of this efficient procedure to successfully generate polyrotaxanes and oligotriazoles from diazides and diacetylenes.[26]

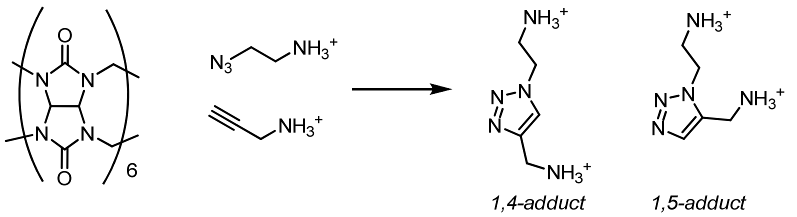

Fig. 1.4: 1,3-Dipolar cycloaddition catalyzed by a cucurbit[6]uril derivative.

The power of rational design was remarkably illustrated by Sanders *et al.* who reported a macrocyclic catalyst made of Zn-porphyrin subunits for the Diels-Alder addition of pyridyl substituted substrates (Fig. 1.5).[27] The dienophile (maleimide) and the diene (furan) are preorganized inside the cavity by coordination to the metal of the pyridyl substituents, which results in selectivity: binding enthalpic gain helps in overcoming the high entropic activation cost. 200-fold rate acceleration with respect to the uncatalyzed process was reported. However, product inhibition was observed: the product binds better to the catalyst than substrates. True catalysis could nevertheless be obtained for the transacylation reaction of 4-(hydroxymethyl) pyridine by *N*-acetylimidazole.[28]

---

[25] 1/1 mixture of 1,4 and 1,5 adducts is obtained without the catalyst

[26] a) Tuncel, D.; Steinke, J. H. G. *Chem. Commun.* **1999**, 1509. b) Krasia, T. C.; Steinke, J. H. G. *Chem. Commun.* **2002**, 22.

[27] a) Walter, C. J.; Anderson, H. L.; Sanders, J. K. M. *J. Chem. Soc., Chem. Commun.* **1993**, 458. b) Clyde-Watson, Z.; Vidal-Ferran, A.; Twyman, L. J.; Walter, C. J.; Mc Callien, D. W. J.; Fanni, S.; Bampos, N.; Wylie, R. S.; Sanders, J. K. M. *New J. Chem.* **1998**, 493. c) Marty, M.; Clyde-Watson, Z.; Twyman, L. J.; Nakash, M.; Sanders, J. K. M. *Chem. Commun.* **1998**, 2265. d) Nakash, M.; Clyde-Watson, Z.; Feeder, N.; Davies, J. E.; Teat, S. J.; Sanders, J. K. M. *J. Am. Chem. Soc.* **2000**, *122*, 5286. e) Nakash, M.; Sanders, J. K. M. *J. Org. Chem.* **2000**, *65*, 7266.

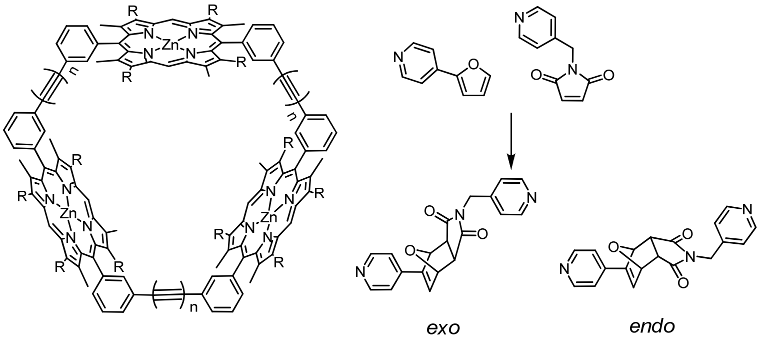

n	**Formed product**
1	*endo*
2	*exo*

Fig. 1.5: Porphyrin macrocycle for Diels-alder catalysis

As a last example of macrocyclic covalent catalysts, deep cavitands such as calixarene and resorcinarene derivatives are able to form strong inclusion complexes in organic media with various cationic and hydrophobic residues.[29] In 2000, Mandolini and de Mendoza reported a calix[6]arene derivative functionalized with a bicyclic guanidinium (catalytic site) able to catalyze the methanolysis of carbonates, as shown on figure 1.6.[30] The fixed cone conformation of the cavitand (enhanced substrate encapsulation) enables 149-fold rate acceleration to be observed. A positive cooperative effect between guanidinium and calixarene was also shown.

---

[28] Mackay, L. G.; Wylie, R. S.; Sanders, J. K. M. *J. Am. Chem. Soc.* **1994**, *116*, 3141.

[29] For a review on host-guest chemistry of resorcinarenes, see: a) Purse, B. W., Rebek, J. Jr. *Proc. Nat. Ac. Sci. U. S. A.* **2005**, *102*, 10777. b) Biros, S. M.; Rebek, J. Jr. *Chem. Soc. Rev.*, **2007**, *36*, 93.

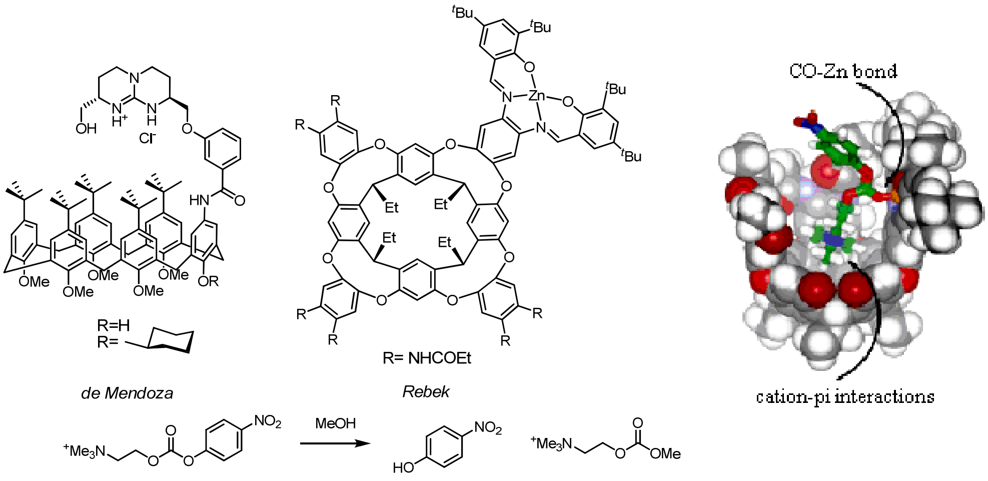
OH
H⁺
H
Cl⁻
HN
O
OMe
OMe
OMe
OMe
OR
R=H
R=
de Mendoza
ᵗBu
ᵗBu
ᵗBu
ᵗBu
N
Zn
O
R
Et
R= NHCOEt
Rebek
CO-Zn bond
cation-pi interactions
⁺Me₃N
NO₂
MeOH
HO
OMe

Fig. 1.6: Reported cavitand derivatives as acetylcholinesterase mimics.

The same reaction was studied four years later by Rebek *et al.*, using an alternative resorcinarene derivative functionalized with a zinc-salphen ligand.[31] Lewis acid activation renders this catalyst quite efficient in the methanolysis of the studied carbonate (Fig. 1.6 shows a computed model of substrate binding to the catalyst, in which the frontal cavity wall was removed for clarity). However, as in many cases, the turnover frequency (TOF) mainly depends on the guest exchange rate of the resorcinarene. Calixarenes have also been used as containers for transition metals for Wacker oxidations[32] and other applications.[33]

---

[30] a) Magrans, J. O.; Ortiz, A. R.; Molins, A.; Lebouille, P. H. P.; Sánchez-Quesada, J.; Prados, P.; Pons, M.; Gago, F.; de Mendoza, J. *Angew. Chem. Int. Ed. Engl.* **1996**, *35*, 1712. b) Cuevas, F.; di Stefano, S.; Magrans, J. O., Prados, P.; Mandolini, L.; de Mendoza, J. *Chem. Eur. J.* **2000**, *6*, 3228.

[31] Richeter, S.; Rebek, J. Jr. *J. Am. Chem. Soc.* **2004**, *126*, 16280.

In catalysis inside a macrocyclic reactor, encapsulation of the substrate is thermodynamically driven (entropic source: the release of solvent molecules) but depends on size, shape, and guest-cavity surface chemical complementarities. The turnover is in most cases guaranteed by the reversible release of the guest molecule from the cavity[34] (*vide infra*). Encapsulation creates a microenvironment that differs from the bulk by alteration of the motion and solvation of the guest (cavity effects). A traffic problem however subsists and kinetics of catalysis in capsules most often depend on the guest exchange rate (nature usually uses open cavities such as channels or pores). Covalent macrocycles therefore represent promising potential supramolecular catalysts, though they often require a tedious multi-step preparation. For this reason, a large number of systems based on the same principles are prepared by self-assembly.

---

[32] Maksimov, A. L.; Sakharov, D. A.; Filippova, T. Y.; Zhuchkova, A. Y.; Karakhanov, E. A. *Ind. Eng. Chem. Res.* **2005,** *44,* 8644.

[33] Capsule containing diphosphine for transition metal complexation: Koblenz, T. S.; Dekker, H. L.; de Koster, C. G.; van Leeuwen, P. W. N. M.; Reek, J. N. H. *Chem. Commun.* **2006**, 1700.

[34] Pluth, M. D.; Raymond, K. N. *Chem. Soc. Rev.* **2007**, *36*, 161.

1.2.2 Self-assembled nanoreactors. [11, 35]

Self-assembly indeed appears as a promising way in successful designs, yet control in the size and geometry of the self-assembled species can be achieved. Suitable programming of the binding functionalities and size and shape complementarities of the building blocks enable a better optimization of the catalytic site(s). Furthermore, the reversibility and directionality of the used interactions for the self-assembly process usually enables the formation of a discrete and thermodynamically stable entity.[36] In numerous cases, guest templation is however necessary for capsule amplification.[37]

H-bonded self-assembled capsules as catalysts were first reported by Rebek *et al*. Hydrogen bonds are usually rather weak interactions but are highly directional, which makes them suitable enough for self-assembly purposes. Capsule stability can then be tuned by a variation of the number of hydrogen bonds in the binding array. A resorcin[4]arene derivative substituted with imide functionalities at the upper rim gives rise to a self-

---

[35] For a review, see: Koblenz, T. S.; Wassenaar, J.; Reek, J. N. H. *Chem. Soc. Rev.* **2008**, *37*, 247.

[36] For a review on self assembled capsules, see: a) MacGillivray, L. R.; Atwood, J. L. *Angew. Chem. Int. Ed.* **1998**, *38*, 1018. b) Hof, F.; Craig, S. L.; Nuckolls, C.; Rebek, J. Jr. *Angew. Chem. Int. Ed.* **2002**, *41*, 1488. (host-guest chemistry of self-assembled capsules) c) Amijs, C. H. M.; van Klink, G. P. M., van Koten, G. *Dalton Trans.* **2006**, 308. (metallasupramolecular architectures and applications).

[37] For a review on metal templation, see: Linton, B.; Hamilton, A. D. *Chem. Rev.* **1997**, *97*, 1669. For reviews on anion templation, see: a) Gimeno, N.; Vilar, R. *Coord. Chem. Rev.* **2006**, *250* , 3161. b) Lankshear, M. D.; Beer, P. D. *Acc. Chem. Res.* **2007**, *40*, 657.

assembled capsule by formation of an array made of 16 H-bonds (Fig. 1.7a). The capsule was shown to be large enough (425 Å^3) to encapsulate two different substrates (though it was also shown that optimal occupation of the capsule lies around 55%).[38]Based on the same principles, a "soft ball" was prepared thanks to the assembly of glycoluril moieties placed at the ends of a spacing group of suitable rigidity and curvature to allow the capsule formation with 16 hydrogen bonds (Fig. 1.7b).[39] Capsule opening proceeds through a gating mechanism by removal of one interaction between two of the glycoluril subunits. The capsule A was then used in regioselective 1,3-dipolar cycloadditions between two aromatic substrates (phenylacetylene and phenylazide).[40] Substrates encapsulate and react in a few days to give the 1,4-adduct selectiviely (without catalyst, hardly no reaction is observed). As shown in Fig. 1.8, reaction rate is also dependent on the distribution of the included species (guest exchange rate). Finally, the capsule showed a rather high affinity for the product of the reaction, which produced some product inhibition (no true catalysis was observed).

---

[38] a) Palmer, L. C.; Rebek, J. Jr. *Org. Biomol. Chem.* **2004**, *2*, 3051. b) Rebek, J. Jr *Angew. Chem. Int. Ed.* **2005**, *44*, 2068 and references therein.

[39] a) Meissner, R. S.; Rebek, J., Jr.; de Mendoza, J. *Science*. **1995**, *270*, 1485. b) Rebek, J. Jr. *Chem. Soc. Rev.* **1996**, *25*, 255. c) Conn, M.; Rebek, J. Jr. *Chem. Rev.* **1997**, *97*, 1647. d) Rebek, J. Jr. *Acc. Chem. Res.* **1999**, *32*, 278. e) Hof, F.; Rebek, J. Jr. *Proc. Nat. Ac. Sci. U. S. A.* **2002**, *99*, 4775.

[40] a) Heinz, T.; Rudkevich, D. M.; Rebek, J. Jr. *Nature* **1998**, *394*, 764. b) Chen, J.; Rebek, J. Jr. *Org. Lett.* **2002**, *4*, 327.

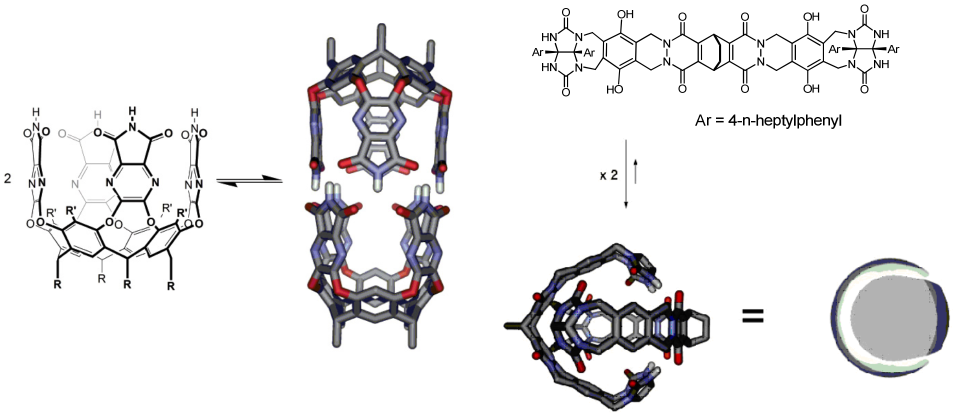

a) b)

Fig. 1.7: H-bonded capsules for catalysis applications: a) Capsule A. b) Soft ball.

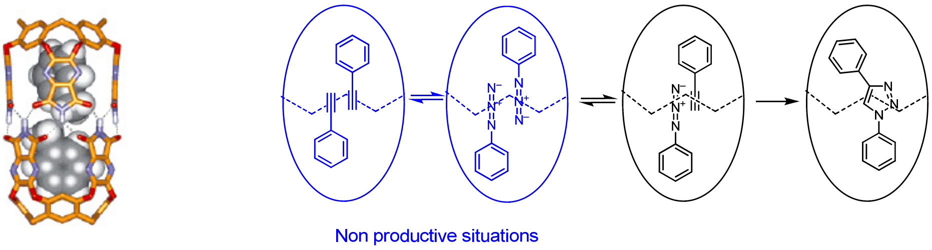

a) b)

Fig. 1.8: 1,3-Dipolar cycloaddition catalyzed by capsule A:
a) Inclusion complex with two toluene molecules. b) Species distribution.

The same trouble was found for the Diels-Alder addition of *p*-benzoquinone and cyclohexadiene catalyzed by the previously described “soft ball”, though a 170-fold rate acceleration with respect to the bulk reaction was observed (Fig. 1.9).[41] This means that the reaction is slower than the exchange of substrates within the cavities. True catalysis could however be obtained using a thiophene dioxide derivative as shown below. Since a higher affinity of the capsule for two benzoquinone molecules than for the product was observed, it is likely that the inclusion of the two cycloaddition components would also be favored, so that turnover could be promoted. Cavity effects are therefore controlled by the opening rates of the capsules and the differences between reaction rates inside and outside the capsule.

---

[41] a) Kang, J.; Rebek, J. Jr. *Nature* **1997**, *385*, 50. b) Kang, J.; Hilmersson, G.; Santamaría, J.; Rebek, J. Jr. *J. Am. Chem. Soc.* **1998**, *120*, 3650. c) Kang, J.; Santamaría, J.;

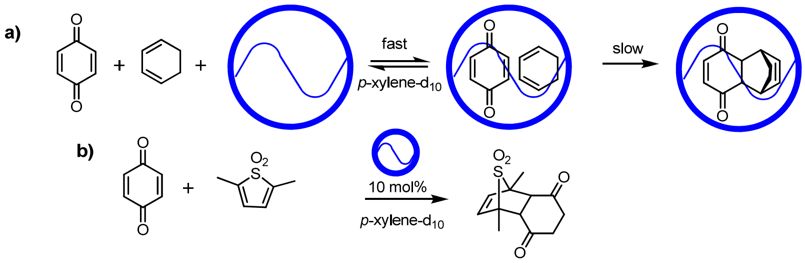

Fig. 1.9: Diels-Alder reaction catalyzed by the "*soft ball*".

Some capsules were also obtained by self-assembly using hydrophobic forces and $\pi-\pi$ stacking interactions by Gibb and co-workers. However, formation of the capsule required a hydrophobic template (a rigid steroid or small alkanes).[42] The resulting water-soluble capsule was then used as a catalyst for an aqueous phase photo-oxidation process.[43] Addition of one equivalent of 1-methylcyclohexene to one equivalent of cavitand resulted in

---

Hilmersson, G.; Rebek, J. Jr. *J. Am. Chem. Soc.* **1998**, *120*, 7389.

[42] Gibb, C. L. D.; Gibb, B. C. *J. Am. Chem. Soc.* **2004**, *126*, 11408.

[43] a) Natarajan, A.; Kaanumalle, L. S.; Jockush, S.; Gibb, C. L. D.; Gibb, B. C.; Turro, N. J.; Ramamurthy, V. *J. Am. Chem. Soc.* **2007**, *129*, 4132. b) Greer, A. *Nature* **2007**, *447*, 273.

the formation of a capsule filled with two alkene substrates. Preferential conformation and restricted motion of substrates inside the capsule led to the observed remarkable regioselectivity (Fig. 1.10).

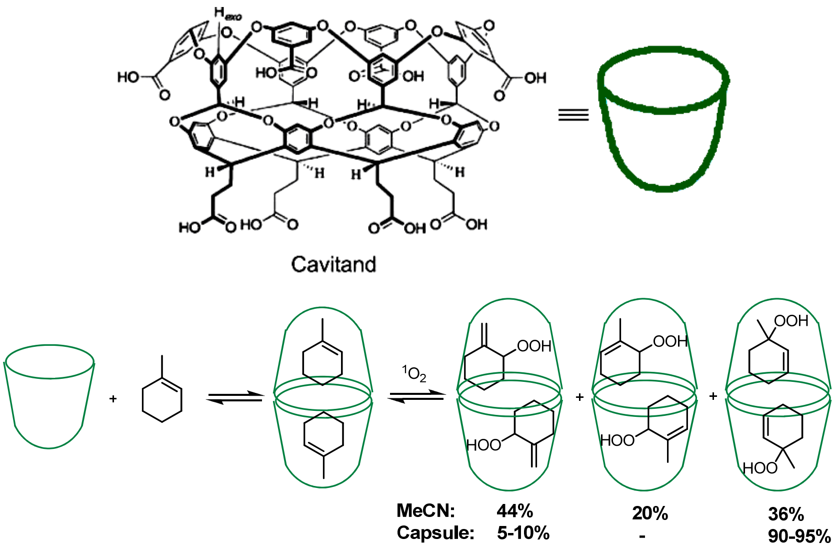

Fig. 1.10: Photooxidation catalyzed by a self-assembled capsule in water.

Another approach for the preparation of self-assembled cavities is to use transition metal-ligand interactions.[44] These strong interactions are highly directional and define a precise angle between the interacting species. In most cases, fast ligand exchange enables a quick equilibration of the possible aggregates and the obtention of a discrete one (thermodynamic control). The advantage of this approach is that the spacer can be linearly rigid, since the angle provided by the metal coordination creates the curvature required for the cavity to form. Exchange between the inside and the outside of the capsule usually takes place without full disruption of the aggregate and is attributed to the expansion of the cage windows.[34]

---

[44] a) Leininger, S.; Olenyuk, B.; Stang, P. J. *Chem. Rev.* **2000**, *100*, 853. b) Holliday, B. A.; Mirkin, C. A. *Angew. Chem., Int. Ed.* **2001**, *40*, 2022. c) Seidel, S. R.; Stang, P. J. *Acc. Chem. Res.* **2002**, *35*, 972. d) Sun, W.-Y.; Yoshizawa, M.; Kusukawa, T.; Fujita, M. *Curr. Opin. Chem. Biol.* **2002**, *6*, 757. e) Pinalli, R.; Cristini, V.; Sottili, V.; Geremia, S.; Campagnolo, M.; Caneschi, A.; Dalcanale, E. *J. Am. Chem. Soc.* **2004**, *126*, 6516.

Based on these principles, Fujita *et al.* designed well-defined cages of various shapes by multi-component transition metal mediated self-assembly processes for use as reaction chambers. The designs were based on a triangular rigid heterocyclic ligand and the forced *cis* square planar geometry of Pd(II) and Pt(II) for the production of octahedral capsules of general formula M_6L_4 (metals occupy the corners of the octahedron, whereas ligands correspond to some of the faces).[45] The *cis* coordination mode to the transition metal was forced by using a bidentate ligand such as ethylenediamine and 2,2'-bipyridine (Fig. 1.11).[46]

---

[45] a) Fujita, M. *Chem. Soc. Rev.* **1998**, *27*, 417. b) Fujita, M.; Tominaga, M.; Hori, A.; Therrien, B. *Acc. Chem. Res.* **2005**, *38*, 371.

[46] a) Fujita, M.; Oguro, D.; Miyazawa, M.; Oka, H.; Yamaguchi, K.; Ogura, K. *Nature* **1995**, *378*, 469. b) Kusukawa, T.; Fujita, M. *Angew. Chem., Int. Ed.* **1998**, *37*, 3142. c) Kusukawa, T.; Fujita, M. *J. Am. Chem. Soc.* **1999**, *121*, 1397. d) Kusukawa, T.; Fujita, M. *Angew. Chem., Int. Ed.* **2001**, *40*, 1879. e) Kusukawa, T.; Fujita, M. *J. Am. Chem. Soc.* **2002**, *124*, 13576.

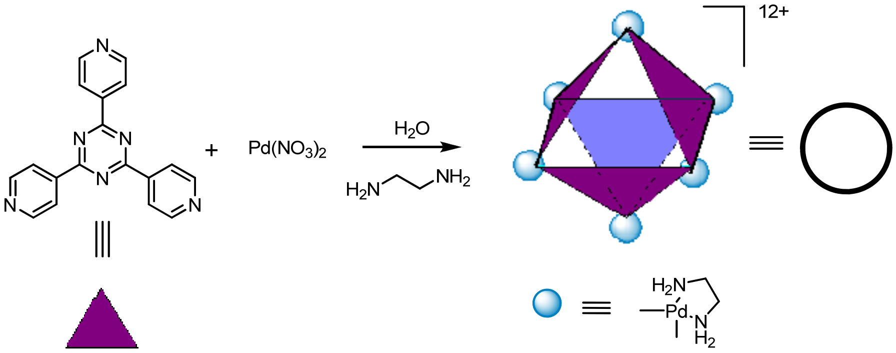

Fig. 1.11: $[M_6L_4]^{12+}$ Octahedral cage reported by Fujita.

This octahedral cage encapsulates up to four organic molecules in aqueous media (depending on the guest sizes) thanks to its 500 Å^3 cavity volume. This capsule was first thought as a potential phase-transfer catalyst because of its water solubility. Indeed, the Wacker oxidation of styrene to acetophenone was catalyzed by the cage (Fig. 1.12).[47] The same octahedral cage was used in Diels-Alder cycloadditions[48] and homo- and hetero-photodimerization of olefins[49], showing outstanding selectivities and enhanced reactivities. The same cavity was used for the controlled trimerization of trialkoxysilanes to give a chair-like derivative that is stabilized by the capsule (kinetically unstable in its absence).[50]

---

[47] Ito, H.; Kusukawa, T.; Fujita, M. *Chem. Lett.* **2000**, 598.

[48] Yoshizawa, M.; Tamura, M.; Fujita, M. *Science* **2006**, *312*, 251.

[49] a) Yoshizawa, M.; Takeyama, Y.; Kusukawa, T.; Fujita, M. *Angew. Chem., Int. Ed.* **2002**, *41*, 1347. b) Yoshizawa, M.; Takeyama, Y.; Okano, T.; Fujita, M. *J. Am. Chem. Soc.* **2003**, *125*, 3243.

[50] Yoshizawa, M.; Kusukawa, T.; Fujita, M.; Sakamoto, S.; Yamaguchi, K. *J. Am. Chem. Soc.* **2001**, *123*, 10454.

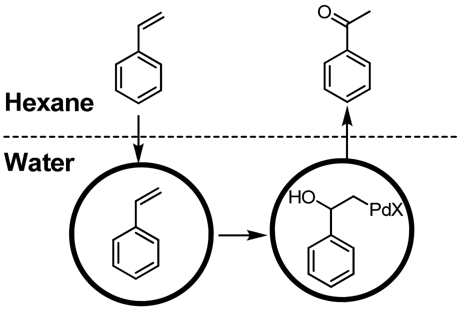

Catalyst	yield %
$Pd(en)(NO_3)_2$	4
metallocage	82
Poisoned metallocage	3

Fig. 1.12: Wacker oxidation of styrene to acetophenone catalyzed by $[M_6L_4]^{12}$.

Raymond and co-workers reported another tetrahedral cage obtained by the self-assembly of a bis-bidentate catechol amide with four metal ions (Al^{3+}, Ga^{3+}, In^{3+}, Fe^{3+}, Ti^{4+}, Ge^{4+}).[51] This chiral negatively charged capsule is soluble in water and presents a cavity of 300-500 Å^3 suitable for encapsulation of cationic guests such as ammonium salts and inorganic species. Metals occupy the corners of the tetrahedron, whereas the bis-catechol derivatives span the edges of the tetrahedron (see Fig. 1.13, metal is represented in red and guest in blue).

---

[51] a) Caulder, D. L.; Raymond, K. N. *Acc. Chem. Res.* **1999**, 32, 975. b) Caulder, D. L.; Brückner, C.; Powers, R. E.; König, S.; Parac, T. N.; Leary, J. A.; Raymond, K. N. *J. Am. Chem. Soc.* **2001**, *123*, 8923. c) Terpin, A. J.; Ziegler, M.; Johnson, D. W.; Raymond, K. N. *Angew. Chem. Int. Ed.* **2001**, *40*, 157. d) Ziegler, M.; Davis, A. V.; Johnson, D. W.; Raymond, K. N. *Angew. Chem. Int. Ed.* **2003**, *42*, 665. e) Fiedler, D.; Leung, D. H.; Bergman, R. G.; Raymond, K. N. *Acc. Chem. Res.* **2005**, *38*, 349.

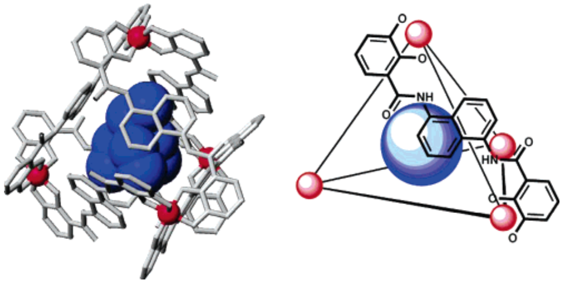

a) b)

Fig. 1.13: a) Model of tetraethylammonium encapsulated in a catechol cage formed with Fe^{3+}. b) Schematic representation of the cage.

The water soluble M_4L_6 assembly was shown to catalyze the 3-aza Cope rearrangement (up to 850-fold acceleration),[52] and the acidic hydrolysis of orthoformates in basic media.[53] The high affinity of the tetrahedral cage for cationic species indeed facilitates the protonation of the orthoformate, even in basic solution. This acid hydrolysis works efficiently for small molecules (tripentylorthoformate and higher substrates do not react) at pH 11 in presence of 1 mol% catalyst. 890-fold rate acceleration was obtained in the case of triisopropyl orthoformate. The kinetics of the process obeyed Michaelis-Menten equation, a characteristic of enzymatic systems.

---

[52] Fiedler, D.; van Halbeek, H.; Bergman, R. G., Raymond, K. N. *J. Am. Chem. Soc.* **2006**, *128*, 10240.

[53] a) Pluth, M. D.; Bergman, R. G.; Raymond, K. N. *Science* **2007**, *316*, 85. b) Pluth, M. D.; Bergman, R. G.; Raymond, K. N. *Angew. Chem. Int. Ed.* **2007**, *46*, 8587.

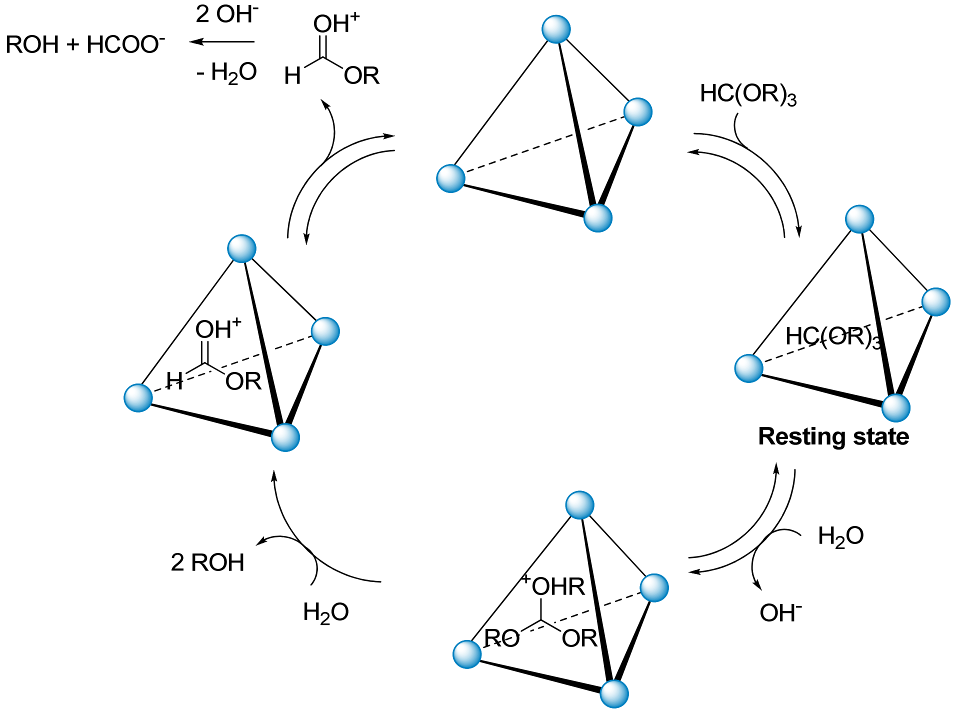

Quantitative: R= Me, Et, Pr, *n*-Pr, *i*-Bu, *n*-Bu
No reaction: R= *n*-pentyl

Fig. 1.14: Mechanism of the catalytic hydrolysis of orthoformates

The mechanism involves encapsulation of the neutral orthoformate driven by hydrophobic forces, followed by protonation of the substrate by a water molecule (encapsulation complex thus increases stability). Two successive hydrolysis steps (in the cavity) lead to the release of two alcohol molecules. The protonated formate ester in the capsule is then released in the basic medium and hydrolyzed (Fig. 1.14). This example clearly reflects the differences in acidity that can be reached upon creation of microenvironments. This macrocyclic catalyst has also been used for the encapsulation of catalytically active inorganic species.

1.2.3 Active site encapsulation.

The self-assembled capsule prepared by Raymond *et al*. was then used for the encapsulation of a metal-ligand complex, rendering the catalyst size-selective *via* substrate encapsulation. This approach is however only successful when host-guest exchange is slower than the reaction itself, otherwise the “cavity effect” is lost. The M_4L_6 assembly can indeed acomodate Ir(III) complexes. C-H bond activation of aldehydes and ethers was then studied and high selectivity (substrate size and shape) was observed. However, product inhibition prevented true catalysis from being effective.[54]

The isomerization of allylic alcohol catalyzed by an encapsulated cationic rhodium(I) complex proved to be more successful.[55] $[(PMe_3)_2Rh(COD)]^+$ was successfully encapsulated in the tetrahedral M_4L_6 assembly and activated *in situ* upon hydrogenation. Isomerization of allylic alcohols was the only possible application for reasons related to the stability of the active catalyst inside the metallocage. Substrate encapsulation and therefore reaction were selective in terms of size and shape as shown in Fig. 1.15. Allyl alcohol was isomerized successfully to propanal by the encapsulated catalyst and the non encapsulated one (95% yield), whereas substituted allylic alcohols only reacted in absence of the capsule (size and shape selection).

---

[54] Leung, D. H.; Bergman, R. G.; Raymond, K. N. *J. Am. Chem. Soc.* **2006**, *128*, 9781.

[55] Leung, D. H.; Bergman, R. G.; Raymond, K. N. *J. Am. Chem. Soc.* **2007**, *129*, 2746.

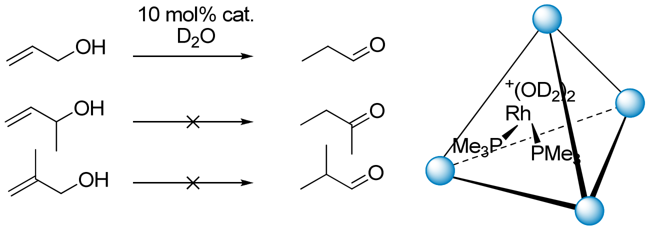
10 mol% cat.
D2O
OH
OH
OH
O
O
O
+(OD2)2
Rh
Me3P
PMe3

Fig. 1.15: Isomerization of allylic alcohols catalyzed by an encapsulated Rh(I) complex.

Encapsulation may provide also catalyst immunity towards poisoning. Nguyen and Hupp reported a molecular square made of four zinc porphyrin (square's faces) units linked through their pyridyl ligand by coordination to four Re(I) atoms (corners).[56] This molecular square accommodates a Mn(III) porphyrin through zinc coordination (K_a=10^6 M^{-1}) (Fig. 1.16).

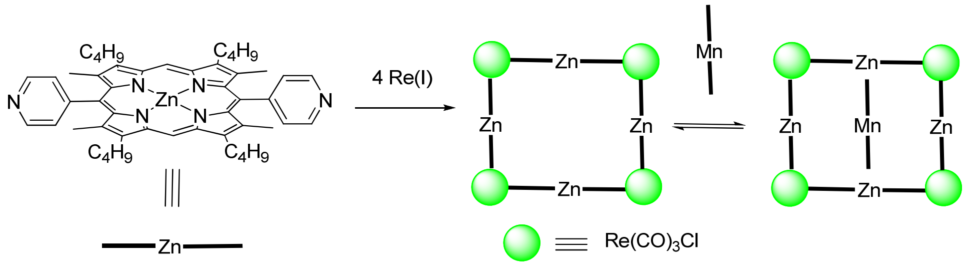
C4H9
C4H9
C4H9
C4H9
N
N
N
N
N
N
Zn
Zn
4 Re(I)
Zn
Zn
Zn
Zn
Mn
Zn
Zn
Mn
Zn
Zn
Re(CO)3Cl

Fig. 1.16: Encapsulation of Mn porphyrin into a molecular square.

Epoxidation of olefins catalyzed by Mn(III) porphyrin derivatives is well described but catalyst usually deactivates rapidly through dimerization (μ-oxo-bridges), therefore giving rise to low turnover numbers (TONs)

---

[56] a) Merlau, M.; Del Pilar Mejia, M.; Nguyen, S. T.; Hupp, J. T. *Angew. Chem., Int. Ed.* **2001**, *40*, 4239. b) Slone, R. V.; Hupp, J. T. *Inorg. Chem.* **1997**, *36*, 5422.

(around 500). Encapsulation of a manganese (III) porphyrin in this self-assembled molecular square enables to epoxidize a wide range of olefins (large and open cavity) and to protect the catalyst from deactivation: TONs as high as 21,000 were obtained in some cases. Some selectivity could also be observed, since substrate size is still determinant for reaction rate.

Ligand-template directed assembly for catalyst encapsulation where the ligand itself templates the capsule formation is also still conceptually promising.[57] Ligand complexation inside the capsule by the transition metal gives rise to the encapsulated (pre)-catalyst. Reek and co-workers reported a tripyridylphosphine that can coordinate to three zinc porphyrins or three zinc salens and therefore give rise to an encapsulated ligand.[58] Apart from being protected in some extent from oxidation by encapsulation, coordination chemistry of the ligand is modified due to its high space occupancy (presence of the cavity): addition of zinc porphyrin to $Pd(P(pyridyl)_3)_4$ gave rise to the monophosphane complex, as a result of steric congestion brought by the coordination to the zinc porphyrins. This resulted in a catalyst with an enhanced reactivity for the Heck reaction of iodobenzene with styrene when $Pd(P(pyridyl)_3)_4$ proved to be inactive as a catalyst. This approach also offers the possibility to vary the studied metal and therefore enlarges the scope of possible catalytic applications.

---

[57] For a conceptual review, see: Kleij, A. W.; Reek, J. N. H. *Chem. Eur. J.* **2006**, *12*, 4218.

[58] Slagt, V. F.; Reek, J. N. H.; Kamer, P. C. J.; van Leeuwen, P. W. N. M. *Angew. Chem. Int. Ed.* **2001**, *40*, 4271.

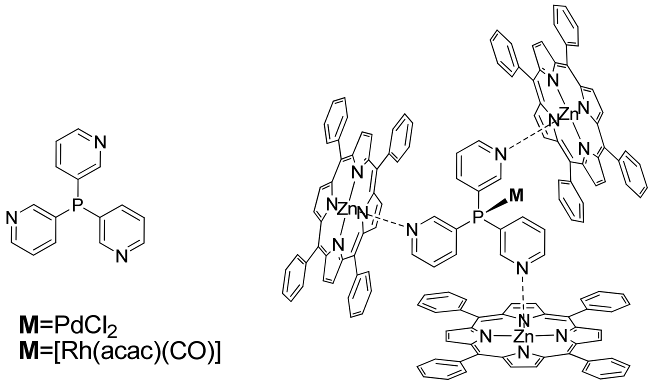

Fig. 1.17: Ligand-template directed assembly for catalyst encapsulation.

The rhodium complex of the encapsulated ligand (see Fig. 1.17) catalyzes the hydroformylation of 1-octene (10-fold rate acceleration) and reverses the obtained selectivity for the non encapsulated catalyst (l/b without Zn-porphyrins: 74/26; l/b with Zn-porphyrins: 28/62).[59]

All the examples described above report the use of capsules as confined reaction chambers in which at least two reactive species are bound, or as phase-transfer catalysts. However, other applications were described for such molecular containers that were used as inducers of chemical amplification and selection by the groups of Rebek[60] and Sanders (Dynamic Combinatorial Libraries).[61]

---

[59] Slagt, V. F.; Kamer, P. C. J.; van Leeuwen, P. W. N. M.; Reek, J. N. H. *J. Am. Chem. Soc.* **2004**, *126*, 1526.

[60] Chen, J.; Körner, S.; Craig, S. L.; Rudkevich, D. M.; Rebek, J., Jr. *Nature* **2002**, *415*, 385.

[61] Otto, S.; Furlan, R. L. E.; Sanders, J. K. M. *Science* **2002**, *297*, 590.

1.3 Self-assembly as a tool for ligand construction.

Supramolecular construction of bidentate ligands from monodentate ones for the stabilization of organometallic catalysts has also been reported. A library of potential catalysts can then be studied with a minimum of effort, using high throughput screening methods.[62] The rational design of such systems also enables the ligand to adopt the ideal bite angle (catalyst optimization).[63] This approach looks promising since a wide family of N,N, N,P and P,P bidentate ligands can be easily screened from a library of monodentate ligands.

Reek and co-workers reported a diphenyl(pyridyl)phosphine derivative that was connected to a bis Zn-porphyrin.[64] Pyridyl coordination to the zinc atoms provided a bidentate ligand that was complexed with rhodium for hydroformylation applications (Fig. 1.18). In the presence of the chiral phosphite ligand and the bis-porphyrin template, hydroformylation of 1-octene took place with a decreased catalyst activity but a higher selectivity for the linear product (94%). When zinc tetraphenylporphyrin was used instead of the bis-porphyrin derivative, a 83% linear selectivity was observed. Higher enantioselectivites were also obtained in the branched selective hydroformylation of styrene (33% *ee* vs. 7% for the rhodium complex prepared from monodentate phosphite). The surprising selectivity and activity arise from the use of a template that preorganizes the system in terms of optimized bite angle and increased steric bulk.

---

[62] a) Wilkinson, M. J.; van Leeuwen, P. W. N. M.; Reek, J. N. H. *Org. Biomol. Chem.* **2005**, *3*, 2371. b) Sandee, A. J.; Reek, J. N. H. *Dalton Trans.* **2006**, 3385.

[63] Van Leeuwen, P. W. N. M.; Kamer, P. C. J.; Reek, J. N. H.; Dierkes, P. *Chem. Rev.* **2000**, *100*, 2741.

[64] Slagt, V. F.; van Leeuwen, P. W. N. M.; Reek, J. N. H. *Chem. Commun.* **2003**, 2474.

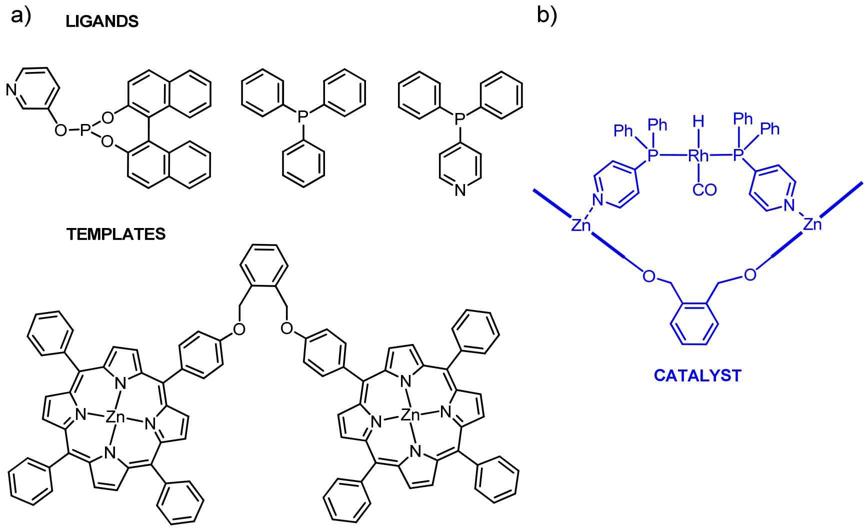

Fig. 1.18: a) Studied ligands and templates assemblies. b) Metal coordination within the template of the assembled bidentate ligand.

In a similar way, Takacs and co-workers reported a bisoxazoline (box) ligand substituted with one phosphite linked to a tether that could form heterodimers in a selective fashion upon coordination with Zn(II) (Fig. 1.19).[65] A library of 13 phosphite box derivatives giving rise to 50 potential bidentate ligands upon zinc coordination was screened for the Pd(II) catalyzed amination of allylic esters. At equal conversions, enantiomeric excesses varied from 20 to about 98% (48% *ee* in a control experiment). This proves that good selectivities can be reached for a specific reaction following this "combinatorial catalysis" approach. More recently, the same library of ligands was used for the rhodium (I) catalyzed asymmetric hydroboration of *ortho* substituted styrenes.[66] This confirmed the high substrate dependence of the catalyst efficiency.

---

[65] Takacs, J. M.; Reddy, D. S.; Moteki, S. A.; Wu, D.; Palencia, H. *J. Am. Chem. Soc.* **2004**, *126*, 4494.

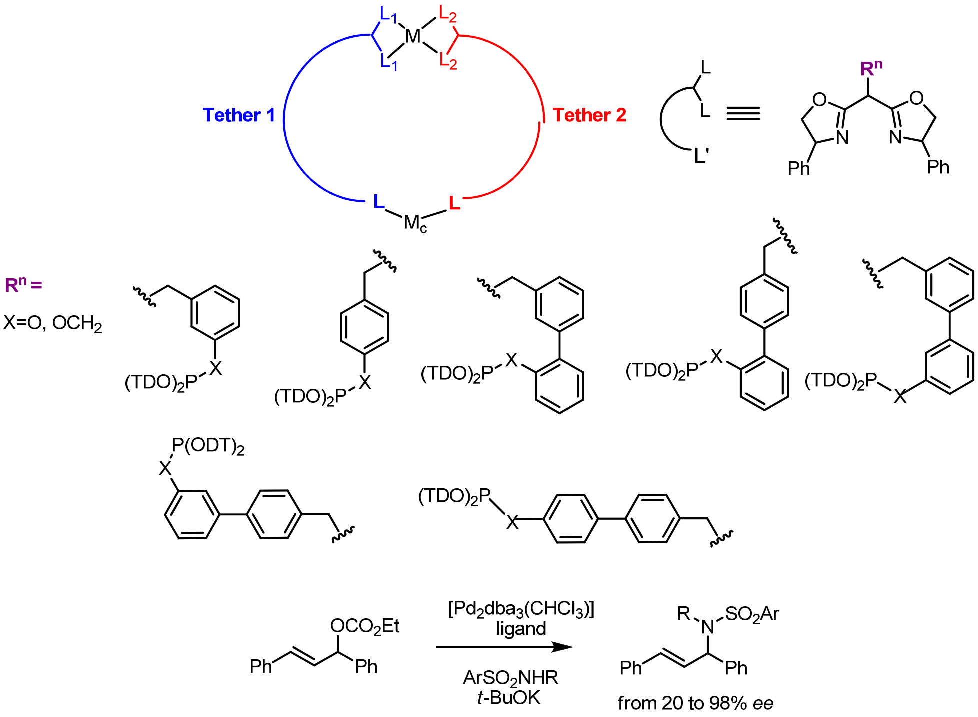
Tether 1
Tether 2
L1
L2
M
Mc
L
L'
Rn
O
N
Ph
Rn =
X=O, OCH2
(TDO)2P
X
P(ODT)2
OCO2Et
[Pd2dba3(CHCl3)]
ligand
ArSO2NHR
t-BuOK
R
N
SO2Ar
from 20 to 98% ee

Fig. 1.19: Phosphite functionalized bisoxazolines for catalysts library and their performance in asymmetric allylic amination.

Another approach inspired by the base pairing observed in DNA was brought by Breit *et al* (Fig. 1.20). Adenine (A) and thymine (T) are indeed bound through hydrogen bonds in the DNA core. Monodentate phosphines bearing heterocyclic units for intermolecular H-bonding were thus prepared and investigated in hydroformylation reactions.[67] This combinatorial approach also enables to screen a wide family of catalysts thanks to the easy formation of the bidentate ligand.

---

[66] Moteki, S. A.; Takacs, J. M. *Angew. Chem. Int. Ed.* **2008**, *47*, 894.

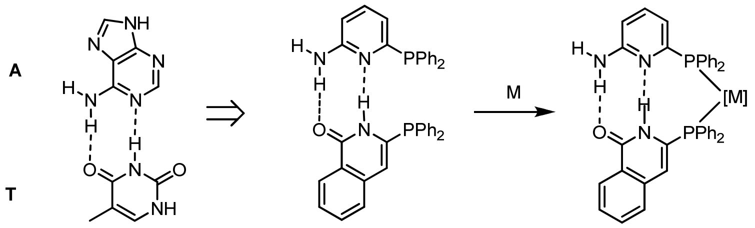

Fig. 1.20: Concept of the H-bonding driven bidentate ligand formation inspired by DNA base-pairing.

A wide family of substituted phosphines were prepared and screened in the hydroformylation reaction. Upon assembly, thiazole and azaindole based phosphines induced a 99% selectivity for the linear product in the hydroformylation of 1-octene (Fig. 1.21). If the azaindole is replaced by an isoquinolone, the dimer survives in methanol and catalyzes the reaction with similar selectivities. The selectivity of the reaction thus depends on the strength of the hydrogen bonds: the stronger the interactions, the higher the selectivity. Assemblies of this kind were also used for the rhodium catalyzed asymmetric hydrogenation of olefins under hydrogen atmosphere

---

[67] a) Seiche, W.; Breit, B. *J. Am. Chem. Soc.* **2003**, *125*, 6608. b) Seiche, W.; Breit, B. *Angew. Chem. Int. Ed.* **2005**, *44*, 1640. c) Waloch, C.; Wieland, J.; Keller, M.; Breit, B. *Angew. Chem. Int. Ed.* **2007**, *46*, 3037.

(phosphine and chiral phosphite linked to complementary heterocycles).[68] Finally, these assemblies were also found to play an important role in the hydration of alkynes and nitriles catalyzed by ruthenium complexes.[69]

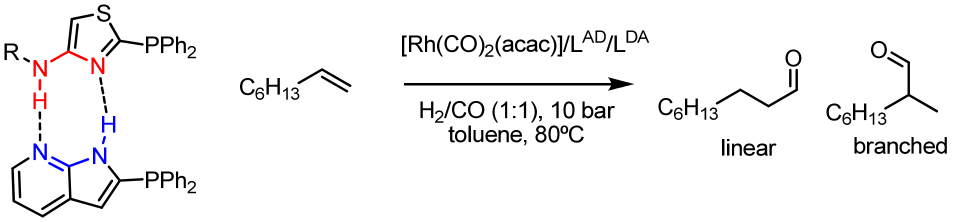
R
N
H
S
N
PPh2
H
N
N
PPh2
C6H13
[Rh(CO)2(acac)]/LAD/LDA
H2/CO (1:1), 10 bar
toluene, 80ºC
C6H13
O
linear
O
C6H13
branched

Fig. 1.21: Hydroformylation of 1-octene in the presence of an H-bonded ligand.

H-Bonding driven self-assembly has also been used by Ding and co-workers to make polymeric heterogeneous inorganic catalysts. Polymerization was ensured by stable ureidopyrimidinone quadruple H-bonding arrays. Homogeneous inorganic catalyst then turned heterogeneous thanks to this H-bonding driven polymerization (easier catalyst recovery) (Fig. 1.22). Asymmetric hydrogenation of dehydro α-aminoacid and enamides occurred with *ee*s lying between 91 and 96% (>99% conversion) in presence of the catalyst.[70] This strategy also proved successful for aromatic ketone hydrogenation when a rigid spacer replaced the hydrogen bonds.[71]

---

[68] a) Weis, M.; Waloch, C.; Seiche, W.; Breit, B. *J. Am. Chem. Soc.* **2006**, *128*, 4188. b) Birkholz, M.-N.; Dubrovina, N. V.; Jiao, H.; Michalik, D.; Holz, J.; Paciello, R.; Breit, B.; Börner, A. *Chem. Eur. J.* **2007**, *13*, 5896.

[69] a) Chevallier, F.; Breit, B. *Angew. Chem. Int. Ed.* **2006**, *45*, 1599. b) Šmejkal, T.; Breit, B. *Organometallics* **2007**, *26* (9), 2461.

[70] Shi, L.; Wang, X.; Sandoval, C. A.; Li, M.; Qi, Q.; Li, Z.; Ding, K. *Angew. Chem. Int.*

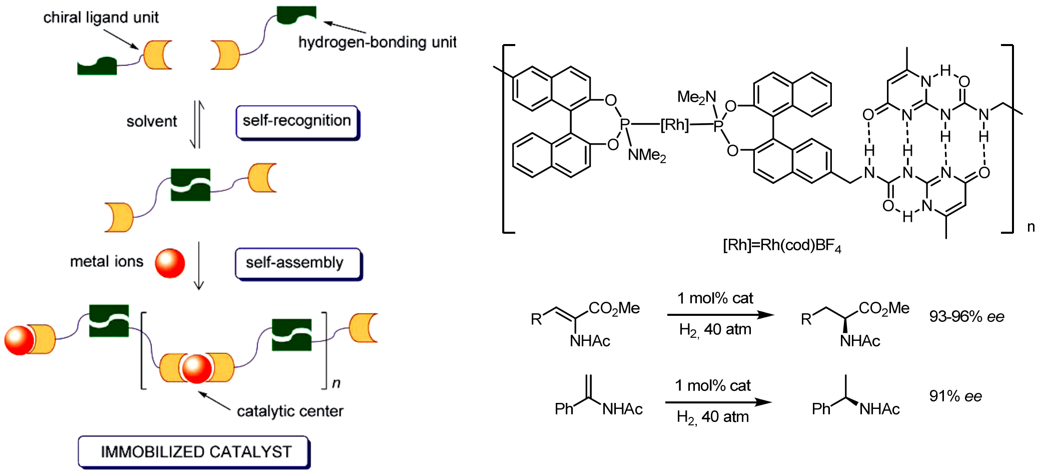
chiral ligand unit
hydrogen-bonding unit
solvent
self-recognition
metal ions
self-assembly
n
catalytic center
IMMOBILIZED CATALYST
Me2N
[Rh]
NMe2
n
[Rh]=Rh(cod)BF4
1 mol% cat
H2, 40 atm
93-96% ee
91% ee

Fig. 1.22: Self-assembly driven catalyst immobilization.

These examples show that supramolecular catalytic systems constitute a promising and solid approach to enzyme mimics and sustainable chemical processes, which nowadays represents a key issue, given the constantly increasing mankind's demand for chemicals and the need for sustainibility.

Ed. **2006**, *45,* 4108.

[71] a) Wang, X.; Ding, K. *J. Am. Chem. Soc.* **2004**, *126*, 10524. b) Liang, Y.; Li, X.; Shi, L.; Ding, K. *J. Am. Chem. Soc.* **2005**, *127*, 7694.

1.4 Objectives.

Guanidinium groups are known to stabilize negatively charged transition states in Michael addition to unsaturated lactones.[72] The guanidinium group is indeed well known for its ability to form highly stable hydrogen bonds with oxoanions, thanks to ion pairing and favoured crossed dipolar interactions.[73] This project mainly aims at developping a conceptually new approach to asymmetric homogeneous catalysis based on the principles of self-assembly for catalyst formation and anion recognition for transition state stabilization. A general design is shown on Fig. 1.23:

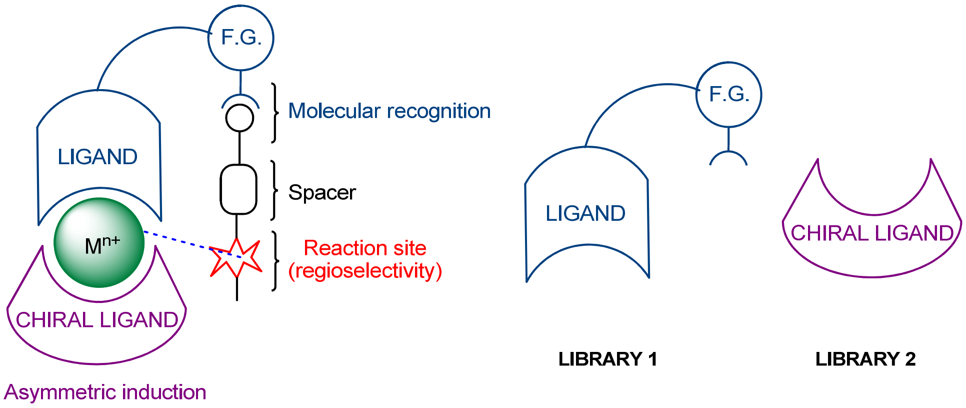
F.G.
Molecular recognition
LIGAND
Spacer
M^n+
Reaction site
(regioselectivity)
CHIRAL LIGAND
Asymmetric induction
F.G.
LIGAND
CHIRAL LIGAND
LIBRARY 1
LIBRARY 2

Fig. 1.23: A new approach to asymmetric homogeneous catalysis using self-assembly and anion recognition.

---

[72] a) Alcazar, V.; Morán, J. R.; de Mendoza, J. *Tetrahedron Lett.* **1995**, *36*, 3941. b) Martin-Portugués, M.; Alcazar, V.; Prados, P.; de Mendoza, J. *Tetrahedron* **2002**, *58*, 2951.

[73] a) Best, M. D.; Tobey, S. L.; Anslyn, E. V. *Coord. Chem. Rev.* **2003**, *240*, 3 and references therein. b) Schug, K. A.; Lindner, W. *Chem. Rev.* **2005**, *105*, 67.

The design involves an H-bonding moiety (urea, thiourea or guanidinium) connected to a transition metal through a heterocyclic spacer for the stabilization of a negatively charged transition state (organocatalysis)[74] and/or substrate fixation *via* molecular recognition (H-bonding). Catalyst's chirality is expected to arise from a "standard" chiral exogenous ligand. Coordination of the H-bonding and chiral ligand to a suitable transition metal is expected to give rise to the heteroleptic complex. The choice of the appropriate metal is therefore critical, since it dictates catalyst's geometry and stability. This new approach also offers the possibility to work in a combinatorial fashion from a ligand library (tuning of the catalyst). Nevertheless, three different situations are to be considered:

Situation 1: The metal is catalytically inactive and the H-bonding moiety might be used as organocatalyst, whereas metal is present as a structural element responsible for asymmetric induction thanks to the chiral ligand.

Situation 2: The metal is catalytically active and the H-bonding moiety might be used as a substrate fixation agent, placing the substrate at a given distance from the active site, which might result in regioselectivity induction.

---

[74] For a review on organocatalysis see: a) Dalko, P. I.; Moisan, L. *Angew. Chem. Int. Ed.* **2004**, *43*, 5138. Thiourea mediated organocatalysis: b) Okino, T., Hoashi Y., Furukawa, T., Xu, X., Takemoto, Y. *J. Am. Chem. Soc.* **2005**, *127*, 119. c) Hoashi, Y., Yabuta, T., Takemoto, Y. *Tetrahedron Lett.* **2004**, *45*, 9185. d) Takemoto, Y. *Org. Biomol. Chem.* **2005**, 4299.

Situation 3: The metal is catalytically active and the H-bonding moiety might activate the substrate in a cooperative fashion along with the transition metal.

Aiming at establishing some guidelines for the construction and study of such systems, a stepwise approach to the project has been adopted:

a) Influence of the acidity of guanidinium cation on the binding strength with oxoanions and its catalytic activity.

Chapter 2 of this Thesis reports on the synthesis and the oxoanion binding study of guanidinium derivatives of different acidic strength. Isothermal Titration Calorimetry (ITC) and ^{1}H NMR techniques were used for these binding studies. Finally, the potential of these compounds as organocatalysts for the 1,4-addition of pyrrolidine to 2-(5*H*)-furanone was studied (Fig. 1.24). These studies aim at giving tips about which guanidinium scaffold is most suitable for the situations 1 and 2 described above (optimization of substrate binding and organocatalyst character).

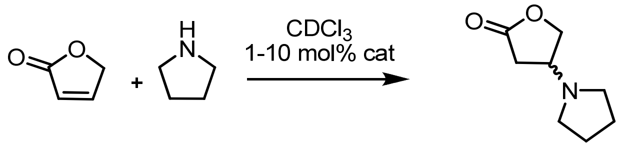

Fig. 1.24: Studied 1,4-addition of pyrrolidine to 2-(5*H*)-furanone.

b) Cooperativity study of metal-substrate and H-bonding interactions in model catalytic systems.

Cooperative working fashion of metal-substrate and H-bonding interactions in a model system, where both activating moieties are connected covalently in order to force cooperativity (situation 3), will be studied in Chapter 3.

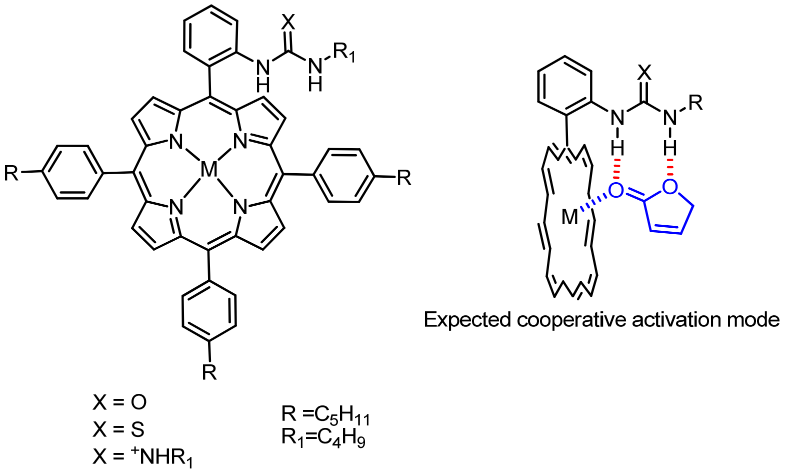

Fig. 1.25: Metalloporphyrins as catalysts for hetero-Michael additions.

Cooperativity between a metal catalyst and an organocatalyst is then studied for the 1,4-addition of pyrrolidine to 2-(5*H*)-furanone (Fig.1.24). In summary, three porphyrin derivatives functionalized with various H-bonding moieties were prepared (urea, thiourea, guanidinium, see Fig. 1.25). Metal screening experiments as well as a complete cooperativity study are reported.

c) *Functionalized ligands for substrate binding in catalysis.*

Chapter 4 reports on the preparation of a small library of heterocycles functionalized with a urea, a thiourea or a guanidinium, as well as on the synthesis of chiral ligands. Monodentate (pyridine, isoquinoline…) and bidentate (dipyrromethene, bipyridine) heterocyclic cores were investigated. Formation of the desired heteroleptic complex has also been studied with Cu(I), Zn(II) and Ru(II), taking into account both the geometries of the metals and their affinities for nitrogen-containing ligands. C-H activation reactions of fatty acids were then targeted. On the one hand, efforts towards Cu(I) catalyzed cyclopropanation and aziridination of unsaturated acids are reported. Finally, the Ru(IV) catalyzed regioselective asymmetric epoxidation of unsaturated fatty acids was targeted. Catalysis and control experiments performed to achieve this goal are herein described.

CHAPTER 2

INFLUENCE OF THE ACIDITY OF GUANIDINIUM CATIONS ON BINDING AND CATALYSIS

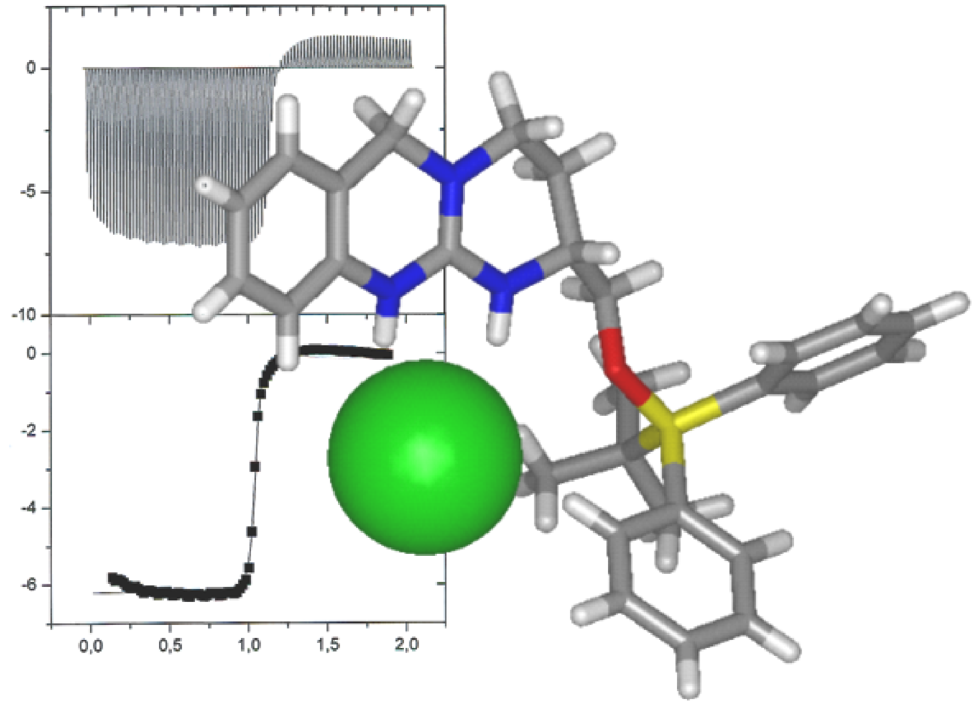
0
-5
-10
0
-2
-4
-6
0,0
0,5
1,0
1,5
2,0

2. Influence of the acidity of guanidinium cations on binding and catalysis.

2.1 Introduction.

2.1.1 The guanidinium group.

Nature frequently uses the guanidinium group to bind oxoanions in enzymatic active sites and protein recognition domains. Present in the side chain of the amino acid arginine, the guanidinium group forms strong ion pairs with oxoanions such as carboxylates and phosphates of enzymes and antibodies, and also takes part in the stabilization of tertiary protein structures *via* internal salt bridging. Most artificial receptors for oxoanions such as carboxylates and phosphates are therefore based on guanidines.[1] The geometrical Y-shape of the three heteroatoms enables the formation of parallel, highly directional hydrogen bonds and its high basicity makes it protonated over a broad pH range (pK_a = 12-13). The positive charge is delocalized between the three nitrogen atoms, which gives this cation its remarkable stability.

From the point of view of energy, oxoanion binding is driven by the high directionality of hydrogen bonds, the ion pairing electrostatic interaction and the presence of favorable dipolar crossed interactions (Fig. 2.1a). The guanidinium/carboxylate ion pair is expected to be more stable than the guanidine/carboxylic acid pair, since guanidinium cation and acetate are nine pK_a units apart in water. Thus, transprotonation is unlikely, also because it would lead to loss of the ion pairing electrostatic interaction and of the attractive crossed dipolar interactions.[2] The objective of this chapter is to explore the frontiers of guanidine's basicity and study the consequences on oxoanion binding affinity and catalysis.

---

[1] a) Best, M. D.; Tobey, S. L.; Anslyn, E. V. *Coord. Chem. Rev.* **2003**, *240*, 3. b) For a recent review on the topic, see: Blondeau, P.; Segura, M.; Pérez-Fernandez, R.; de Mendoza, J. *Chem. Soc. Rev.* **2007**, *36*, 198.

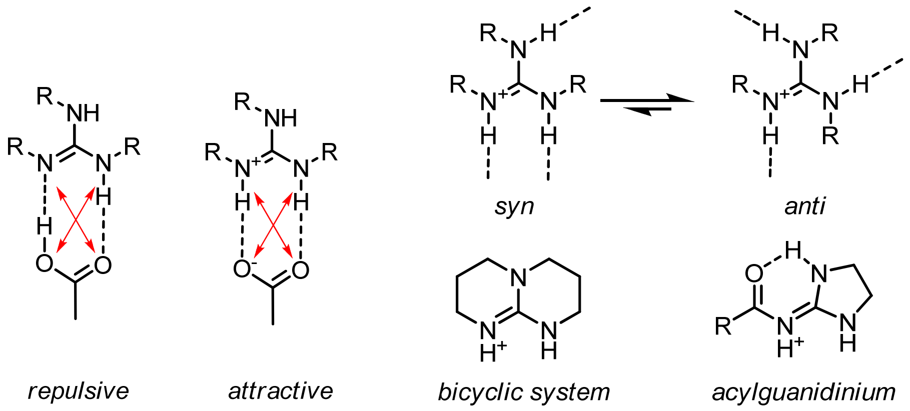

a) Crossed dipolar interactions.

b) Conformational interconversion and ways to prevent it.

Fig.2.1: Basics of the guanidinium-carboxylate recognition

In the case of *N*-alkylguanidines, fast interconversion between the *syn* and the more stable but unproductive (in terms of H-bonded ion-pairing)

---

[2] Jorgensen, W. L.; Pranata, J. *J. Am. Chem. Soc.* **1990**, *112*, 2008.

anti conformers causes anion binding to be weaker (Fig. 2.1b). This issue can be efficiently overcome by introduction of the guanidinium cation in a bicyclic decaline system[3] or by the use of intramolecular H-bonding (acylguanidinium cations) in monocyclic systems. Over the last two decades, our group investigated the molecular recognition of relevant anions (chiral recognition and transport of biologically relevant anions, construction of supramolecular architectures) by functionalized bicyclic chiral guanidinium salts.[4]

---

[3] a) Echavarren, A. M.; Galán, A.; de Mendoza, J.; Salmerón, A.; Lehn, J.-M. *Helv. Chim. Acta* **1988**, *71*, 685. b) Kurzmeier, H.; Schmidtchen, F. P. *J. Org. Chem.* **1990**, *55*, 3749.

[4] Amino acid recognition: a) Echavarren, A.; Galán, A.; Lehn, J.-M.; de Mendoza, J. *J. Am. Chem. Soc.* **1989**, *111*, 4994. b) Galán, A.; Andreu, D.; Echavarren, A. M.; Prados, P.; de Mendoza, J. *J. Am. Chem. Soc.* **1992**, *114*, 1511. c) Breccia, P.; Van Gool, M.; Pérez-Fernández, R.; Martín-Santamaría, S.; Gago, F.; Prados, P.; de Mendoza, J. *J. Am. Chem. Soc.* **2003**, *125*, 8270. Molecular recognition of oligonucleotides: d) Galán, A.; Pueyo, E.; Salmerón, A.; de Mendoza, J. *Tetrahedron. Lett.* **1991**, *32*, 1827. e) Galán, A.; de Mendoza, J.; Toiron, C.; Bruix, M.; Deslongchamps, G.; Rebek, J. Jr. *J. Am. Chem. Soc.* **1991**, *113*, 9424. f) Andreu, C.; Galán, A.; Kobiro, K.; de Mendoza, J.; Park, T. K.; Rebek J. Jr.; Salmerón, A.; Usman, N. *J. Am. Chem. Soc.* **1994**, *116*, 5501. Protein surface recognition by a tetraguanidinium oligomer: g) Peczuh, M. W.; Hamilton, A. D.; Sánchez-Quesada, J.; de Mendoza, J.; Haack, T.; Giralt, E. *J. Am. Chem. Soc.* **1997**, *119*, 9327. h) Haack, T.; Peczuh, M.; Salvatella, X.; Sánchez-Quesada, J.; de Mendoza, J.; Hamilton, A. D.; Giralt, E. *J. Am. Chem. Soc.* **1999**, *121*, 11813. Tetraguanidinium as a cell internalization vector: i) Fernández-Carneado, J.; Van Gool, M.; Martos, V.; Castel, S.; Prados, P.; de Mendoza, J.; Giralt, E. *J. Am. Chem. Soc.* **2005**, *127*, 869. Guanidinium based macrocycles for selective anion recognition: j) Alcázar, V.; Segura, M.; Prados, P.; de Mendoza, J. *Tetrahedron. Lett.* **1998**, *39*, 1033.

2.1.2 Anion binding versus transprotonation.

Ammonium ions, amides, ureas, thioureas and guanidinium cations have been commonly used for anion recognition. Upon their introduction into a given scaffold, they can give rise to a wide range of affinities for specific anions through hydrogen bonding. This is mainly attributed to geometrical factors, but also to electronic ones. Nevertheless, most of these receptors proved efficient only in non competitive, aprotic solvents. To increase anion affinity in more polar or protic solvents, further polarization of the H-bond donor must be introduced using either positively charged groups or vicinal electron withdrawing ones, although overpolarization may ultimately lead to proton transfer, especially in the presence of highly basic anion partners.[5] H-bonding between an A-H donor and a B acceptor has therefore to be regarded as a frozen proton transfer from A to B. Consequently, high association constants are obtained when charge transfer between A and B is favored, but not to a too high extent.[6] This concept was illustrated by Licchelli and co-workers who reported a urea derivative substituted with electron withdrawing groups (**I**) (Fig. 2.2), which was shown to coordinate acetate with a high binding constant (4.1×10^6 M^{-1} in acetonitrile, UV-Vis titration).[7]

---

[5] Amendola, V.; Esteban-Gómez, D.; Fabbrizzi, L.; Licchelli, M. *Acc. Chem. Res.* **2006**, *39*, 343.

[6] Steiner, T. *Angew. Chem. Int. Ed.* **2002**, *41*, 48.

[7] Boiocchi, M.; Del Boca, L.; Gomez, D. E.; Fabbrizzi, L.; Licchelli, M.; Monzani, E. *J. Am. Chem. Soc.* **2004**, *126*, 16507.

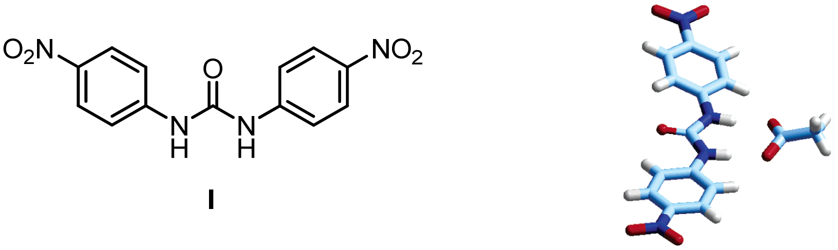

I

Fig. 2.2: Structure of urea **I** and the X-Ray structure of **I** (AcO^-).

This strong binding constant was attributed to the high acidity of the urea NHs. Various oxoanions were studied under identical conditions and a good correlation between K_s and the computed partial charge on the oxoanion was found (related to anion's basicity). However, upon addition of the highly basic fluoride anion, **I** shows a different behavior in acetonitrile (Fig. 2.3): After addition of one equivalent of tetrabutylammonium fluoride (TBAF), the anion was fully complexed by the urea (orange solution), but addition of a second equivalent caused the highly stable HF_2^- anion (self-complex) to form by deprotonation of the urea (dark red solution), and binding was cancelled. The differences in the measured binding constant explain the sequential behavior of the system ($K_2 < K_1$).[8]

---

[8] For receptors with $K_2 > K_1$, direct receptor deprotonation should be expected.

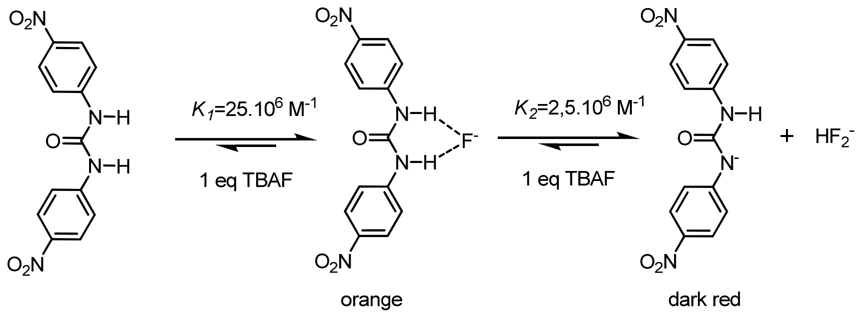
O2N
N-H
O=
N-H
O2N
K1=25.10^6 M^-1
1 eq TBAF
N-H
F-
N-H
orange
K2=2,5.10^6 M^-1
1 eq TBAF
N-H
N-
+ HF2-
dark red

Fig. 2.3: Equilibria accounting for deprotonation of **I** by fluoride (MeCN).

The acidity of the receptor was then increased by replacing a 4-nitrophenyl substitutent for a 5-nitrobenzofurazan one: a crystal structure of the deprotonated receptor **II**, stabilized by its mesomeric forms, was obtained (Fig. 2.4).

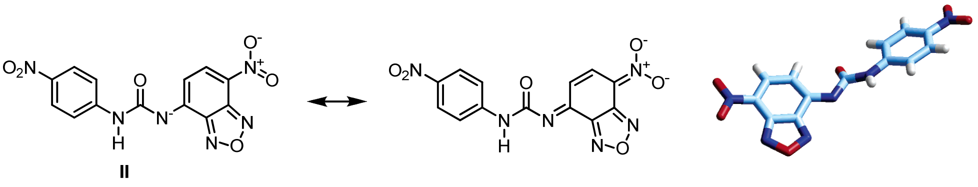
O2N
O
N
H
N-
O-
N+
O
N
N-O
II
O2N
O
N
H
N
O-
N+
O-
N
N-O

a) b)

Fig. 2.4: a) Resonance forms of the deprotonated receptor **II**. b) X-ray crystal structure of deprotonated **II**, in the presence of an excess F$^-$.

The most acidic proton was taken by fluoride.[9] Interestingly, upon addition of acetate and dihydrogen phosphate salts to a solution of **II**, deprotonation and formation of the $[HX_2]^-$ species was observed, highlighting the importance of the acidity on anion binding (Fig. 2.5).

---

[9] Boiocchi, M.; Del Boca, L.; Esteban-Gómez, D.; Fabbrizzi, L.; Licchelli, M.; Monzani, E. *Chem. Eur. J.* **2005**, *11*, 3097.

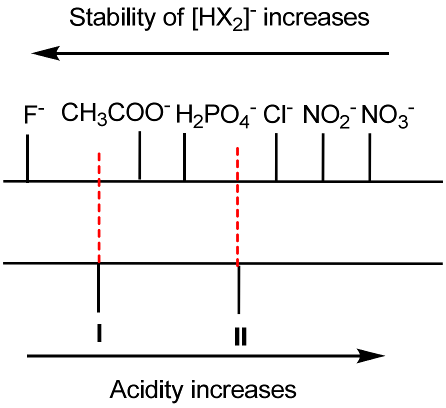

Fig. 2.5: Juxtaposition of acidity scales of **I** and **II** and stability scale of HX_2^- (deprotonation takes place above the dashed line).

Other systems presenting a similar behavior have been reported and explored as specific anion sensors.[10]

---

[10] a) Camiolo, S.; Gale, P. A.; Hursthouse, M. B.; Light, M. E. *Org. Biomol. Chem.* **2003**, *1*, 741. b) Gunnlaugsson, T.; Kruger, P. E.; Jensen, P.; Pfeffer, F. M.; Hussey, G. M. *Tetrahedron Lett.* **2003**, *44*, 8909. c) Esteban-Gómez, D.; Fabbrizzi, L.; Licchelli, M. *J. Org. Chem.* **2005**, *70*, 5717. d) Gunnlaugsson, T.; Kruger, P. E.; Jensen, P.; Tierney, J.; Paduka Ali, H. D.; Hussey, G. M. *J. Org. Chem.* **2005**, *70*, 10875. e) Pfeffer, F. M.; Gunnlaugsson, T.; Jensen, P.; Kruger, P. E. *Org. Lett.* **2005**, *7*, 5357. f) Evans, L. S.; Gale, P. E.; Light, M. E.; Quesada, R. *Chem. Commun.* **2006**, 965. g) Kim, Y.-J.; Kwak, H.; Lee, S. J.; Lee, J. S.; Kwon, H. J.; Nam, S. H.; Lee, K.; Kim, C. *Tetrahedron* **2006**, *62*, 9635. h) Gunnlaugsson, T.; Glynn, M.; Tocci, G. M.; Kruger, P. E.; Pfeffer, F. M. *Coord. Chem. Rev.* **2006**, *250*, 3094. i) Lin, C.; Simov, V.; Drueckhammer, D. G. *J. Org. Chem.* **2007**, *72*, 1742.

2.1.3 Guanidinium cations as organocatalysts.

Guanidinium cations have also been studied as potential organocatalysts. Their binding ability suggests that negatively charged oxygenated transition states may be strongly stabilized by guanidinium derivatives. Indeed, de Mendoza and co-workers first reported that guanidinium significantly accelerates the 1,4-addition of pyrrolidine to 2-(5*H*)-furanone.[11] A chiral bicyclic guanidine was subsequently endowed with bulky groups in order to induce asymmetry but the stereogenic centers were located too far away from the binding pocket to allow any chiral induction to take place (Fig. 2.6).

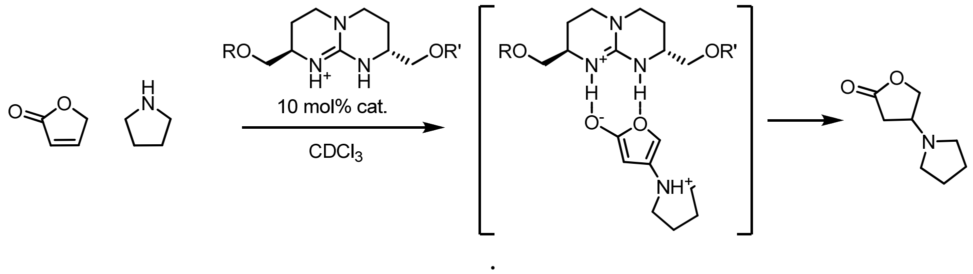

Fig. 2.6: Guanidinium-catalyzed conjugate addition.

Other catalytic application of the bicyclic chiral guanidine implies its use as an organobase, its high pK_a enabling the possible deprotonation of organic substrates. In this field, Casas and de Mendoza studied a guanidine-catalyzed procedure for the preparation of amino acids with a quaternary carbon.[12] Guanidine was used as a base for the deprotonation of an azlactone that was then trapped with an electrophile (ethyl acrylate) to give, after hydrolysis, the quaternized amino acid, obtained in reasonable yields and good enantioselectivities (Fig. 2.7). Other guanidines have also been reported as organocatalysts for nitroaldol[13] and transfer reactions (phosphoryl, acyl).[14]

---

[11] a) Alcázar, V.; Morán, J. R.; de Mendoza, J. *Tetrahedron. Lett.* **1995**, *36*, 3941. b) Martín-Portugués, M.; Alcázar, V.; Prados, P.; de Mendoza, J. *Tetrahedron* **2002**, *58*, 2951.

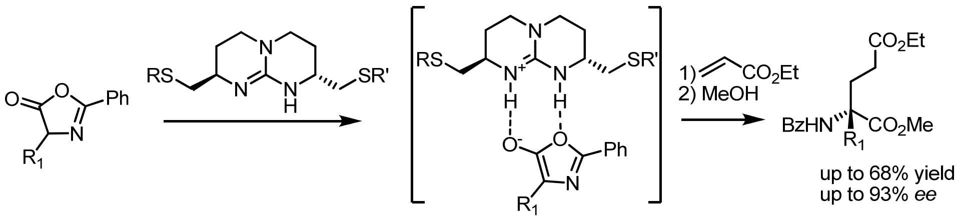

Fig. 2.7: Guanidine as an organobase: chiral amino acids with a quaternary carbon.

---

[12] Casas, J.; Nonell-Canals, A.; Maseras, F.; de Mendoza, J. to be submitted.

[13] a) Chinchilla, R.; Nájera, C.; Sánchez-Agallo, P. *Tetrahedron:* Asymmetry **1994**, *5*, 1393. b) Bernardi, L.; Bonini, B. F.; Capitò, E.; Dessole, G.; Comes-Franchini, M.; Fochi, M.; Ricci, A. *J. Org. Chem.* **2004**, *69*, 8168. c) Sohtome, Y.; Hashimoto, Y.; Nagasawa, K. *Adv. Synth. Catal.* **2005**, *347*, 1643. d) Sohtome, Y.; Nagasawa, K. ; Hashimoto, Y. *Eur. J. Org. Chem.* **2006**, 2894. e) Sohtome, Y.; Takemura, N.; Takada, K.; Takagi, R.; Iguchi, T.; Nagasawa, K. *Chem. Asian J.* **2007**, *2*, 1150.

[14] a) Piątek, A. M.; Gray, M.; Anslyn, E. V. *J. Am. Chem. Soc.* **2004**, *126*, 9878. b) Pratt, R. C.; Lohmeijer, B. G. G.; Long, D. A.; Waymouth, R. M.; Hedrick, J. L. *J. Am. Chem. Soc.* **2006**, *128*, 4556.

2.2 Synthesis of model guanidinium cations.

The acidity of our bicyclic guanidinium cations was modified by insertion of one or two adjacent aromatic rings. Coplanarity of the final structure allows electron delocalization through the aromatic rings and results in a pronounced increase in the acidic character (Fig. 2.8).

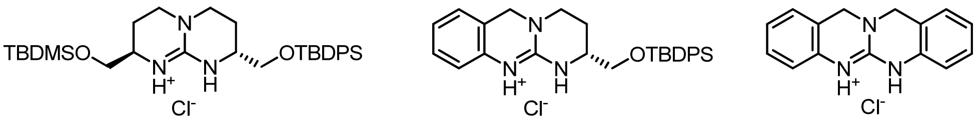

1 (Cl$^-$) **2 (Cl$^-$)** **3 (Cl$^-$)**

Fig. 2.8: Structures of the studied guanidinium cations.

2.2.1 Bicyclic chiral guanidinium cation 1.

The synthesis of bicyclic chiral guanidinium cations was described independently in the late 1980's by the groups of de Mendoza and Schmidtchen.[3a] This convergent eight-step synthesis involves enantiomerically pure amino acids as starting materials (all four possible diastereomers can be prepared). The key step of the large scale synthesis is a double cyclization process that converts thiourea **9** in a protected guanidine (Fig. 2.9). Recently, we scaled up the synthesis of the thiourea precursors **6** and **8** at the pilot plant scale (about 500 g each).[15] The remaining steps were then performed according to usual procedures (at a 80 g scale).

---

[15] Frédéric Ratel, *Tesis de Licenciatura* **2005**, Universidad Autónoma de Madrid.

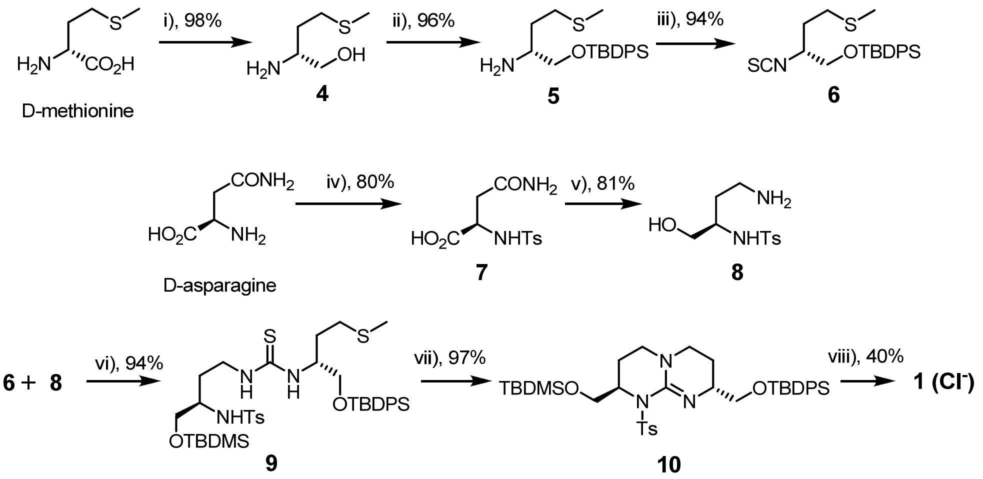
D-methionine
i), 98%
4
ii), 96%
5
iii), 94%
6
D-asparagine
iv), 80%
7
v), 81%
8
6 + 8
vi), 94%
9
vii), 97%
10
viii), 40%
1 (Cl⁻)

i) $BH_3.Me_2S$, THF; ii) TBDPSCl, imidazole, MeCN; iii) $CSCl_2$, Na_2CO_3, H_2O, CH_2Cl_2 iv) TsCl, NaOH, H_2O; v) $LiBH_4$, TMSCl, THF; vi) MeCN, then imidazole, TBDMSCl; vii) TfOMe, DIPEA, CH_2Cl_2; viii) Al/Hg, THF, H_2O

Fig. 2.9: Synthesis of the bicyclic chiral guanidinium salt **1**.

This procedure is well known in our laboratory since **1** is a common starting material for various applications in oxoanion recognition. The p*K*a value of **1** was then evaluated by a UV-Vis measurement in MeCN:H_2O (1:1)[16] as 12.8 ± 0.3 (Fig. 2.10).

---

[16] By measuring the absorbance at different p*H* values. Equations for acid-base equilibria in water were used as an approximation.

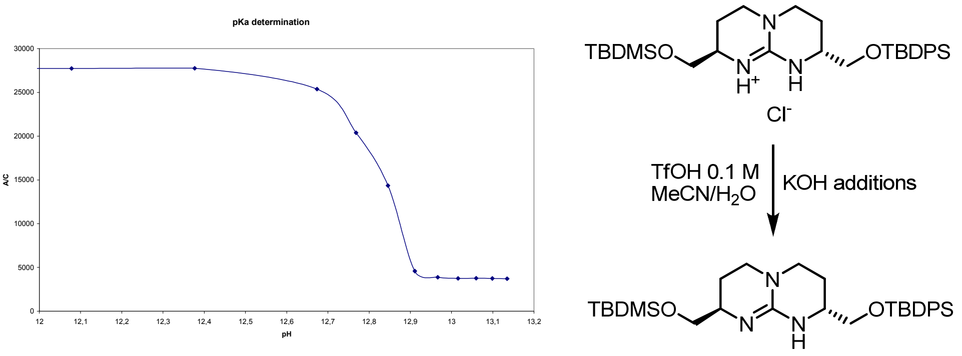

Fig. 2.10: UV-Vis monitored pK_a determination of **1** (at 204 nm).

2.2.2 Chiral benzoguanidinium cation 2.

Following a similar synthetic route, the double cyclization step applied to thiourea **11** might lead directly to **2** (Fig. 2.11). Regioselective formation of **11** was anticipated to occur without the need of amine protection (as a sulfonamide), because the benzylic amine is likely more nucleophilic than the aromatic one.

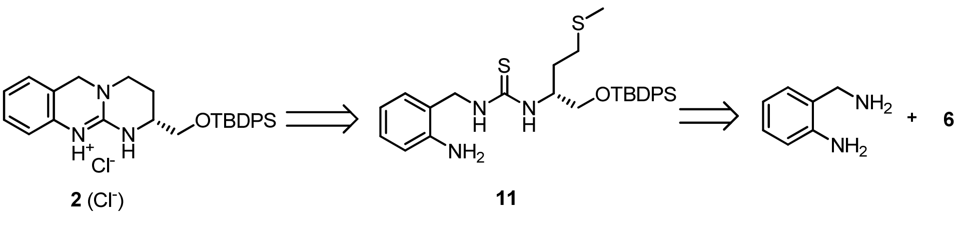

Fig. 2.11: Retrosynthetic approach for chiral benzoguanidinium cation **2.**

A screening of reaction conditions for the exclusive formation of **11** was performed and the concentration of reactants optimized.[15] **11** could thus be obtained in a 77% yield after column chromatography. Upon treatment with methyl trifluoromethane sulfonate in basic medium, **11** was converted into **2,** which was isolated by precipitation of its hydrochloride salt in diethyl ether (29% yield). The low yield could be attributed to the precipitation step, but no attempts to optimize the purification procedure were performed (Fig. 2.12).

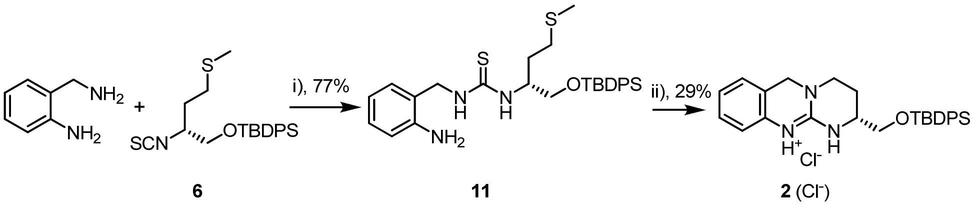

i) MeCN, RT; ii) TfOMe, DIPEA, CH_2Cl_2, 0ºC to reflux

Fig. 2.12: Synthesis of chiral benzoguanidinium cation **2** (Cl$^-$).

This new straightforward synthetic procedure enables to introduce chirality as well as rigidity into benzoguanidines, thus paving the way for new applications. As for **1**, the pK_a of **2** was measured by UV-Vis measurements, and a value of 12.3 ± 0.2 was estimated (Fig. 2.13). The pK_a difference between **1** and **2** is in accordance with the one observed for acetic acid (pK_a = 4.76) and benzoic acid (pK_a = 4.20). The more acidic character of benzoguanidinium cation **2** is due to delocalization of the positive charge through the aromatic ring, therefore rendering the positive charge distribution non symmetric (the two NHs should have different pK_a values). This was reflected in the NMR chemical shifts of both guanidinium protons: the proton adjacent to the aromatic ring resonates at 11.67 ppm whereas the more distal one appears at 9.35 ppm.

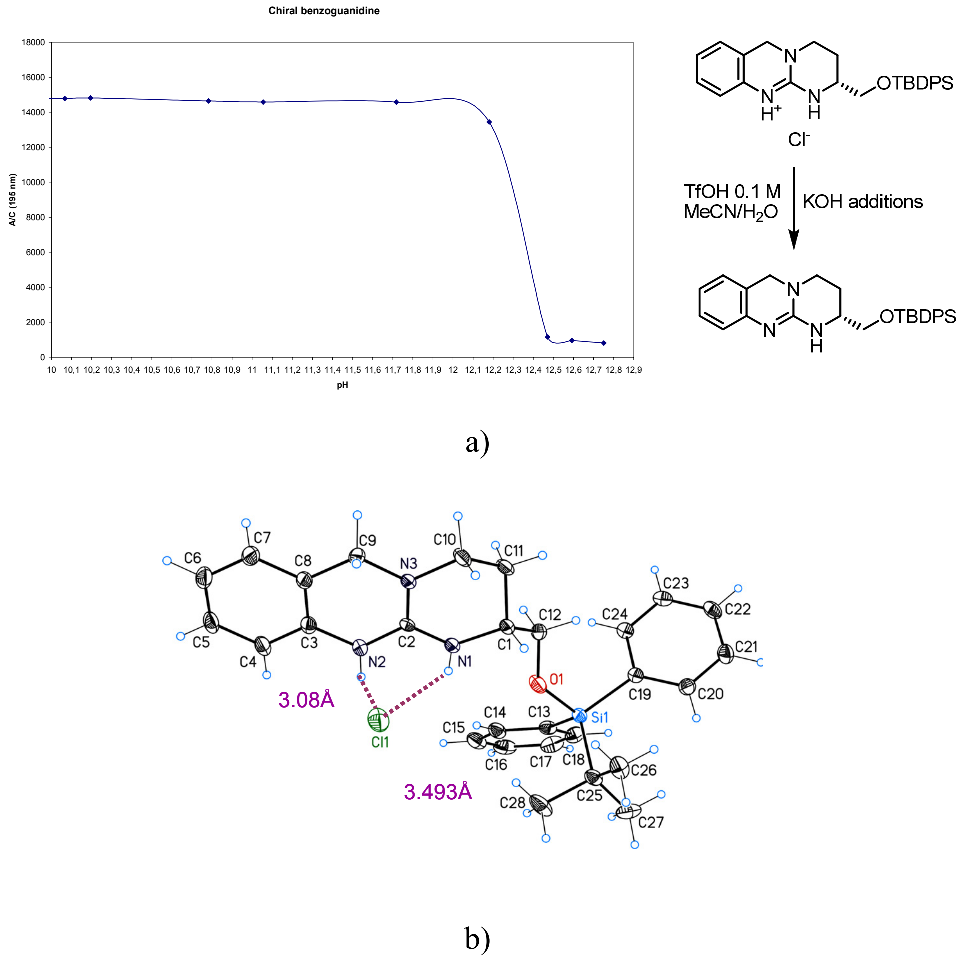

Fig. 2.13: a) UV-Vis monitored pK_A determination of **2** (196 nm). b) Ortep plot of the X-ray structure of **2** (Cl^-) ($MeCN/Et_2O$).

In agreement with the different acidities, the NH····Cl^- distances in the X-ray structure of **2** are significantly different (3.08 vs. 3.493 Å), the counterion being significantly closer to the more acidic proton of the guanidinium group.

2.2.3 Dibenzoguanidinium cation 3.

Preparation of **3** was achieved following a synthetic route previously reported by our group (Fig. 2.14).[17] Anthranilonitrile was hydrogenated in the presence of rhodium[18] to yield the secondary amine **12** (37% yield) which was converted to thiourea **13** upon treatment with thiocarbonyldiimidazole (65% yield). Intramolecular cyclization took place by activation of the thiourea with methyl iodide at room temperature for two weeks (yield not determined, *lit.* 97%).[17]

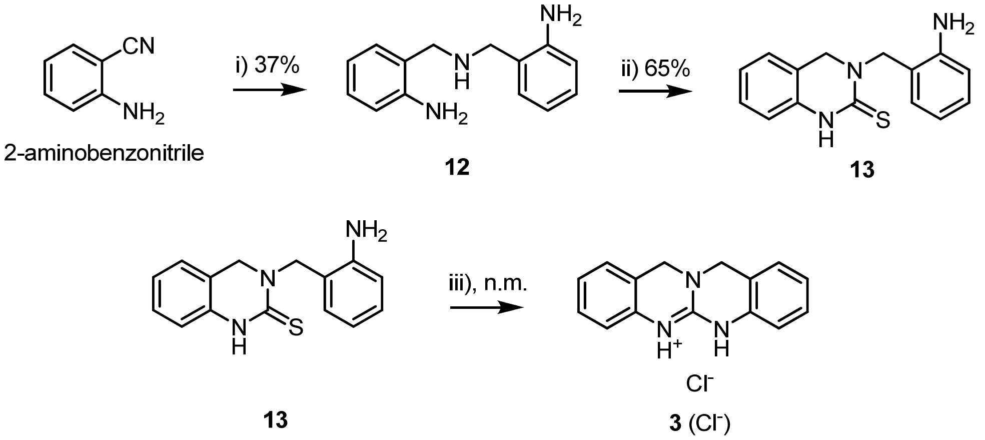

i) H_2, $Rh.Al_2O_3$, MeOH ii) Thiocarbonyldiimidazole, $CHCl_3$ iii) MeI, THF

Fig. 2.14: Synthesis of dibenzoguanidinium cation **3**.

---

[17] Chicharro, J. L.; Prados, P.; de Mendoza, J. *Chem. Commun.* **1994**, 1193.

[18] Galán, A.; de Mendoza, J.; Prados, P.; Rojo, J.; Echavarren, A. E. *J. Org. Chem.* **1991**, *56*, 452.

The increased acidity of the guanidinium cation was again reflected in the NMR chemical shift of the NH protons at 11.45 ppm ($CDCl_3$). As for **1** and **2**, a pK_a value lying between 11.7 and 12.2 was estimated by UV-Vis, which is consistent with the observed general trend. Finally, crystals of **3** could be grown in acetonitrile (Fig. 2.15), which confirmed the structure (poor resolution).

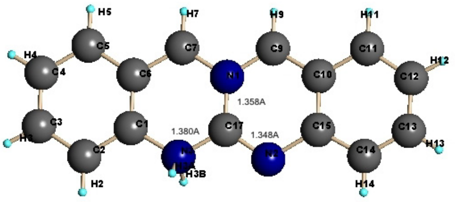

Fig. 2.15 X-ray structure of **3** (MeCN)

2.3 Binding studies.

2.3.1 ^{1}H NMR experiments.

The complexation of **1** (Cl^- and PF_6^-) with acetate has been reported[19] and exhibits a 1:1 stoichiometry. Job plots display a bell shaped curve, accounting for a 1:1 complex, as expected. However, ^{1}H NMR binding studies of **2** (Cl^- or PF_6^-) with acetate did not give rise to the expected bell-shaped curve (Job Plot). Below one equivalent of acetate added, signals of **2** do not shift significantly ($CDCl_3$). With one equivalent, NH signals are strongly shifted ($\Delta\delta = 0.8$ ppm) and further acetate addition does not alter the chemical shifts of the species in equilibrium. This suggests a 1:1 stoichiometry along with an "all-or-nothing" behavior for the complexation of **2** with acetate. Thus, the complex equilibria indicate that ^{1}H NMR is not a suitable and simple method for the study of the binding of **2** with acetate. For the same reason, experiments with **3** were not carried out. Similar NMR experiments were then performed with **2** (Cl^-) and benzoate (pK_a = 4.2), 4-nitrobenzoate (pK_a = 3.44), 3,5-dinitrobenzoate (pK_a = 2.8), as well as with **2** (PF_6^-) and chloride (pK_a = -5) in order to study the effects of anion basicity on binding. Bell shaped curves for the Job experiments were expected for poorly basic anions, for which transprotonation with **2** is unlikely (Fig. 2.16). However, similar results were obtained, suggesting that no transprotonation was taking place.

---

[19] Blondeau, P.; Benet-Buchholz, J.; de Mendoza, J. *New J. Chem.* **2007**, *31*, 736.

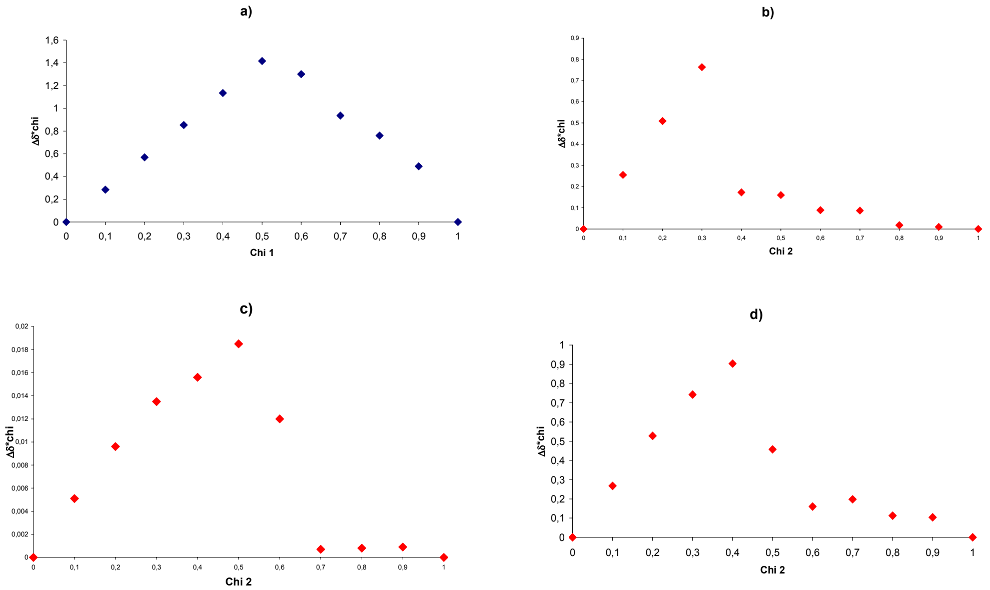

Fig. 2.16: Job plots determined by ^{1}H NMR ($CDCl_3$) for: a) **1** (PF_6^-) with Cl^-. b) **2** (PF_6^-) with Cl^-. c) **2** (Cl^-) with acetate. d) **2** (Cl^-) with *p*-nitrobenzoate.

2.3.2 Isothermal titration calorimetry (ITC).

This technique is based on a titration experiment where a solution of the guest is added dropwise to a solution of the host in an adiabatic cell. Measurement of the heat transfered during the addition (related to the electric energy received by the apparatus to bring the solution back to a constant temperature) enables the determination of the stoichiometry of the binding and its thermodynamic components (ΔG, ΔH and ΔS).

Binding with poorly basic anions was first studied (Table 2.1, Fig. 2.17).[20] Hexafluorophosphate salts of **1**, **2** and **3** were complexed with tetrabutylammonium chloride (TBACl), which enabled to exclude anion-induced transprotonation. The results clearly show that the binding affinity for chloride is higher for the most acidic guanidinium cations: **1** < **2** < **3**. As a result, difference in Gibb's binding free energy is about 1 kcal.mol^{-1} between **3** and **2**, as well as between **2** and **1** (binding constants roughly differ in one order of magnitude). The shapes of the titration curves also reflect this tendency. In both studied solvents, binding is mainly entropically driven, which is related to the release of solvent molecules and the voluminous anion (PF_6^-) from the binding pocket. In a more competitive solvent, such as DMSO, the enthalpic term decreases significantly and becomes slightly positive (endothermal process due to solvent competition).

---

[20] For ITC studies of guanidinium cations see: a) Wiseman, T.; Willinston, A. S.; Brandts, J. F.; Lin, L.-N. *Anal. Biochem.* **1989**, *179*, 131. b) Berger, M.; Schmidtchen, F. P. *Angew. Chem. Int. Ed.* **1998**, *37*, 2694. c) Linton, B.; Hamilton, A. D. *Tetrahedron* **1999**, *55*, 6027.

Table 2.1: Thermodynamics of the binding of **1-3** (PF_6^-) with TBACl.

		MeCN	DMSO
1 (PF_6^-)	$K_a\,(10^3)$	4.58	0.549
	ΔG	-5.07	-3.81
	ΔH	-1.164	0.068
	ΔS	12.9	12.8
2 (PF_6^-)	$K_a\,(10^3)$	21.6	0.686
	ΔG	-6	-3.94
	ΔH	-1.495	0.215
	ΔS	14.9	13.7
3 (PF_6^-)	$K_a\,(10^3)$	119	n.m.
	ΔG	-7.03	-
	ΔH	-1.368	-
	ΔS	18.7	-

K_a in $L.mol^{-1}$, ΔG and ΔH in $kcal.mol^{-1}$, ΔS in $cal.mol^{-1}.K^{-1}$, errors < 10%

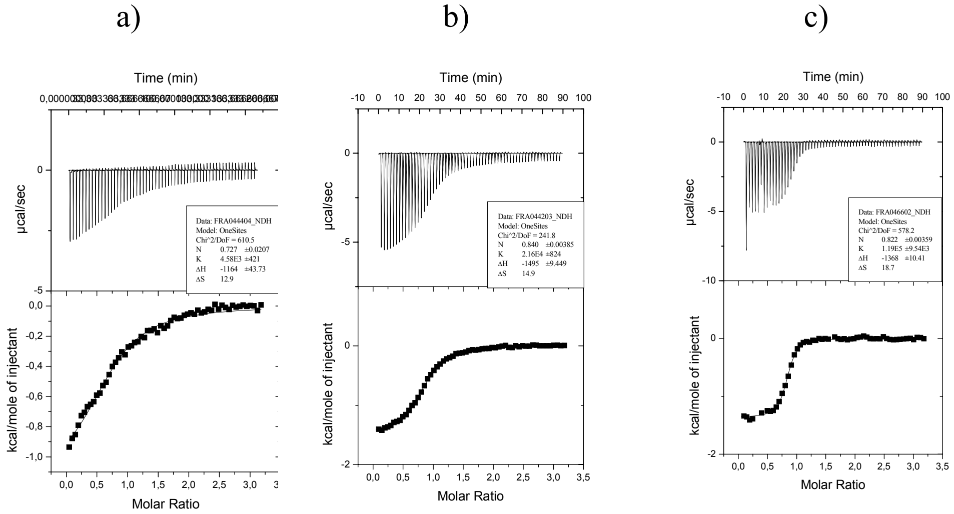

Fig. 2.17: ITC curves at 30 ºC in MeCN of: a) **1** (PF_6^-) with TBACl. b) **2** (PF_6^-) with TBACl. c) **3** (PF_6^-) with TBACl.

In less competitive solvents, the enthalpic component is expected to increase. In general, the association displays enthalpy/entropy compensation. Therefore, for poorly basic anions (for which host deprotonation is unlikely), hydrogen bonding strength depends on receptor's acidity: the more acidic the guanidinium is, the higher the binding is observed.

Acetate complexation with these receptors was also studied by ITC in MeCN and DMSO at 30 ºC, all binding data showing a neat 1:1 stoichiometry (Table 2.2, Fig. 2.18):

Table 2.2: Thermodynamic parameters of binding of guanidinium cations with tetrabutylammonium acetate in MeCN and DMSO at 30 ºC (errors<10%)

		1 (Cl$^-$)	**1** (PF$_6^-$)	**2** (Cl$^-$)	**2** (PF$_6^-$)	**3** (Cl$^-$)	**3** (PF$_6^-$)
MeCN	K_s (10^3)	136	440	1260	3400	113	443
	ΔG	-7.1	-7.85	-8.46	-9.04	-7	-7.83
	ΔH	-3.47	-4.7	-4.79	-6.21	-4.36	-4.936
	ΔS	12	10.4	12.1	9.35	8.73	9.55
DMSO	K_s (10^3)	10.2	11.4	82.1	120	n.m.	n.m.
	ΔG	-5.55	-5.62	-6.8	-7.04	-	-
	ΔH	-2.31	-2.5	-2.41	-2.4	-	-
	ΔS	10.7	10.3	14.5	15.3	-	-

K_s expressed in L.mol^{-1}, ΔG and ΔH in kcal.mol^{-1}, ΔS in cal.mol^{-1}.K^{-1}

As observed in the case of chloride, **2** binds better to acetate than **1** because of its higher acidity. Remarkably, **3** shows lower affinity for acetate than **1** (**3** ≤ **1** < **2**). In a general manner, use of competitive counterions such as chloride tends to lower the association constant (if compared with hexafluorophosphate). Benzoguanidinium cation **2** gives higher binding constants because of an increased enthalpic term, which can be attributed to the formation of strong hydrogen bonds with the more acidic NHs. In acetonitrile, the energy difference between **1** and **2** is solely due to the enthalpic contribution, whereas in DMSO, both enthalpy and entropy differ (entropy/enthalpy compensation). Furthermore, complexation of **2** (PF_6^-) with the less basic 3,5-dinitrobenzoate in acetonitrile gives an association constant of 6×10^3 M^{-1} for an enthalpically driven binding ($K_a = 3.4 \times 10^6$ M^{-1} for acetate), which also illustrates the pK_a dependence of association strength of both host and guest.

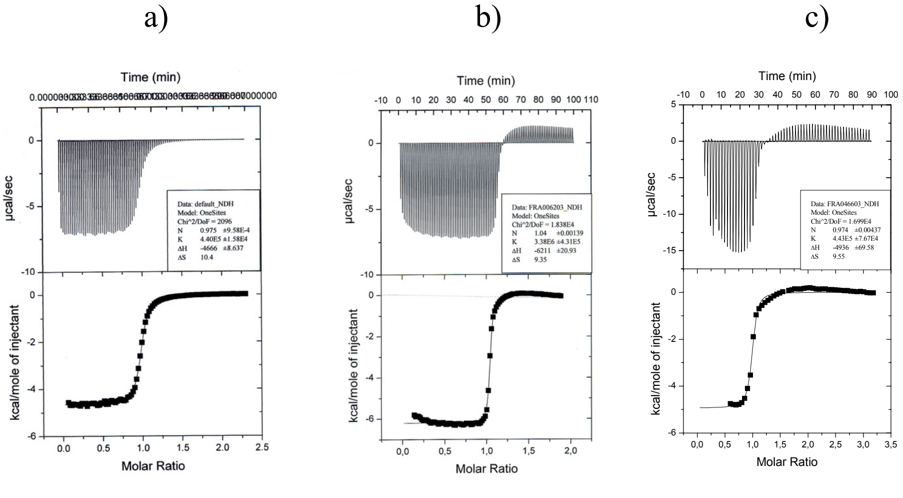

Fig. 2.18: Titration curves in MeCN for: a) **1** (PF_6^-) with AcO^-. b) **2** (PF_6) with AcO^-. c) **3** (PF_6^-) with AcO^-.

Since unprotonated **3** has been reported to form bridged dimers,[17] the unusual shape of its titration curve before equivalence was attributed to a possible dimer formation in competition with the 1:1 complex.[21] The lower affinity observed for **3**, despite its high acidity, was then attributed to transprotonation, giving rise to the less stable guanidine/acetic acid pair (non favored dipolar crossed interactions), likely to compete with the formation of the guanidine dimer. To check this hypothesis, a thermodynamic cycle was considered (Fig. 2.19), taking only into account the enthalpic component of the binding (the entropic terms would not compensate in the cycle because of the release of salts upon complexation); ITC experiments performed in acetonitrile were taken into account.

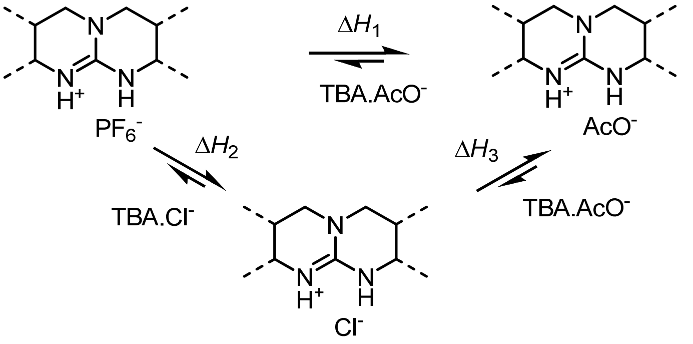

$\Delta H_1 = \Delta H_2 + \Delta H_3$

[a]	ΔH_1	ΔH_2	ΔH_3	$\Delta H_1 - \Delta H_2 - \Delta H_3$
1	-4700	-1164	-3470	-66 (43)
2	-6210	-1495	-4790	75 (21)
3	-4936	-1368	-4360	792 (76)

[a] ΔH expressed in cal.mol^{-1}, numbers in parenthesis refer to accepted error from ITC experiments in MeCN

Fig. 2.19: Thermodynamic cycle for anions binding to **1-3**.

---

[21] The corresponding points of the titration were removed for data fitting.

Experimental results fit rather well the thermodynamic cycle for **1** and **2**, since the deviation is rather low (though it is higher than the accepted experimental error), indicating the absence of competing processes. For **1** and **2**, the error is less than 1.4% of the ΔH_1 value, which is remarkable.[22] However, in the case of **3**, a 16% error was observed, suggesting the existence of a competing process, likely to be transprotonation between acetate and guanidinium. All these observations can be taken as evidences for transprotonation and show that binding should be higher as the acidity of the H-bond donors increases provided that transprotonation between host and guest is avoided.

Finally, **1-3** (AcO^-) salts were prepared[23] and studied by IR spectroscopy in the solid state, to check the differences in their aggregation states. Detailed hydrogen bonding studies by IR usually require use of solutions, as well as different concentrations to distinguish intramolecular (chelation) from intermolecular hydrogen bonds, but we were here just interested in seeing the differences between the spectra. The results (Fig. 2.20) confirmed that compound **3** behaves differently from **1** and **2**. For **1** and **2**, broad peaks were seen above 3000 cm^{-1} (low intensity) and sharp ones between 2800 and 300 cm^{-1} (strong), corresponding respectively to non-bonded and bonded NHs of the guanidine, a common feature of guanidinium salts. The IR spectrum for 1,5,7-triazabicyclo[4.4.0]dec-5-

---

[22] Errors were estimated as the ratio of ΔH_1- ΔH_2- ΔH_3 over ΔH_1.

[23] A solution of **1-3** (PF_6^-) in CH_2Cl_2 was wahed with NH_4OAc. The organic phase was dried and the solvent eliminated under vacuum.

ene (bicyclic guanidine) exhibits broad peaks in the 2800-3000 cm^{-1} area. However, for **3**, a broad peak can be observed between 2200 and 2800 cm^{-1} and two sharp ones of low intensity between 2800 and 3000 cm^{-1} (see fig. 2.20). Furthermore, the spectrum of **3** (PF_6^-) exhibits a sharp and intense band at 3392 cm^{-1}, attributed to the NHs, which is absent in **3** (AcO^-). This provides additional support for a transprotonation process between **3** and acetate.

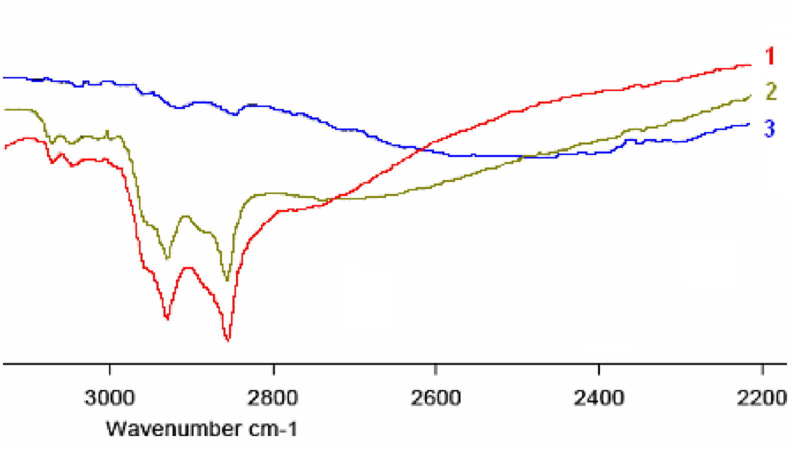

Fig. 2.20: IR Spectra of **1-3** (AcO^-).

2.4 Catalysis.

2.4.1 General.

Bicyclic guanidinium cations derived from **1** were previously shown to stabilize the oxoanionic transition state of the 1,4-addition of pyrrolidine to 2-(5*H*)-furanone[11] (Fig. 2.7). The influence of the acidity of the guanidinium scaffold on its catalytic activity was however not reported. For this reason, **1-3** were investigated as potential catalysts for this reaction, which can be easily monitored by ^{1}H NMR (Fig. 2.21), therefore enabling the construction of its kinetic profile by signal integration.

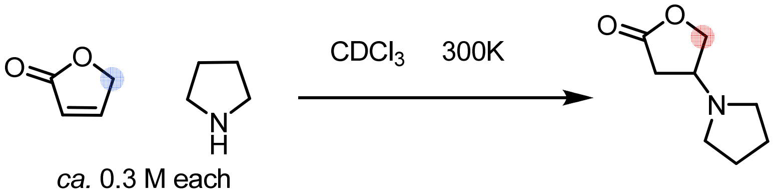

$$\mathcal{V} = k_0\ [\text{2-(5}H\text{)-furanone}]\ [\text{pyrrolidine}]^2$$

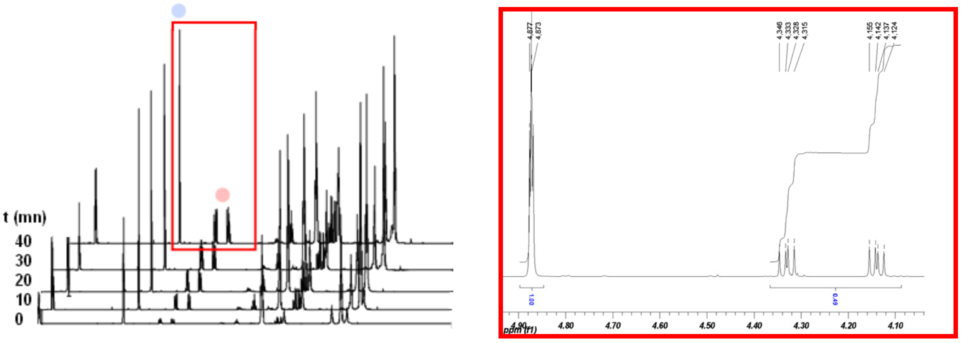

Fig. 2.21: Uncatalyzed reaction monitored by ^{1}H NMR spectroscopy.

The reaction displays third-order kinetics, as was previously shown in our group.[24] The second partial order for pyrrolidine is attributed to its participation in the deprotonation of the zwitterionic transition state; the resulting pyrrolidinium cation then deprotonates upon proton transfer to enolate, thus regenerating the pyrrolidine. Therefore, the reaction might also be catalyzed by water (protonation of the enolate and/or deprotonation of the pyrrolinium moiety by water) (Fig. 2.22), though it is difficult to determine which of these two steps is faster under the reaction conditions. The role of water in the reaction made it difficult to reproduce the previous results, for which half-time of the reaction was reached after 180 minutes.

---

[24] Martín-Portugués, M. *Tesis de Licenciatura* **1996**, Universidad Autónoma de Madrid.

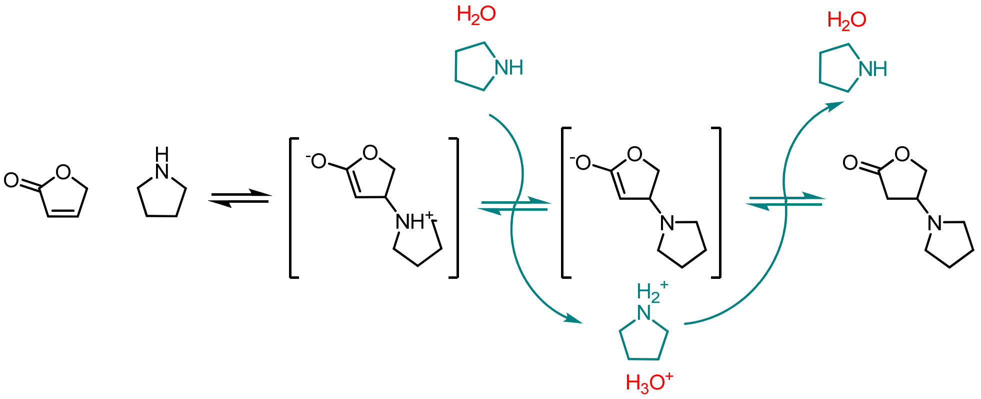

Fig. 2.22: Proposed mechanism of the reaction and water catalysis.

When commercially available reagents and no catalyst were used, half completion was reached after only 90 minutes ($t_{1/2}$). However, careful distillation of the reagents in a glass oven, afforded a $t_{1/2}$ of 192 minutes, close to the previously published results. Finally, after distillation of pyrrolidine over calcium hydride, half completion of reaction was obtained after 235 minutes. This clearly shows that water has to be strictly avoided in these experiments to obtain reliable and reproducible data. In the case of guanidinium cations, dried pyrrolidine and distilled 2-(5*H*)-furanone were used, whereas in the case of porphyrins (see Chapter 3), distilled substrates were used.

2.4.2 Catalysis experiments.

Similar kinetic measurements were then performed in the presence of catalytic amounts of **1-3**. In order to reproduce the previously obtained results, experiments with 10 mol % catalyst were performed with **1** (Cl$^-$) and **2** (Cl$^-$) (Fig. 2.23). The results were rather positive, since **2** proved to be an excellent catalyst for the reaction and half completion was reached after only 10 minutes [*vs*. 235 minutes for the blank reaction and 75 minutes with 10 mol% of **1** (Cl$^-$)].[25]

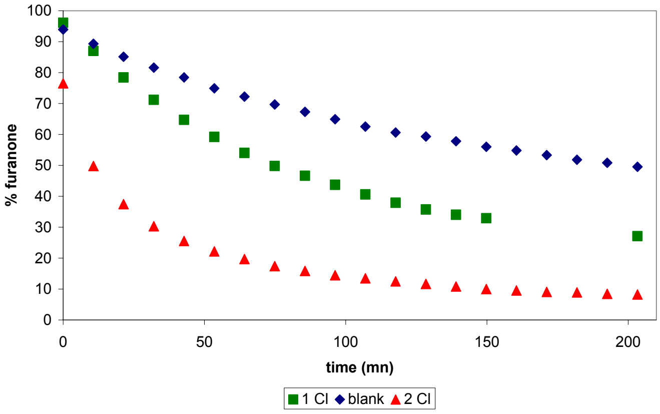

Catalyst	$t_{1/2}$ (mn)
none	235
1 (Cl$^-$)	75
2 (Cl$^-$)	10

Fig. 2.23: Kinetic measurements performed with 10 mol % **1-2**.

In the presence of 10 mol% of **2** (Cl$^-$), a 23.5 fold-rate acceleration was observed, whereas with **1** (Cl$^-$), 3.1 fold-rate acceleration was observed. These high differences are in agreement with the acetate binding studies performed previously. Anionic transition state of the reaction is indeed likely to have a higher binding constant with **2** than with **1** (increased guanidinium acidity). ^{1}H NMR titrations of these two guanidinium cations (chloride) with 2-(5*H*)-furanone were then performed but binding constants could not be calculated: signal shifts were not significant enough, especially for **2**. This evidences our design hypothesis, namely that affinity with the transition state is essential for catalytic activity (lowering of activation energy by enhanced transition state stabilization). Furthermore, the negative charge in the zwitterionic transition state of the reaction is not distributed symmetrically between the two oxygens, as is the case of the guanidinium positive charge in **2**, which might also enable to explain the observed results (better electronic fit). However, the reaction catalyzed by the benzoguanidinium cation is much too fast to allow an accurate determination of the reaction half-time. For this reason, a set of experiments was performed at a lower catalyst loading (1 mol %). Results of the experiments are summarized in Fig. 2.24. As expected, at low catalyst loading, the activity decreases but can nevertheless be detected. **2** (Cl^-) proves to be the best catalyst for the reaction since a 4.12 fold-rate acceleration is obtained in presence of just 1 mol% catalyst. No direct correlation can however be made between the pK_a of the catalyst and its catalytic efficiency and it seems that a similar phenomenon as the one described for anion binding is taking place: for a given guanidinium pK_a, there is a drop in the catalyst efficiency: more acidic guanidinium **3** and **14** are worst catalysts than **2**. Actually, **14** might act as a bifunctional catalyst, for which the carboxyguanidinium would activate the lactone (likely product inhibition could appear) and the pyridyl residue would participate in the transition state deprotonation (as usually does the pyrrolidine).

---

[25] Literature results are significantly different ($t_{1/2}$ = 22 minutes for **1** (Cl$^-$)),[11]probably due to the use of wet reactants in the experiments.

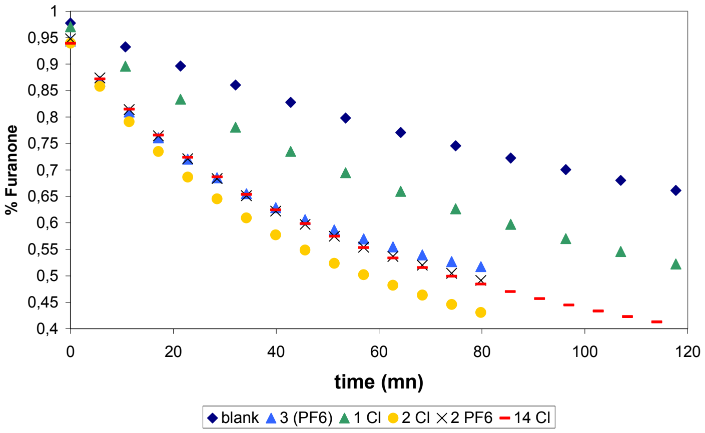

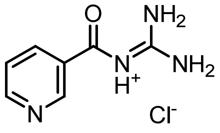

14

Catalyst	none	**1 (Cl^-)**	**2 (Cl^-)**	**2 (PF_6^-)**	**3 (PF_6^-)**	**14 (Cl^-)**
$t_{1/2}$ (min)	235	128	57	74	91	74
acceleration	-	1.83	4.12	3.18	2.58	3.18

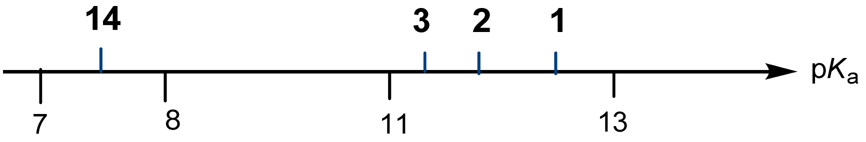

Fig. 2.24: Kinetic measurements performed with 1 mol % **1**, **2**, **3** and **14**.[26]

It was previously reported that catalytic activity was enhanced for non competitive counterions due to easier binding of the oxoanionic transition state[11]. Differences observed between **2** (PF_6^-) and **2** (Cl^-) however tend to show the contrary, which is unexpected. This might however be explained by the high sensitivity of the reaction to water and the obtained results may therefore belong to the same range (within experimental error).[27] The effect of the counterion was here not studied systematically and no clear conclusion can be drawn. Furthermore, guanidinium cations are Brönsted acids, so transprotonation with the transition state is likely. However, an enolate-like transition state might protonate in various competitive fashions. Hypothetically, acidity of the catalyst may determine which proton exchange processes are faster.

---

[26] The synthesis of **14** will be described in the last chapter of this manuscript.

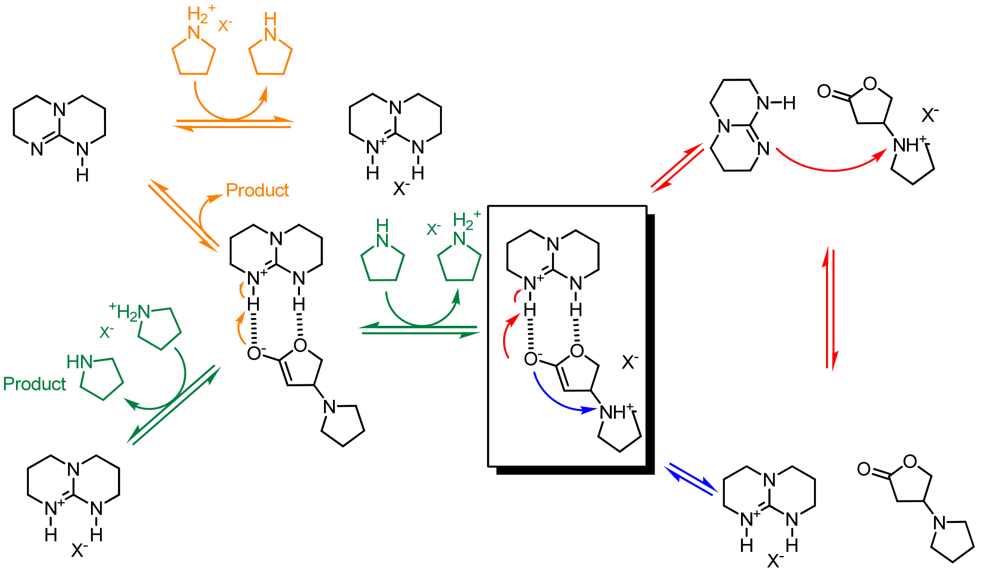

Fig. 2.25: Proposed equilibria for the protonation/deprotonation of the zwitterionic transition state (among others).

On the one hand, deprotonation of the zwitterionic transition state can occur following an intramolecular proton transfer mechanism (blue arrows,

---

[27] Experiments were performed only once from the same mother solutions of substrates, to keep the water content as constant as possible.

Fig. 2.25) or by participation of a pyrrolidine molecule (green arrows). However, kinetics of the uncatalyzed reaction suggest that intramolecular proton transfer is unlikely: the mechanism involves a second pyrrolidine molecule (second partial order for pyrrolidine). On the other hand, Brönsted acidity of guanidinium cations also suggests that oxoanionic transition state is likely to deprotonate the guanidinium cation (red and orange arrows) to yield the free guanidine that is likely to protonate with the cationic moiety of the transition state or the pyrrolidinium cation ($pK_a = 11.27$).[28] Surprisingly, the catalytic activity of **2** might therefore arise from adequate balance of acidity and basicity for the protonation and deprotonation of the zwitterionic transition state.

To check this hypothesis, a deprotonated sample of **2** (Cl^-) was deuterated with DCl. If transprotonation takes place, use of a stoichiometric amount of deuterated **2** would result in deuteration of the product. The ^1H NMR spectrum of the catalyst was recorded prior to its use and deuteration, though not complete, was evidenced. The reaction was then performed with a stoichiometric amount of $\mathbf{2}^D$ (Cl^-) and the Michael adduct analyzed after column chromatography (Fig. 2.26).

In the product from the deuterated experiment (spectrum (a)), a new broad signal appears at 3.17 ppm with respect to the experiment performed with non-labelled catalyst. The splitted signal corresponds to the α-proton of the carbonyl (acidic position), where deuteration is expected to take place (this was confirmed by a 2D COSY NMR experiment). Though some deuteration of the Michael adduct could be observed, it is difficult to assess whether the labelling is caused by transprotonation or by fast intermolecular proton exchange. As a last remark, for each experiment involving a chiral catalyst, optical rotation of the reaction product was measured and appeared to be close to 0, as previously observed when derivatives of **1** were used.

---

[28] Hall, H. K. Jr. *J. Am. Chem. Soc.* **1957**, *79*, 5441.

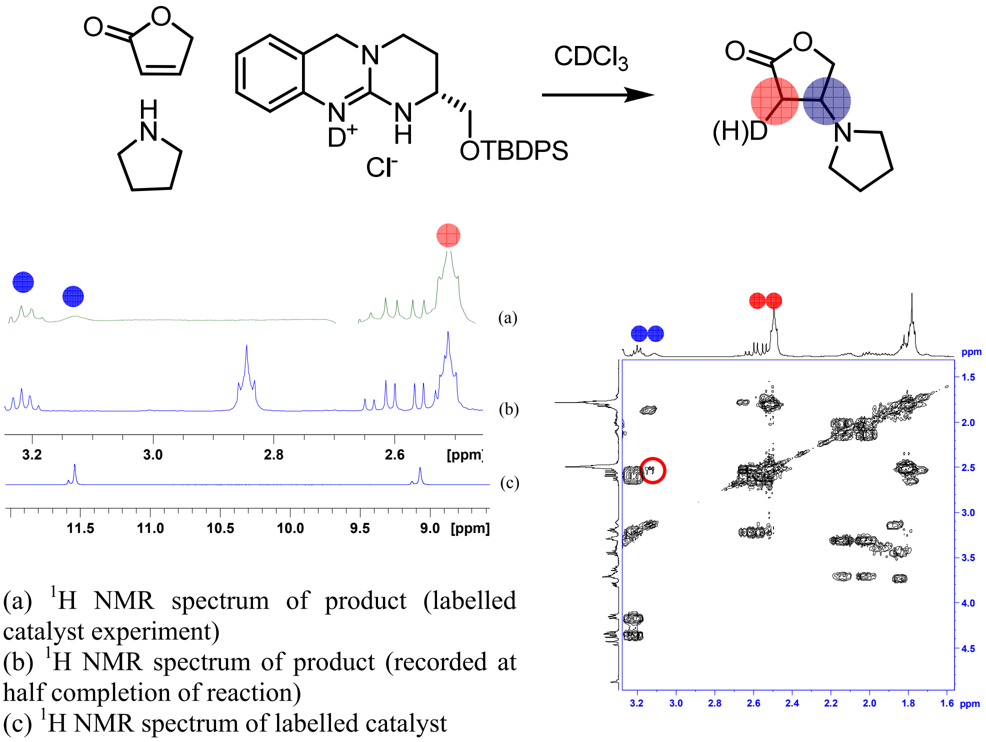

(a) ^{1}H NMR spectrum of product (labelled catalyst experiment)
(b) ^{1}H NMR spectrum of product (recorded at half completion of reaction)
(c) ^{1}H NMR spectrum of labelled catalyst

Fig. 2.26: Results of the D-labelled guanidinium catalyzed experiment.

These studies show that acidity of the catalyst mainly influences the rate of proton transfers, which is decisive for catalyst efficiency and observation of high turnover frequencies in the studied case.

2.5 Conclusions.

In this chapter, a series of guanidinium cations (**1-3**) bearing different acidities by attachment of aromatic rings to the bicyclic guanidinium core were prepared. Their anion binding affinity as a function of acidity was then investigated by ITC. It was shown that, for acetate, high association constants attributed to enthalpic binding terms (related to hydrogen bonding strength) could be obtained for benzoguanidinium cations such as **2**. For highly acidic guanidinium cations, anion protonation is likely, which causes a drop in the association constant (binding of **3** with AcO^-). A direct correlation between H-bonding strength and receptor's acidity could also be evidenced.

The acidity of H-bond donors also has consequences on their behavior as catalysts for the Michael addition of pyrrolidine to 2-(5*H*)-furanone. Rates of proton transfer steps were altered by catalyst's acidity, which was decisive for the definition of catalyst's efficiency. This study renders benzoguanidinium cations catalysts of choice for anion binding and organocatalysis applications.

2.6 Experimental part.

a) General procedures.

Synthesis. All commercially available reagents (Aldrich, Fluka, Acros, Novabiochem, and Panreac) were used without any further purification, unless otherwise stated. Solvents were dried with a Solvent Purification

System for deoxygenation and drying of solvents. All reactions were performed under argon atmosphere and anhydrous conditions unless otherwise stated.

Chromatography. Thin Layer Chromatography (TLC) was performed on glass supported Alugram Sil G/UV 254 (Macherey-Nagel). Column chromatography was done using silica gel by SDS (Chromagel 60 ACC, 40-60 μm mesh) following the previously reported procedure.[29]

Analysis. NMR spectra were recorded on a Bruker Avance 400 Ultrashield NMR spectrometer using the residual solvent peak as internal standard. Melting points were recorded on a Büchi B-540 apparatus. Optical rotations $[\alpha]^{20}_{D}$ were determined on a Perkin-Elmer 241 MC polarimeter (Na_D 589 nm). Mass spectra were recorded on a Waters LCT Premier spectrometer using ESI technique or on a Bruker Autoflex MALDI-TOF instrument. Crystal structures were determined on a Bruker-Nonius diffractometer equipped with a APPEX 2 4K CCD area detector, a FR591 rotating anode with MoKalpha radiation, Montel mirrors as monochromator and a Kryoflex low temperature device (T = 100 K). UV-Vis measurements were performed on a Shimadzu UV-2401PC with a thermostated (7-60 ºC) sample holder.

Job plot experiments. 0.01M standard solutions of **1-2** and tetrabutylammonium acetate (or other anion) in $CDCl_3$ were mixed in a NMR tube in order to get solutions with various known compositions. ^1H NMR spectra were then recorded (400 MHz).

ITC titrations. ITC titrations were performed using an isothermal titration Microcal VP-ITC calorimeter. All measurements were performed at 303 K and reproduced three times at least. Host solution (1 mM in MeCN, 5 mM in DMSO) was filled in the ITC cell and guest solutions (8 mM in MeCN, 50 mM in DMSO) were added through the syringe. Control experiments for guest dilution were also performed and heat evolution was found to be negligible. Solvent was previously degassed by sonication during 15 minutes. Analysis and data fitting was done using Origin 7 software. Samples were weighted in a Mettler Toledo MX5 microbalance. Tetrabutylammonium acetate and chloride salts were weighted in a dry box.

---

[29] Still, W. C.; Kahn, M.; Mitra, A. *J. Org. Chem.* **1978**, *43*, 2923.

Kinetic measurements. 2-(5*H*)-furanone and pyrrolidine were previously distilled in a Büchi glass oven B580 under vacuum unless otherwise stated. Then, 0.3 M stock solutions of each substrate were prepared in deuterated chloroform. The catalyst was weighed on a Mettler Toledo MX5 microbalance. 0.5 mL of each solution and the catalyst were placed in a NMR tube and the ^{1}H NMR spectra were recorded every 10 minutes under the automation mode on a Bruker Avance 500 Ultrashield spectrometer.

b) Synthesis.

The characterization of the synthetic intermediates of **1** has been extensively reported in previous accounts of our group and will not be described in this manuscript. The large scale synthesis of **6** and **8** is however reported here. Preparation of **9**, **10** and **1** was performed according to well known procedures at the usual scales.

(2*R*)-*N*-*p*-Toluenesulphonylasparagine (7).

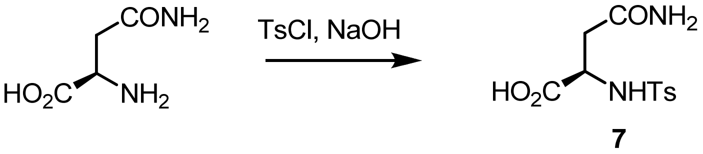

Procedure

In a 10 L reactor D-asparagine (400 g, 2.66 mol) was dissolved in 4.8 L of a 0.8N aqueous solution of NaOH. Then *p*-toluenesulfonyl chloride (672 g, 3.34 mol) was added within two hours. 5N NaOH (700 mL) was added so that the pH of the mixture remains above the value of 10. The reaction mixture was stirred at room temperature for 24 h and filtered. The aqueous phase was placed in the reactor and acidified with 37% HCl (290 mL) to reach pH 1.5. The reaction mixture was stirred at room temperature for 1 h at 5 ºC and the resulting precipitate was filtered, washed with water and dried in the oven at 50 ºC, to afford **7** (603.18 g, 73%).

(2*R*)-*N*-[2-(4-Amino-1-hydroxybutyl)]-*p*-toluenesulphonamide (8).

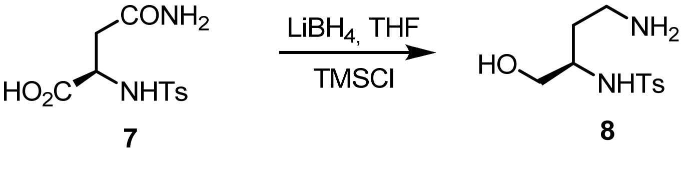

Procedure

In a 10 L reactor, equipped with a reflux condenser and an addition funnel, a lithium borohydride solution (2M in THF, 3.13 L, 6.26 mol) was diluted in anhydrous THF (1.33 L) and the mixture was flushed with nitrogen. TMSCl (1.58 L, 12.5 mol) was added dropwise and the reaction mixture was cooled at 0 ºC. Compound **7** (553.18 g, 1.33 mol) was then slowly added as a fine powder. Once the addition over, the reaction mixture was stirred at room temperature for 1 h and then refluxed overnight. Methanol (2.5 L) was then carefully added and the solvent was eliminated *in vacuo*. The resulting residue was dissolved in water (2.5 L) and the solvent was once again eliminated. The solid was then dissolved in water (1.8 L) and the solution was basified to pH 11 by adding a 5N aq solution of NaOH, thus allowing the product to precipitate at 4 ºC overnight. The product was filtered off and recrystallized in water (3.3 L), yielding **8** (433 g, 87%).

(2*R*)-Amino-5-thia-1-hexanol (4).

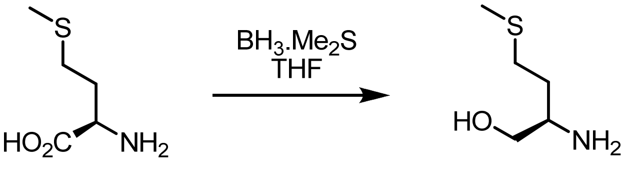

4

Procedure

In a 10 L reactor D-methionine (275 g, 1.82 mol) was dissolved in anhydrous THF (4.62 L) at room temperature. Borane-dimethylsulfide complex (370 mL, 3.7 mol) was then added and the reaction mixture was stirred at room temperature for 1 h and then refluxed overnight. A solution of 10% HCl in MeOH (1.33 L) was added at -2 ºC, and the reaction mixture was refluxed for 1 h. The mixture was cooled to room temperature and concentrated at reduced pressure to yield a colorless oil that was dissolved in water (320 mL). The aqueous phase was basified with 4N NaOH (650 mL) and extracted with CH_2Cl_2 (11 × 2 L). The combined organic phases were dried (Na_2SO_4) and concentrated to dryness to yield **4** (192.56 g, 78%).

(2*R*)-Amino-1-(*tert*-butyldiphenylsilyloxy)-5-thiahexane (5).

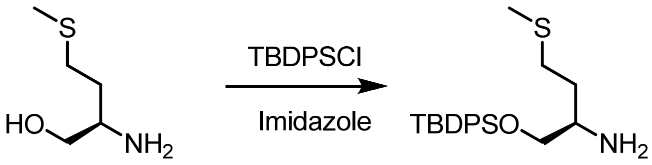

4 **5**

Procedure

In a 3 L reactor compound **4** (192.56 g, 1.46 mol) was dissolved in acetonitrile (1.5 L) under inert atmosphere and a solution of imidazole (134.16 g, 2.85 mol) and *tert*-butyldiphenylsilyl chloride (503.48 g, 1.85 mol) in acetonitrile (280 mL) was added at room temperature. The reaction mixture was stirred at room temperature for 44 h (*lit.* 12 h), the solvent was eliminated at reduced pressure and the resulting orange oil was then placed in a 10 L reactor and distributed at 50 ºC between 1N NaOH (4.5 L) and hexane (3.75 L). The aqueous phase was extracted with hexane (2 × 2 L) and the combined organic phases were washed with water (3 × 1.5 L) and with a mixture of H_2O/MeCN/AcOH (30:20:1, 1 × 3 L then 3 × 700 mL). The combined aqueous phases were then washed with hexane (6 × 1 L) and basified with solid sodium carbonate (180 g). The acetonitrile was eliminated at reduced pressure until formation of an emulsion that was extracted with diethyl ether (2 × 2 L). The combined organic phases were dried (Na_2SO_4) and concentrated to dryness to afford **5** (437.12 g, 82%) as a yellow oil.

(2*R*)-1-(*tert*-Butyldiphenylsilyloxy)-5-thia-2-hexyl isothiocyanate (6).

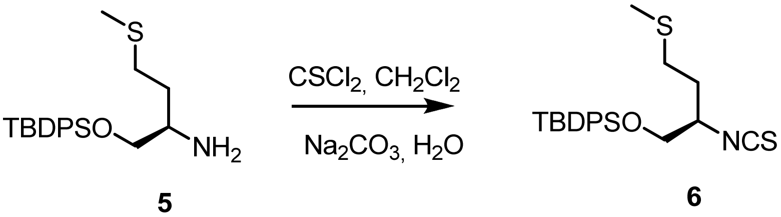
TBDPSO
S
NH2
CSCl2, CH2Cl2
Na2CO3, H2O
5
TBDPSO
S
NCS
6

Procedure

To a solution of **5** (437.11 g, 1.26 mol) in CH_2Cl_2 (2.05 L) a solution of sodium carbonate (653.7 g) in water (3.46 L) was added. The mixture was then vigorously stirred at room temperature and a solution of thiophosgene (102.6 mL, 1.46 mol) in CH_2Cl_2 (1.26 L) was added dropwise. The reaction mixture was stirred at room temperature for 2 h, the organic phase was washed with water (4 × 1.5 L) and brine (1 ×1.5 L), dried (Na_2SO_4) and concentrated to dryness to yield **6** (468.57 g, 83%) as a red oil.

(*R*)-1-(2-Aminobenzyl)-3-(1-(*tert*-butyldiphenylsilyloxy)-4-(methylthio) butan-2-yl) thiourea (11).

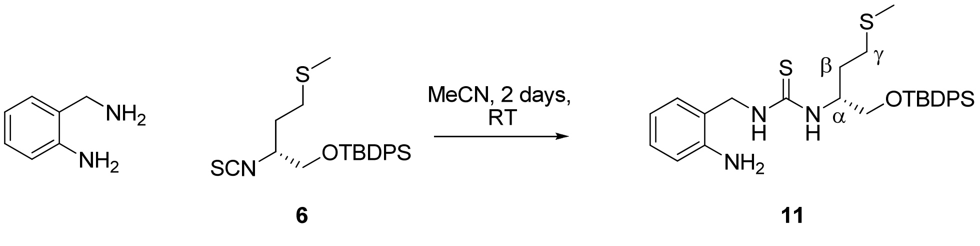
NH2
NH2
S
SCN
OTBDPS
6
MeCN, 2 days, RT
S
β
γ
N H
N H
α
OTBDPS
S
NH2
11

Procedure

A solution of **6** (2.14 g, 5.1 mmol) and 2-aminobenzylamine (680 mg, 6.2

mmol) in acetonitrile (10 mL) was stirred two days at room temperature After this time, solvent was eliminated *in vacuo* and the crude reaction mixture was directly purified *via* column chromatography using a 30% to 45% diethyl ether/hexane as an elution mixture. 2.1017 g of the desired thiourea were isolated after elimination of the solvents (77% yield). **^{1}H NMR** (400 MHz, $CDCl_3$): δ ppm 7.63-7.59 (m, 4H, Ph-Si), 7.45-7.35 (m, 6H, Ph-Si), 7.1 (td, 1H, *J* = 8.0, 1.6 Hz), 7.02 (d, 1H, *J* = 7.4 Hz), 6.67 (t, 1H, *J* = 7.6 Hz), 6.63 (d, 1H, *J* = 8.0 Hz), 6.40-5.95 (m, 3H, NH thiourea, NH_2 ar), 4.82 (broad s, 1H, NH thiourea), 4.52 (dd, 1H, *J* = 14.0, 3.2 Hz, C$\underline{H}$ α), 4.14 (broad s, 2H, benzyl C$\underline{H_2}$), 3.69 (m, 2H, C$\underline{H_2}$-OSi), 2.4 (t, 2H, *J* = 6.8 Hz, C$\underline{H_2}$ γ), 2-1.75 (m, 5H, S$\underline{Me}$, and C$\underline{H_2}$ β), 1.06 (s, 9H, $SiC(C\underline{H_3})_3$); **^{13}C NMR** (100 MHz, $CDCl_3$): δ ppm 180.3 (C=S); 144.6 (C_{Ar}-NH_2); 134.6, 131.8, 129.5, 129.0, 128.4, 126.9, 119.7 (C-Si), 116.9, 114.8 (C arom.), 64.5 (CH_2-O), 53.3 (CH α), 46.3 (Ph-CH_2-NH), 29.6 (CH_2 β, γ), 25.9 (CH_3 *tert*-butyl), 18.2 (*tert*-butyl), 14.11 (SCH_3).

2,3,4,6-Tetrahydro-2-(*tert*-butyldiphenylsilyloxymethyl)-1H-pyrimido [2,1-b]quinazoline hydrochloride (2 (Cl$^-$)).

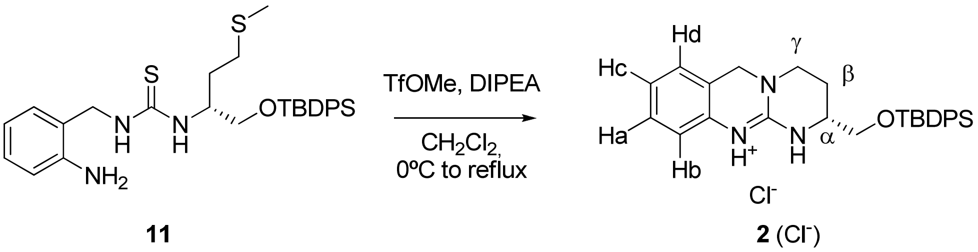

11 **2** (Cl$^-$)

Procedure

To a solution of **11** (537.9 mg, 1 mmol) in dry dichloromethane were added diisopropylethylamine (10 µL) and methyl trifluoromethanesulfonate (distilled in a vacuum oven at 40 ºC (7 mbar), 234 µL, 2.07 mmol) at 0 ºC and under argon. The obtained mixture was stirred two hours at room temperature and more diisopropylethylamine (1.45 mL, > 8 mmol) was added dropwise. The obtained mixture was then heated to reflux for 12 hours. Solvents were then eliminated *in vacuo* and the residue distributed between NaOH 1N (5 mL) and diethyl ether (10 mL). The organic phase was washed with NaOH 1N (50 mL), followed by water (50 mL). The organic phase was then collected in a flask and NH_4Cl 1N was added. **2** (Cl^-) was obtained by filtration of the precipitate (89.9 mg, 29%). **M.p.:** 165-166 ºC. **^{1}H NMR** (400 MHz, $CDCl_3$): δ ppm 11.67 (broad s, 1H, Ph-NH gu), 9.35 (broad s, 1H, NH gu), 7.67-7.62 (m, 4H, Ph-Si), 7.47-7.36 (m, 6H, Ph-Si), 7.22 (d, 1H, J = 7.6 Hz, H_d), 7.10 (d, 1H, J = 8.0 Hz, H_a), 7.03 (t, 1H, J = 8.0 Hz, H_b), 6.97 (d, 1H, J = 7.6 Hz, H_c), 4.40 (dd, 2H, J = 17.6, 14.4 Hz, Ph-CH_2-N), 3.91-3.85 (m, 1H, CHα), 3.75-3.61 (m, 2H, CH_2O), 3.36-3.21 (m, 2H, CH_2 γ), 2.21-2.01 (m, 2H, CH_2 β), 1.06 (s, 9H, $SiC(CH_3)_3$); **^{13}C NMR** (100 MHz, $CDCl_3$): δ ppm 149.7 (C guan.), 135.5, 135.4, 132.5, 132.4, 129.9, 128.9, 127.8, 125.3, 123.8, 115.6, 115.5 (C arom.), 65.1 (CH_2O); 49.6 ($PhCH_2N$); 49.2 (CH α); 44.4 (CH_2 γ); 26.8 (*tert*-Bu); 22.5 (CH_2β); 19.0 (C_{tBu}-Si). **MS (ESI$^+$)**: [M^+] calcd. for $C_{28}H_{34}ClN_3OSi$ 491.22; found 491.22; **$[\alpha]^{20}_D$:** -56.6 (c=0.6, CH_2Cl_2).

Crystal structure determination[32].

Compound **2 (Cl^-)** crystallizes in the chiral space group *P*$2_12_12_1$. The elementary cell contains two independent molecules of the same compound with different conformations (Fig. 2.27). The absolute configuration with ***R***(C1) could also be confirmed (Flack 0.04(4)). The shortest distances from the chloride atoms to the molecules are: Cl1···N2: 3.070 Å; Cl1···N1: 3.493 Å; Cl1B···N2B: 3.080 Å and Cl1B···N2B: 3.426 Å. The elementary cell contains additionally one molecule of water. The hydrogen atoms of the water molecule could not be localized.

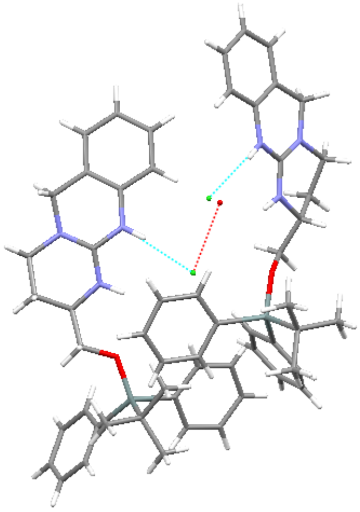

Fig. 2.27: Crystal elementary cell of **2 (Cl^-)**.

---

[32] J. Benet Buchholz and E. Escudero (ICIQ X-ray diffraction unit) are acknowledged.

Bis-(2-aminobenzyl)amine (12).

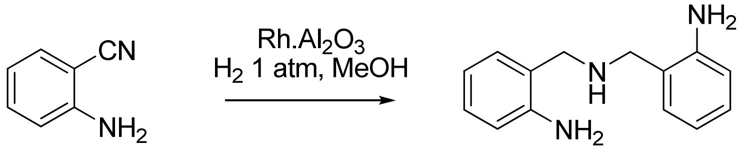

12

Procedure

To a solution of anthranilonitrile (413.6 mg, 3.5 mmol) in dry methanol (10 mL), 5% rhodium on alumina (450.3 mg) was added and the solution was bubbled with hydrogen for 15 min. The mixture was then stirred at RT for 24 hours under a hydrogen atmosphere. The mixture was filtered over celite and the solvent was eliminated *in vacuo*. The residue was dissolved in CH_2Cl_2 and the resulting organic phase was washed with 5% aqueous HCl. The organic phase was dried with Na_2SO_4, filtered and the solvent was then eliminated under vacuum. The resulting yellow oil was purified by silica gel column chromatography (CH_2Cl_2/MeOH 3%) to yield **12** as a slightly yellow oil (146 mg, 37%). ^{1}**H NMR** ($CDCl_3$, 400 MHz): δ ppm 7.11 (dt, 2H, J = 7.3 Hz, J = 0.9 Hz), 7.09 (d, 2H, J = 7.3 Hz), 6.72 (dt, 2H, J = 7.2, 0.9 Hz), 6.67 (d, 2H, J = 7.66 Hz), 3.80 (s, 4H, CH_2); ^{13}**C NMR** ($CDCl_3$, 100 MHz): δ ppm 145.9, 130.1, 128.5, 123.6, 118.1, 115.8, 51.7.

3-(2-Aminobenzyl)-3,4-dihydro-(*1H*)-2-quinazolinethione (13).

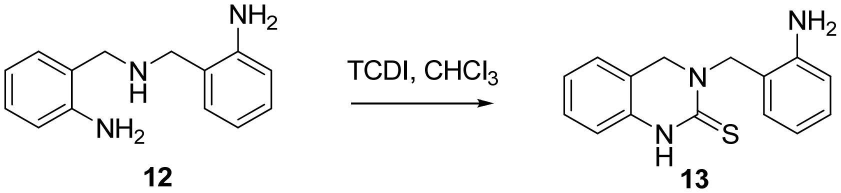

12 **13**

Procedure

To a solution of **12** (130 mg, 572 μmol) in chloroform (27 mL), thiocarbonyldiimidazole (122.3 mg, 686 μmol) was added and the resulting mixture was stirred at room temperature for three days. The solvent was then eliminated under vacuum and the residue was purified by silica gel column chromatography (AcOEt:Hexane 1:2), yielding **13** as a white solid (100 mg, 65%). **M.p**: 236.9 ºC. **^{1}H NMR** ($CDCl_3$, 400 MHz): δ ppm 8.35 (s, 1H), 7.16 (t, 1H, J = 5.9 Hz), 7.14 (d, 2H, J = 7.1 Hz), 6.95 (t, 2H, J = 6.5 Hz), 6.72 (t, 1H, J = 6.5 Hz), 6.71 (d, 2H, J = 7.6 Hz), 5.22 (s, 2H), 4.35 (s, 2H).

11,12 Dihydro-(*5H*)-5,6,11a-triazanaphthacene hydrochloride (3 (Cl^-)).

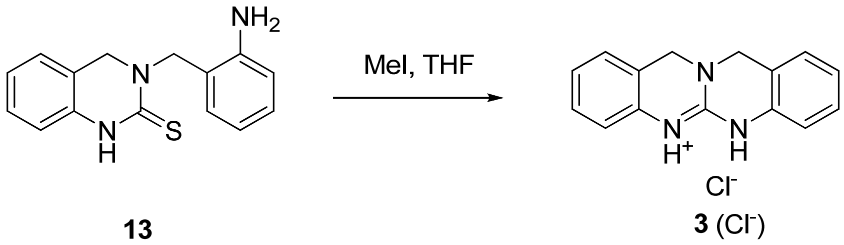

Procedure

To a solution of **13** (100 mg, 371 μmol) in dry THF (50 mL) was added methyl iodide (321 μL, 5.15 mmol) at room temperature. The reaction mixture was stirred under argon for two weeks. The solvent was then eliminated *in vacuo* and the residue was dissolved in dichloromethane. The resulting organic phase was then washed with HCl 1N, dried with Na_2SO_4, filtered and the solvent was eliminated *in vacuo* to yield **3** (Cl^-) as an air sensitive yellow solid. A white solid was obatined after recrystallisation in acetonitrile (yield not measured, *lit.* 97%).[17] **^{1}H NMR** (CDCl$_3$, 400 MHz): δ ppm 11.45 (s, 2H), 7.27-7.12 (m, 2H), 7.06 (d, 4H, *J* = 4.3 Hz), 6.96 (d, 2H, *J* = 7.7 Hz), 4.7 (s, 4 H); **^{13}C NMR** (CDCl$_3$, 100 MHz): δ ppm 131.2, 129.2, 125.6, 125.1, 115.8, 115.4, 49.5; **MS (ESI$^+$)**: [M-Cl$^+$] calc. for $C_{15}H_{14}N_3$ 236.12; found 236.11.

General procedures for anion exchange.

1) A solution of **1-3** (Cl$^-$) in CH_2Cl_2 was successively washed with 2N KOH and 0.1 N NH_4PF_6 (3 times each). The organic phase was then dried over anhydrous sodium sulfate, filtered and the solvent eliminated under vacuum to yield the corresponding hexafluorophosphate guanidinium salt.
2) A methanol solution of **1-3** was passed through an anion exchange resin (Dowex®) for hexafluorophosphate. Elution was performed with 1:1 MeOH:H_2O. The guanidinium salt was recovered by evaporation of the eluate.

1 (PF$_6^-$): ^{1}H NMR (400 MHz, CDCl$_3$): δ ppm 7.59-7.54 (m, 4H), 7.37-7.28 (m, 6H), 6.09 (s, 1H, NH), 6.07 (s, 1H, NH), 3.62-3.55 (m, 3H), 3.55-3.50 (m, 1H), 3.49-3.44 (m, 1H), 3.43-3.36 (m, 1H), 3.36-3.28 (m, 1H), 3.26-3.21 (m, 3H), 2.05 (s, 6H), 2.0-1.85 (m, 2H), 1.84-1.72 (m, 2H), 0.98 (s, 9H), 0.81 (s, 9H).

2 (PF$_6^-$): ^{1}H NMR (400 MHz, CDCl$_3$): δ ppm 8.29 (broad s, 1H, Ph-NH gu), 7.67-7.62 (m, 4H, Ph-Si), 7.47-7.36 (m, 6H, Ph-Si), 7.22 (d, 1H, *J* = 7.6 Hz, H_d), 7.10 (d, 1H, *J* = 8.0 Hz, H_a), 7.03 (t, 1H, *J* = 8.0 Hz, H_b), 6.97 (d, 1H, *J* = 7.6 Hz, H_c), 6.71 (broad s, 1H, NH gu), 4.40 (dd, 2H, *J* = 17.6, 14.4 Hz, Ph-CH_2-N), 3.91-3.85 (m, 1H, CHα), 3.75-3.61 (m, 2H, CH_2O), 3.36-3.21 (m, 2H, CH_2 γ), 2.21-2.01 (m, 2H, CH_2 β), 1.06 (s, 9H, $SiC(CH_3)_3$); **^{13}C NMR** (100 MHz, $CDCl_3$): δ ppm 149.7 (C guan.), 135.5, 135.4, 132.5, 132.4, 129.9, 128.9, 127.8, 125.3, 123.8, 115.6, 115.5 (C arom.), 65.1 (CH_2O), 49.6 ($PhCH_2N$), 49.2 (CH α), 44.4 (CH_2 γ), 26.8 (*tert*-Bu), 22.5 (CH_2β), 19.0 (C-Si).

3 (PF_6^-): ^{1}H NMR (400 MHz, $CDCl_3$): δ ppm 7.17 (t, 2H, *J* = 7.8 Hz), 7.015 (d, 2H, *J* = 7.2 Hz), 6.95 (t, 2H, *J* = 7.5 Hz), 6.88 (d, 2H, *J* = 7.8 Hz), 4.51 (s, 4H).

CHAPTER 3

FUNCTIONALIZED METALLOPORPHYRINS AS COOPERATIVE CATALYSTS

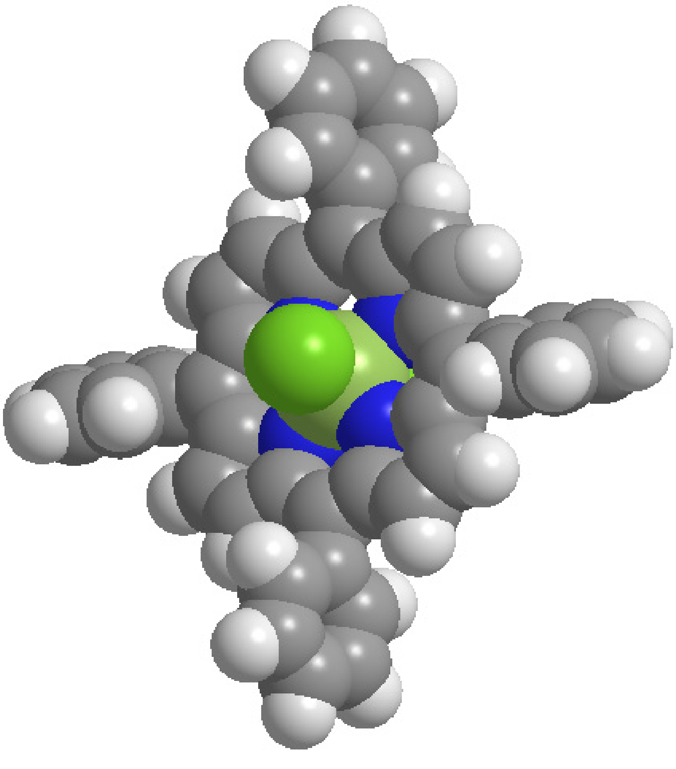

3. Functionalized metalloporphyrins as cooperative catalysts.

3.1 Introduction.

This chapter aims at studying the efficiency of multifunctional catalysts, for which metal activation and hydrogen bonding are expected to work in a cooperative fashion (dual activation). Metal-substrate interactions and hydrogen bonding are known to give rise to cooperativity in enzymatic systems such as staphylococcal nuclease (SNase).[1] In nature, phosphodiester hydrolysis (DNA, RNA) is indeed guaranteed by cooperation between metal centers and amino acid residues which act as general acid/base catalysts. Positively charged residues of lysine, arginine and histidine are thought to stabilize the phosphorane-like transition states by electrostatic interactions, hydrogen bonding and/or proton transfer. A few systems able to reproduce this observed cooperativity have been reported so far and, in most cases, emphasis was put on enzyme mimics. One of the most representative examples is RNA phosphodiesterase mimic. Phosphodiester hydrolysis was previously shown to be catalyzed by both mono- and dinuclear metal complexes and hydrogen bond donors (such as ammonium and guanidinium),[2] independently. Multifunctional catalysts for

---

[1] a) Serpersu, E. H.; Shortle, D.; Mildvan, A. S. *Biochemistry* **1987**, *26*, 1289. b) Wilcox, D. E. *Chem. Rev.* **1996**, *96*, 2435. c) Perreault, D. M.; Anslyn, E. V. *Angew. Chem. Int. Ed. Engl.* **1997**, *36*, 432.

[2] a) Jubian, V.; Dixon, R. P.; Hamilton, A. D. *J. Am. Chem. Soc.* **1992**, *114*, 1120. b) Smith, J.; Ariga, K.; Anslyn, E. V. *J. Am. Chem. Soc.* **1993**, *115*, 362. c) Muche, M.-S.; Kamalaprija, P.; Gobel, M. W. *Tetrahedron Lett.* **1997**, *38*, 2923.

RNA cleavage have therefore been designed, as shown in Fig. 3.1.

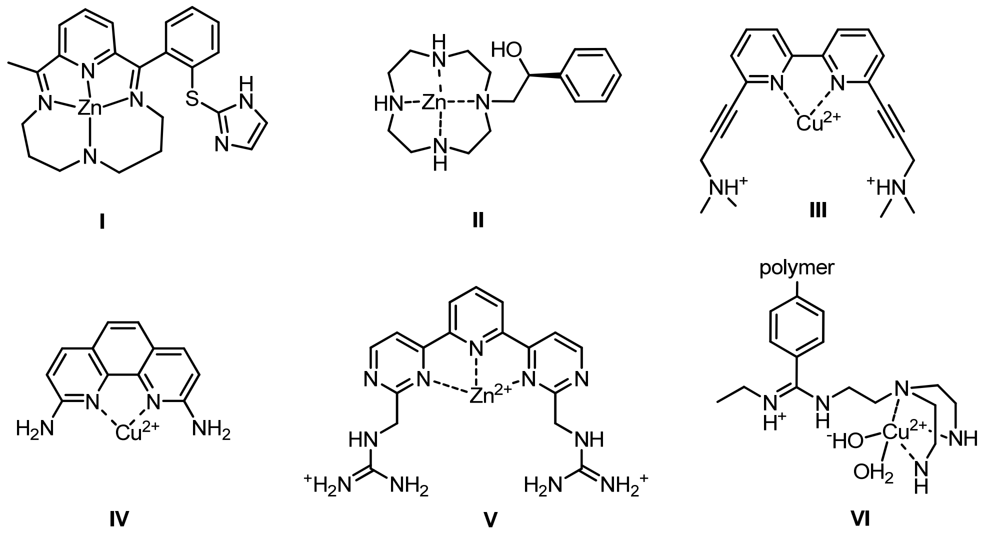

Fig. 3.1: Reported cooperative catalysts for phosphodiester hydrolysis.

In the first step of hydrolysis of RNA, transesterification of the phosphodiester by the 2'-OH group takes place to give rise to a 2',3'-cyclic phosphodiester that is hydrolyzed in the second step (nucleophilic attack of a water molecule) (Fig. 3.2). This process takes place in the enzyme active site where phosphodiester is bound to two guanidiniums of arginine residues and one calcium cation fixed to aspartate residues. A water molecule is activated as nucleophile by the carboxylate residue of glutamate while calcium and guanidinium cations stabilize the phosphorane-like transition state; proton transfer from guanidinium cation to phosphorane is likely.[3]

---

[3] Perreault, D. M.; Cabell, L. A.; Anslyn, E. V. *Bioorg. Med. Chem.* **1997**, *5*, 1209.

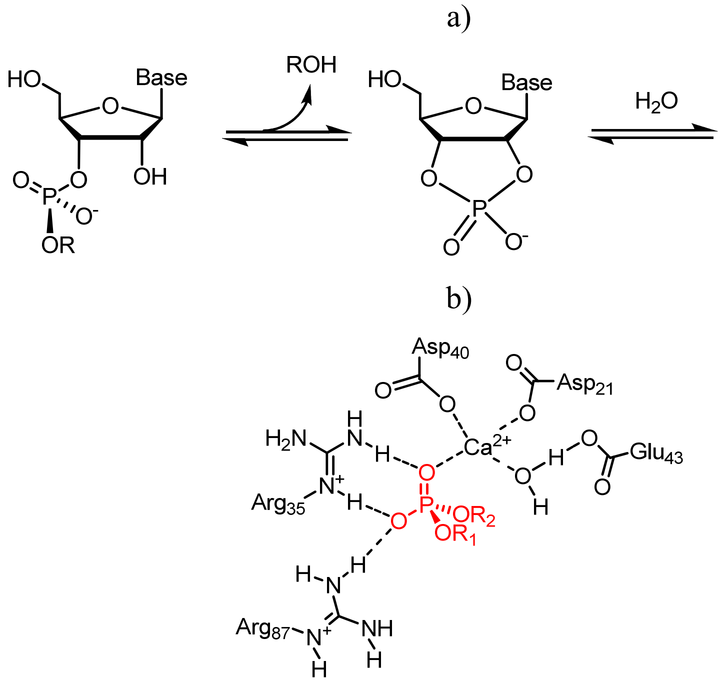

Fig. 3.2: a) Simplified mechanism of phosphodiester hydrolysis;
b) Schematic representation of the active site of SNase.

Breslow *et al.* pioneered work on an artificial bifunctional catalyst able to reproduce the cooperativity observed between a base and a metal in enzymatic systems.[4] **I** indeed bears an imidazole functionality and a Zn binding site, located at suitable distances through a rigid enough spacer (avoided catalyst collapsing), which enable the cyclization *via* transesterification of **VII** (Fig. 3.3). The metal ion is then responsible for the activation of the phosphodiester as electrophile and imidazole for the activation of the hydroxyl group as a nucleophile (OH deprotonation). *p*-

---

[4] Breslow, R.; Berger, D.; Huang, D.-L. *J. Am. Chem. Soc.* **1990**, *112*, 3686.

nitrophenol is often used as a good leaving group in these model reactions due to its high acidity. 20-fold rate acceleration with respect to the reaction catalyzed by a imidazole free Zn(II) complex could be achieved, showing the cooperative effect brought by the imidazole.

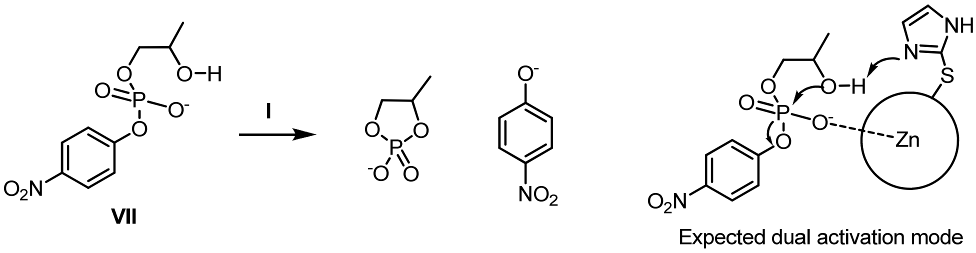

Fig. 3.3: Intramolecular cyclization of **VII** by **I**-catalyzed transesterification.

Five years later, Kimura and co-workers reported a functionalized Zn-cyclen able to cleave phosphodiesters, thus elucidating part of the action mechanism of alkaline phosphatase.[5] System **II** however could not be used as a catalyst, since it could not be reactivated, but did prove that the simultaneous action of the metal and a hydroxy residue (from Ser102 in the natural enzyme) is at the origin of the enzymatic activity. These studies also proved the essential role of pH in such reactions. A phosphoryl intermediate **II'** is created upon attack of the hydroxy group that is deprotonated in physiological conditions and is then hydrolyzed by the Zn-OH intermediate that only forms in alkaline media (Fig. 3.4).

---

[5] Kimura, E.; Kodama, Y.; Koike, T.; Shiro, M. *J. Am. Chem. Soc.* **1995**, *117*, 8304.

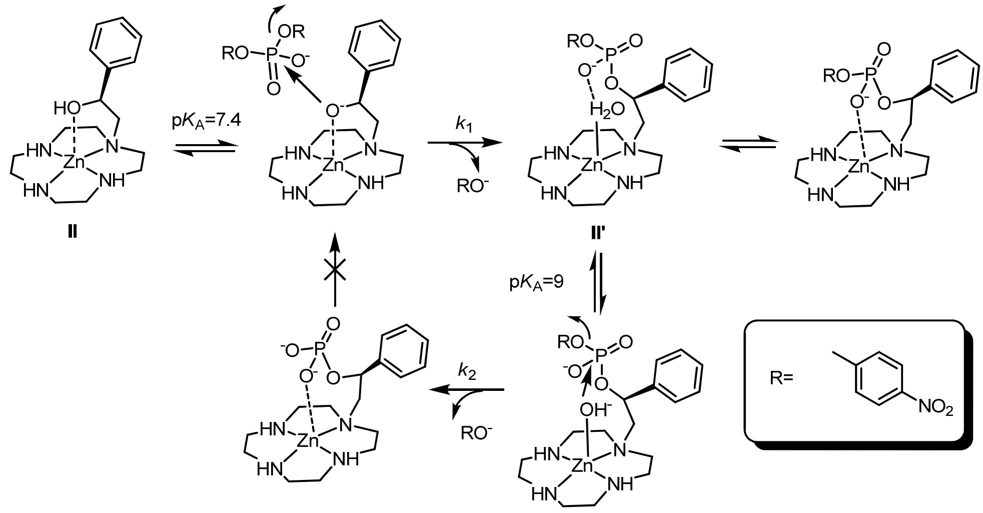

Fig. 3.4: Mechanism of phosphodiester hydrolysis by **II.**

In 1996, Krämer and Kövári reported a catalyst made of a bipyridine core substituted with two amine groups for the hydrolysis of **VIII**.[6] An impressive 4 × 10^7 fold rate acceleration for the hydrolysis of **VIII** could be obtained (Fig. 3.5).

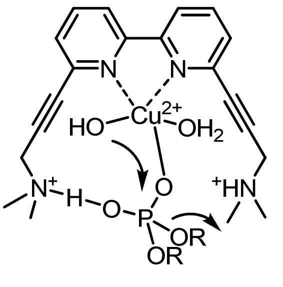

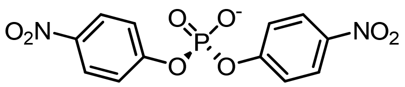

VIII

Fig. 3.5: Proposed mechanism for the hydrolysis of **VIII** by **III.**

---

[6] Kövári, E.; Krämer, R. *J. Am. Chem. Soc.* **1996**, *118*, 12704.

This unpreceeded efficiency was attributed to the presence of the ammonium groups which form hydrogen bonds with the metal coordinated phosphodiester and thus provide an additional electrostatic activation. Hydrolysis begins by the nucleophilic attack of the metal hydroxide to the phosphorus, thus releasing an alcoholate.

Linkletter and Chin reported in 1999 the first artificial cooperative catalyst for the cleavage of RNA. **IV** was indeed shown to induce a 10^9-fold rate acceleration with respect to the copper(II) hydroxide catalyzed experiment for the hydrolysis of 2',3'-cyclic adenosine monophosphate (Fig. 3.6).[7] The amino groups present in **IV** were shown to lower the pK_a of the water molecules coordinated to Cu(II), showing the existence of hydrogen bonds between the amine groups and the water molecules coordinated to the metal ion. These hydrogen bonds were also shown to play an important role in the reaction mechanism, since nucleophilicity of metal-hydroxide is significantly modified by the hydrogen bonding, therefore facilitating the hydrolysis process of 2',3'c-AMP.

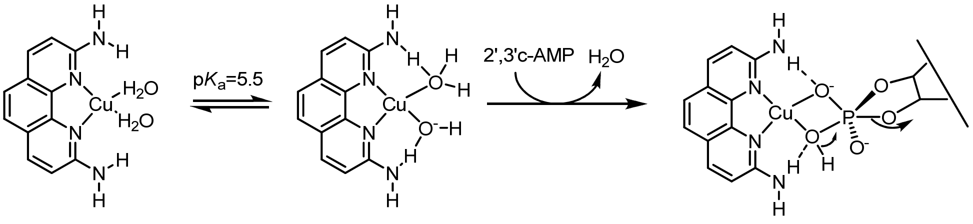

IV

Fig. 3.6: Proposed mechanism of 2',3'c-AMP hydrolysis catalyzed by **IV.**

---

[7] Wall, M.; Linkletter, B.; Williams, D.; Lebuis, A.-M.; Hynes, R. C.; Chin, J. *J. Am. Chem. Soc.* **1999**, *121*, 4710.

Inspired by these results, Anslyn and co-workers reported catalyst **V** in 2002, for which high cooperativity between the Zn(II) cation and the guanidinium groups was observed for the hydrolysis of phosphodiesters.[8] The mechanism is similar to the one described by Chin, that is to say that guanidinium groups not only help in activating the metal hydroxide (pK_a lowering) but also form strong hydrogen bonds with the transition state of the reaction (Fig. 3.7). A 3300-fold rate enhancement was obtained for the hydrolysis of 2',3'c-AMP with respect to an experiment performed with a guanidine free analog of **V**. This catalyst was however used in supstoichiometric amounts, which means that no turnover was possible.

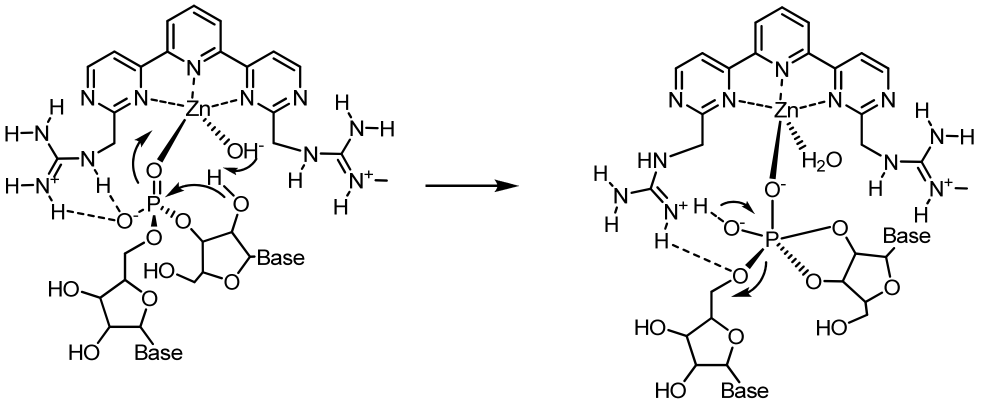

Fig. 3.7: Cooperative working fashion of metal and hydrogen bonds in phosphodiester hydrolysis.

This cooperative behaviour was then translated to molecularly imprinted polymers by Wulff *et al.*. Polymer **VI** is indeed functionalized with an amidinium group linked to a Cu(II) coordinating group and is formed in presence of a template. This polymer was used for the hydrolysis of carbonates and proved highly efficient since a 110000-fold rate enhancement could be obtained with respect to the uncatalyzed process in the hydrolysis of model substates.[9]

---

[8] Aït-Haddou, H.; Sumaoka, J.; Wiskur, S. L.; Folmer-Andersen, J. F.; Anslyn, E. V. *Angew. Chem. Int. Ed.* **2002**, *41*, 4013.

At the biological level as in supramolecular chemistry, cooperativity describes how the binding of one ligand can influence the receptor's affinity towards further binding interactions (allosteric effects).[10] Positive cooperativity implies increased further binding affinity upon ligand binding, while, on the contrary, negative cooperativity refers to decreased binding affinity. Non-cooperativity therefore refers to identical binding affinity for further ligand. The best known example in a biological system is the allosteric oxygenation of hemoglobin.[11] This tetrameric protein binds four individual oxygen molecules with increasing affinity until all four binding sites are occupied in a positively cooperative manner. In the catalysis field, cooperativity refers to dual activation of electrophile and/or nucleophile, which often leads to higher reactivities and/or selectivities.[12] Most organocatalysts are also based on bifunctionality for dual activation (*e.g.* proline and functionalized thioureas).[13]

---

[9] Liu, J. Q.; Wulff, G. *J. Am. Chem. Soc.* **2006**, *126*, 7452.

[10] a) Ercolani, G. *J. Am. Chem. Soc.* **2003**, *125*, 16097. b) Badjić, J. D.; Nelson, A.; Cantrill, S. J.; Turnbull, W. B.; Stoddart, J. F. *Acc. Chem. Res.* **2005**, *38*, 723.

[11] Eaton, W. A.; Henry, E. R.; Hofrichter, J.; Mozzarelli, A. *Nat. Struct. Biol.* **1999**, *6*, 351.

[12] For a complete review on bimetallic dual activation see: Cahard, D.; Ma, J.-A. *Angew. Chem. Int. Ed.* **2004**, *43*, 4566.

[13] Reviews on organocatalysis: a) Dalko, P. I., Moisan, L. *Angew. Chem. Int. Ed.* **2004**, *43*, 5138. b) Takemoto, Y. *Org. Biomol. Chem.* **2005**, 4299.

In order to study the dual activation of 2-(5*H*)-furanone in its pyrrolidine Michael addition by metal-substrate and hydrogen bonding interactions, scaffolds **14a-c** were chosen because of the known ability of porphyrins to accommodate a wide range of metals and their easy functionalization.

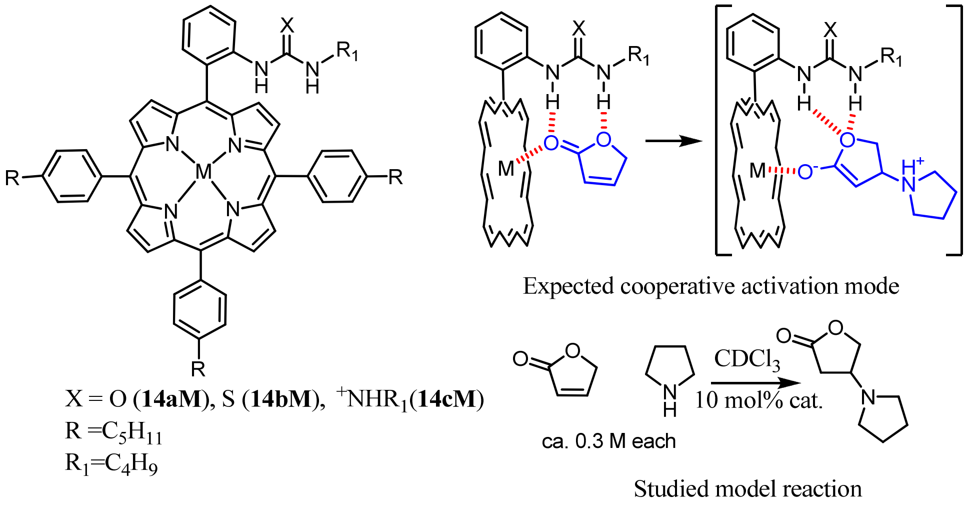

X = O (**14aM**), S (**14bM**), $^+$NHR$_1$(**14cM**)
R =C_5H_{11}
R$_1$=C_4H_9

Expected cooperative activation mode

Studied model reaction

Fig. 3.8: Designed systems **14a-c** (**M** = metal) and expected dual activation.

On the one hand, this scaffold enables metal screening experiments since porphyrins can easily be metallated with a wide range of metals. The porphyrin skeleton can also be functionalized with hydrogen bond donor groups such as urea, thiourea[14] and guanidinium, allowing for screening the H-bond donor abilities. Lactone activation is then expected to take place in a cooperative way thanks to both interactions.

---

[14] Urea and thiourea porphyrins in carbohydrate recognition: a) Kim, Y.-H.; Hong, J. *Angew. Chem. Int. Ed.* **2002**, *41*, 2947. b) Ladomenou, K.; Bonar-Law, R. P. *Chem. Commun.* **2002**, 2108. c) Rusin, O.; Hub, M.; Král, V. *Materials Science & Engineering* **2001**, C18, 135.

3.2 Results and discussion.

3.2.1 Synthesis of functionalized porphyrin derivatives 14aH-14cH.

Retrosynthetic analysis of the designed compounds was performed in collaboration with Dr. P. Ballester's group[†,15]. Following known procedures, the formation of H-bonding groups is expected to take place from amine **15**, easily accessible from the nitro porphyrin derivative **16** (Fig. 3.9).

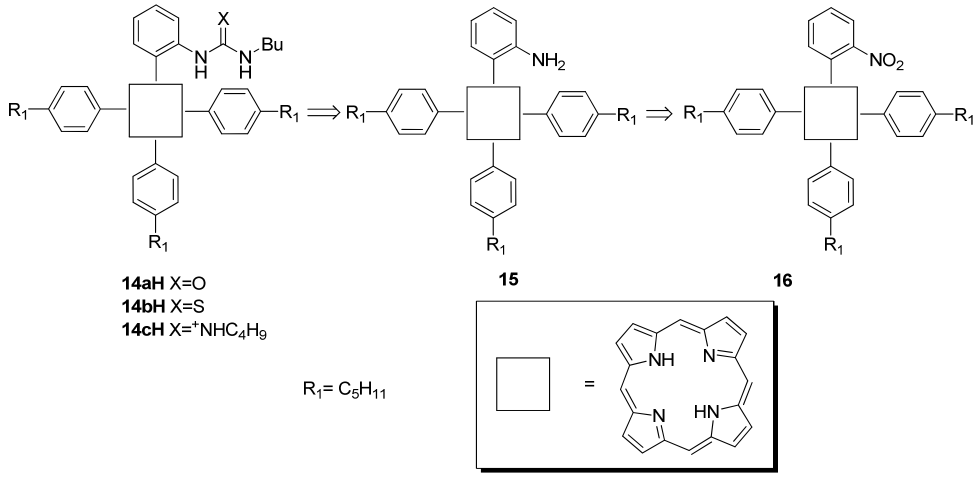

Fig. 3.9: Retrosynthetic analysis of porphyrins **14aH-14cH.**

[†] Institut Català d'Investigació Química (ICIQ), Tarragona.

[15] Gomila Ribas, R. *PhD Thesis*, Universitat de les Illes Balears, **2004**.

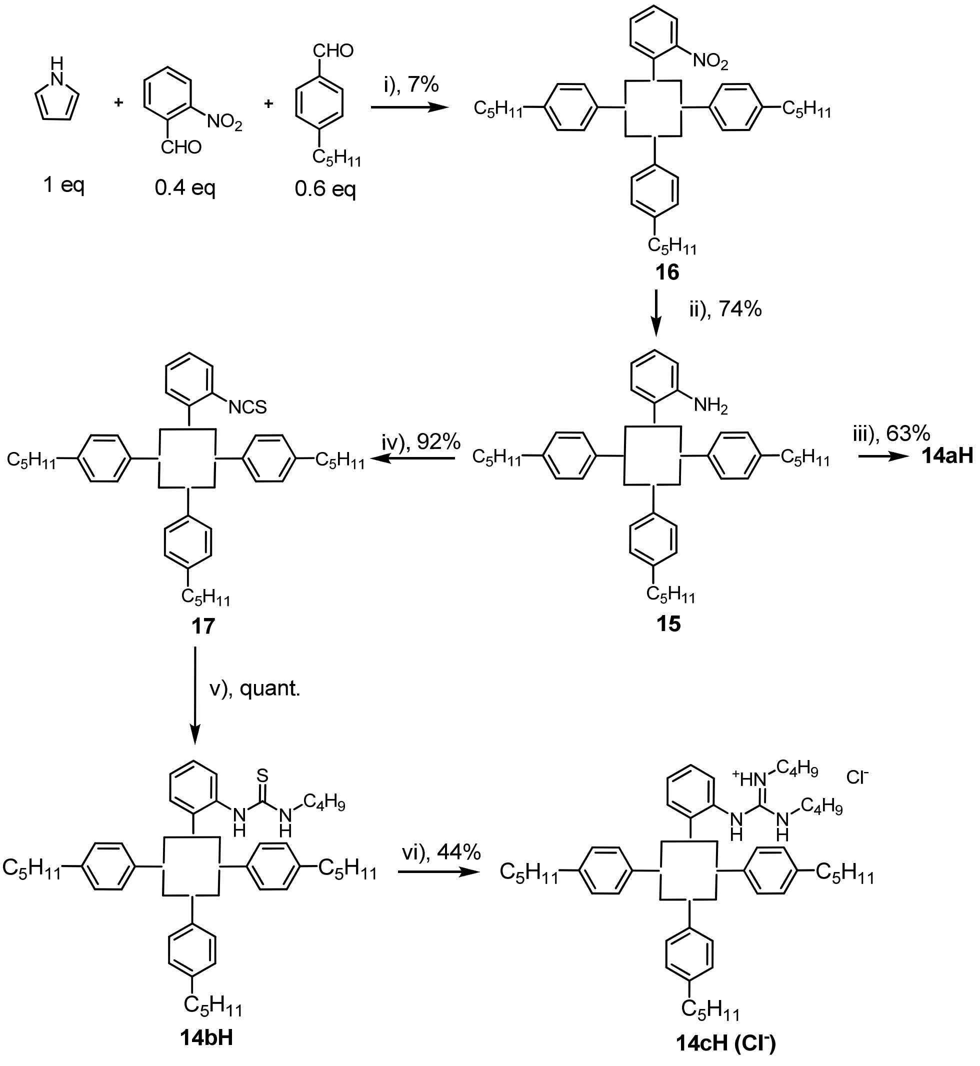
1 eq
0.4 eq
0.6 eq
i), 7%
16
ii), 74%
15
iii), 63%
14aH
iv), 92%
17
v), quant.
14bH
vi), 44%
14cH (Cl⁻)

i) $BF_3.Et_2O$, CH_2Cl_2 then DDQ, NEt_3; ii) $SnCl_2$, 1,4 dioxane, HCl, 70ºC; iii) BuNCO, CH_2Cl_2; iv) $CSCl_2$, Na_2CO_3, CH_2Cl_2, H_2O; v) $BuNH_2$; vi) TfOMe, CH_2Cl_2, microwave, then $BuNH_2$, Δ

Fig. 3.10: Synthesis of porphyrins **14aH-14cH.**

Compound **16** was obtained following a statistical porphyrin synthesis from 2-nitrobenzaldehyde, pyrrole and 4-pentylbenzaldehyde, leading to the mono-nitroporphyrin derivative **16** isolated in 7% yield from a mixture of compounds after column chromatography (Fig. 3.10). Tetra 4-pentylphenylporphyrin **TPPP** was also isolated in 15% yield; and regioisomers of dinitroporphyrins and trinitroporphyrin were detected but not isolated. The nitro group of **16** was then reduced in acidic medium by tin (II) chloride to the corresponding aminoporphyrin **15** (a key intermediate), isolated in 74% yield after chromatography. This amine derivative was treated with butylisocyanate in a sealed tube for three days to form the resulting ureidoporphyrin **14aH**, isolated in 63% yield after column chromatography.

Remarkably, treatment of **15** with excess butylisothiocyanate in a sealed tube or under microwave irradiation leads to recovery of unreacted **15**. The lack of reactivity was attributed to the tendency of porphyrins to aggregate in solution (crowded amino group). This issue was overcome by formation of isothiocyanatoporphyrin **17** by treatment of **15** with thiophosgene (93% yield after column chromatography). Thiourea **14bH** was then obtained in nearly quantitative yield by treatment of **17** with butylamine in absence of solvent. Preparation of **14cH** proved only efficient upon activation of thiourea **14bH** with methyl trifluoromethanesulfonate followed by treatment with butylamine under microwave irradiation. Several strategies for the direct guanidylation of **15** proved unsuccessful (Fig. 3.11).[16]

---

[16] a) Feichtinger, K.; Zapf, C.; Sings, H. L.; Goodman, M. *J. Org. Chem.* **1998**, *63*, 3804. b) Mundla, S. R.; Wilson, L. J.; Klopfenstein, S. R.; Seibel, W.; Nikolaides, N. N. *Tetrahedron Lett.* **2000**, *41*, 6563.

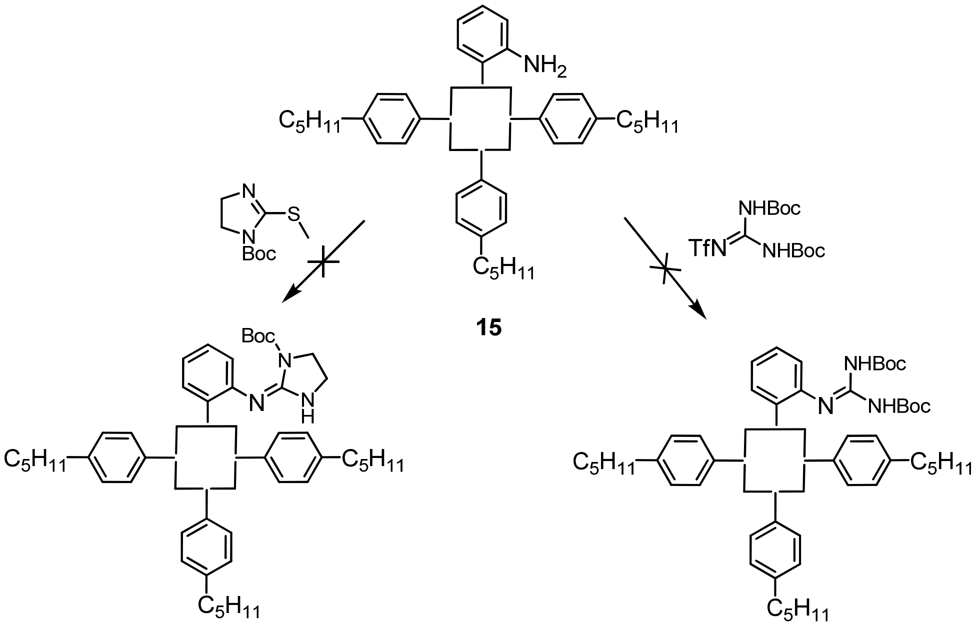

Fig. 3.11: Attempts for direct guanidylation of **15.**

In order to compare the efficiency of the prepared covalent derivatives with equivalent systems for which the H-bonding moiety and metalloporphyrin are not covalently linked, model compounds were also prepared, as shown on Fig. 3.12. This aimed at studying the cooperativity of the prepared bifunctional catalysts. The urea derivative **19** was obtained by treatment of aniline with butylisocyanate in a sealed tube in 84% yield after column chromatography (as performed for **14aH**). Following the same route as for **14bH**, phenylisothiocyanate was obtained by treatment of aniline with thiophosgene. Treatment of the resulting isothiocyanate in neat butylamine afforded thiourea **18** in 83% overall yield after column chromatography. Compound **2**, described in the previous chapter, was used for comparisons with **14cH**.

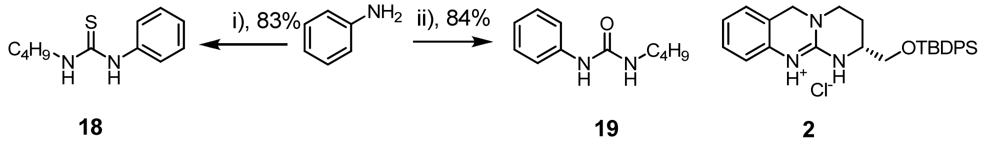

i) $CSCl_2$, Na_2CO_3, CH_2Cl_2, H_2O then $C_4H_9NH_2$; ii) C_4H_9NCO, CH_2Cl_2, sealed tube

Fig.3.12: Synthesis of model compounds for cooperativity study.

3.2.2 Metallation of porphyrin derivatives 14aH-14cH.

Treatment of free base porphyrin derivatives with an appropriate metal salt leads to the formation of the corresponding metalloporphyrin derivative. Zinc(II), nickel(II), magnesium(II) and tin(IV) porphyrin derivatives were thus prepared, as shown in Table 3.1, according to known procedures.[17]

Table 3.1: Metallation of studied porphyrin derivatives.

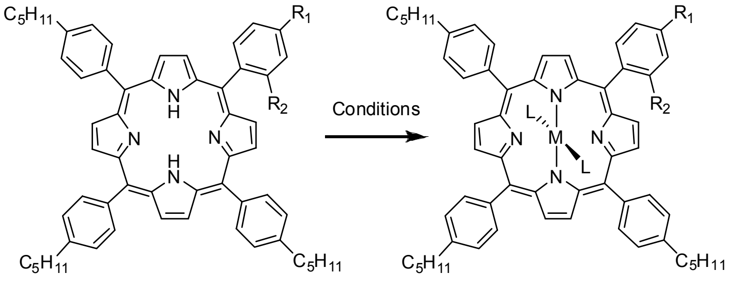

---

[17] Procedures for preparation of Zn(II), Ni(II), and Mg(II) porphyrins: a) Strohmeier, M.; Orendt, A. M.; Facelli, J. C.; Solum, M. S.; Pugmire, R. J.; Parry, R. W.; Grant, D. M. *J. Am. Chem. Soc.* **1997**, *119*, 7114. Procedure for preparation of Sn(IV) porphyrins: b) Crossley, M. J.; Thordarson, P., Wu, R. A.-S. *J. Chem. Soc., Perkin Trans. 1* **2001**, 2294.

R_1	**R_2**	**conditions**	**M**	**L**	**yield (%)**
C_5H_{11}	H	*(a)*	Zn(II)	-	90 **ZnTPPP**
H	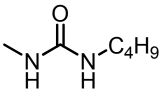	*(a)*	Zn(II)	-	81 **14aZn**
C_5H_{11}	H	*(b)*	Ni(II)	-	78 **NiTPPP**
C_5H_{11}	H	*(c)*	Mg(II)	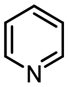	98 **MgPy₂TPPP**
C_5H_{11}	H	*(d)*	Mg(II)	-	decomposition **MgTPPP**
C_5H_{11}	H	*(e)*	Sn(IV)	Cl	91 **SnCl₂TPPP**
C_5H_{11}	H	*(f)*	Sn(IV)	OH	100 **Sn(OH)₂TPPP**
H	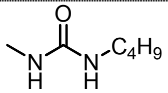	*(e)*	Sn(IV)	Cl	85 **14aSnCl₂**
H	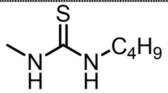	*(e)*	Sn(IV)	Cl	93 **14bSnCl₂**
H	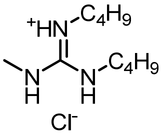	*(e)*	Sn(IV)	Cl	n.m. **14cSnCl₂**

(a) $Zn(OAc)_2$, CH_2Cl_2, MeOH, room temperature; *(b)* Ni $(OAc)_2$, CH_2Cl_2, MeOH reflux; *(c)* $MgClO_4$, Pyridine, reflux; *(d)* ΔΔ, high vacuum (from **MgPy₂TPPP**); *(e)* $SnCl_2$, Pyridine; *(f)* K_2CO_3, THF, H_2O (from **SnCl₂TPPP**)

The metal was selected by its known affinity for oxygen ligands, its hardness and the ease of porphyrin metallation. Zinc porphyrins are readily available and highly stable, which makes them potential catalysts of choice. However, upon insertion of Zn(II) to **14aH**, unexpected conformational changes take place. ^{1}H NMR monitoring of the aromatic proton adjacent to the urea (H_o) in **14aH** and **14aZn** indicates that urea's oxygen is coordinated intramolecularly to the metal center. As shown in Fig. 3.13, the signal of H_o is upfield shifted upon metal insertion, indicating that the carbonyl group of the urea is no longer close to H_o in **14aZn** as it was in **14aH**. Additionnally, the downfield shift observed for the NHs in **14aZn** reveals that the urea is close to an electron withdrawing group. The likely conformation of **14aZn** was confirmed by 2D NMR experiments (COSY, NOESY).

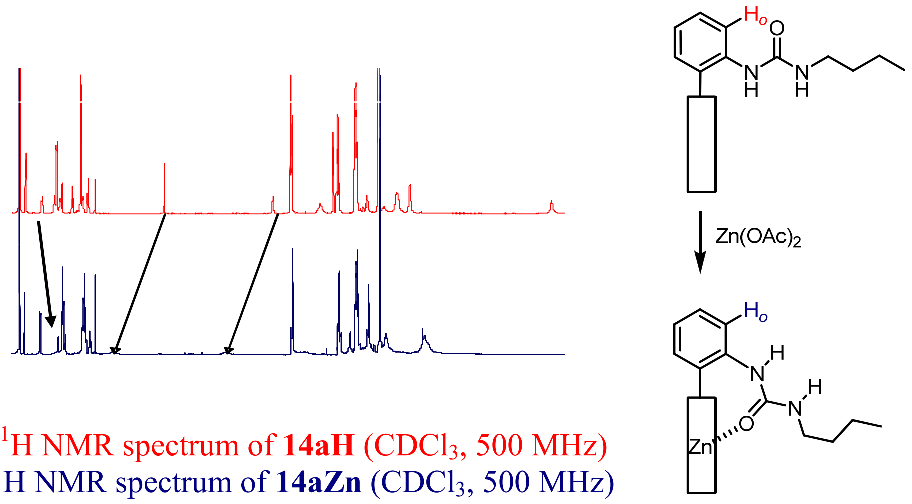

^{1}H NMR spectrum of **14aH** (CDCl$_3$, 500 MHz)
^{1}H NMR spectrum of **14aZn** (CDCl$_3$, 500 MHz)

Fig. 3.13: Intramolecular metal coordination in **14aZn.**

This undesired coordination is likely to compete with substrate coordination in catalysis experiments. Competition experiments with acetate as a guest were performed to see if the addition of an external coordinating agent would remove the intramolecular coordination. Indeed, addition of acetate[18] partially removed the intramolecular coordination (Fig. 3.14). Several complexes of various stoichiometries are however expected to form at equilibrium, which might explain the complexity of some signals in the ^{1}H NMR spectrum.

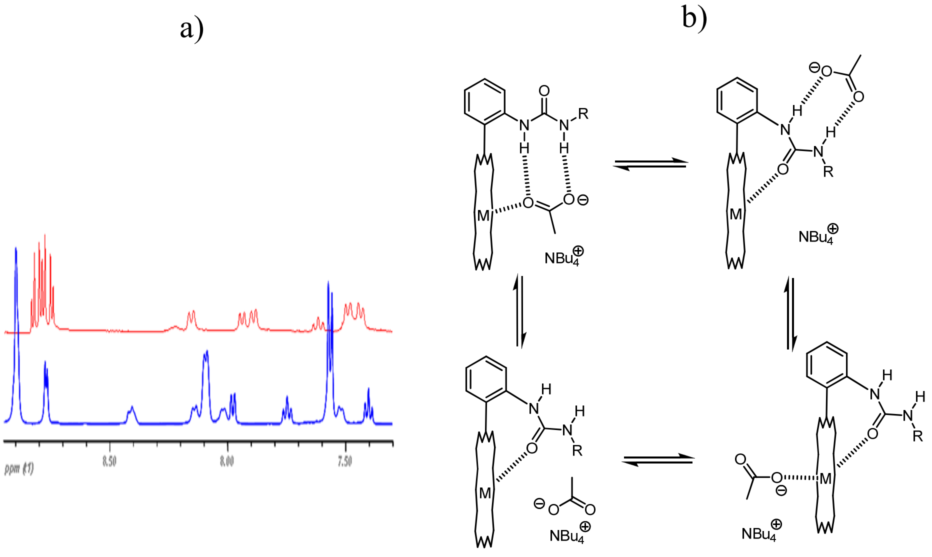

Fig. 3.14: a) Binding of **14aZn** with acetate: ^{1}H NMR spectra ($CDCl_3$, 500 MHz) of free **14aZn** (blue) and with 10 eq. of acetate (red); b) Possible conformations of a 1:1 **14aZn**-TBA.AcO$^-$ complex.

Various binding experiments with some reaction substrates were also performed in order to screen the optimal metals. A suitable metal for catalysis is expected to shown higher affinity for 2-(5*H*)-furanone than for pyrrolidine. ^{1}H NMR titrations, ITC and UV-Vis experiments were run, but no direct conclusion could be drawn. However, a UV-Vis titration of

---

[18] 10 equivalents were used to reproduce the conditions of the catalysis experiments where 10 mol% of catalyst would be used.

ZnTPPP with pyrrolidine revealed an association constant of 4 × 10^4 M^{-1} (Fig. 3.15).[19]

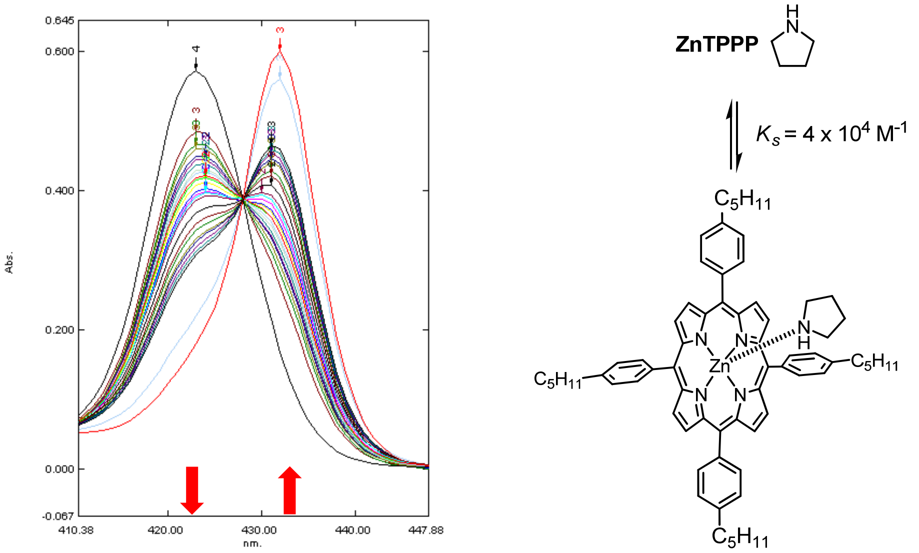

Fig. 3.15: UV-Vis monitored titration of **ZnTPPP** with pyrrolidine.

Given the difficulty to accurately measure the binding constants between our metalloporphyrins and the substrates of the reaction, it was decided to perform catalysis experiments for metal screening.

3.2.3 Metal screening experiments.

Kinetic measurements of the 1,4-addition of pyrrolidine to 2-(5*H*)-furanone in the presence of 10 mol% of the metalloporphyrin derivative were monitored by ^{1}H NMR as described in the previous chapter. Stock solutions of distilled substrates[20] were used in order to ensure reproducibility of results (same water content in all experiments) and measurements were performed in the minimal interval of time.

---

[19] Zn(II)-porphyrins are well known for their axial coordination of nitrogen bases, typically pyridine, DABCO... A similar experiment performed with 2-(5*H*)-furanone gave no optical response.

3.2.3.1 Zinc(II) porphyrins.

Instead of a catalyst, **14aZn** proved to be a strong inhibitor of the reaction, as shown on Fig. 3.16. Intramolecular coordination of urea's oxygen to the zinc efficiently competes with the coordination of the substrates and favors exclusively the coordination of pyrrolidine, resulting in a decreased effective concentration, thus leading to the observed reaction slowering. Indeed, an experiment performed in the presence of catalytic amounts of **ZnTPPP** shows a kinetic profile similar to uncatalyzed experiment, which suggests that the activation of 2-(5*H*)-furanone is cancelled by coordination of the pyrrolidine to the metal. As expected, quinuclidine ($pK_a = 11.3$) also catalyzes the reaction[21], since a 1.27-fold rate acceleration is observed. It was also expected that, in the presence of **ZnTPPP** and a tertiary amine such as quinuclidine (competitive metal binding), the amount of metal-bound pyrrolidine would decrease, giving rise to an enhanced catalytic activity. The results show, however, that quinuclidine does not displace the coordinated pyrrolidine to a significant extent, since an intermediary reaction half-time is observed (1.17-fold acceleration). Given the results obtained with quinuclidine, it was not surprising to observe a 1.67-fold rate acceleration in the presence of **TPPP**.

---

[20] Distillation was performed in an oven glass and substrates were not dried. Experimental methods and water sensitivity of the reaction were discussed in the previous chapter.

[21] Participation of bases in the mechanism was discussed in Chapter 2.

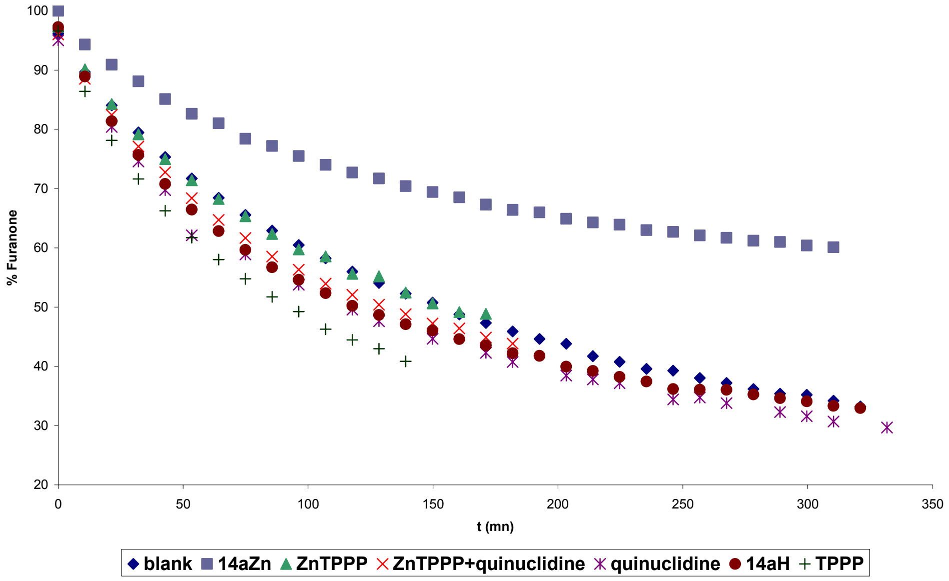

Catalyst (10 mol %)	$t_{1/2}$ (min)	Acceleration
none	150	-
14aZn	> 250	<1
ZnTPPP	150	1
ZnTPPP+quinuclidine	128	1.17
14aH	118	1.27
TPPP	90	1.67
quinuclidine	118	1.27

Fig. 3.16: Kinetic measurements and control experiments for Zn(II)-porphyrins.

This rate acceleration was attributed to the basicity of the inner nitrogen atoms of the porphyrin (pK_a around 16) that might enter in the base assisted mechanism of the reaction. In the presence of **14aH**, a moderate rate enhancement was observed (1.27-fold), which might be attributed to the steric congestion caused by the urea and/or to alteration of the pK_a of the free base porphyrin by the urea group. These results show however that zinc is not a suitable metal.

3.2.3.2 Nickel(II) porphyrins.

Similar to **ZnTPPP**, the kinetic profile in the presence of a 10 mol% amount of **NiTPPP** overlays the one of the uncatalyzed reaction, which either indicates that no activation takes place or that lactone activation is cancelled by the binding of pyrrolidine to the metal, as for Zn(II). Although axial coordination to nickel(II) porphyrins is known[22], coordination of reaction substrates could not be demonstrated by spectroscopic methods.

3.2.3.3 Magnesium(II) porphyrins.

Results reveal that **MgPy$_2$TPPP** tends to slower significantly the reaction, which is attributed to a fast ligand exchange of the axially coordinating pyridine with pyrrolidine, while 2-(5*H*)-furanone does not exchange with pyridine or exchange more slowly. A control experiment performed in presence of 20 mol% pyridine (maximal pyridine amount released upon axial substrate coordination) shows that pyridine ($pK_a = 5.14$) also catalyzes the reaction, though its lower basicity makes it a worse catalyst than pyrrolidine (hence the observed inhibition with **MgPy$_2$TPPP**) (Figs. 3.17 and 3.18).

---

[22] a) Retsek, J. L.; Drain, C. M.; Kirmaier, C.; Nurco, D. J.; Medforth, C. J.; Smith, K. M.; Sazanovich, I. V.; Chirvony, V. S.; Fajer, J.; Holten, D. *J. Am. Chem. Soc.* **2003**, *125*, 9787. b) Song, Y.; Haddad, R. E.; Jia, S.-L.; Hok, S.; Olmstead, M. M.; Nurco, D. J.; Schore, N. E.; Zhang, J.; Ma, J.-G.; Smith, K. M.; Gazeau, S.; Pécaut, J.; Marchon, J.-C.; Medforth, C. J.; Shelnutt, J. A. *J. Am. Chem. Soc.* **2005**, *127*, 1179.

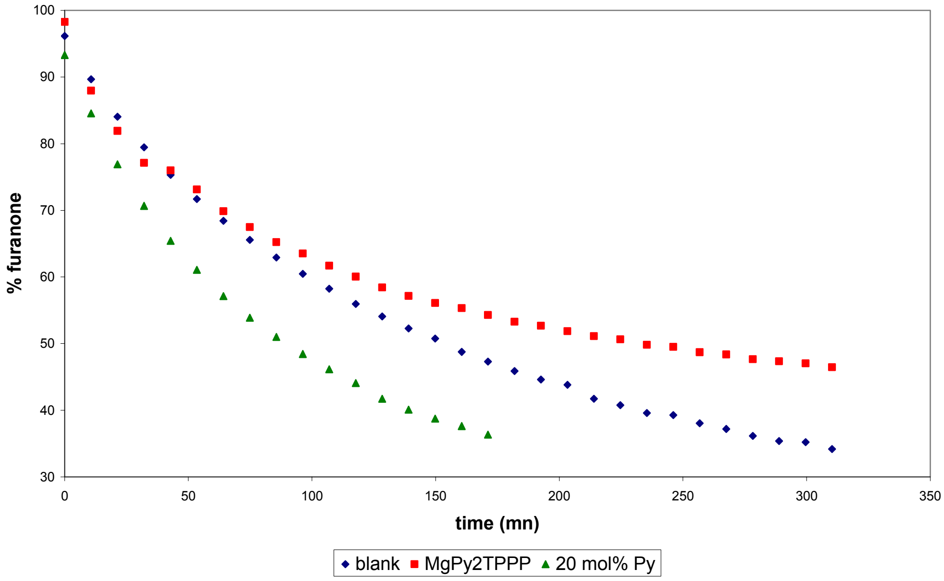

Catalyst (10 mol%)	$t_{1/2}$ (min)	Acceleration
none	150	-
MgPy$_2$TPPP	225	<1
Pyridine (20 mol%)	86	1.74

Fig. 3.17: Kinetic measurements and control experiments for Mg(II) porphyrin derivatives.

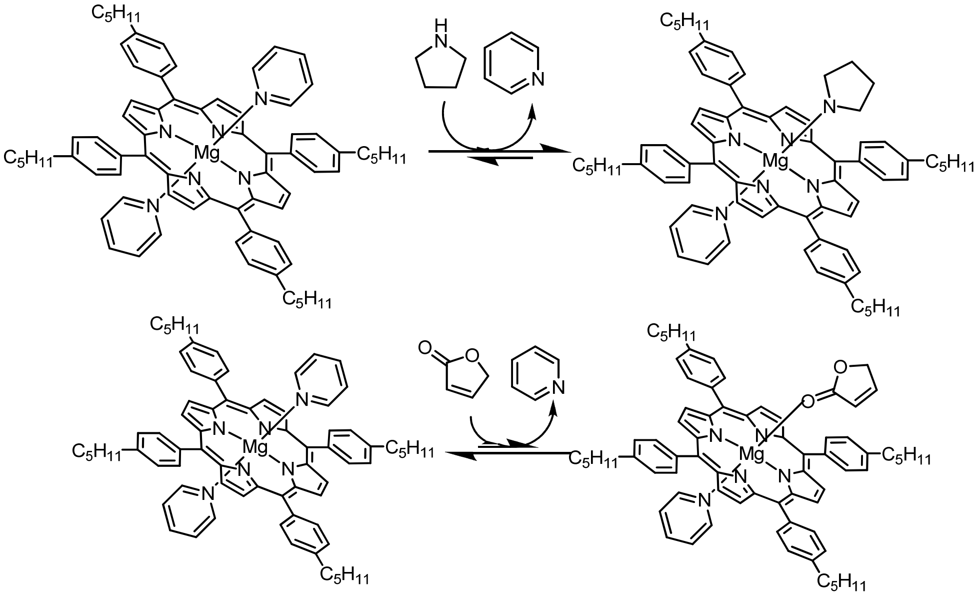

Fig. 3.18: Proposed equilibria for ligand exchange of **MgPy$_2$TPPP**.

Since magnesium is a rather hard metal, **MgTPPP** is expected to significantly accelerate the reaction. Mg (II)-porphyrins however tend to accomodate axial ligands: preparation of **MgTPPP** was indeed poorly reproducible and decomposition was observed after heating of **MgPy$_2$TPPP** under vacuum (removal of pyridine axial ligands). Axially uncoordinated Mg(II)-porphyrins proved to be unstable catalysts and easy to get contaminated by moisture, which produces unaccurate results since water is also a catalyst for the reaction (experiments were not reproducible).

3.2.3.4 Tin(IV) porphyrins.

Sn(IV) being a highly oxophilic transition metal, a significant lactone activation was expected.[23] Tin(IV) porphyrins are readily available and air stable species, which also makes them candidates of choice.

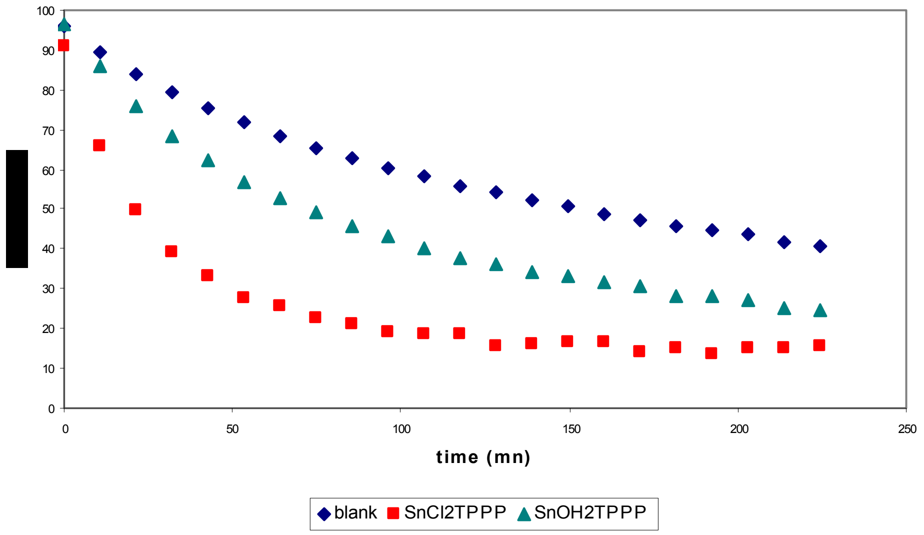

Catalyst (10 mol%)	**$t_{1/2}$ (min)**	**Acceleration**
none	150	-
$SnCl_2$TPPP	21	7.14
$Sn(OH)_2$TPPP	74	2.03

Fig. 3.19: Kinetic measurements performed with tin(IV) porphyrins.

As expected, tin porphyrins significantly increase the rate of the studied Michael addition. Up to 7.14-fold rate accelerations could be obtained in the case of dichlorotin(IV) tetraarylporphyrin, which is a good example of catalysis. The observed differences between dichloro and dihydroxo derivatives are attributed to the rate of ligand exchange between the metalloporphyrin and the lactone. Ligand exchange is much faster for the dichloro tin porphyrin than for the dihydroxo one, which is directly related to the respective affinity of tin(IV) for these anions: the Sn···OH bond is stronger than Sn···Cl one. Tin was then chosen for the metallation of **14aH-14cH** (see Table 3.1) and for the study of the cooperative action of the catalysts, since high turnover and activation were observed with this metal.

---

[23] Tin(IV) porphyrin catalysts were described for: Ring opening of epoxides: Moghadam, M.; Tangestaninejad, S.; Mirkhani, V.; Shaibani, R. *Tetrahedron* **2004**, *60*, 6105. Alcohol acetylation: Moghadam, M.; Tangestaninejad, S.; Mirkhani, V.; Mohammadpour-Baltork, I.; Shaibani, R. *J. Mol. Cat. A* **2004**, *219*, 73.

3.2.4 Cooperativity studies.

The catalytic activities of **14aSnCl$_2$-14cSnCl$_2$** were measured following the same protocol as for metal screening experiments, except that the catalyst loading was lowered to 1 mol% in order to slower the reaction and enable a more accurate comparison of results. The results for **14aSnCl$_2$-14cSnCl$_2$** were then systematically compared with catalysis experiments performed in the presence of 1 mol% **SnCl$_2$TPPP** and **18**, **19**, and **2**, which gives information about the benefits of the covalent linkage between the Lewis acid and the H-bonding moiety. The results are sumarized in Fig. 3.20. In the presence of 1 mol% **SnCl$_2$TPPP**, a 3-fold rate acceleration is observed, whereas in the presence of 1 mol% of a tin(IV) porphyrin substituted with a H-bonding moiety (**14aSnCl$_2$-14cSnCl$_2$**), 3.26 to 3.33-fold rate accelerations were observed. This suggests that Lewis acid and H-bonding activation modes work in a cooperative fashion in the lactone activation in the studied cases.

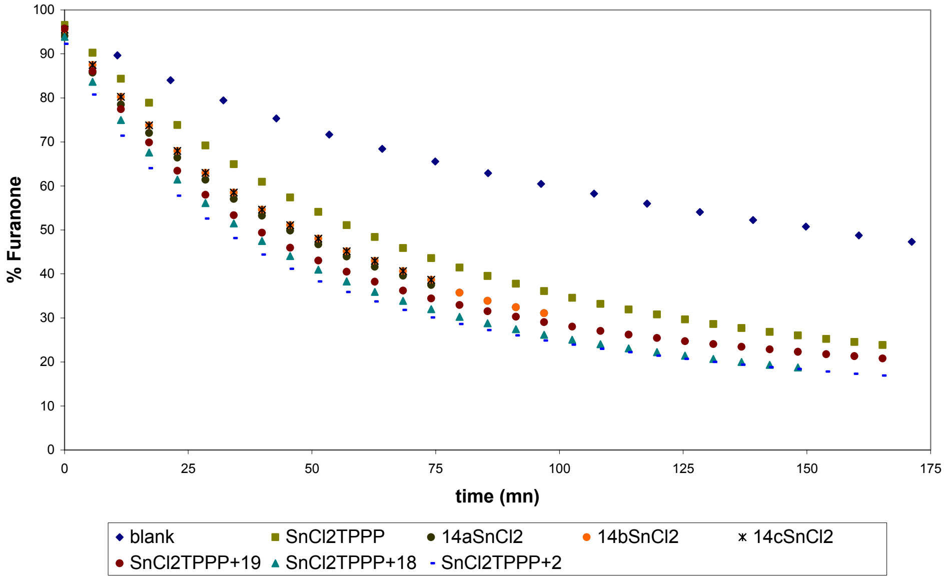

Catalyst (1 mol%)	$t_{1/2}$ (min)	Acceleration
none	150	-
$SnCl_2TPPP$	50	3
$14aSnCl_2$	45	3.33
$SnCl_2TPPP+19$	40	3.75
$14bSnCl_2$	46	3.26
$SnCl_2TPPP+18$	35	4.29
$14cSnCl_2$	46	3.26
$SnCl_2TPPP+2$	32	4.69

Fig. 3.20: Results of the kinetic measurements for cooperativity study of **$14aSnCl_2$-$14cSnCl_2$**

Remarkably, the kinetic profiles for **$14aSnCl_2$-$14cSnCl_2$** are quite similar and almost superimpose, showing that little discrimination of the H-bonding moiety is performed during the catalysis, probably due to the high participation of the Lewis acid in the substrate activation. Our results indicate that **14aSnCl₂** is a slightly better catalyst than thiourea **14bSnCl₂** or guanidinium cation **14cSnCl₂**. The reason for this is probably steric, since the H-bonding moiety is not fully coplanar, as required for an ideal orientation of the H-bonded hydrogens towards the metal bound lactone. As shown on Fig. 3.21, the twisting degree actually reflects the relative performances of the series: **14aSnCl₂** < **14bSnCl₂** ≤ **14cSnCl₂**.

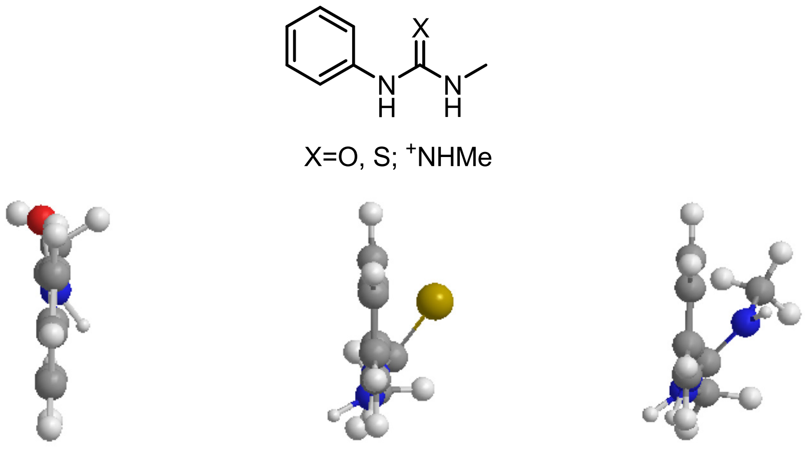

14aSnCl₂ **14bSnCl₂** **14cSnCl₂**

Fig. 3.21: Lateral views of the modelled H-bonding moieties (ChemBio3D, MMFF94).[24]

Surprisingly, when using the activating moieties as independent molecules, the general trend is to observe that the bimolecular catalytic system (**$SnCl_2$TPPP**+**18**, **19**, or **2**) is significantly more efficient than the covalent system (**14a$SnCl_2$-14c$SnCl_2$**), revealing that the position of the substituent in the covalently linked systems is not optimal and an improved design is necessary. Bimolecular system might also offer a higher turnover frequency (substrates might not bind so tightly to **$SnCl_2$TPPP** than to the bifunctional catalysts). In that case, it is observed that the catalysis performance follows the trend **19 < 18 < 2**, probably for reasons related to acidity of the H-bond donor.

---

[24] *n*-Butyl chains were replaced by methyl groups in the calculations for simplicity.

3.3 Conclusions.

Tetraarylporphyrins functionalized with various H-bonding moieties (urea, thiourea, guanidine) were successfully prepared following standard procedures of porphyrin chemistry. Unfunctionalized **TPPP** was then successfully metallated with Zn(II), Ni(II), Mg(II) and Sn(IV). Metal screening experiments were performed by kinetic measurements of the 1,4-addition of pyrrolidine to 2-(5*H*)-furanone in the presence of a 10 mol% of the metalloporphyrin derivative. Tin(IV) porphyrins appeared as candidates of choice for catalysis of the studied reaction, since up to 7.14-fold rate acceleration was observed in presence of 10 mol% catalyst. After stannylation of the functionalized porphyrins **14aH-14cH**, kinetic measurements were performed in the presence of a 1 mol% catalyst and compared with similar bimolecular catalytic systems. Cooperativity of the H-bonding moiety and the Lewis acid subunit was demonstrated, although the metal was shown to be responsible for most of the activation. Bimolecular systems also proved more efficient than the covalent systems, which was attributed to entropic factors related to the distance between the H-bond donor and the metal center and the conformation of the H-bonding moieties in the covalent systems.

3.4 Experimental part.

a) General procedures.

The general procedures for synthesis, chromatography, analysis and kinetic measurements were described in Chapter 2.

UV-Vis titration. Two standard solutions were prepared in dichloromethane, one for **ZnTPPP** ([**ZnTPPP**] = 1×10^{-6} M) and another one for both pyrrolidine and **ZnTPPP** ([**ZnTPPP**] = 1×10^{-6} M, [pyrrolidine] = 2×10^{-5} M). The titration was performed placing in the cuvette 2 mL of the solution of **ZnTPPP** and adding an increasing amount of standard solution of pyrrolidine (10 μL = 0.1 eq). After each addition, the absorbance at 400-450 nm was registered and its variation at $\lambda = 423$ nm was plotted against the concentration of pyrrolidine. Data fitting was performed using SPECFIT® software.

b) Synthesis.

5-(2-Nitrophenyl)-10,15,20-tris(4-pentylphenyl)-21*H*,23*H*-porphyrin (16).

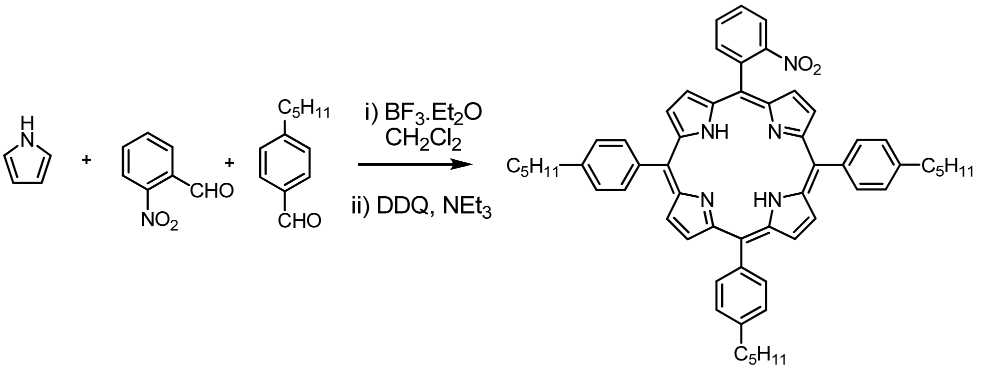

16

Procedure

A mixture of freshly distilled pyrrole (1.39 mL, 20.00 mmol), *o*-nitrobenzaldehyde (1.21 g, 8.00 mmol) and *p*-pentylaldehyde (2.11 g, 12 mmol) was dissolved in anhydrous ethanol (13 mL) and dry CH_2Cl_2 (1000 mL) and the solution was degassed by bubbling with argon for 10 min. and protected from light. $BF_3.Et_2O$ (1 mL, 6.6 mmol) was then added and the reaction was stirred at room temperature for one hour. Then 2,3-dicycano-5,6-dichloro-1,4-benzoquinone (DDQ) (4.54 g, 20 mmol) was added and the mixture was stirred at room temperature for 90 min. Triethylamine (6 mL) was added to quench the reaction. Solvent was eliminated under reduced pressure and the resulting black residue was extracted overnight with methanol in a Soxhlet device. The remaining solid was then dissolved in CH_2Cl_2 and passed through a Florisil bed (hexane/CH_2Cl_2, 1:1). After solvent elimination *in vacuo*, crude was preadsorbed on silica and purified by column chromatography on silica gel (80 g SiO_2, CH_2Cl_2/hexane, 1:2). The first product to come out from the column was the tetraalkylporphyrin derivative **TPPP** (15% yield), followed by **16** (511.6 mg, 7.6%) as violet solids that can be recrystallized from CH_2Cl_2/MeOH.

16: **M.p.** 199-201 ºC; **^{1}H NMR** (400 MHz, $CDCl_3$): δ ppm 8.88 (d, 2H, J = 7.0 Hz, H β-pyrr), 8.86 (s, 4H, H β-pyrr), 8.64 (d, 2H, J = 7.0 Hz, H β-pyrr), 8.45 (d, 1H, J = 7.0 Hz), 8.24 (d, 1H, J = 7.0 Hz), 8.10 (m, 6H), 7.95 (m, 2H), 7.50 (d, 6H, J = 7.0 Hz), 2.94 (t, 6H, J = 7.0 Hz, CH_2), 1.95 (m, 6H, CH_2), 1.50 (m, 12H, CH_2), 1.05 (t, 9H, J = 7.0 Hz, CH_3), -2.72 (s, 2H, NH); **FAB-MS**: *m/z* 870.0 [M^+]

TPPP: **^{1}H NMR** (400 MHz, $CDCl_3$): δ ppm 8.77 (s, 8H), 8.03 (d, 8H, J = 7.8 Hz), 7.46 (d, 8H, J = 7.8 Hz), 2.86 (t, 8H, J = 7.6 Hz), 1.90-1.75 (m, 8H), 1.50-1.35 (m, 16H), 0.94 (t, 12H, J = 7.0 Hz), -2.82 (broad s, 2H).

5-(2-Aminophenyl)-10,15,20-tris(4-pentylphenyl)-21*H*,23*H*-porphyrin (15).

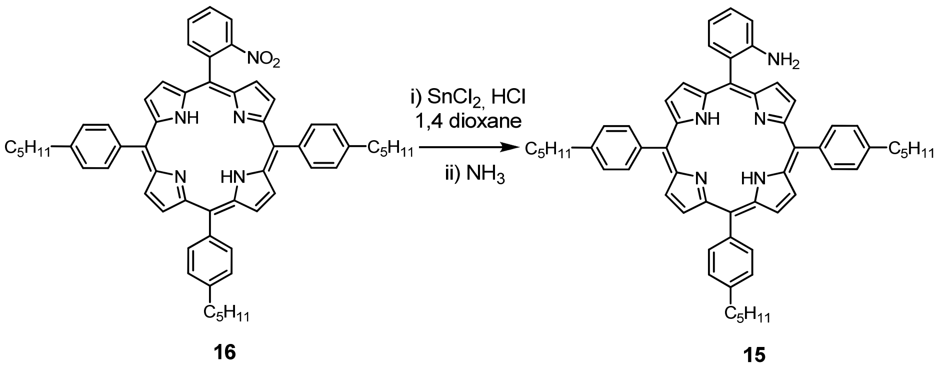

Procedure

To a solution of **16** (230 mg, 0.264 mmol) in 1,4-dioxane (50 mL), tin(II) chloride dihydrate (690 mg, 3.06 mmol) and 37% HCl (80 mL) were added. The reaction was protected from light and heated to 70 ºC for 1 h. The mixture was then basified with concentrated ammonia. Mixture was then allowed to cool to room temperature and extracted with ethyl acetate (3 × 50 mL). The combined organic phases were washed with water, dried over Na_2SO_4 and the solvent eliminated *in vacuo*. The resulting residue was purified by column chromatography on silica gel (hexane/CH_2Cl_2, 1:4), affording **15** (164 mg, 74%) as a violet solid, after recrystallization from a CH_2Cl_2/MeOH mixture. **M.p.** 169-171 ºC; **^{1}H NMR** (400 MHz, $CDCl_3$): δ ppm 8.80 (s, 8H, H β-pyrr), 8.86 (s, 4H, H β-pyrr), 8.05 (m, 6H), 7.84 (d, 1H, J = 7.0 Hz), 7.53 (t, 1H, J = 7.0 Hz), 7.50 (d, 6H, J = 7.0 Hz), 7.25 (t, 1H, J = 7.0 Hz), 7.10 (d, 1H, J = 7.0 Hz), 3.50 (s, 2H, NH_2), 2.94 (t, 6H, J = 7.0 Hz, $ArCH_2$), 1.95 (m, 6H, CH_2), 1.50 (m, 12H, CH_2), 1.05 (t, 9H, J = 7.0 Hz, CH_3), -2.8 (s, 2H, NH); **FAB-MS**: *m/z* 840.0 [M^+].

5-(2-(3-Butylureido)-phenyl)-10,15,20-tris(4-pentylphenyl)-21*H*,23*H*-porphyrin (14aH).

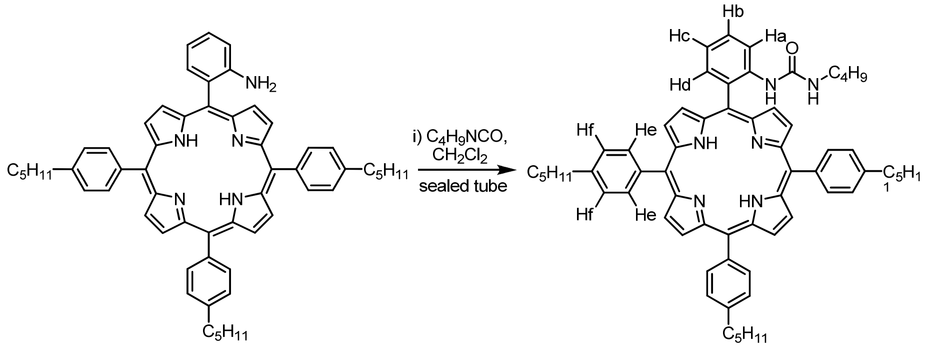
NH2
NH
N
N
HN
C5H11
C5H11
C5H11
i) C4H9NCO,
CH2Cl2
sealed tube
Hb
Hc
Ha
O
Hd
N
H
N
H
C4H9
Hf
He
Hf
He
NH
N
N
HN
C5H11
C5H11
C5H11

15 **14aH**

Procedure

To a solution of **15** (100 mg, 0.12 mmol) in dry dichloromethane (4 mL) placed in a sealed tube was added butyl isocyanate (1.2 mL, 9 eq). The reaction mixture was stirred for three days at 40 ºC. After this time, reaction was stopped and solvent eliminated *in vacuo*. The crude mixture was purified by column chromatography (CH_2Cl_2/hexane) to afford the corresponding urea porphyrin derivative **14aH** as a violet solid (70 mg, 63% yield). **M.p.** 164-166 ºC; **^{1}H NMR** (500 MHz, $CDCl_3$): δ ppm 8.90 (s, 6H, H β-pyrr), 8.76 (d, 2H, *J* = 5.0 Hz, H β-pyrr), 8.40 (m, 1H, H_a), 8.15-8.01 (m, 6H, H_e), 7.98 (d, 1H, *J* = 5.6 Hz, H_d), 7.75 (t, 1H, *J* = 6.4 Hz, H_b), 7.57-7.53 (m, 6H, H_f), 7.40 (t, 1H, *J* = 6.0 Hz, H_c), 5.70 (s, 1H, NH_{urea}), 3.37 (s, 1H, NH_{urea}), 2.97 (t, 6H, *J* = 6.0 Hz, CH_2), 2.34 (m, 2H, CH_2 Bu), 1.95 (m, 6H, CH_2), 1.56 (m, 12H, $2CH_2$), 1.01 (m, 9H, CH_3), 0.66 (broad s, 4H, 2 CH_2), 0.38 (broad s, 3H, CH_3), -2.72 (s, 2H, NH); **HR-MS** (ESI^+): *m/z* calc. for $C_{64}H_{71}N_6O$ 939.5689, obt. 939.566 [M^+]; **IR**: ν(CO) = 1812.5 cm^{-1}, ν(NH) = 3316.0 cm^{-1} (free), ν(NH) = 2954.0 cm^{-1} (associated).

5-(2-Isothiocyanatophenyl)-10,15,20-tris(4-pentylphenyl)-21*H*,23*H*-porphyrin (17).

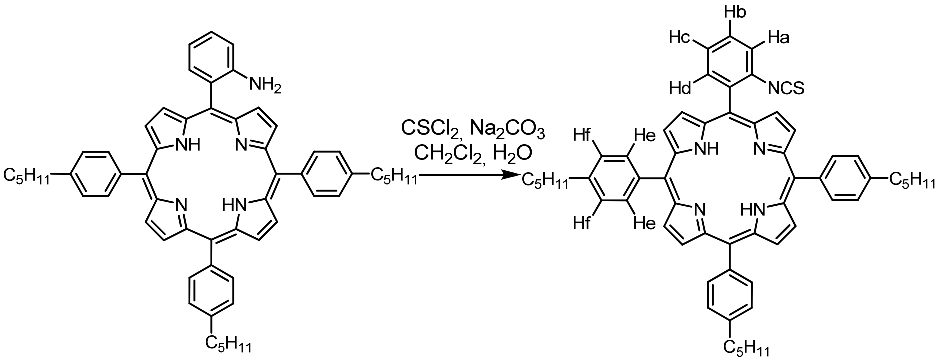

15 17

Procedure

To a solution of **15** (393.7 mg, 0.47 mmol) in CH_2Cl_2 (40 mL) were added a solution of sodium carbonate (263.2 mg, 2.48 mmol) in 80 mL of water and thiophosgene (80 µL, 1.03 mmol). The mixture was protected from light and stirred at room temperature for 3 h. The organic phase was washed with water (4 × 50 mL) and brine (50 mL), dried (Na_2SO_4), and concentrated to dryness. The resulting residue was purified by column chromatography on silica gel (40% CH_2Cl_2/hexane), yielding **17** as a violet solid (386 mg, 93%). **^{1}H NMR** (400 MHz, $CDCl_3$): δ ppm 8.95- 8.85 (s, 6H, H β-pyrr), 8.71 (d, 2H, $J = 4.8$ Hz, H β-pyrr), 8.20-8.10 (m, 7H, He, Ha), 7.80 (dt, 1H, $J = 8.6$, 1.2 Hz, Hb), 7.70-7.62 (m, 2H, Hc, Hd), 7.60-7.50 (d, 6H, $J = 6.8$ Hz, Hf), 2.96 (t, 6H, $J = 8.0$ Hz, CH_2), 2.00-1.90 (m, 6H, CH_2), 1.60-1.45 (m, 12H, CH_2), 1.30-1.20 (m, 6H, CH_2), 1.04 (t, 9H, $J = 6.4$ Hz, CH_3), -2.7 (s, 2H, NH); **HR-MS** (ESI$^+$): *m/z* calc. for $C_{60}H_{60}N_5S$ 882.4569, obt. 882.4567 [M^+].

5-(2-(3-Butylthioureido)-phenyl)-10,15,20-tris(4-pentylphenyl)-21*H*,23*H*-porphyrin (14bH).

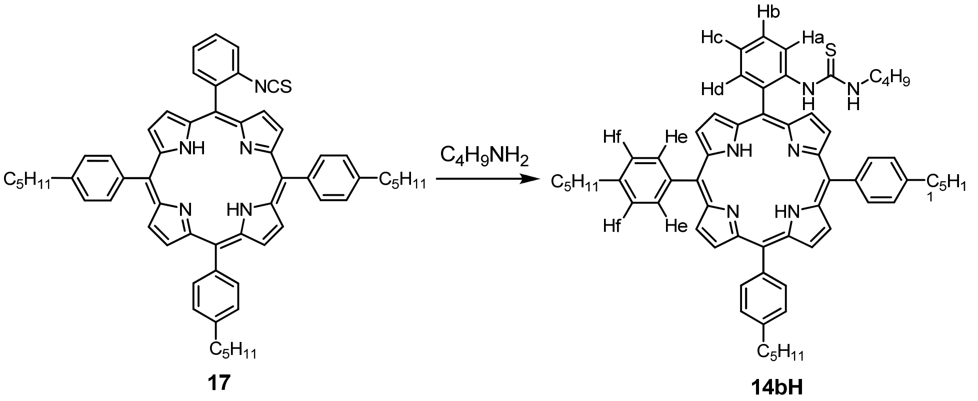

Procedure

Isothiocyanate **17** (264 mg, 0.3 mmol) was dissolved at room temperature in butylamine (3 mL), previously flushed with argon for 10 minutes. The mixture was protected from light and stirred at room temperature for 30 min under argon. The solvent was concentrated to dryness and the residue was dried on a vacuum line to eliminate the excess of butylamine. The residue was purified by column chromatography on basic alumina (50 to 70% CH_2Cl_2/hexane), affording **14bH** (276 mg, 99%) as a violet solid. **^{1}H NMR** (400 MHz, $CDCl_3$): δ ppm 8.90- 8.80 (m, 6H, Hβ-pyrr), 8.70 (d, 2H, J = 4.0 Hz, Hβ-pyrr), 8.20-8.00 (m, 8H, He, Ha, Hd), 7.85 (dt, 1H, J = 8.0, 1.6 Hz, Hb), 7.70-7.62 (dt, 1H, J = 8.0, 1.6 Hz, Hc), 7.60-7.50 (m, 6H, Hf), 7.06 (s, 1H, NH thiourea), 5.90 (broad s, 1H, NH thiourea), 2.95 (t, 8H, J = 8.0 Hz, CH_2), 2.00-1.80 (m, 8H, CH_2), 1.60-1.45 (m, 14H, CH_2), 1.04 (t, 12H, J = 7.0 Hz, CH_3), -2.70 (s, 2H, NH); **HR-MS** (ESI$^+$): *m/z* calc. for $C_{64}H_{71}N_6S$ 955.5461, obt. 955.5418 [M$^+$].

5-(2-(3,3’-Dibutyltguanidinio)-phenyl)-10,15,20-tris(4-pentylphenyl)-21*H*,23*H*-porphyrin (14cH).

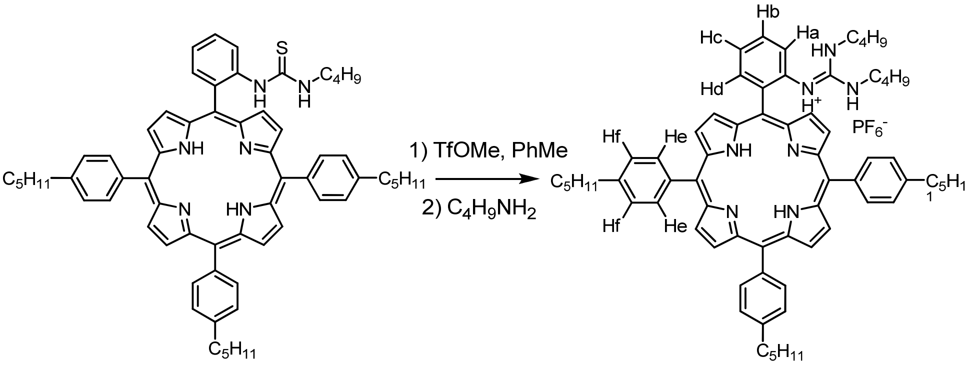
S
N
H
N
H
C4H9
NH
N
N
HN
C5H11
C5H11
C5H11
1) TfOMe, PhMe
2) C4H9NH2
Hb
Hc
Ha
Hd
HN
C4H9
N
H+
N
H
C4H9
PF6-
Hf
He
Hf
He
NH
N
N
HN
C5H11
C5H11
C5H11

14bH

14cH

Procedure

To a solution of **14bH** (97 mg, 0.10 mmol) in dry toluene (6 mL) and under argon was added methyl trifluoromethane sulfonate (23 μL, 0.20 mmol) and butylamine (40 μL, 0.4 mmol). The reaction mixture was protected from light and stirred at room temperature for 20 hours. The solvent was eliminated *in vacuo* and replaced by butylamine (3 mL). The resulting reaction mixture was then treated in the microwave at 80 ºC during 60 min. After elimination of the excess butylamine under vacuum, the residue was distributed between NaOH 1N (10 mL) and diethyl ether (10 mL) and the organic phase was washed with water, HPF_6 0.1N and finally water. After drying the organic phase (Na_2SO_4) and elimination of the solvents, the crude compound was adsorbed on silica gel and purified by column chromatography (elution from neat CH_2Cl_2 to 10% AcOEt/CH_2Cl_2) to afford **14cH** (50.6 mg, 44% yield) as a violet solid. **^{1}H NMR** (400 MHz, $CDCl_3$): δppm 8.89 (d, 2H, $J = 4.8$ Hz, H β-pyrr), 8.83 (m, 4H, H β-pyrr), 8.62 (d, 2H, J = 4.8 Hz, H β-pyrr), 8.32 (d, 1H, J = 6.8 Hz, Ha), 8.10-7.80 (m, 6H, He), 7.89 (t, 1H, J = 7.2 Hz, Hb), 7.79 (t, 1H, J = 7.2 Hz, Hc), 7.69 (d, 1H, J = 8.0 Hz, Hd), 7.55-7.49 (m, 6H, Hf), 6.4 (s, 1H, NHgu), 5.2 (broad s, 2H, NHgu), 2.9 (t, 6H, J = 7.2 Hz, CH_2), 2.2 (s, 4H, CH_2), 1.9-1.8 (m, 6H, CH_2), 1.6-1.4 (m, 14H, CH_2), 1.1-0.95 (m, 9H, CH_3), 0.6-0.1 (m, 8H, CH_2), 0.1- -0.2 (m, 4H, CH_2), -2.78 (s, 2H, NH); **HR-MS** (ESI^+): *m/z* calc. for $C_{68}H_{80}N_7^+$994.6470, obt. 994.6255 [$(M+H)^+$].

1-Butyl-3-phenyl-thiourea (18).

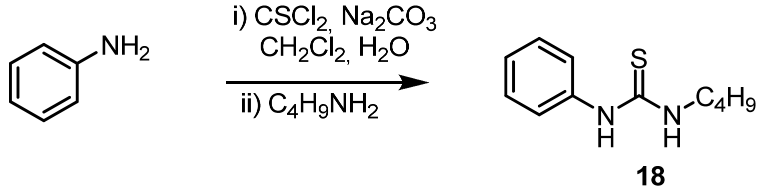

18

Procedure

To a biphasic system made from a solution of aniline (0.2 mL, 2.20 mmol) in CH_2Cl_2 (25 mL) and a solution of sodium carbonate (1.233 g, 11.63 mmol) in water (50 mL), was added thiophosgene (0.37 mL, 4.83 mmol). The resulting mixture was stirred for 2 hours at room temperature, and then the organic phase was washed four times with water. The solvent was then eliminated under vacuum after drying with anhydrous sodium sulfate. To the crude residue excess butylamine (2 mL) was added under argon and the mixture was stirred at room temperature for 15 min. The excess amine was then eliminated *in vacuo* and the residue was dried on the vacuum line to yield **18**, that was purified by silica gel column chromatography (378.2 mg,

83%). **^{1}H NMR** ($CDCl_3$, 400 MHz): δ ppm 7.36-7.29 (m, 3H, H_{Ar}), 7.22-7.15 (m, 2H, H_{Ar}), 6.28 (s, 1H, NH), 3.58-3.49 (m, 2H, CH_2), 1.53-1.41 (m, 2H, CH_2), 1.33-1.20 (m, 2H, CH_2), 0.85 (t, 3H, J = 7.9 Hz, CH_3); **^{13}C NMR** (CDCl3, 100 MHz): δ (ppm) 180.2, 136.8, 129.9, 126.7, 124.9, 44.8, 30.9, 20.1, 13.7.

1-Butyl-3-phenylurea (19).

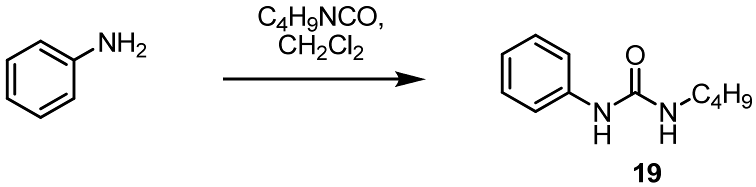

19

Procedure

To a solution of aniline (0.10 mL, 1.10 mmol) in dry CH_2Cl_2 (25 mL) was added butylisocyanate (0.13 mL, 1.15 mmol) at room temperature and under argon. The reaction mixture was stirred at reflux during two days. The solvent was then eliminated *in vacuo* after cooling down the vessel. The residue was dissolved in ethyl acetate (20 mL) and the resulting organic phase was washed with HCl 1N (to remove unreacted aniline) and then with water. The organic phase was dried with anhydrous sodium sulfate and the solvent was eliminated under vacuum to yield **19** (177.6 mg, 84% yield). **^{1}H NMR** ($CDCl_3$, 400 MHz): δ ppm 7.32-7.27 (m, 4H, H_{Ar}), 7.12-7.05 (m, 2H, H_{Ar} + NH), 5.15 (t, 1H, J = 5.3 Hz, NH), 3.3-3.21 (m, 2H, CH_2), 1.59-1.45 (m, 2H, CH_2), 1.41-1.31 (m, 2H, CH_2), 1.27 (t, 3H, J = 7.0 Hz, CH_3); **^{13}C NMR** ($CDCl_3$, 100 MHz): δ ppm 156.5 (CO), 138.8, 129.5, 124.0, 121.2, 40.3 (CH_2), 32.2 (CH_2), 20.1 (CH_2), 13.9 (CH_3).

The preparation of benzoguanidinium derivative **2** is reported in Chapter 2.

General procedure for the preparation of zinc(II) porphyrins.

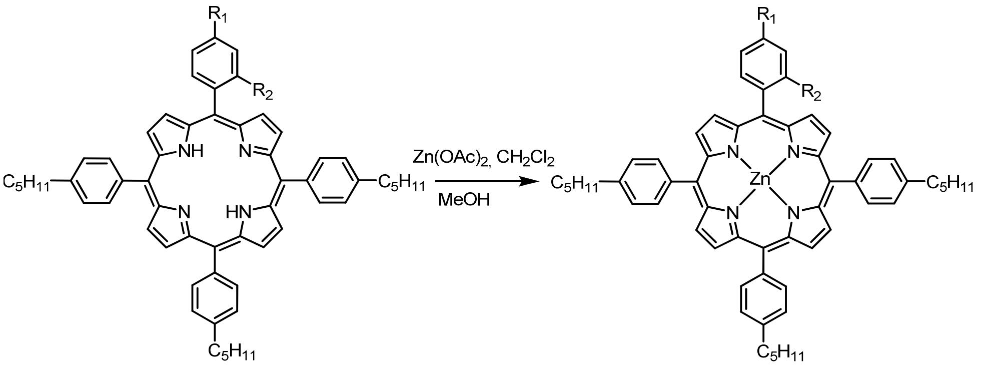

Procedure

To a solution of the porphyrin derivative (1 eq.) in a dichloromethane-methanol mixture ([porphyrin] = 10^{-6} M) was added zinc(II) acetate (10 eq) and the resulting mixture was stirred at room temperature for one hour. Solvents were then eliminated under vacuum and the crude compound was filtered on silica gel. After elimination of the solvents *in vacuo*, the metallated porphyrin derivative was obtained in high yields.

14aZn: 81% yield; **^{1}H NMR** (500 MHz, $CDCl_3$): δ ppm 8.90 (s, 4H, H β-pyrr), 8.80 (d, 2H, J = 4.5 Hz, H β-pyrr), 8.45 (d, 2H, J = 4.5 Hz, H β-pyrr), 8.07 (d, 1H, J = 7.5 Hz, H_a), 7.97 (t, 5H, J = 8.1 Hz, H_e), 7.90 (d, 1H, J = 7.0 Hz, H_d), 7.50-7.40 (m, 7H, H_f and H_b), 7.37 (t, 1H, J = 7.5 Hz, H_c), 6.86

(s, 1H, NH_{urea}), 4.40 (s, 1H, NH_{urea}), 2.94 (t, 6H, *J* = 8.0 Hz, CH_2), 1.96-1.91 (m, 6H, CH_2), 1.69 (broad s, 2H, CH_2 Bu), 1.59-1.30 (m, 12H, 2 CH_2), 1.30-1.26 (m, 5H, CH_3 and CH_2 Bu), 1.06-1.02 (m, 9H, CH_3), 0.90 (m, 2H, CH_2 Bu), 0.06 (s, 2H, NH). **HR-MS** (ESI^+): *m/z* calc. for $C_{64}H_{69}N_6OZn$ 1001.4824, obt. 1001.4874 [M^+].

ZnTPPP: 90% yield. **^{1}H NMR** ($CDCl_3$, 400 MHz): δ ppm 8.97 (s, 8H, pyrr H), 8.12 (d, 8H, *J* = 7.6 Hz, He), 7.55 (d, 8H, *J* = 7.6 Hz, Hf), 2.96 (t, 8H, *J* = 7.6 Hz, CH_2), 1.94 (q, 8H, *J* = 7.6 Hz, CH_2), 1.60-1.40 (m, 16H, CH_2), 1.03 (t, 12H, *J* = 7.2 Hz, CH_3). **X-ray** Structure was confirmed by X-ray diffraction, though definition of the alkyl chains was not optimal (Fig. 3.22). Packing of the crystal is achieved by parallel Zn(II)-porphyrin units interacting through π-stacking interactions between the aryl residues with an additional porphyrin ring that connects the two parallel strands, thus forming an angle between the porphyrins. Hydrophobic interactions between the alkyl chains are also involved in packing determination.

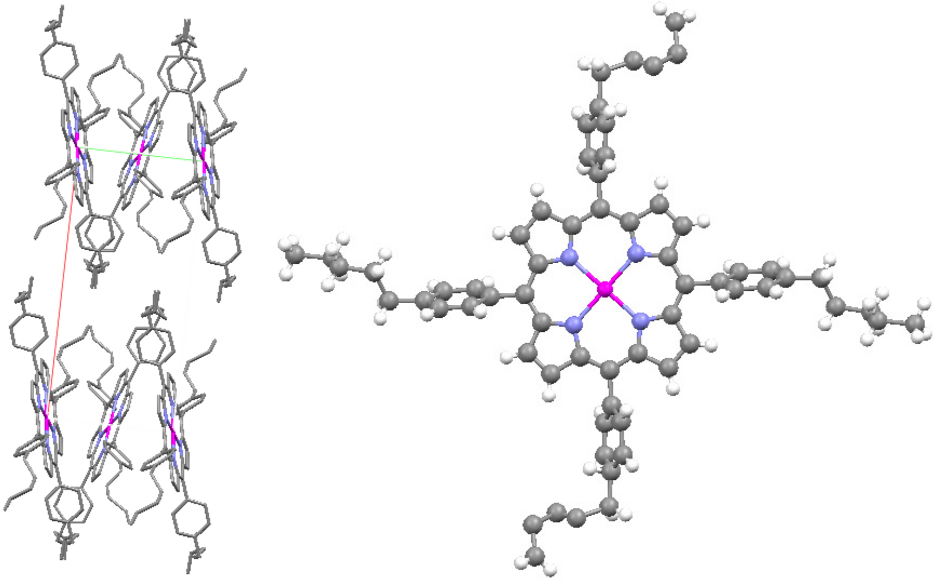

Fig. 3.22: X-ray structure and crystal packing of **ZnTPPP**.

Tetra-(4-pentylphenyl)porphyrinato nickel(II) NiTPPP.

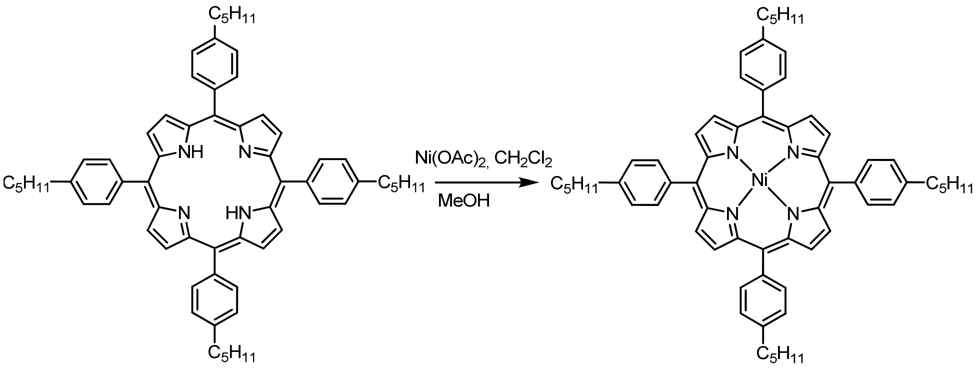
C5H11
NH
N
N
HN
Ni(OAc)2, CH2Cl2
MeOH
N
N
Ni
N
N

Procedure

To a solution of **TPPP** (50 mg, 55 μmol) in dichloromethane (10 mL) was added a solution of nickel(II) acetate (153 mg, 0.61 mmol) in methanol (5 mL) and the resulting mixture was stirred at reflux during 5 days. The reaction mixture was then evaporated under vacuum and the residue was purified by alumina supported column chromatography using 10% CH_2Cl_2/hexane as elution system. After evaporation of the fractions, a slight blue to red solid is obtained (41.5 mg, 78% yield). **^{1}H NMR** ($CDCl_3$, 400 MHz): δ ppm 8.76 (s, 8H, H β-pyrr), 7.91 (d, 8H, J = 7.6 Hz, He), 7.47 (d, 8H, J = 7.6 Hz, Hf), 2.90 (t, 8H, J = 7.6 Hz, CH_2), 1.87 (q, 8H, J = 7.6 Hz, CH_2), 1.60-1.40 (m, 16H, CH_2), 1.05 (t, 12H, J = 7.2 Hz, CH_3).

Dipyridino(5,10,15,20-tetra-(4-pentylphenyl)porphyrinato) magnesium(II) MgPy$_2$TPPP.

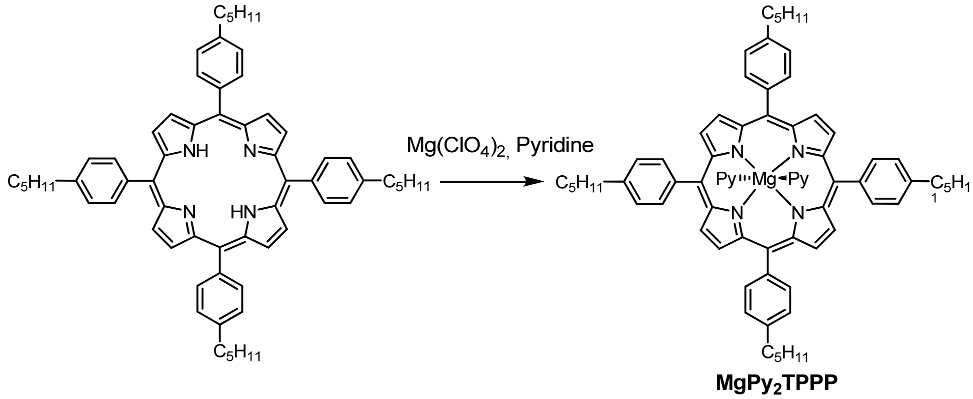

Procedure

TPPP (100 mg, 0.12 mmol) was dissolved in pyridine (13 mL) and magnesium perchlorate (623 mg, 2.79 mmol) was added. The reaction mixture was then refluxed overnight and then allowed to cool at room temperature. After cooling, the reaction mixture was filtered and solid washed with diethyl ether until obtention of a colorless filtrate. The resulting organic phase was washed three times with water and dried with Na_2SO_4. After filtration and evaporation of the solvent, **Mg(Py)$_2$TPPP** was obtained as purple to blue needles (118 mg, 98% yield). **^{1}H NMR** (400 MHz, $CDCl_3$): δ ppm 8.98 (s, 8H, H β-pyrr), 8.16 (d, 8H, J = 7.7 Hz, H_{Ar}), 7.58 (d, 8H, J = 7.7 Hz, H_{Ar}), 7.02 (tt, 2H, J = 7.6, 1.7 Hz, H_{Py}), 6.46-6.41 (m, 4H, H_{Py}), 5.78-5.74 (m, 4H, H_{Py}), 3.02 (t, 8H, J = 7.7 Hz, CH_2), 2.05-1.95 (m, 8H, CH_2), 1.67-1.53 (m, 16H, CH_2), 1.10 (t, J = 7.0 Hz, CH_3); **HR-MS** (MALDI): *m/z*: calc. for $C_{64}H_{68}MgN_4$ 916.6138, obt. 916.514 [(M-2 Py)$^+$].

General procedure for the preparation of dichlorotin(IV) porphyrins.

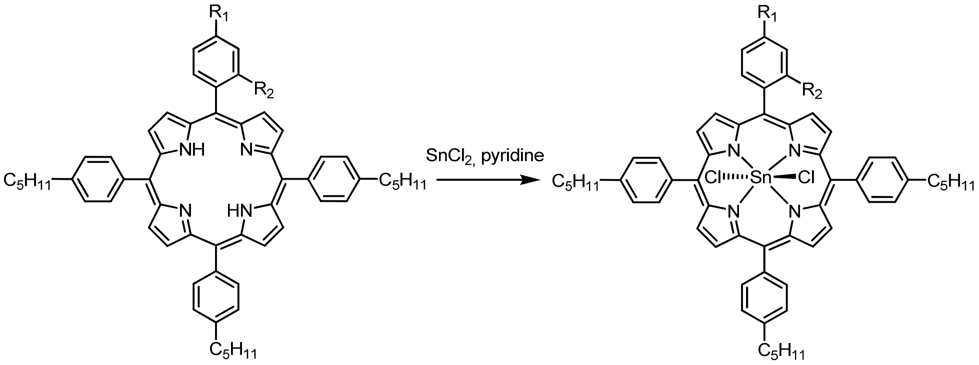

Procedure

To a solution of the porphyrin derivative (1 eq.) dissolved in dry pyridine ([porphyrin] = 4 × 10^{-3} M) was added tin(II) chloride dehydrate (20 eq.) and the resulting reaction mixture was refluxed for three hours. After cooling down at room temperature, water was added to the mixture and the resulting precipitate was collected by filtration. The resulting solid was dissolved in dichloromethane and the organic phase was washed with water, HCl 1N solution, and again with water. After drying with anhydrous sodium sulfate, filtration and elimination of the solvents *in vacuo*, the dichlorotin(IV) porphyrin derivative were obtained as blue/red solids.

$SnCl_2TPPP$: 91% yield. **^{1}H NMR** (400 MHz, $CDCl_3$): δ ppm: 9.26 (s, 8H, H β-pyrr), 8.25 (d, 8H, J = 8.0 Hz, H_{Ar}), 7.65 (d, 8H, J = 8.0 Hz, H_{Ar}), 3.02 (t, 8H, J = 7.6 Hz, CH_2), 2.03-1.96 (m, 8H, CH_2), 1.66-1.51 (m, 16H, CH_2), 1.08 (t, J = 7.1 Hz, CH_3); **HR-MS** (MALDI): *m/z* calc. for $C_{64}H_{68}ClN_4Sn$ 1047.4164, obt. 1047.4139 [$(M-Cl)^+$] (^{120}Sn isotope detected).

$14aSnCl_2$: 85% yield. **^{1}H NMR** ($CDCl_3$, 400 MHz): δ ppm 9.30-9.18 (m, 6H, H β-pyrr, satellites), 9.12 (d, 2H, J = 5.0 Hz, H β-pyrr), 8.51 (dd, 1H, J = 1.7, 7.5 Hz), 8.27-8.14 (m, 6H), 8.06 (dd, 1H, J = 7.5, 1.4 Hz), 7.81 (td, 1H, J = 8.0 Hz, 1.5Hz), 7.67-7.60 (m, 6H), 7.57 (td, 1H, J = 7.7, 1.3 Hz), 2.98 (t, 6H, J = 7.8 Hz, CH_2), 2.00-1.90 (m, 6H, CH_2), 1.61-1.46 (m, 14H, CH_2), 1.03 (t, 9H, J = 7.1 Hz, CH_3), 0.91-0.81 (m, 3H, CH_3), 0.49-0.37 (m, 2H, CH_2), 0.29 (t, 2H, J = 6.4 Hz, CH_2); **HR-MS** (MALDI): *m/z* calc. for $C_{64}H_{68}ClN_6OSn$ 1091.3803, obt. 1091.4178 [$(M-Cl)^+$] (^{120}Sn isotope detected).

$14bSnCl_2$: 93% yield. **^{1}H NMR** ($CDCl_3$, 400 MHz): δ ppm 9.30-9.16 (m, 8H, H β-pyrr, satellites), 8.78 (d, 1H, J = 5.7 Hz), 8.26-8.17 (m, 6H), 8.09 (dd, 1H, J = 7.6, 1.6 Hz), 7.84-7.77 (m, 1H), 7.68-7.62 (m, 6H), 7.13 (dd, 1H, J = 8.2, 0.9 Hz), 2.99 (t, 6H, J = 7.6 Hz, CH_2), 2-1.9 (m, 6H, CH_2), 1.70-1.40 (m, 14H, CH_2), 1.30-1.25 (m, 2H, CH_2), 1.05 (t, 9H, J = 7.0 Hz,

CH_3), 0.99-0.91 (m, 3H, CH_3), 0.10-0.07 (m, 2H, CH_2).

14cSnCl$_2$ (Cl$^-$): Yield not measured. **^{1}H NMR** ($CDCl_3$, 400 MHz): *δ* ppm 9.40-9.30 (broad s, 2H, H β-pyrr), 9.29-9.21 (m, 4H, H β-pyrr, satellites), 8.80 (broad s, 2H, H β-pyrr), 8.62 (s, 1H, NH), 8.55 (d, 1H, *J* = 6.8 Hz); 8.27-8.12 (m, 6H), 8.08-7.80 (m, 3H), 7.70-7.55 (m, 8H, 6H arom., 2 NHs), 3.00 (t, 6H, *J* = 7.7 Hz, CH_2), 2.00-1.90 (m, 6H, CH_2), 1.77-1.75 (m, 4H, CH_2), 1.64-1.48 (m, 14H, CH_2), 1.08-1.02 (m, 9H, CH_3), 0.60-0.44 (m, 6H, CH_2), 0.40-0.32 (m, 9H, CH_3); **HR-MS** (MALDI): *m/z* calc. for $C_{68}H_{78}ClN_7OSn^+$ 1147.5, obt. 1146.5 (M-2Cl)$^+$] (^{120}Sn isotope detected).

Dihydroxo(5, 10, 15, 20-tetra-p-(pentyl)phenylporphyrinato)tin(IV) (Sn(OH)$_2$TPPP).

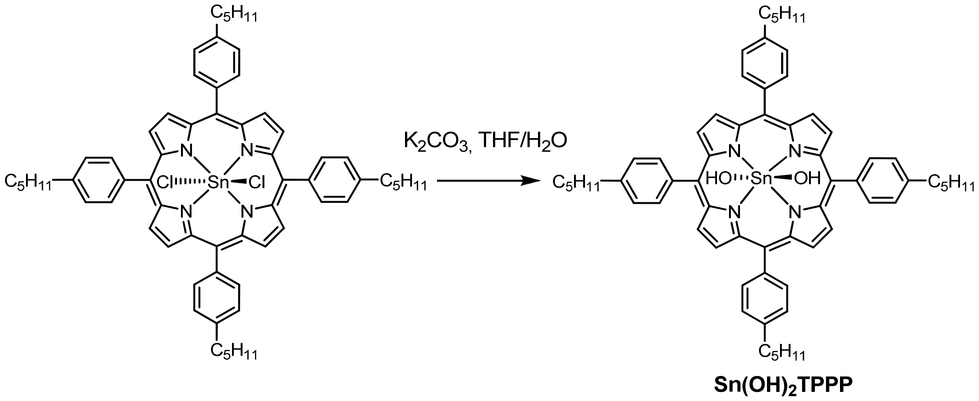

Procedure

A mixture of **Sn(Cl)$_2$TPPP** (50 mg, 46 μmol) and potassium carbonate (262 mg, 1.9 mmol) in a mixture of THF/water (50/12.5 mL) was refluxed for one hour. After cooling the reaction mixture at room temperature, the solvent was eliminated *in vacuo* and the residue was distributed between dichloromethane and water. The organic phase was washed with additional water, dried with anhydrous sodium sulfate, filtered and the solvent was finally eliminated under vacuum to yield **$Sn(OH)_2TPPP$** (54.8 mg, quantitative) as a blue-purple solid. **^{1}H NMR** ($CDCl_3$, 400 MHz): δ ppm 9.17 (s, 8H), 8.25 (d, 8H, J = 7.8 Hz), 7.64 (d, 8H, J = 7.8 Hz), 3.01 (t, 8H, J = 7.6 Hz), 2.10-1.90 (m, 8H), 1.67-1.47 (m, 16H), 1.07 (t, 12H, J = 7 Hz). **HR-MS** (MALDI): *m/z* calc. for $C_{64}H_{71}N_4O_2Sn$ 1047.4599, obt. 1047.4598 (^{120}Sn isotope detected) [$(M+H)^+$].[25]

---

[25] Mass peaks for the loss of one or two axial hydroxo ligands are also seen at 1029.4896 and 1012.5040 $g.mol^{-1}$, respectively.

CHAPTER 4

FUNCTIONALIZED LIGANDS FOR SUBSTRATE BINDING IN CATALYSIS

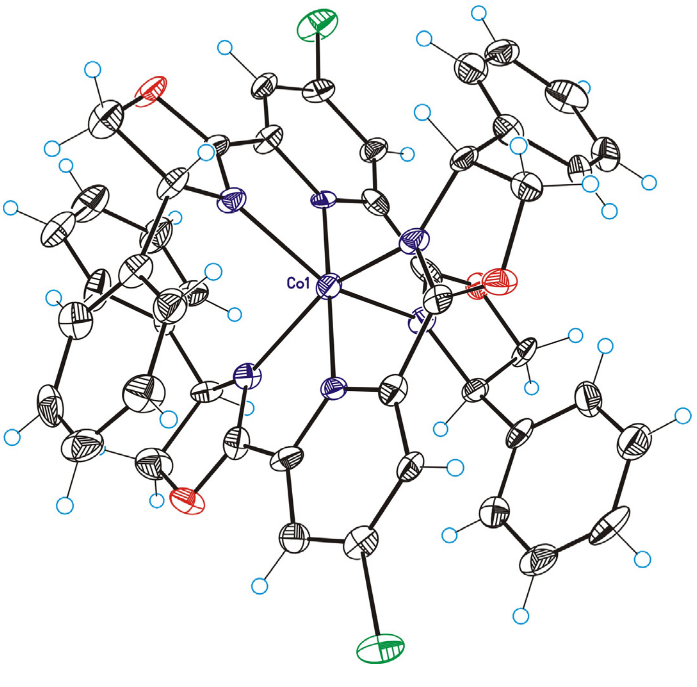

4. Functionalized ligands for substrate binding in catalysis.

4.1 Introduction.

The outstanding regioselectivity observed in enzymatic catalysis is mainly attributed to substrate fixation in the enzyme active site to fix the substrate in an optimal way and to restrict its molecular motions. Translation of these principles to homogeneous catalysis is therefore one of the longstanding goals of supramolecular chemistry. Surprisingly, the combination of molecular recognition with catalytically active metal centers in artificial systems has not been deeply investigated although some successful examples have been recently described.

Crabtree and co-workers reported in 2006 a terpyridyl ligand substituted with a Kemp's acid subunit able to fix a carboxylic acid substrate at a given distance of a metal binding site (Fig. 4.1), which resulted in remarkable selectivites in the C-H oxidation of ibuprofen (μ-oxo manganese dimer catalyzed C-H oxidation assisted by oxone).[1] Use of the Kemp acid provides the catalyst with a U-shaped geometry that enables suitable substrate orientation, while the phenylene linker provides some spacing between the remote recognition unit and the catalytic active site. The terpyridyl residue is used for metal binding.

---

[1] a) Das, S.; Incarvito, C. D.; Crabtree, R. H.; Brudvig, G. W. *Science* **2006**, *312*, 1941. b) Das, S.; Brudvig, G. W.; Crabtree, R. H. *J. Am. Chem. Soc.* **2008**, *130*, 1628.

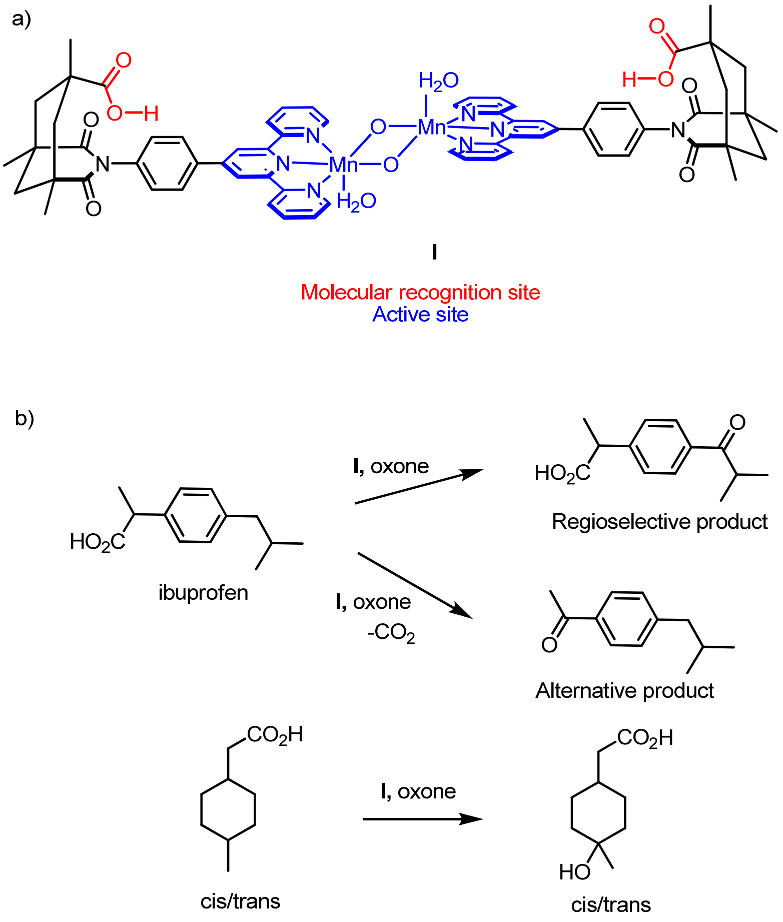
a)
O
O—H
O
N
N
N
N
Mn
O
O
H_2O
H_2O
Mn
N
N
N
H—O
O
O
N
O
I
Molecular recognition site
Active site
b)
I, oxone
HO_2C
O
Regioselective product
HO_2C
ibuprofen
I, oxone
$-CO_2$
O
Alternative product
CO_2H
I, oxone
CO_2H
HO
cis/trans
cis/trans

Fig. 4.1: a) Catalytic system for regioselective C-H oxidation of carboxylic acid derivatives developed by Crabtree and Brudvig. b) Regioselective C-H oxidation of carboxylic acids.

Control experiments with non functionalized terpyridine ligands were not regioselective. In the presence of 0.1 mol% catalyst and five equivalents of oxone, the regioselective oxidation product could be observed in 96.5% selectivity with a remarkable turnover of 710 (in CD_3CN). Inhibition of the reaction was then evidenced by the addition of *p-tert*-butylbenzoic acid, which sterically blocks the active site by formation of the carboxylic acid heterodimer without oxidizing. This inhibition is totally reversed by addition of acetic acid, which competes in binding with the inhibitor and, thanks to its small size, frees to some extent the catalytic active site, thus regenerating the catalyst.

Recently, Breit and co-workers reported a catalyst for the regioselective hydroformylation reaction of unsaturated carboxylic acids.[2] In that case, molecular recognition was based on a carboxyguanidinium/carboxylate ion pair (Fig. 4.2). The pyridyl core of the ligand fixes the desired conformation of the carboxyguanidine group by increasing the rotation barrier of the carbonyl group (lone pairs electronic repulsion). A rhodium(I) complex was tested in hydroformylation reactions of unsaturated carboxylic acids (unconjugated), with remarkable selectivities (linear over branched product, expressed as l/b ratio) and turnover frequencies (TOF of 250 h^{-1}) relative to usual systems (xantphos, triphenylphosphine) or to the equivalent free system (PPh_3+**III**: TOF: 12 h^{-1}; l/b: 1.5). The role of the guanidine moiety in the molecular recognition event was established by competition experiments (addition of non reacting acid such as AcOH), for which inhibition and decreased selectivity were observed. Substrate selectivity of the process for β,γ-unsaturated carboxylic acids in competition experiments with non acidic olefinic substrates was also observed.

---

[2] Šmejkal, T.; Breit, B. *Angew. Chem. Int. Ed.* **2008**, *47*, 311.

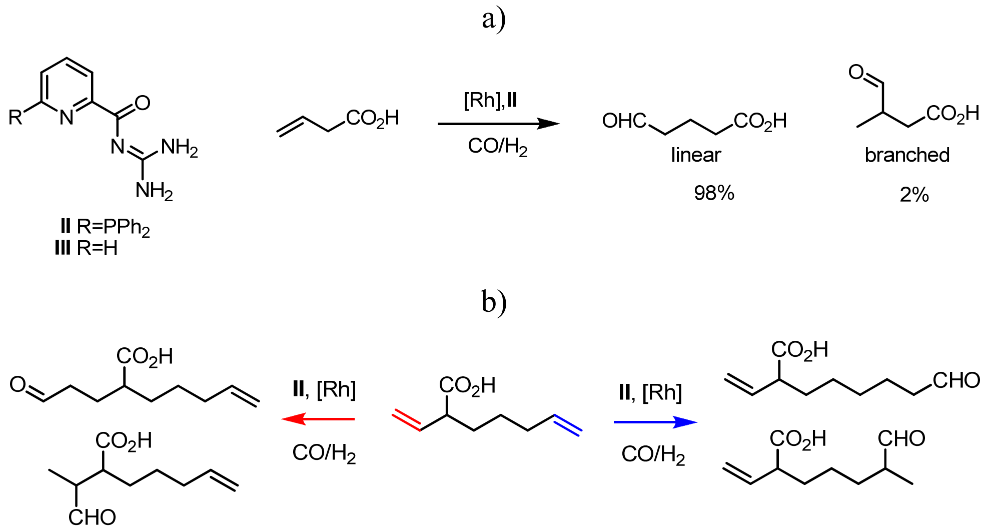
a)
R
N
O
N
NH2
NH2
II R=PPh2
III R=H
CO2H
[Rh],II
CO/H2
OHC
CO2H
linear
98%
O
CO2H
branched
2%
b)
CO2H
O
II, [Rh]
CO/H2
CO2H
II, [Rh]
CO/H2
CO2H
CHO
CO2H
CHO
CO2H
CHO

Fig. 4.2: Functionalized ligand for highly regioselective hydroformylations.

A substrate bearing two reactive sites (double bonds) was then investigated (Fig. 4.2b) and ligand **II** was shown to induce a high regioselectivity in the reaction (the red pathway was ten times faster than the blue one), the linear aldehyde obtained from the red pathway being isolated in 75% yield (among the five possible products of mono- and dihydroformylation).

Surprisingly, when *α,β* unsaturated acids were used as substrates for the reaction, some decarboxylation was observed, resulting in the corresponding aliphatic aldehyde, whereas when PPh_3 was used as a ligand, hydrogenation of the double bond was observed.[3] In the presence of ligand **II**, hydroformylation is preferred to olefin hydrogenation, the formed product then undergoing decarboxylation (Fig. 4.3). A supramolecular interaction between substrate and ligand might therefore provide remarkable levels of selectivity and activity in transition metal catalyzed processes.

---

[3] Šmejkal, T.; Breit, B. *Angew. Chem. Int. Ed.* **2008**, *47*, 3946.

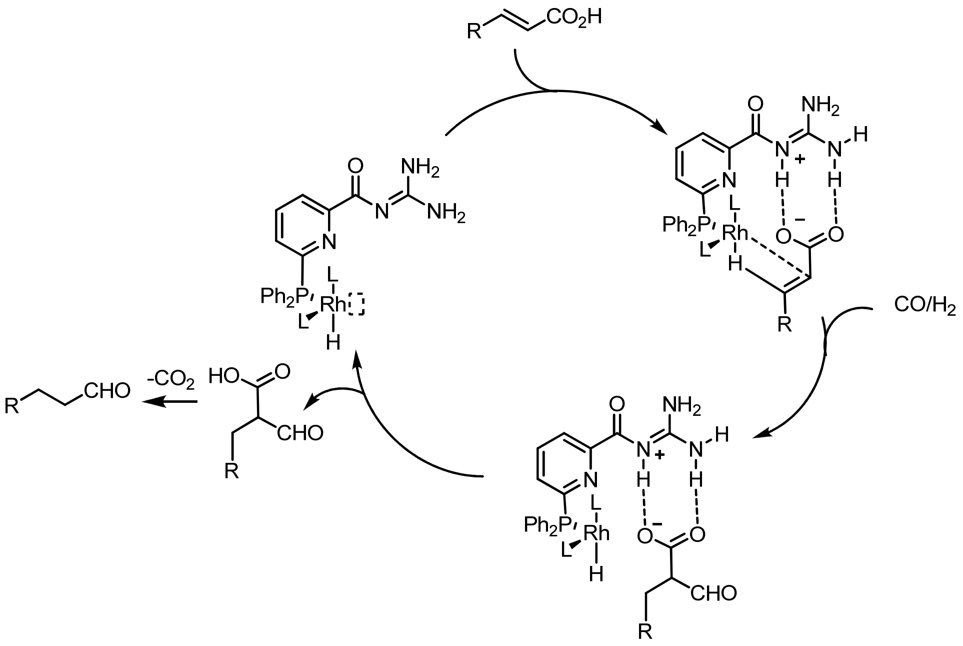

Fig. 4.3: Proposed mechanism for the formation of aliphatic aldehydes from *α,β*-unsaturated carboxylic acids.

This chapter deals with the synthesis of a library of readily accessible ligands functionalized with H-bond donating groups such as urea, thiourea and guanidine and their formation of heteroleptic metal complexes with a second library of chiral ligands, in order to create and screen a wide library of chiral catalysts with molecular recognition of the substrate, which might result in regioselective asymmetric catalysis. Such a combinatorial approach was previously illustrated by Ding and co-workers, as summarized in Fig. 4.4.[4]

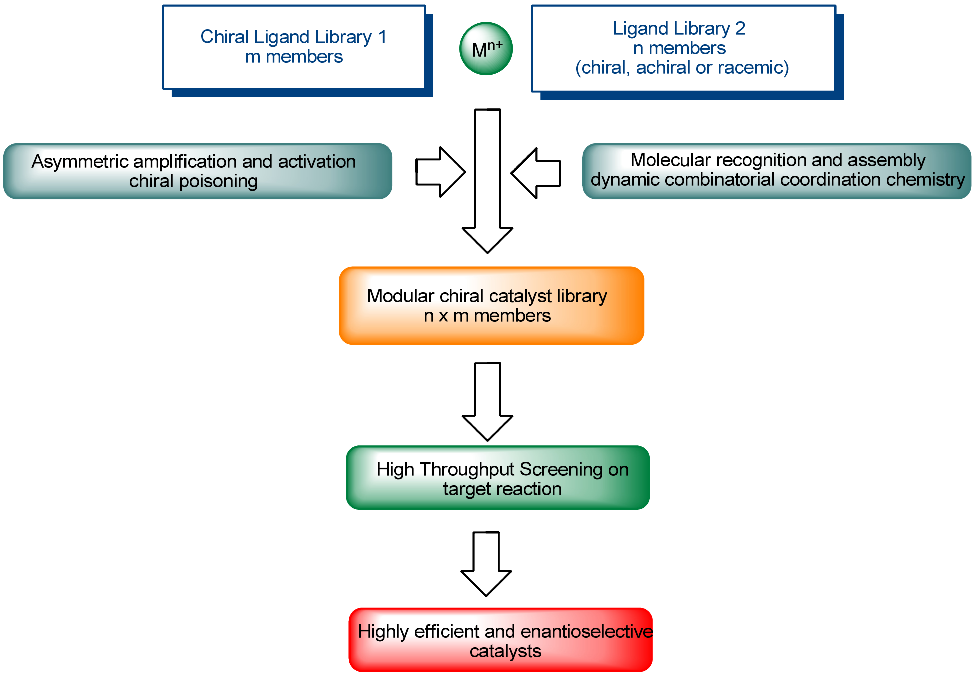
Chiral Ligand Library 1
m members
M^{n+}
Ligand Library 2
n members
(chiral, achiral or racemic)
Asymmetric amplification and activation
chiral poisoning
Molecular recognition and assembly
dynamic combinatorial coordination chemistry
Modular chiral catalyst library
n x m members
High Throughput Screening on
target reaction
Highly efficient and enantioselective
catalysts

Fig. 4.4: Conceptual approach for combinatorial catalyst engineering and screening.

This approach was used in tandem hetero Diels-Alder reactions and diethylzinc additions on formylbenzaldehyde derivatives with a single catalyst (**IV**), giving rise to high yields and stereoselectivities in a one-pot sequence (Fig. 4.5).[5] Catalyst **IV** showed asymmetric induction for both reactions when performed separately, which enabled the construction of a tandem procedure (>94% *ee* for each isolated step).

---

[4] Ding, K.; Du, H.; Yuan, Y.; Long, J. *Chem. Eur. J.* **2004**, *10*, 2872.

[5] Du, H.; Ding, K. *Org. Lett.* **2003**, *5*, 1091.

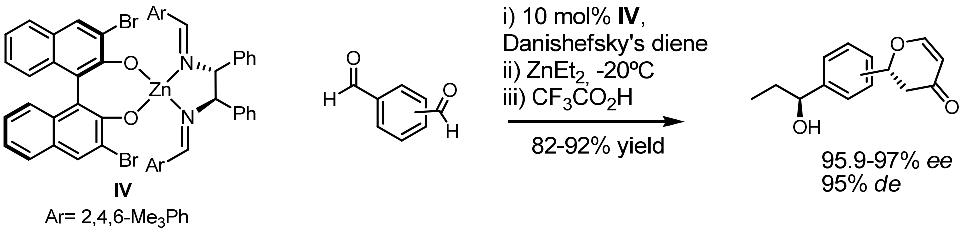
Br
Ar
O
N
Ph
Zn
O
N
Ph
Br
Ar
IV
Ar= 2,4,6-Me$_3$Ph
O
H
O
H
i) 10 mol% **IV**, Danishefsky's diene
ii) ZnEt$_2$, -20ºC
iii) CF$_3$CO$_2$H
82-92% yield
O
O
OH
95.9-97% *ee*
95% *de*

Fig. 4.5: Tandem enantioselective hetero Diels-Alder and diethylzinc addition reactions performed by a screened catalyst from a library.

Given the relevance of the combinatorial approach to catalysis and of the use of substrate specific molecular recognition sites on the ligands, combination of both concepts might lead to highly selective homogeneous catalysis in terms of regioselectivity and enantioselectivity.

For this reason, we designed a library of mono- and bidentate achiral ligands functionalized with hydrogen bonds donating groups, as well as a library of chiral ligands (Fig. 4.6). Upon coordination with a suitable transition metal and formation of the heteroleptic ligand, this approach offers the possibility to screen a broad family of catalysts and study a wide scope of applications.

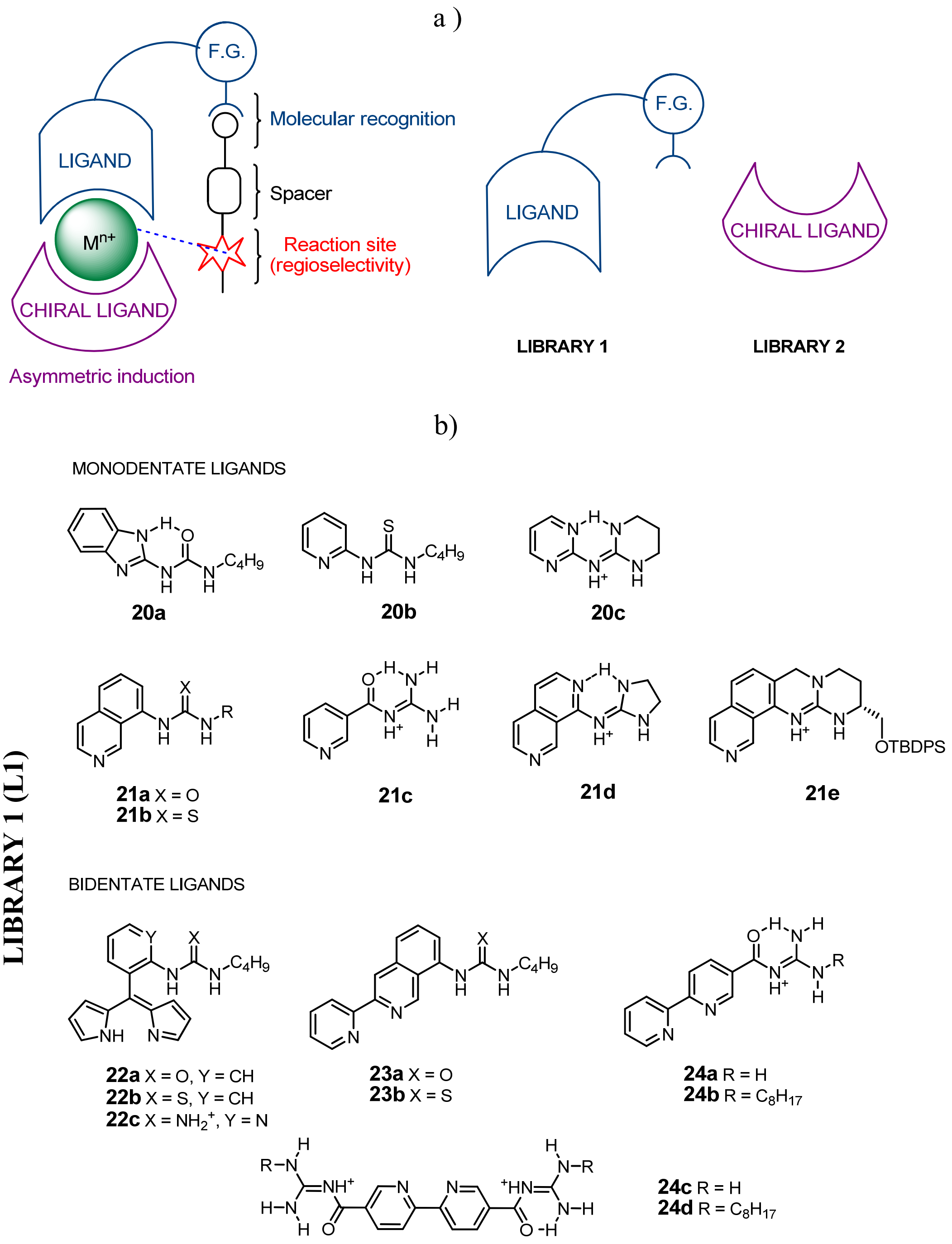
a)
F.G.
LIGAND
Molecular recognition
Spacer
Reaction site
(regioselectivity)
Mn+
CHIRAL LIGAND
Asymmetric induction
F.G.
LIGAND
CHIRAL LIGAND
LIBRARY 1
LIBRARY 2
b)
LIBRARY 1 (L1)
MONODENTATE LIGANDS
20a
20b
20c
21a X = O
21b X = S
21c
21d
21e
OTBDPS
BIDENTATE LIGANDS
22a X = O, Y = CH
22b X = S, Y = CH
22c X = NH2+, Y = N
23a X = O
23b X = S
24a R = H
24b R = C8H17
24c R = H
24d R = C8H17

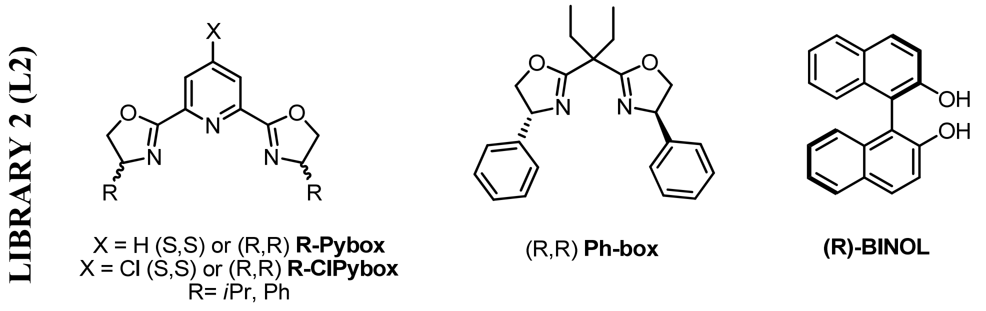

Fig. 4.6: a) Schematic representation of the concept of our combinatorial supramolecular approach to catalysis; b) Studied ligand libraries.

Regarding the library of hydrogen bonding achiral ligands (Library 1, L1), a series of monodentate and bidentate ligands were designed with various spacing groups (2-pyridyl, 8-isoquinolyl, dipyrromethenes) in order to study the influence of the distance between the metal and the H-bonding moiety on the catalytic activity and the formation of the heteroleptic complex. However, at this initial proof-of-concept step, the study was limited to N-heterocyclic ligands (phosphines, alcohols, phosphites, etc were excluded). The 2-pyridyl spacer was selected because of the easy synthetic accessibility of the corresponding ligands **20a-20c**. Furthermore, the 8-isoquinolyl spacing group was found in the literature to form cooperative anion binding when complexed with a metal and was therefore considered as a potential spacer (**21a-21e**).[6] The carboxyguanidine derived from nicotinic acid **21c** was expected to be readily accessible and to present a conformation similar to the one obtained with the 8-isoquinolyl spacer, though rotation of the carbonyl group is possible. Regarding the bidentate ligand series, dipyrromethenes **22a-22c** were also studied, given the encouraging results described in the previous chapter. For the same reasons, the 3-(pyridin-2-yl)-isoquinolyl spacer (**23a-23b, 24a-24d**) was designed and studied. Urea, thiourea and guanidinium derivatives were also systematically studied in order to screen the H-bonding moiety. Finally, in order to obtain a planar ligand and thus enhance both binding affinity and catalyst's efficiency (as discussed in the previous chapters), designs include the use of intramolecular hydrogen bonds (when possible) between the H-bonding moiety and the heterocycle, which is expected to favour the planar conformation (**20a**, **20c**, **21c**, **21d**, **24a-24d**).

---

[6] Bondy, C. R.; Gale, P. A.; Loeb, S. J. *J. Am. Chem. Soc.* **2004**, 5030.

Chiral ligands (Library 2, L2) were chosen according to their versatility, valency, chiral environment and ease of preparation, though this list is obviously not exhaustive. In the following sections, the synthesis of libraries L1 and L2, the attempts of formation of the heteroleptic complex and some trials of catalysis will be presented.

4.2 Synthesis of ligands.

4.2.1 Synthesis of chiral ligands (L2).

(R)-BINOL was used as delivered by commercial sources without any further purification. The general procedure for the preparation of oxazoline derivatives involves the formation of an amide from a carboxylic acid and a chiral aminoalcohol (obtained by reduction of aminoacids), followed by the cyclization of the amidoalcohol derivative to the corresponding oxazoline by activation of the alcohol as a leaving group (Fig. 4.7). Oxazoline derivatives were prepared as reported in the literature.[7]

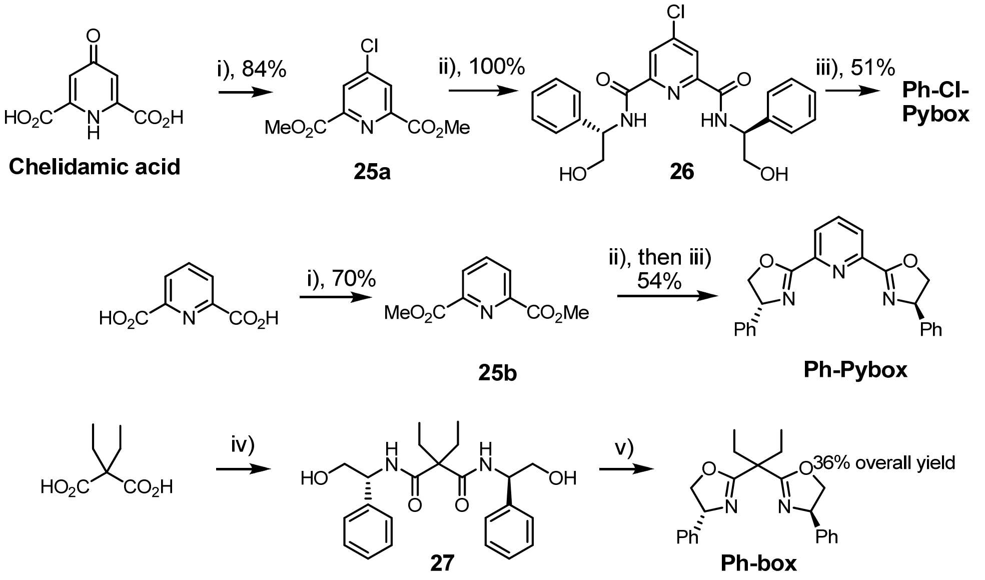
Chelidamic acid
i), 84%
25a
ii), 100%
26
iii), 51%
Ph-Cl-Pybox
i), 70%
25b
ii), then iii) 54%
Ph-Pybox
iv)
27
v)
36% overall yield
Ph-box

i) PCl_5, CCl_4, then MeOH; ii) L-phenylglycinol, 120 °C overnight; iii) TsCl, NEt_3, CH_2Cl_2, refl.; iv) 1) $SOCl_2$ 2) (*R*)-phenylglycinol, CH_2Cl_2, NEt_3; v)TsCl, DMAP, NEt_3, CH_2Cl_2.

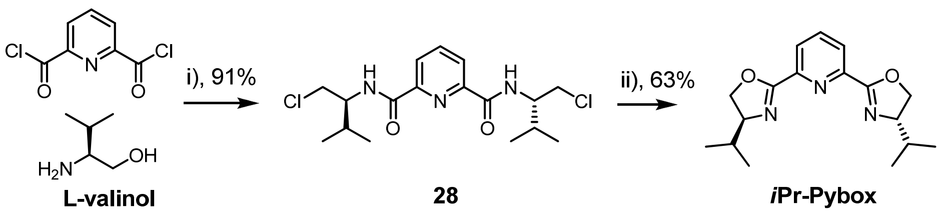
L-valinol
i), 91%
28
ii), 63%
*i*Pr-Pybox

i) $CHCl_3$, 24 h, then $SOCl_2$, reflux; ii) NaH, dry THF, room temperature.

Fig. 4.7: Synthesis of oxazoline derivatives.

As described on Fig. 4.7, two pathways were followed for the synthesis of the diamidoalcohol intermediates from the dicarboxylic acid derivatives. A diacid chloride was formed upon treatment of the diacid, either with phosphorous pentachloride, or with thionyl chloride. In the case of **Ph-box** and ***i*****Pr-Pybox**, the resulting acid chloride was treated with the aminoalcohol to form the diamide derivatives **27** and **28** in 56 and 91% yields, respectively. Alternatively, the diacid chloride was treated with methanol to form the corresponding diester. Treatment of the diester with the aminoalcohol (valinol, phenylglycinol) at high temperature in a sealed tube readily afforded the diamides in almost quantitative yields. Cyclization of the diamidoalcohol to the oxazoline derivatives proceeded through alcohol activation, either by tosylation (TsCl) or by chlorination (thionyl chloride) and through the action of a strong base for amide deprotonation (DMAP or sodium hydride). Pybox derivatives were then obtained in reasonable overall yields after recrystallization in ethanol (from 38 to 57% yield). **Ph-box** was however isolated by silica gel column chromatography (36% overall yield).

---

[7] a) Nishiyama, H.; Yamaguchi, S.; Kondo, M.; Itoh, K. *J. Org. Chem.* **1992**, *57*, 4306. b) Lundgren, S.; Lutsenko, S.; Jönsson, C.; Moberg, C. *Org. Lett.* **2003**, *20*, 3663.

4.2.2 Synthesis of functionalized ligands (L1).

4.2.2.1 Synthesis of 20a-20c.

The ureidobenzimidazole derivative **20a** precipitated upon treatment of 2-aminobenzimidazole with butylisocyanate in dichloromethane and was obtained in 87% yield (Fig 4.8). Similarly, treatment of 2-aminopyridine with butylisothiocyanate afforded 2-thioureidopyridine **20b** in 46% yield. The rather low yield was due to non completion of the reaction, attributed to the low reactivity of the substrates and the harsh reaction conditions (unstability of butylisothiocyanate).

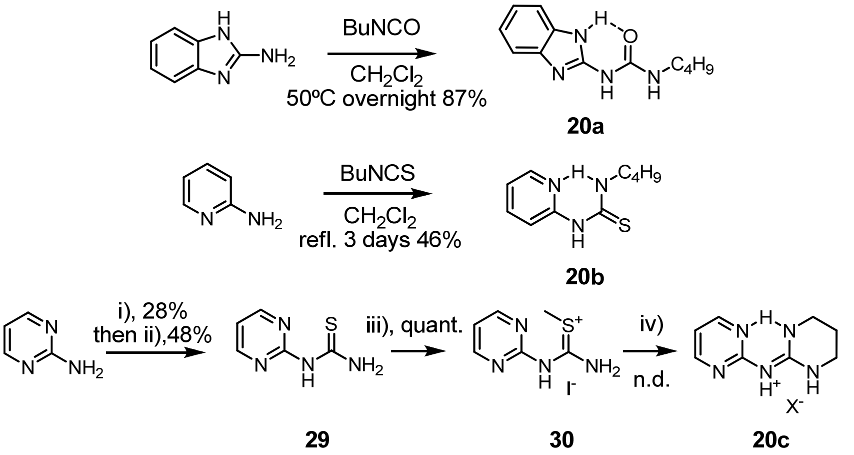
BuNCO
CH_2Cl_2
50ºC overnight 87%
20a
BuNCS
CH_2Cl_2
refl. 3 days 46%
20b
i), 28%
then ii),48%
iii), quant.
iv)
n.d.
29
30
20c

i) Benzoyl isothiocyanate, toluene,100 ºC, overnight; ii) NaOH/H_2O; iii) MeI, EtOH, reflux, overnight; iv) 1,3 diaminopropane, DMSO, 110 ºC, overnight.

Fig. 4.8: Synthesis of **20a-20c.**

As described in the literature for its pyridyl analogue,[8] preparation of **20c** was expected to take place by activation of thiourea **29** followed by nucleophilic substitution with 1,3-diaminopropane. Preparation of thiourea **29** proceeded by reaction of benzoylisothiocyanate with 2-aminopyrimidine to yield a protected thiourea that was debenzoylated in basic medium to yield **29** in a poor 13% overall yield. Thiourea **29** was then treated with methyl iodide for activation as the thiouronium salt **30**, which was heated in the presence of 1,3-diaminopropane. The isolated compound was unfortunately poorly soluble in common organic solvents and purification was therefore tedious, resulting in low yields. For this reason, **20c** was not studied for metal complexation and catalysis experiments.

---

[8] a) Rasmussen, C. S.; Villani, F. J. Jr.; Weaner, L. E.; Reynolds, B. E.; Hood, A. R.; Hecker, L. R.; Nortey, S. O.; Hanslin, A.; Costanzo, M. J.; Powell, E. T.; Molinari, A. J. *Synthesis* **1988**, 456. b) Zafar, A.; Melendez, R.; Geib, S. J.; Hamilton, A. D. *Tetrahedron* **2002**, *58*, 683.

4.2.2.2 Synthetic studies for 21a-21e.

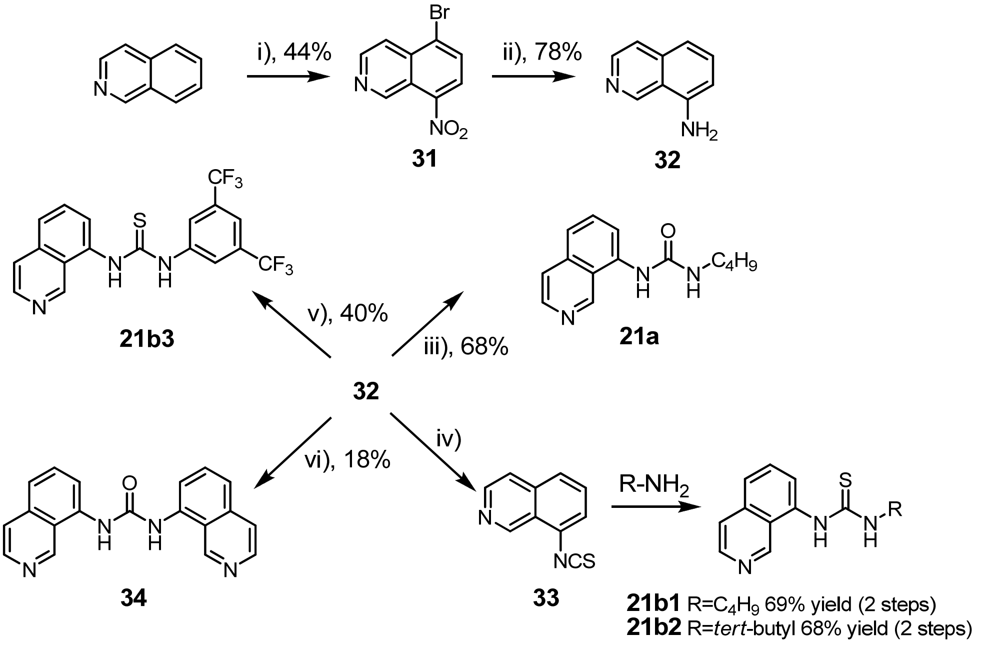
i), 44%
Br
N
NO2
31
ii), 78%
NH2
32
CF3
S
CF3
21b3
v), 40%
iii), 68%
O
C4H9
21a
32
vi), 18%
iv)
O
34
NCS
33
R-NH2
S
R
21b1 R=C4H9 69% yield (2 steps)
21b2 R=tert-butyl 68% yield (2 steps)

i) N-Bromosuccinimide, H_2SO_4, -10ºC then KNO_3; ii) DMF, NEt_3, H_2 60 psi, Pd/C; iii) butylisocyanate, CH_2Cl_2; iv) 1,1'-thiocarbonyldiimidazole, CH_2Cl_2; v) 1-isothiocyanato-3,5-bis(trifluoromethyl)benzene; Et_2O; vi) CDI, CH_2Cl_2.

Fig. 4.9: Synthesis of **21a-21b.**

Compound **21a** was prepared as described in a previous work published by Gale and co-workers.[6] Isoquinoline was first monobrominated at the 5-

position by electrophilic aromatic substitution and nitration was then performed regioselectively at the 8-position of the isoquinoline ring. 5-bromo-8-nitroisoquinoline **31** was thus obtained in 44% yield after recrystallization in methanol (Fig. 4.9). This step could be performed easily on multigram scale. Palladium catalyzed hydrogenation of the resulting compound under high pressure yielded the 8-aminoisoquinoline **32**, a key intermediate for the preparation of **21a-b**, in 78% yield. Treatment of **32** with butylisocyanate for five days at room temperature afforded urea **21a** in 68% yield after precipitation in hexanes. Preparation of **21b1** and **21b2** proceeded through the synthesis of 8-isothiocyanatoisoquiniline **33** that could be obtained upon treatment of **32** with 1,1'-thiocarbonyldiimidazole at room temperature for one day. Alternatively, obtention of 8-isocyanatoisoquinoline for further derivatization of the urea series by treatment of **32** with 1,1'-carbonyldiimidazole provided compound **34** as a major product (18% isolated yield in non optimized conditions), due to the nucleophilicity of **32**. Finally, thiourea **21b3** was obtained in 40% yield by treatment of **32** with 1-isothiocyanato-3,5-bis(trifluoromethyl)benzene in diethyl ether.

A conformational analysis of this compound was then performed by ^{1}H NMR bidimensional experiments (NOESY) at various temperatures. The most stable conformer is shown in Fig. 4.10.

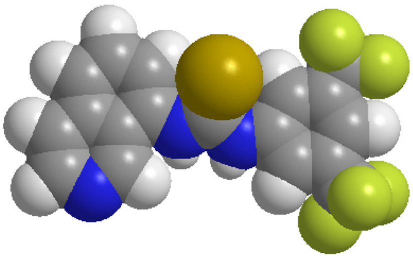

Fig. 4.10: MM2 model of **21b3** (Chem 3D)® and the most stable conformer as seen by NMR experiments.

The guanidinium **21d** was expected to be prepared by amination of 1-chloro-2,7-naphthyridine and further derivatization with guanidylation agents or by a similar synthetic route as for **20c** (Fig. 4.11).

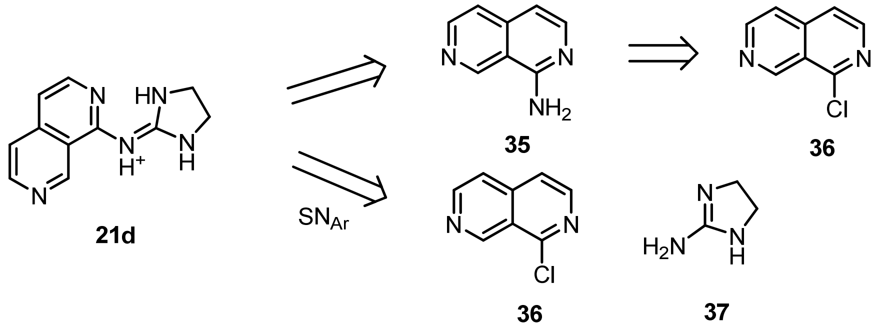

Fig. 4.11: Retrosynthetic analysis for **21d.**

1-Hydroxy-2,7-naphthyridine was prepared by intramolecular cyclization of the cyanoenamine derivative **38** following a described procedure.[9] On the other hand, 1-chloro-2,7-naphthyridine **36** was quantitatively prepared by treatment of 1-hydroxy-2,7-naphthyridine with phosphorous oxychloride (Fig. 4.12a). Compound **36** was then treated with sodium amide in THF in an attempt to substitute the chlorine atom for an amine function. Unfortunately, a mixture of products of the Chichibabin reaction was obtained and could hardly be separated (Fig. 4.12b).

---

[9] a) Baldwin, J. J.; Mensler, K.; Ponticello, G. S. *J. Org. Chem.* **1978**, *43*, 4878. b) Van den Haak, H. J. W.; Van der Plas, H. C.; Van Veldhuisen, B. *J. Heterocycl. Chem.* **1981**, *18,* 1349.

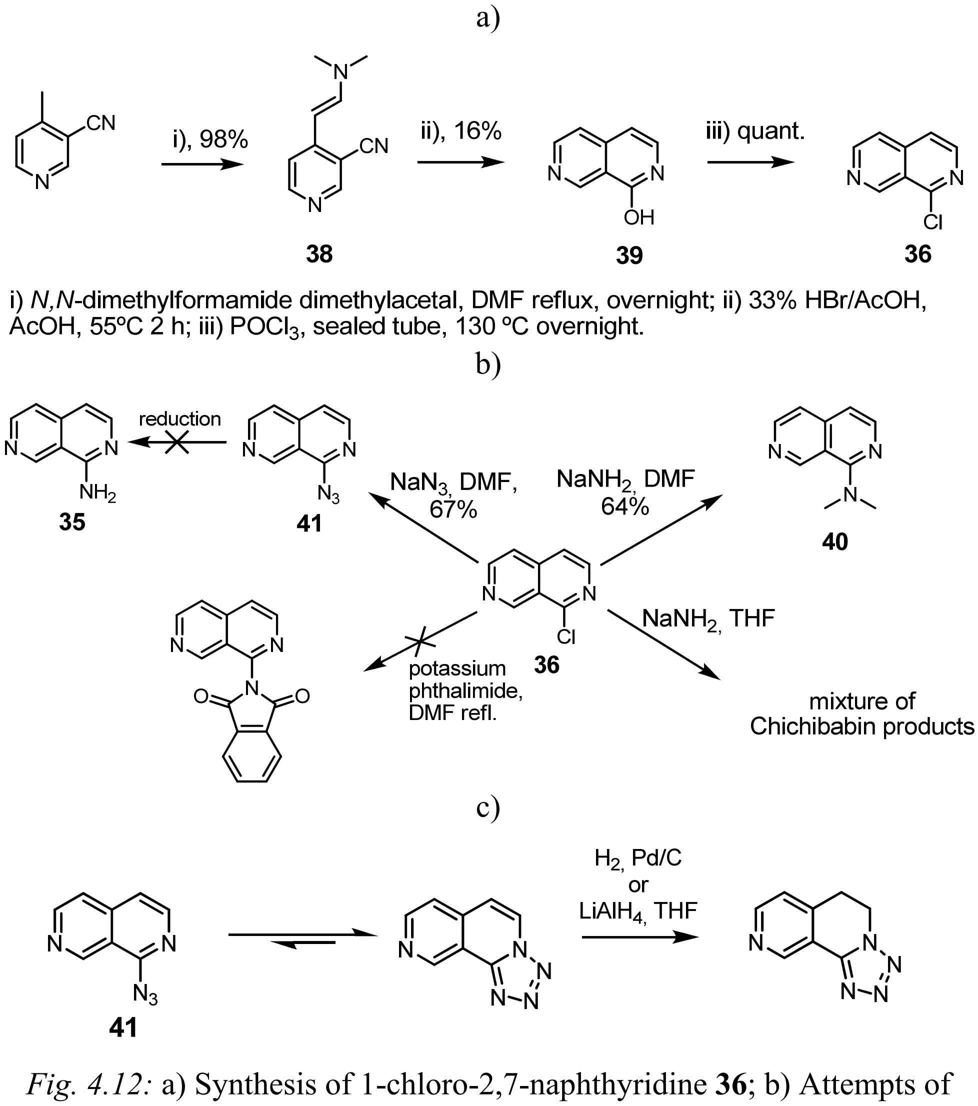
a)
i), 98%
ii), 16%
iii) quant.
38
39
36
b)
reduction
NaN$_3$, DMF, 67%
NaNH$_2$, DMF 64%
NaNH$_2$, THF
potassium phthalimide, DMF refl.
mixture of Chichibabin products
35
41
40
36
c)
H$_2$, Pd/C or LiAlH$_4$, THF
41

i) *N,N*-dimethylformamide dimethylacetal, DMF reflux, overnight; ii) 33% HBr/AcOH, AcOH, 55°C 2 h; iii) $POCl_3$, sealed tube, 130 °C overnight.

Fig. 4.12: a) Synthesis of 1-chloro-2,7-naphthyridine **36**; b) Attempts of amination of **36**; c) Evidence for the azide/tetrazole equilibrium.

Surprisingly, in DMF, this reaction gave rise to only one product, namely the 1-dimethylamino-2,7-naphthyridine **41** (obtained in 64% yield after column chromatography), resulting from the nucleophilic attack of sodium dimethylamide, product of the fast transamidation reaction between sodium amide and *N,N*-dimethylformamide. Gabriel's amine synthesis was also investigated but substitution of the chlorine atom with phthalimide by reflux in DMF gave rise to a complex mixture of products. Substitution of the chlorine atom by an azido group was also attempted, but the obtained product (67% yield) appeared to be the tautomeric tetrazole (Fig. 4.12c). Evidence for this process was the absence of the characteristic azide absorption band on the IR spectrum of **41**, and the hydrogenation of the aromatic naphthyridine core instead of reduction of the azide by catalytic hydrogenation or by reaction with lithium aluminium hydride.

As a last trial, a direct nucleophilic aromatic substitution between the monocyclic guanidine **42** and **36** was attempted (Fig. 4.13). Compound **42** was prepared according to described procedures from 1,2-diaminoethane and dimethylcyanamide.[10] 1,2-diaminoethane was first transformed into the monotosylate ammonium salt by *p*-toluenesulfonic acid in quantitative yield. The resulting salt was heated at 120 ºC in a sealed tube in dimethylcyanamide to give the corresponding guanidinium tosylate in 53% yield after recrystallization in ethanol. The anion was then exchanged to hydroxide by an ion exchange resin to yield the corresponding hydrate. Aromatic nucleophilic substitution of the chlorine atom of **36** by **42** was then investigated and the reaction was performed by heating a solution of the substrates in DMF (120 ºC). A white precipitate was formed and collected by filtration. Surprisingly, the product appeared to be the spiro derivative **43** arising from consecutive nucleophilic and electrophilic aromatic substitution reactions, which was evidenced by ^{13}C NMR. The same compound was obtained when the reaction was repeated at room temperature. Preparation of **21d** could therefore not be achieved.

---

[10] Adcock, B.; Lawson, A.; Miles, D. H. *J. Chem. Soc.*, **1961**, 5120.

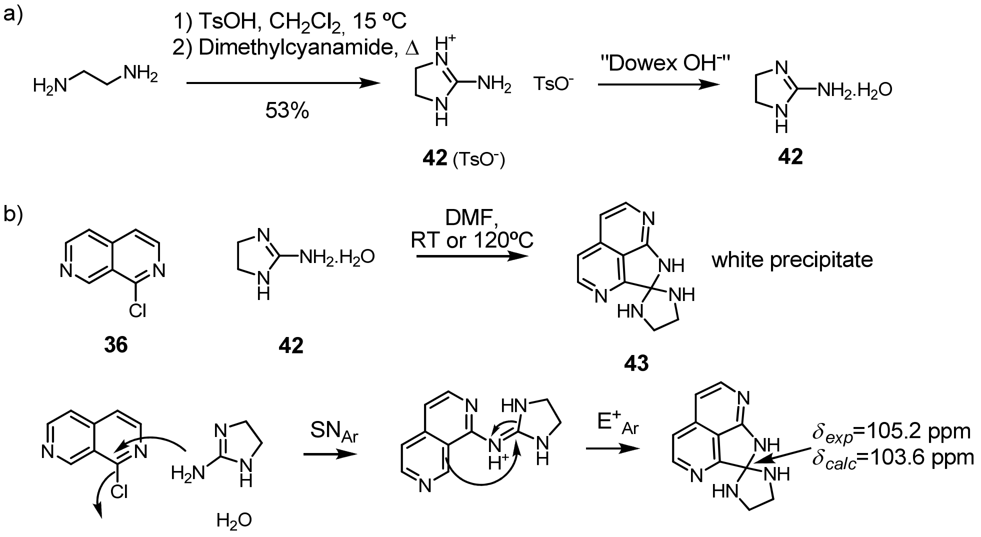
a)
1) TsOH, CH2Cl2, 15 ºC
2) Dimethylcyanamide, Δ
53%
42 (TsO⁻)
"Dowex OH⁻"
42
b)
36
42
DMF,
RT or 120ºC
white precipitate
43
SNAr
E⁺Ar
H2O
δexp=105.2 ppm
δcalc=103.6 ppm

Fig. 4.13: a) Synthesis of monocyclic guanidine **42**; b) Attempts of nucleophilic aromatic substitution between **42** and **36**.

As an alternative, we decided to perform the synthesis of isoquinoliguanidinium **21e**, following a similar route as for the benzoguanidinium derivative **2** (see Chapter 2). Synthesis therefore requires the preparation of diamine **44**, which could be achieved by reduction of 7-cyano-8-aminoisoquinoline **45**, whose preparation from **31** involved the transformation of nitroaryl derivatives to *o*-cyano-aminoaryl derivatives, following a known methodology.[11] Since the synthesis of fluorescent chiral guanidines is also of high interest for our research group, control experiments for the synthesis of naphthoguanidine **46** were also performed (Fig. 4.14).

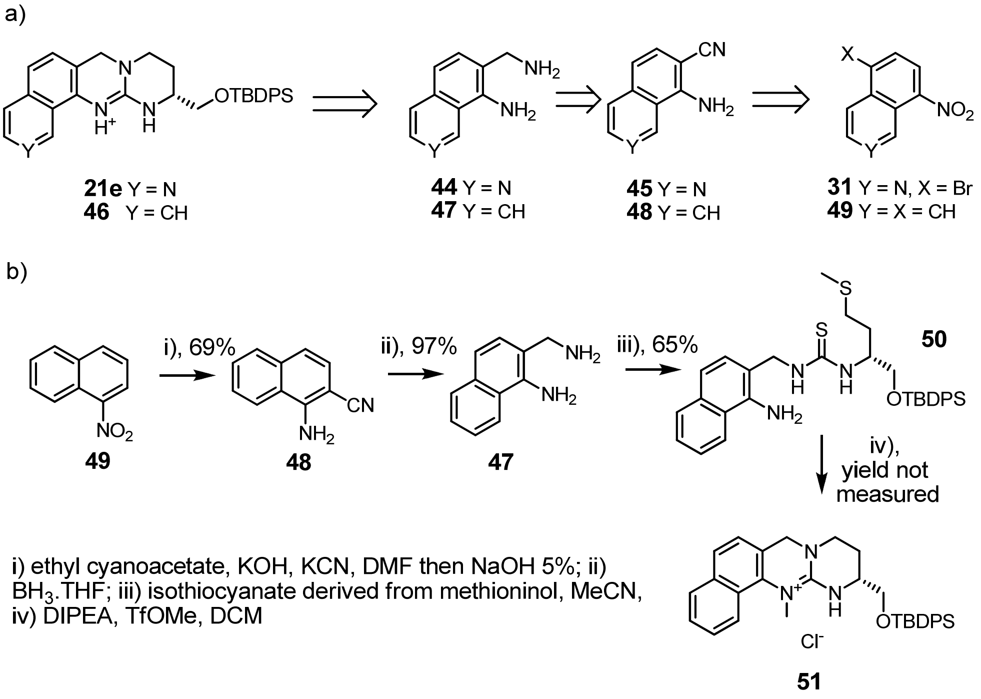
a)
OTBDPS
21e Y = N
46 Y = CH
NH2
44 Y = N
47 Y = CH
CN
45 Y = N
48 Y = CH
X
NO2
31 Y = N, X = Br
49 Y = X = CH
b)
i), 69%
ii), 97%
iii), 65%
49
48
47
50
iv), yield not measured
51
Cl-
i) ethyl cyanoacetate, KOH, KCN, DMF then NaOH 5%; ii) BH3.THF; iii) isothiocyanate derived from methioninol, MeCN, iv) DIPEA, TfOMe, DCM

Fig. 4.14: a) Retrosynthetic analysis of naphthoguanidine **46** and isoquinolinoguanidine **21e**; b) Synthesis of compound **46**.

1-Nitronaphthalene **49** was treated with ethylcyanoacetate in the presence of potassium hydroxide and potassium cyanide, followed by an aqueous solution of sodium hydroxide to yield cyanoamine **48** in 69% yield after purification. Diamine **47** was obtained in 97% yield after reduction of the nitrile with boron hydride. After treatment with the isothiocyanate derived from methioninol in acetonitrile (see Chapter 2), thiourea **50** was isolated in 65% yield after column chromatography. The double cyclization was then performed as previously for the benzoguanidinium derivative. Unfortunately, the major compound was the *N*-methylguanidine **51** as revealed by mass spectrometry and ^{1}H NMR in the reaction crude.[12] This surprising outcome was attributed to the electron rich naphthalene ring that renders the amine (in position 1) more nucleophilic and prompt to both methylation and cyclization. The methodology proved thus suitable for the synthesis of aromatic guanidines from nitroaryl derivatives. For this reason, preparation of **21e** was attempted by the same synthetic scheme.

---

[11] a) Tomioka, Y.; Ohkubo, K.; Yamazaki, M. *Chem. Pharm. Bull.* **1985**, *33*, 1360. b) Zhang, W.; Liu, R.; Cook, J. M. *Heterocycles* **1993**, *36*, 2229.

Upon treatment of **31** (5-bromo-8-nitroisoquinoline) with ethyl cyanoacetate, potassium cyanide and potassium hydroxide in DMF, the unexpected major product **52** was obtained, likely as a result of nucleophilic aromatic substitution on the bromine atom, activated as a leaving group by the electron withdrawing nitro group, followed by decarboxylation in basic medium (Fig. 4.15). This side reaction could be avoided by a Stille reaction performed on **31** with tributyltin hydride in the presence of tetrakis-(triphenylphosphino)palladium, which gave rise to 8-nitroisoquinoline **53** in 99% yield after column chromatography (Fig. 4.16). The aminonitrile **45** was then formed upon treatment of 8-nitroisoquinoline with ethylcyanoacetate in presence of potassium cyanide and potassium hydroxide. However, purification of **45** proved difficult by column chromatography because of its low solubility in chloroform, and, as a result, a low yield (not determined) was obtained.

---

[12] The methylation site was not determined.

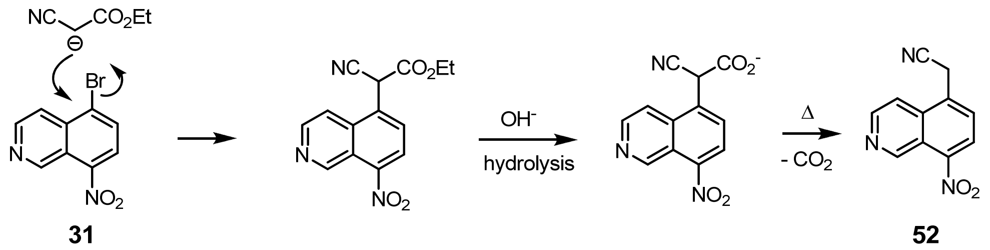
NC CO2Et
Br
N
NO2
31
NC CO2Et
OH-
hydrolysis
NC CO2-
Δ
- CO2
NC
52

Fig. 4.15: Proposed mechanism for the formation of **52**.

Reduction of nitrile **45** to amine **44** was then investigated with various reducing agents (boron hydride, catalytic hydrogenation with Ni Raney, Pd/C with hydrogen pressure). Surprisingly, the reaction gave rise to a mixture of products in all cases, as seen on the ^{1}H NMR and mass spectra (ESI$^+$) analysis of the crude mixtures. Overreduction of the aromatic scaffold was even detected in some cases (such as in palladium catalyzed hydrogenations under acidic medium). Since amine **44** could not be prepared successfully, the synthesis of **21e** was not further investigated.

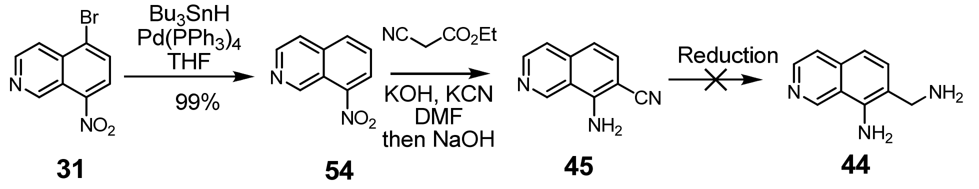
Br
Bu3SnH
Pd(PPh3)4
THF
99%
N
NO2
31
54
NC CO2Et
KOH, KCN
DMF
then NaOH
CN
NH2
45
Reduction
NH2
44

Reduction: i) BH_3.THF, 0 °C to reflux; ii) Ni Raney, H_2 (4 bar), DMF; iii) Pd/C, HCl 1N, H_2 (3 bar); iv) Pd/C AcOH, H_2 (1 atm)

Fig. 4.16: Synthetic efforts towards **21e**.

Given the difficulties encountered to prepare a guanidinium derivative with a spacing group equivalent to the one found in **21a-21b**, we decided to prepare a more flexible, readily available ligand. Carboxyguanidines are easily accessible from carboxylic acids and therefore represent candidates of choice. A carboxyguanidine derived from nicotinic acid (**21c**) would allow to reproduce the conformations obtained with **21d** and **21e**, though some freedom is introduced. Synthesis of **21c** was successfully achieved according to a procedure described by Schmuck *et al.*[13]

Treatment of guanidinium carbonate in alkaline medium with di-*tert*-butyldicarbonate in 1,4-dioxane and water yielded the Boc-protected guanidine **55** in 88% yield.[14] The peptidic coupling was then performed according to described procedures with Pybop® assisted acid activation. Boc-protected carboxyguanidine **56** could be isolated by precipitation in 89% yield. Treatment of **56** in trifluoroacetic acid for 15 minutes at room temperature quantitatively afforded the diprotonated form of **21c** (Fig 4.17a). The x-ray structure of **21c** was determined by addition of saturated picric acid, since the compound precipitated and was easily crystallized (Fig. 4.16b). Treatment of **21c** (trifluoroacetate salt) on an anion exchange resin (chloride) in water afforded **21c** (Cl^-) as a white solid.

---

[13] Schmuck, C.; Machon, U. *Chem. Eur. J.* **2005**, *11*, 1109.

[14] For synthesis, see: Abou-Jneid, R.; Ghoulami, S.; Martin, M.-T.; Dau, E.; Travert, N.; Al-Mourabit, A. *Org. Lett.* **2004**, *6*, 3933.

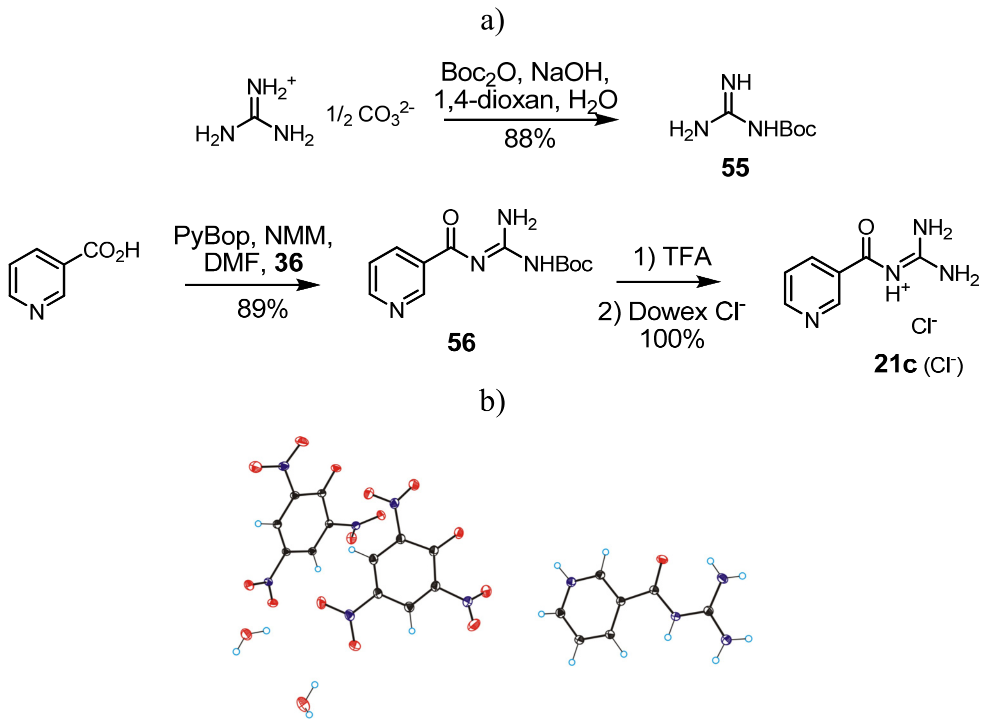
a)
NH2+
H2N
NH2
1/2 CO3 2-
Boc2O, NaOH,
1,4-dioxan, H2O
88%
NH
H2N
NHBoc
55
CO2H
N
PyBop, NMM,
DMF, 36
89%
O
NH2
N
NHBoc
56
1) TFA
2) Dowex Cl-
100%
O
NH2
N
H+
NH2
N
Cl-
21c (Cl-)
b)

Fig. 4.17: a) Synthesis of **21c**; b) X-ray structure of **21c** (picrate).

4.2.2.3 Synthetic studies for 22a-22c.

The cooperativity observed in the porphyrin systems studied in the previous chapter inspired the preparation of dipyrromethenes for the formation of heteroleptic chiral complexes. It was first anticipated that a similar synthetic route as the one used in the previous chapter could be used (from 2-nitrobenzaldehyde). Also, 2-chlorobenzaldehyde was investigated as a possible starting material. Dipyrromethenes were prepared according to known procedures, by treatment of an aromatic aldehyde with pyrrole in

TFA, to form the dipyrromethane.[15] Dipyrromethanes were then oxidized with DDQ to the corresponding dipyrromethenes (Fig. 4.18).

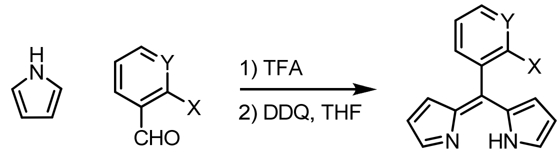

X	**Y**	Yield step 1	Yield step 2
NO_2	CH	72% (**57**)	61% (**60**)
Cl	CH	94% (**58**)	23% (**61**)
Cl	N	84% (**59**)	30% (**62**)

Fig. 4.18: Synthesis of dipyrromethenes.

The preparation of aminodipyrromethene **63** has been reported either by Pd-catalyzed hydrogenation or by tin (II) chloride reduction of **60**.[16] These procedures however proved unsuccessful for compound **57** and **60** since some reduction of the pyrrole ring was also observed in the case of catalytic hydrogenations. For practical reasons (stability, handling…), **60** was complexed with boron trifluoride etherate to give **64** in 86% yield, but application of both reduction methods on **64** failed to give the desired reduction product (Fig. 4.19a). The compound was nevertheless detected by mass spectrometry, but column chromatographies never afforded the pure desired product. Given these negative results, further synthesis was not pursued and emphasis was concentrated on the preparation of the more promising bidentate ligands **23a-b** and **24a-d**. The crystal structure of **64** is represented in Fig. 4.19b.

---

[15] a) Yu, L.; Muthukumaran, K.; Sazanovich, I. V.; Kirmaier, C.; Hindin, E.; Diers, J. R.; Boyle, P. D.; Bocian, D. F.; Holten, D., Lindsey, J. S. *Inorg. Chem.* **2003**, *42*, 6629. b) Wood, T. E.; Berno, B.; Beshara, C. S.; Thompson, A. *J. Org. Chem.* **2006**, *71*, 2964.

[16] Ziessel, R.; Bonardi, L.; Retailleau, P.; Ulrich, G. *J. Org. Chem.* **2006**, *71*, 3093.

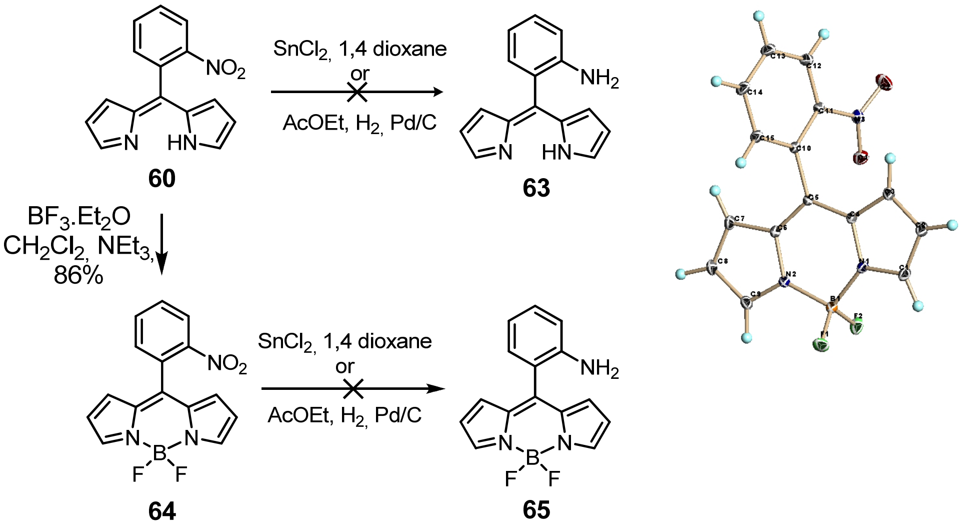
NO2
SnCl2, 1,4 dioxane
or
AcOEt, H2, Pd/C
NH2
60
63
BF3.Et2O
CH2Cl2, NEt3,
86%
NO2
SnCl2, 1,4 dioxane
or
AcOEt, H2, Pd/C
NH2
64
65

a) b)

Fig. 4.19: a) Synthetic efforts towards **63** and **65**; b) ORTEP plot of the X-ray structure of **64**.

4.2.2.4 Towards the preparation of 23a-b.

The retrosynthetic scheme of these bidentate ligands was inspired by the synthetic route used for the monodentate ones (Fig. 4.20a). The key intermediate is amine **66**, and the synthesis of isoquinolines **68** and **69** was based on the preparation of 3,3'-biisoquinoline reported by Sauvage and co-workers.[17]

---

[17] Durola, F.; Hanss, D.; Roesel, P.; Sauvage, J.-P.; Wenger, S. *Eur. J. Org. Chem.* **2007**,

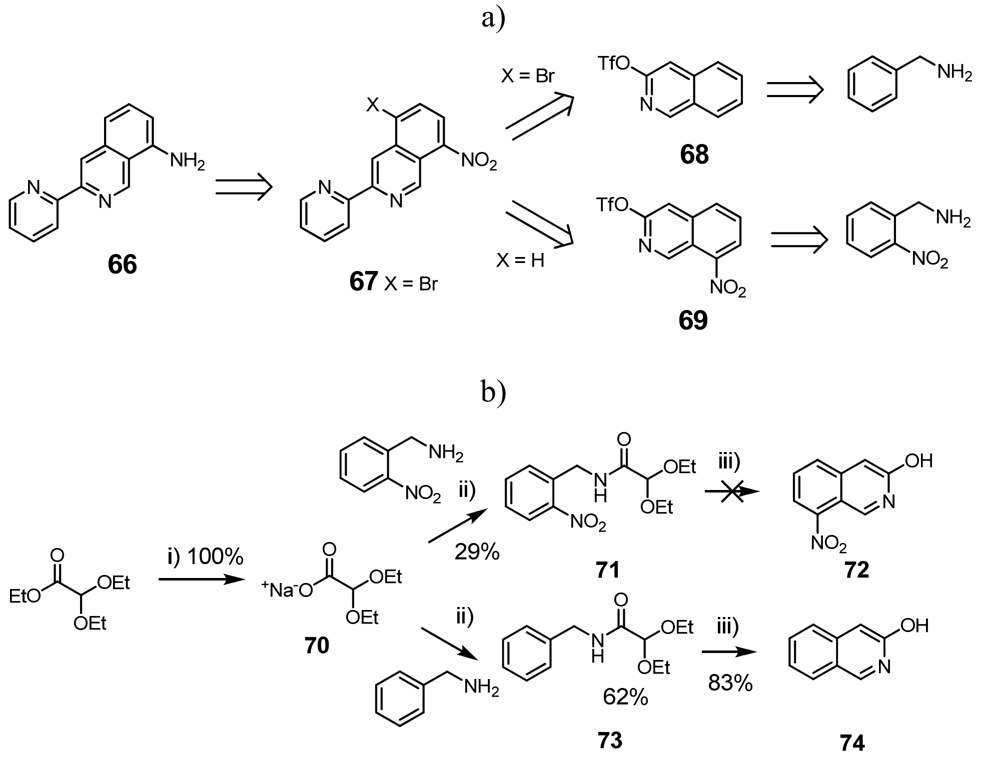
a)
X = Br
TfO
N
NH2
68
X
N
N
NO2
66
67 X = Br
X = H
TfO
N
NO2
69
NH2
NO2
b)
NH2
NO2
ii)
O
N
H
OEt
OEt
NO2
iii)
OH
N
NO2
29%
71
72
O
EtO
OEt
OEt
i) 100%
O
+Na-O
OEt
OEt
70
ii)
NH2
O
N
H
OEt
OEt
62%
73
iii)
83%
OH
N
74

i) NaOH, H_2O, EtOH, o.n.; ii) 1) $SOCl_2$, Et_2O reflux; 2) dry pyridine, dry toluene; iii) H_2SO_4, 1 day.

Fig. 4.20: a) Retrosynthetic analysis of the key intermediate **66**;
b) Synthesis of 3-hydroxyisoquinoline derivatives.

Ethyl diethoxyacetate was first hydrolyzed in a basic aqueous medium to yield sodium diethoxyacetate in quantitative yield after lyophilization. Treatment of the carboxylate with thionyl chloride readily afforded the corresponding acid chloride, to which the benzylamine derivative was added to form the amide bond. In the case of 2-nitrobenzylamine derivative, amide **71** could be isolated in a 29% yield after column chromatography (unstable). In the case of benzylamine, **73** was obtained in a 62% yield after

---

125.

column chromatography. Curiously, cyclization of **71** to the 8-nitro-3-hydroxy-isoquinoline **72** in sulfuric acid at room temperature was unsuccessful.[18] 3-hydroxyisoquinoline **74** was however isolated in 83% yield when amide **73** was treated under the same conditions (Fig. 4.20b).

3-Hydroxyisoquinoline was then treated with trifluoromethanesulfonate anhydride in dry pyridine in order to activate the heterocycle for the following Negishi coupling, to afford compound **56** in a 78% yield after column chromatography.

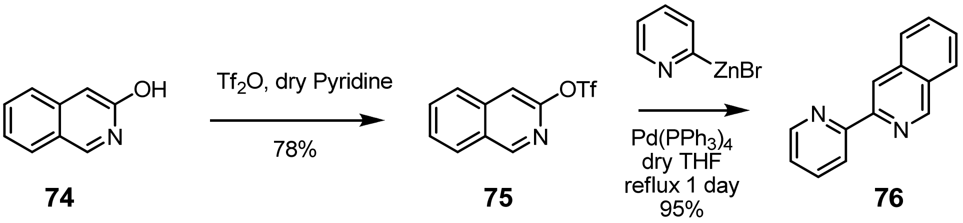

Fig. 4.21: Preparation of 3-(pyridin-2-yl)isoquinoline **76**.

Formation of the pyridine-isoquinoline C-C bond elaboration between the pyridine and the isoquinoline ring could then be achieved by a a Pd(0)-catalyzed C-C coupling in 95% yield. The compound was isolated without chromatography and obtained as a single product after work-up (38% overall yield, 6 steps). Given that the isoquinoline functionalization proved efficient for the synthesis of **21a-b**, selective bromination of **76** at position 5 followed by nitration at position 8 was investigated. **76** was thus treated with *N*-bromosuccinimide in sulfuric acid at -10 ºC for one day, but no reaction could be observed after this time, which was attributed to the lower reactivity of **76** with respect to isoquinoline (the 2-pyridyl moiety behaving as an electron withdrawing substituent). At room temperature a mixture of **76**, **77**, and **78** was obtained; which upon treatment with potassium nitrate (one pot) afforded the desired isoquinoline derivative **79** (Fig. 4.22).

---

[18] Reaction was not investigated further, though gentle heating might favour the cyclization process.

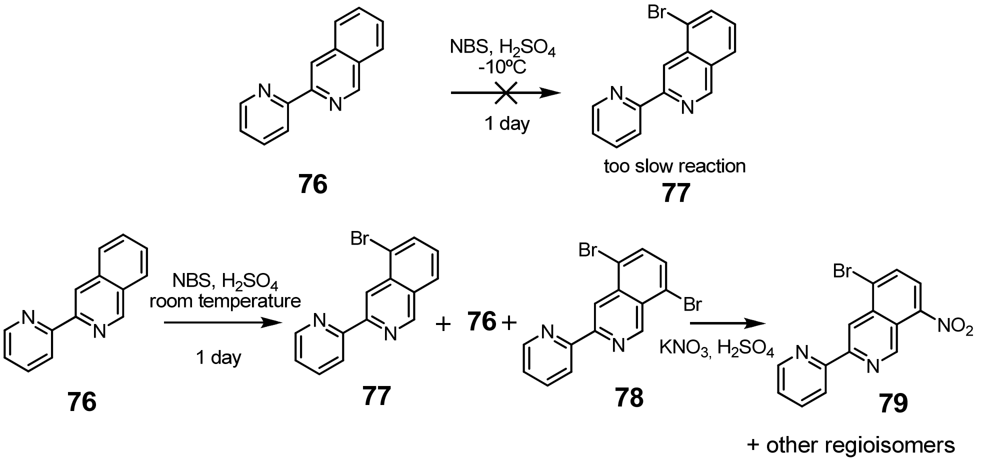
76
NBS, H_2SO_4
-10ºC
1 day
Br
too slow reaction
77
76
NBS, H_2SO_4
room temperature
1 day
Br
77
+ 76 +
Br
Br
78
KNO_3, H_2SO_4
Br
NO_2
79
+ other regioisomers

Fig. 4.22: Functionalization attempts of **76.**

The dibromo derivative **78** could be isolated by recrystallization in methanol and attempts to separate the mixture of products obtained from the reaction by column chromatography were unsuccessful. Compound **77** is actually more reactive than **76**, which results in a mixture of products. Therefore, these synthetic studies were abandoned and the synthesis of carboxyguanidines derived from 2,2'-bipyridines was undertaken.

4.2.2.5 Synthesis of 24a-24d.

As for compound **21c**, carboxyguanidines were expected to be easily prepared from the corresponding aromatic carboxylic acids. 5,5'-dicarboxylic acid-2,2'-bipyridine **80** (for the synthesis of **24c-d**), being commercially available, only the preparation of 2,2'-bipyridine-5-carboxylic acid **81** was required. Negishi coupling between 2-bromo-5-methylpyridine and 2-pyridyl zinc bromide afforded the corresponding 5-methyl-2,2'-bipyridine **82** in 95% yield without column chromatography (Fig. 4.23a).

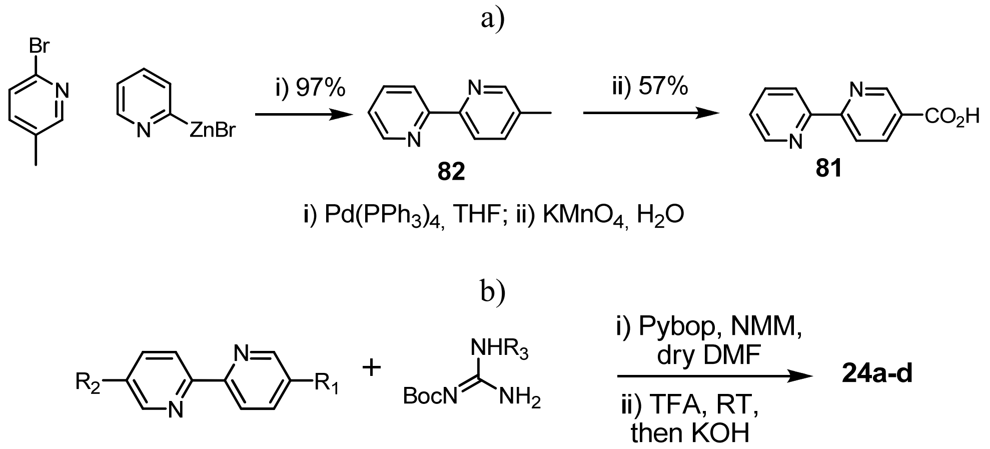
a)
Br
N
N
ZnBr
i) 97%
N
N
82
ii) 57%
N
N
CO2H
81
i) Pd(PPh3)4, THF; ii) KMnO4, H2O
b)
R2
N
N
R1
+
NHR3
BocN
NH2
i) Pybop, NMM, dry DMF
ii) TFA, RT, then KOH
24a-d

R_1	**R_2**	**R_3**	Yield
CO_2H	H	H	63% [**24a (Cl^-)**]
CO_2H	H	C_8H_{17}	76% (**24b**)
CO_2H	CO_2H	H	27% [a, b] (**24c**)
CO_2H	CO_2H	C_8H_{17}	n.m. [a] (**24d**)

[a] The low solubility of the compounds in organic solvents caused low yields, though Boc deprotection is quantitative. [b] Isolated by centrifugation of a NaOH suspension.

Fig. 4.23: a) Synthesis of acid **81**; b) Synthesis of **24a-24d**.

The methyl group was then oxidized to carboxylic acid by potassium permanganate, affording acid **81** in 57% yield after precipitation. A methodology previously described (peptide coupling with *N*-Boc guanidine followed by Boc deprotection) was then applied to the synthesis of **24a-d** (Fig. 4.23b).

N-Boc octyl guanidine was prepared following a methodology reported by Feichtinger *et al.,* offering the possibility to prepare a wide library of *N*-Boc guanidines from primary amines.[19] Guanidinium carbonate was first treated with benzoyl chloride in alkaline medium to yield *N*-Cbz guanidine **83** in 75% yield. **83** was subsequently treated in the same conditions with di-*tert*-butyl dicarbonate to afford the diprotected guanidine **84** in 68% yield. The latter was then activated at low temperature with trifluoromethane sulfonic anhydride to yield the key intermediate **85** in 62% yield. Reaction of octylamine with **85** yielded the diprotected octylguanidine in 89% yield, which was hydrogenated in the presence of palladium over charcoal to yield *N*-Boc-*N'*-octylguanidine **87** in 100% yield (at 78% conversion). Alternatively, **87** could also be prepared in one single step by treatment of octylguanidinium hemisulfate with di-*tert*-butyl dicarbonate in alkaline medium (65% yield) (Fig. 4.24). Thus, this method offers the possibility to extend the family of studied carboxyguanidines (introduction of chirality might also be considered). Octyl group was introduced to enable full solubility of the product; unfortunately, **24b** only proved soluble in dichloromethane.

---

[19] a) Goodman, M.; Feichtinger, K.; Romoff, T.T. *PCT Int. Appl.* **1998,** WO 9852917. b) Feichtinger, K.; Zapf, C.; Sings, H.L.; Goodman, M. *J. Org. Chem.* **1998**, *63*, 3804.

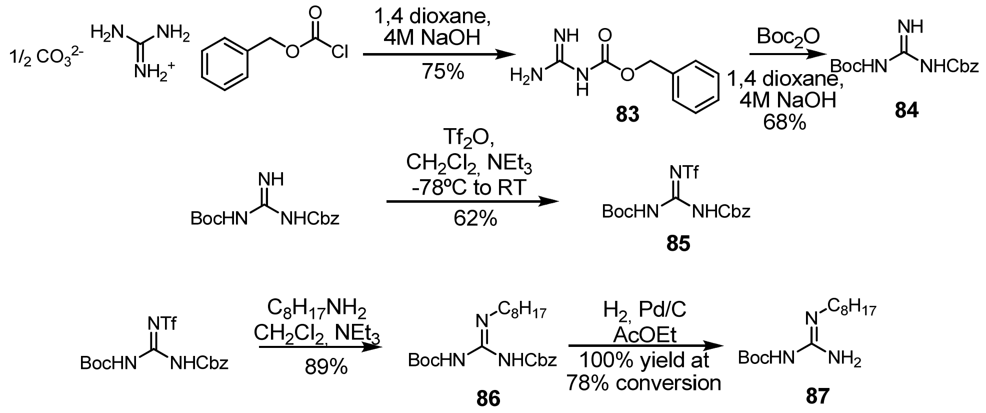
1/2 CO_3^{2-}
H_2N
NH_2
NH_2^+
O
O
Cl
1,4 dioxane,
4M NaOH
75%
NH
O
H_2N
N
H
O
83
Boc_2O
1,4 dioxane,
4M NaOH
68%
NH
BocHN
NHCbz
84
NH
BocHN
NHCbz
Tf_2O,
CH_2Cl_2, NEt_3
-78ºC to RT
62%
NTf
BocHN
NHCbz
85
NTf
BocHN
NHCbz
$C_8H_{17}NH_2$
CH_2Cl_2, NEt_3
89%
N
C_8H_{17}
BocHN
NHCbz
86
H_2, Pd/C
AcOEt
100% yield at
78% conversion
N
C_8H_{17}
BocHN
NH_2
87

Fig. 4.24: Synthesis of *N*-Boc-*N'*-octylguanidine **87**.

4.3 Mixing the ligand libraries with metals.

4.3.1 Monodentate functionalized ligands.

4.3.1.1 Complexation studies for 20a-c.

Since **20a** and **20c** are poorly soluble in common organic solvents, complexation experiments were mainly performed with 2-thioureidopyridyl derivative **20b**, also because thiourea derivatives are widely used in organocatalysis.[20] Complexes were prepared by mixing stoichiometric amounts of **20b**, the chiral ligand, and metal salt. Fast ligand exchange at the NMR time scale prevented to assess for the exclusive formation of the desired heteroleptic complex. In a first series of experiments, complexation of **20b** and ***i*Pr-Pybox** with $ZnCl_2$ was studied. Up to three species were likely to form, given the versatile coordination sphere of Zn(II). First, an entropically favored complex made of two tridentate ***i*Pr-Pybox** ligands surrounding the hexacoordinated metal was expected. On the other hand, **20b** is also likely to act as a bidentate ligand since the soft sulfur atom is an excellent transition metal binder. **20b** might therefore bind the metal through the heteroaromatic nitrogen and the sulfur atom (enthalpically favored), giving rise to either a tetracoordinated (**$ZnCl_2(20b)_2$**) or a pentacoordinated (**$ZnCl_2(20b)$(*i*Pr-Pybox)**) metal center.

---

[20] Connon, S. J. *Chem. Eur. J.* **2006**, *12*, 5419.

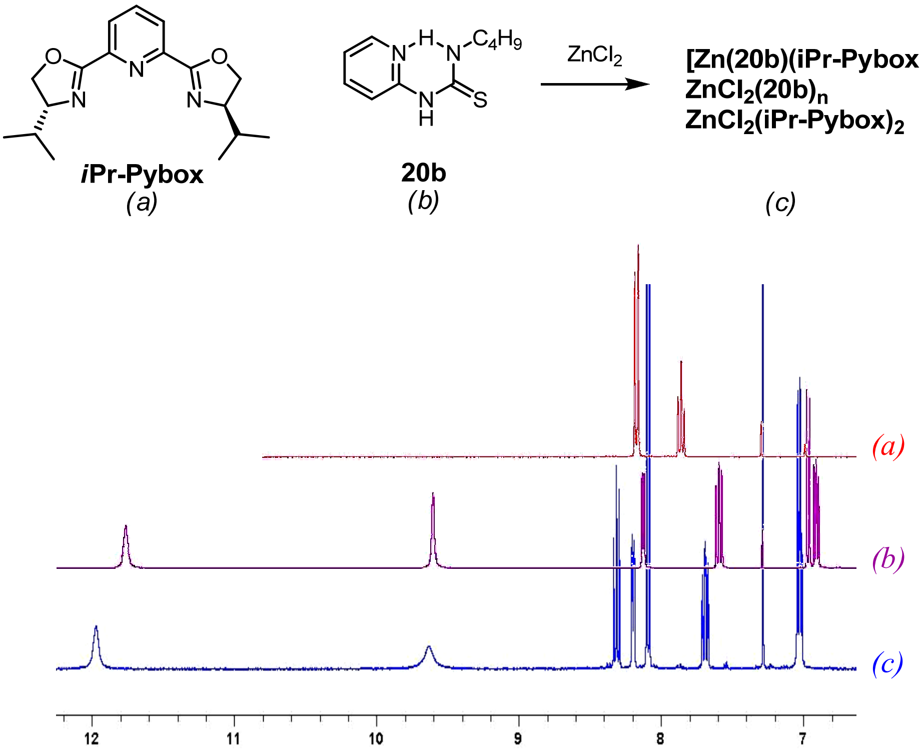

Fig. 4.25: ^{1}H NMR complexation experiment of **20b**, ***i*Pr-Pybox** and $ZnCl_2$

As shown above, every signal of each ligand was shifted upon addition of the metal salt (downfield shifts were observed in most cases), suggesting that both **20b** and ***i*Pr-Pybox** are bound to the metal. However, no specific contacts between these two species were detected by 2D NMR experiments (COSY, NOESY).

Since the chloride anion was expected to form hydrogen bonds with the thiourea group, preparation of the complex with $Zn(OAc)_2$ and $Zn(BF_4)_2$ was also investigated. Indeed, structurally different, well defined species were obtained. However, in the case of tetrafluoroborate, broad peaks and undefined species were observed on the spectrum, probably due to the formation of a bridged dimeric zinc complex in the cases of metal binding anions (chloride, acetate). The NMR spectra would therefore correspond to a mixture of **ZnX_2(*i*Pr-Pybox)$_2$** and **$ZnCl_2$(20b)$_2$** (both enthalpically and entropically favoured related to the desired **$ZnCl_2$(20b)(*i*Pr-Pybox)** complex) (Fig. 4.26). This hypothesis was further supported by the lack of catalytic activity of the system (see Section 4.4).

Similar experiments were then undertaken, replacing ***i*Pr-Pybox** by **(*R*)-BINOL**. Again, NMR signals of **20b** varied siginificantly depending on the metal salt (acetate or tetrafluoroborate), suggesting that for acetate a bridged zinc dimer was likely.

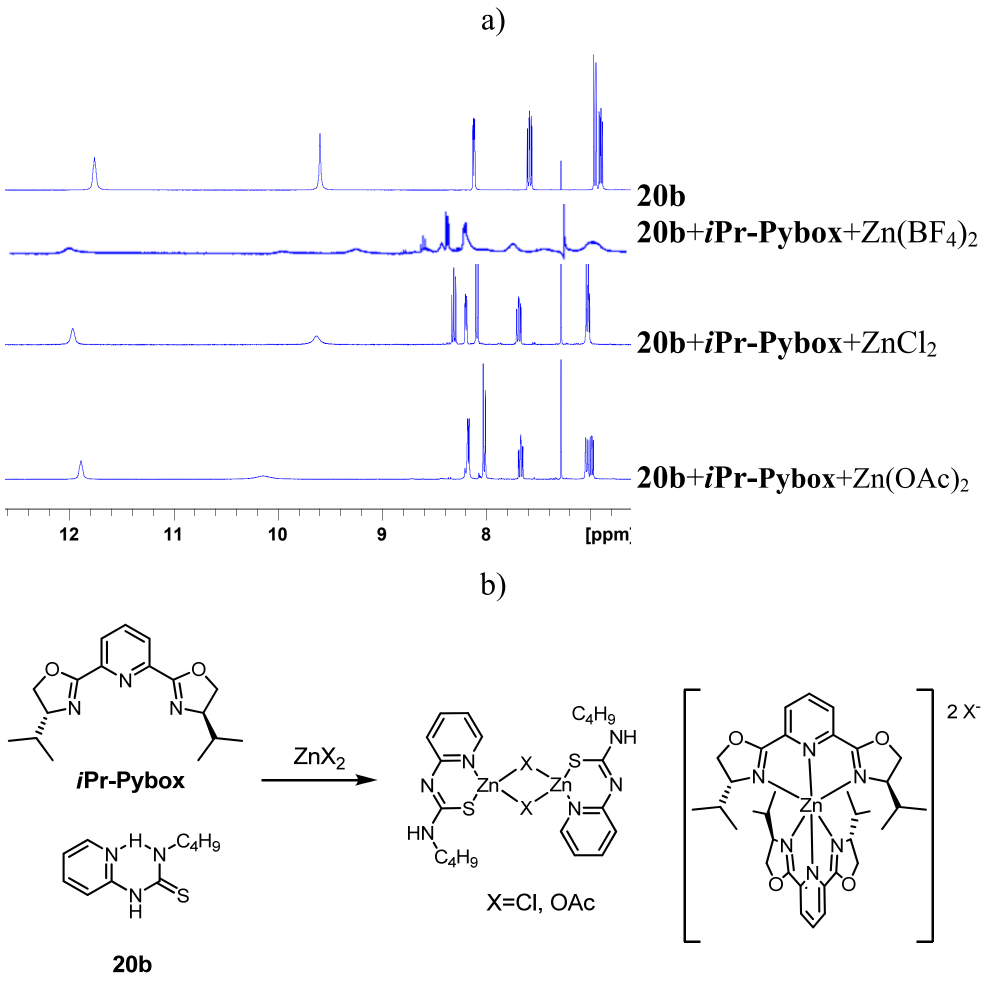

Fig. 4.26: a) Influence of the counterion on complex formation; b) Potential mixtures of complexes with Zn(II).

Copper (I), bearing a tetrahedral environment, was subsequently studied. The NMR spectra in the presence of CuI were similar as for Zn(II), each ligand binding the metal. Upon addition of acetylacetonate, signals of **20b** did not change significantly, suggesting that the hydrogen bonding pocket was deactivated (Fig. 4.27).

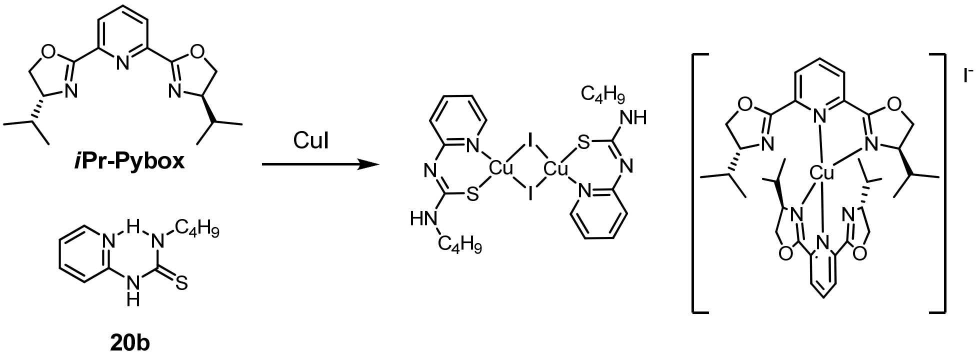

Fig. 4.27: Potential mixture of complexes with Cu(I).

In conclusion, Zn(II) and Cu(I) are not suitable metals for the formation of the desired heteroleptic complex. Additionally, these observations proved that a 2-pyridyl spacing group was not suitable for our purpose, since sulfur coordination to the metal was facilitated by the proximity of the pyridine lone pair. This coordination mode of **20b** has been reported in the literature.[21] For this reason, other functionalized ligands bearing longer spacers, such as isoquinoline, were evaluated.

4.3.1.2 Complexation studies with 21a-b.

Complexation of **21a** and **Ph-Pybox** with Cu(MeCN)$_4$(PF$_6$) was studied by ^{1}H NMR. This Cu(I) source was chosen because of its non coordinating anion, to avoid formation of the anion bridged copper dimer previously observed with **20b**. Addition of **21a** or **21b** to the mixture of **Ph-Pybox** and copper (I), resulted in a precipitate showing broad peaks in the ^{1}H NMR spectrum belonging to **Ph-Pybox**, which means that **Cu(Ph-Pybox)$_2$(PF$_6$)** was formed. The following scheme was then considered (Fig. 4.28):

---

[21] Fan, Y.; Lu, H.; Hou, H.; Zhou, Z.; Zhao, Q.; Zhang, L.; Cheng, F. *J. Coord. Chem.* **2000**, *50*, 65.

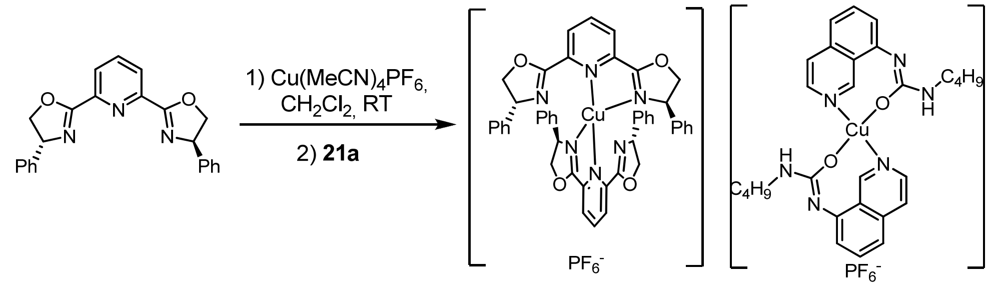

Fig. 4.28: Proposed mixture of complexes obtained with Cu(MeCN$_4$)(PF$_6$), **21a** and **Ph-Pybox**.

Similar experiments were undertaken with thioureas **21b1**, **21b2**, and **21b3**, without significant changes with respect to **21a**. Equimolar amounts of **Ph-Pybox** and tetrakis-(acetonitrile)copper(I) hexafluorophosphate were mixed in dry CH$_2$Cl$_2$ at room temperature, and then one equivalent of *tert*-butyl thiourea derivative **21b2** was added. A yellow precipitate was formed immediately, and its MS analysis suggested that both the nitrogen and sulfur atoms of **21b2** were bound to copper. The remaining brown solution was probably made of **Cu(Ph-Pybox)$_2$**, (a **Ph-pybox** + sodium signal was observed in ESI$^+$-MS). No changes were observed upon adition of another halide, such as bromide. When experiments were performed with **21b1** or **21b3**, identical results were observed (Fig. 4.29).

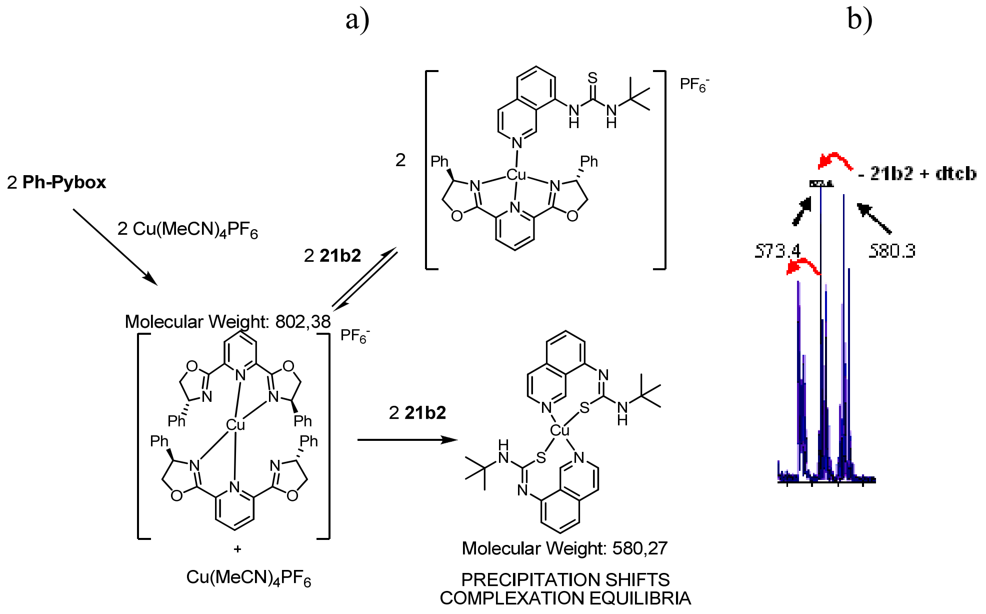
a)
b)
2 Ph-Pybox
2 Cu(MeCN)4PF6
2 21b2
2
Ph
Cu
N
Ph
PF6-
S
Molecular Weight: 802,38
PF6-
+
Cu(MeCN)4PF6
2 21b2
Molecular Weight: 580,27
PRECIPITATION SHIFTS
COMPLEXATION EQUILIBRIA
- 21b2 + dtcb
573.4
580.3

Fig. 4.29: Mixture of **21b2**, **Ph-Pybox** and Cu(I): a) Proposed reaction sequence; b) MALDI (dtcb) spectrum of the precipitate.

Precipitation of the **Cu(21b)$_2$(PF$_6$)** complex shifted all equilibria and **Cu(Ph-Pybox)$_2$(PF$_6$)** was obtained in the remaining solution, which also explains that addition of anions to the system (to prevent sulfur coordination by modifying the electronic properties of the thiourea) caused no changes. In conclusion, O and S atoms of the H-bonding moiety were shown to mainly coordinate to the metal. Furthermore, a similar experiment with the parent isoquinoline heterocycle (**iq**) instead of **21b2** revealed (MALDI) the formation of **Cu(Ph-Pybox)$_2$(PF$_6$)** (Fig. 4.30).

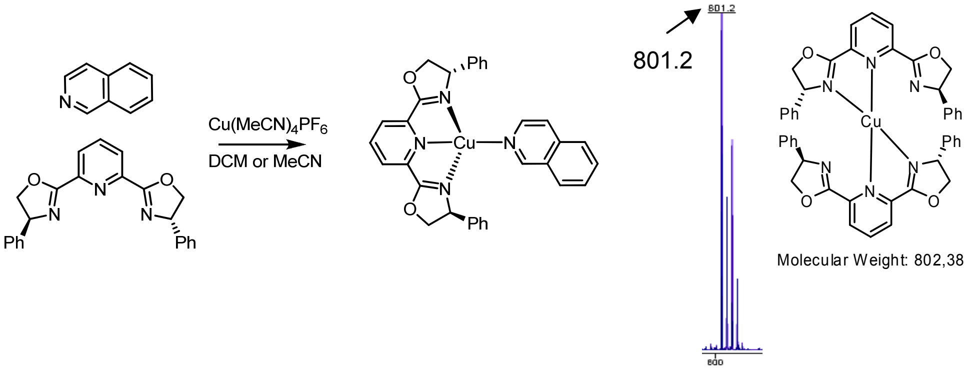

Fig. 4.30: Control experiment with isoquinoline.

This control experiment underlines another important challenge to deal with, namely the entropic cost of using a monodentate instead of a preorganized tridentate ligand. This is why the desired **Cu(iq)(Ph-pybox)** complex is not observed and the **Cu(Ph-pybox)$_2$** is formed instead, even in the presence of a competitive solvent. This set of experiments with Cu(I) revealed that this metal is not suitable for our goal with **21a-21b**.

Complexation experiments of **21a-21b** and **Ph-Pybox** with Zn(II) were then performed, though the situation was identical as for Cu(I) (Fig. 4.31). Zn(II) was chosen for its known ability to coordinate between 4 and 6 ligands, a versatile behavior that makes it quite attractive for our applications. The desired complex was actually formed with Zn(II) (entry 2), but sulfur coordination is likely, according to the first experiment (entry 1). Furthermore, formation of the pybox dimer is likely prevailing.

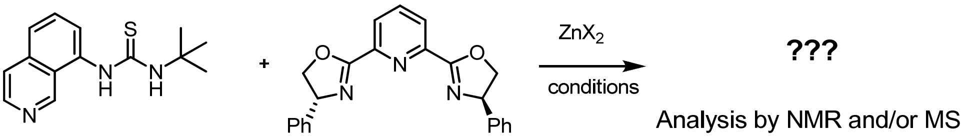

Entry	X	Conditions	Results
1	OAc	MeCN, MeOH, 1 eq. **21b2**, 1 eq $Zn(OAc)_2$	**Zn(21b2)$_2$**: MALDI-MS (dtcb) *m/z* calc. 582.1; obt. 582.2
2	OAc	**Ph-Pybox**, MeOH, **21b2**	**Zn(21b2)(Ph-Pybox)**: MALDI-MS (dtcb) [a] *m/z* calc. 693.2; obt. 691.3 **Zn(Ph-Pybox)$_2$**: MALDI-MS [a] (dtcb) *m/z* calc.804.2; obt. 802.3
3	Br	TBABr*, **21b2**, MeOH, **Ph-Pybox**	Crystallization of pybox dimer (detected by ^{1}H NMR): integrals of pybox signals decrease with time.

[a] Peaks of [M$^+$] and [(M+OH)$^+$] were obtained, data for [M$^+$] are shown.

Fig. 4.31: Summary of results for complexation of **21b2** and **Ph-Pybox** with Zn(II).

Finally, ruthenium (II) was evaluated, taking into account literature precedents with other *N*-heterocyclic ligands (a tridentate ligand and a monodentate one).[22] This metal also opens the way to catalytic C-H activation reactions, such as epoxidations.

A control experiment with isoquinoline was first performed, and formation of ***trans*-RuCl$_2$(iq)(Ph-Pybox)**, as well as isolation of the complex, was achieved in 77% yield. The mode of coordination, as determined by ^{1}H NMR, was assigned to a C_2 symmetry *trans* one reflected in the ^{1}H NMR spectrum by a single set of signals for the **Ph-pybox** phenyl rings. In the alternative *cis* coordination, both phenyl rings are in different chemical environments and are therefore expected to give rise to different sets of signals (Fig. 4.32). The resulting complex proved to be easy to handle and stable enough to be purified by chromatography.

---

[22] Hua, X.; Shang, M., Lappin, G. A. *Inorg. Chem.* **1997**, *36*, 3735.

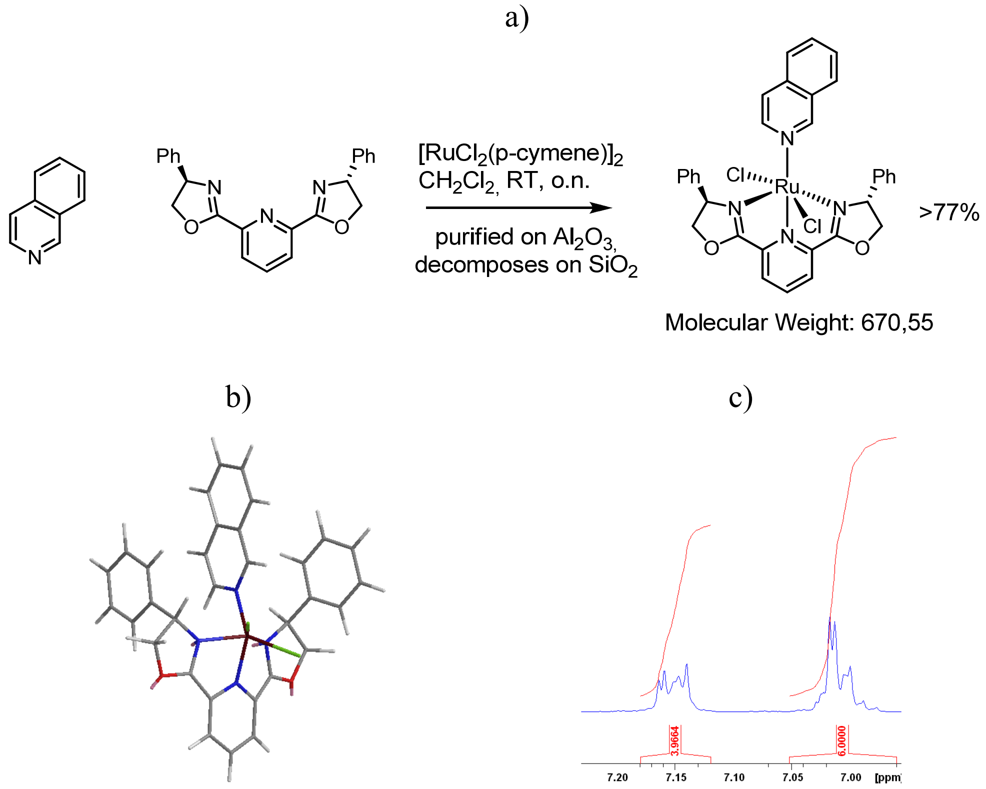
a)
Ph
N
O
[RuCl2(p-cymene)]2
CH2Cl2, RT, o.n.
purified on Al2O3,
decomposes on SiO2
Cl
Ru
>77%
Molecular Weight: 670,55
b)
c)
3.9664
6.0000
7.20
7.15
7.10
7.05
7.00
[ppm]

Fig. 4.32: a) Synthesis of ***trans*-RuCl$_2$(iq)(Ph-Pybox)**; b) MM2 model (Chem3D) of the ***cis*-RuCl$_2$(iq)(Ph-pybox)** complex; c) aromatic region of the ^{1}H NMR spectrum of ***trans*-RuCl$_2$(iq)(Ph-Pybox)**.

Such encouraging results prompted us to investigate the complexation with **21a-b**, under various conditions (Fig. 4.33).

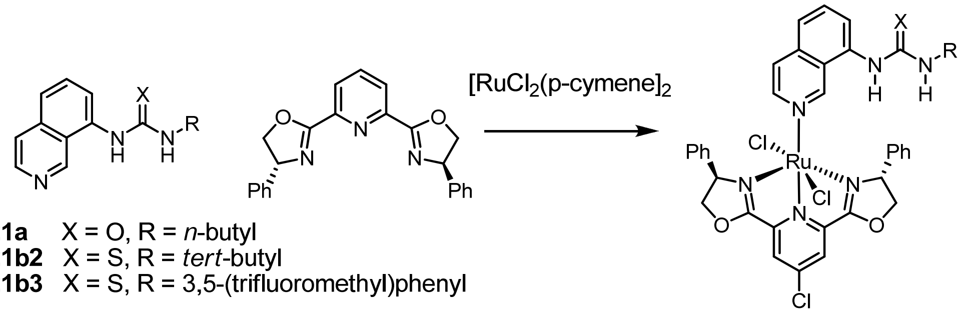

21a X = O, R = *n*-butyl
21b2 X = S, R = *tert*-butyl
21b3 X = S, R = 3,5-(trifluoromethyl)phenyl

Entry	Conditions	MALDI-MS
1	**21b3**, **Ph-Cl-Pybox**, CH_2Cl_2, MeOH, 2 days, room temperature	[Ru(**21b3**)(*p*-cymene)]$^+$: 650 [RuCl$_2$(**21b3**)(**Ph-Cl-Pybox**)]$^+$: 990 [[RuCl(**Ph-Cl-Pybox**)]$_2$(p-cymene)]$^+$: 1216
2	**21b3**, **Ph-Cl-Pybox**, THF, refl., overnight	Complex mixture (12 peaks): [RuCl(**21b3**)(**Ph-Cl-Pybox**)]$^+$: 954 [Ru(**21b3**)(*p*-cymene)]$^+$: 650
3	**21b2**, **Ph-Pybox**, CH_2Cl_2, refl. 4 h	HPLC-MS[1]: RuCl$_2$(**21b2**)(**Ph-Pybox**) detected in a very low amount, [RuCl$_2$(**Ph-Pybox**)$_2$] as a major compound
4	**21b2**, **Ph-Pybox**, CH_2Cl_2, room temperature, 5 days	[RuCl$_2$(**Ph-Pybox**)$_2$]$^+$: 875.2 [RuCl(**Ph-Pybox**)$_2$]$^+$: 840.2 [RuCl$_2$(**21b2**)(**Ph-Pybox**)]$^+$:800.1 [RuCl(**21b2**)(**Ph-Pybox**)]$^+$:765.1 [Ru(**21b2**)(**Ph-Pybox**)]$^+$:729.2 1092 (not identified)
5	**21b2**, **Ph-Pybox**, TBA.AcO$^-$, CH_2Cl_2, room temperature, 1 h	HPLC-MS: RuCl$_2$(**21b2**)(**Ph-Pybox**) detected in a very low amount, [RuCl$_2$(**Ph-Pybox**)$_2$] as a major compound
6	**21b2**, **Ph-Pybox**, TBA.Cl$^-$, CH_2Cl_2, room temperature, 5 days	[RuCl$_2$(**Ph-Pybox**)$_2$]$^+$: 875.2 [RuCl(**Ph-Pybox**)$_2$]$^+$: 840.2 [RuCl$_2$(**21b2**)(**Ph-Pybox**)]$^+$:800.1 [RuCl(**21b2**)(**Ph-Pybox**)]$^+$:765.1 [Ru(**21b2**)(**Ph-Pybox**)]$^+$:729.2
7	**21a**, **Ph-Pybox**, CH_2Cl_2, room temperature, 7 days	[RuCl$_2$(**Ph-Pybox**)$_2$]$^+$: 875.2 [RuCl(**Ph-Pybox**)$_2$]$^+$: 839.2 [RuCl$_2$(**21a**)(**Ph-Pybox**)]$^+$:784.2

Fig. 4.33: Summary of results for complexation of **21a-b** with Ru(II).

Typically, stoichiometric amounts of ligands and the metal precursor were mixed and analyzed, after solvent elimination, either by mass spectrometry (MALDI, pyrene as a matrix) or by HPLC-MS techniques. In most cases, formation of the desired heteroleptic complex **RuCl$_2$(21a-b)(Ph-Pybox)** was observed, though the **RuCl$_2$(Ph-Pybox)$_2$** species was always formed too. Numerous attempts to purify these crude reaction mixtures by column chromatography were unsuccessful, however. Furthermore, HPLC analysis of the reaction mixtures after a few hours of reaction revealed that **RuCl$_2$(Ph-Pybox)$_2$** forms quickly, and is therefore likely to be the kinetic product (larger reaction times do not allow the exclusive formation of **RuCl$_2$(21a-b)(Ph-Pybox)**. For these reasons, it was decided to explore new synthetic routes, preparing the complex in a stepwise fashion.

Initially, formation of **RuCl$_2$(21b2)(p-cymene)** was attempted. It was indeed expected that this complex might lead to the desired heteroleptic complex upon treatment with **Ph-Pybox** (Fig. 4.34).

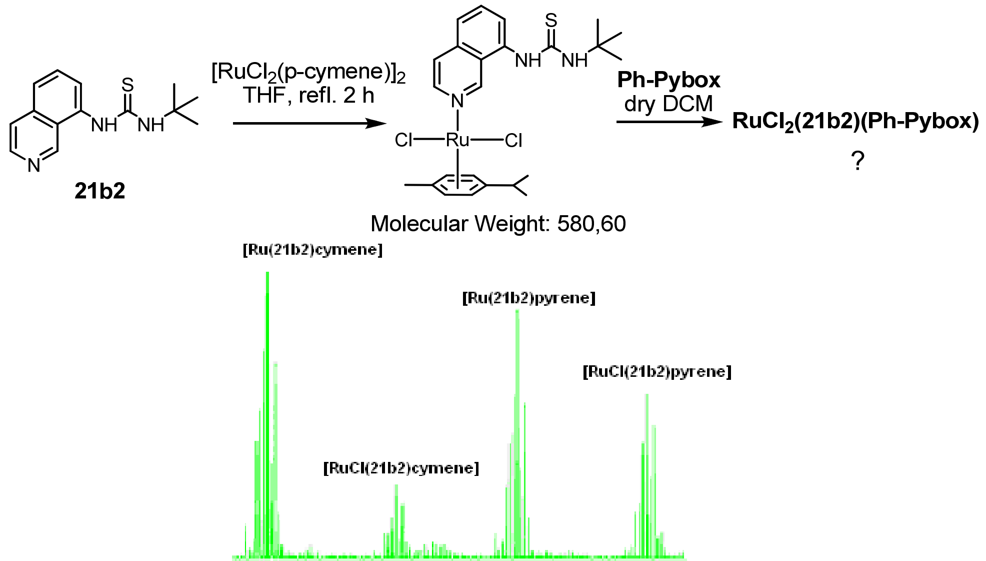
S
NH
NH
N
21b2
[RuCl2(p-cymene)]2
THF, refl. 2 h
Cl—Ru—Cl
Ph-Pybox
dry DCM
RuCl2(21b2)(Ph-Pybox)
?
Molecular Weight: 580,60
[Ru(21b2)cymene]
[Ru(21b2)pyrene]
[RuCl(21b2)pyrene]
[RuCl(21b2)cymene]

Fig. 4.34: Preparation of **RuCl$_2$(21b2)(p-cymene)**.

The intermediate complex was easily formed as seen on the ^{1}H NMR spectrum of the crude mixture and by MALDI-MS analysis. However, upon treatment with **Ph-Pybox**, a crude mixture of **RuCl$_2$(Ph-Pybox)$_2$** and **RuCl$_2$(21b2)(Ph-Pybox)** was obtained, indicating that a rapid equilibration was taking place. On the other hand, according to a literature precedent, the formation of **RuCl$_2$(Ph-Pybox)$_2$** was expected to be inhibited by the trapping of **Ph-Pybox** in a complex formed in presence of carbon monoxide: **RuCl$_2$(Ph-Pybox)(CO)**.[23] Treatment of this complex with **21a-b** should lead to the desired complex. Unfortunately, although the **RuCl$_2$(Ph-Pybox)(CO)** complex was successfully formed, it could not be purified by chromatography. The procedure was also hardly reproducible (Fig. 4.35).

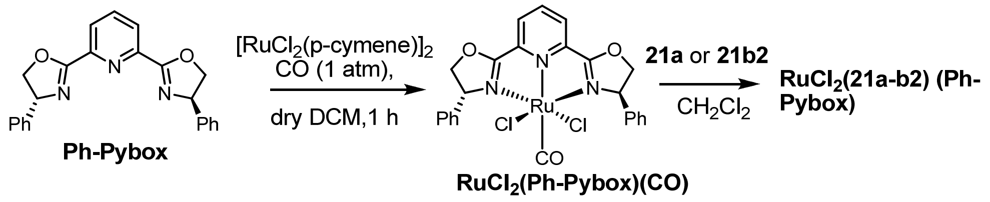

Ligand	MALDI-MS (g.mol^{-1})
21a	[RuCl$_2$(**Ph-Pybox**)$_2$]$^+$: 875.2 [RuCl(**Ph-Pybox**)$_2$]$^+$: 840.2 [RuCl$_2$(**21a**)(**Ph-Pybox**)]$^+$: 784.6 [RuCl(**2a**)(**Ph-Pybox**)]$^+$ and [Ru(**2a**)(**Ph-Pybox**)]$^+$ [RuCl$_2$(**Ph-Pybox**)(*p*-cymene)]: 680.5
21b2	[RuCl(**21b2**)(**Ph-Pybox**)]$^+$:764.2 [Ru(**2b2**)(**Ph-Pybox**)]$^+$:729.2

Fig. 4.35: Preparation of **RuCl$_2$(21a-b2)(Ph-Pybox)** from **RuCl$_2$(Ph-Pybox) (CO)**

---

[23] Nishiyama, H.; Itoh, Y.; Matsumoto, H.; Park, S.-B.; Itoh, K. *J. Am. Chem. Soc.* **1994**, *116*, 2223.

Remarkably, this approach resulted in a significantly lower amount of **$RuCl_2$(Ph-Pybox)$_2$** formed, according to peak intensities on mass spectra relative to previous experiments. However, during the course of the experiment performed with **21b2**, a compound crystallized and appeared to be a metallo-macrocyclic dimer: **[RuCl(21b2)(*p*-cymene)]$_2$**. This unexpected compound was actually also present on the mass spectrum of previous experiments ($[M-2Cl]^+$: 1092 $g.mol^{-1}$) (Fig. 4.36).

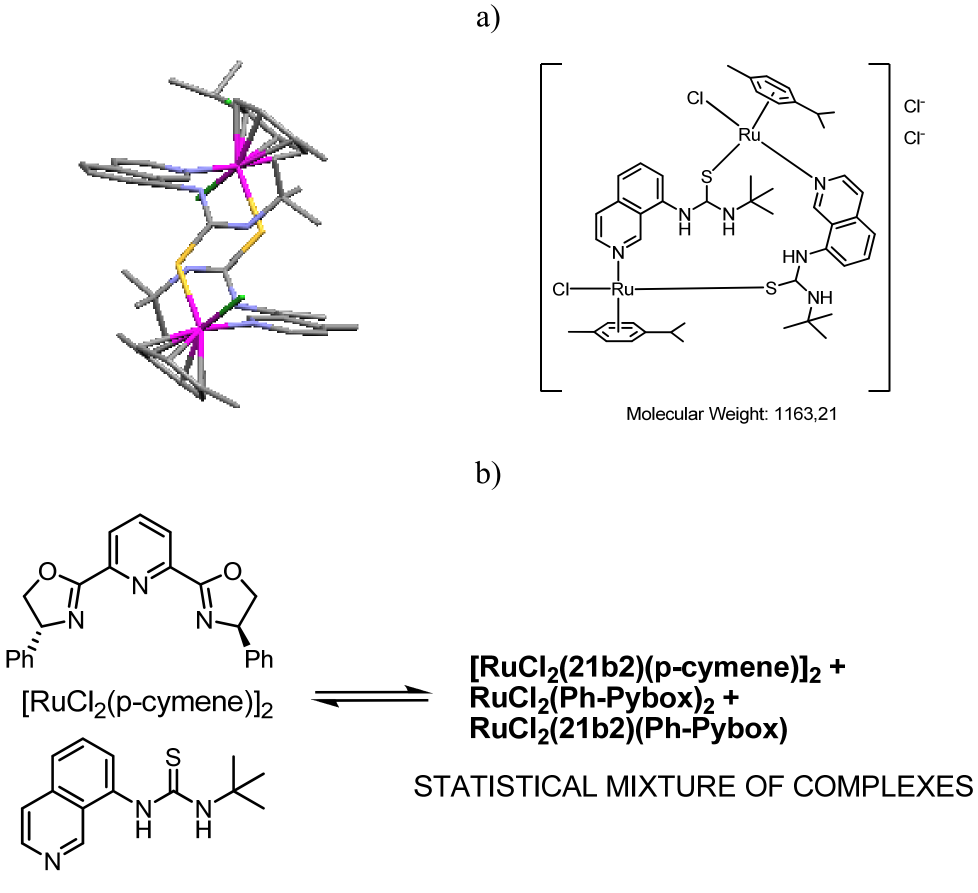
a)
Cl
Ru
S
N
HN
NH
Cl
Ru
Cl^-
Cl^-
Molecular Weight: 1163,21
b)
O
N
N
O
Ph
Ph
[RuCl2(p-cymene)]2
S
N
H
N
H
N
[RuCl2(21b2)(p-cymene)]2 +
RuCl2(Ph-Pybox)2 +
RuCl2(21b2)(Ph-Pybox)
STATISTICAL MIXTURE OF COMPLEXES

Fig. 4.36: a) X-ray structure of the obtained metallo-macrocyclic dimer **[$RuCl_2$(21b2)(*p*-cymene)]$_2$**; b) Equilibria with Ru(II).

From this set of experiments with Ru(II), it must be concluded that the desired complex was successfully formed under some conditions but, due to entropic and enthalpic reasons, a mixture of ligands equilibrates to a mixture of complexes that could be described as a pybox dimer (entropically favored), and a thioureidoisoquinoline dimer. Isolation of the desired complexes could therefore not be achieved. It was then expected that guanidinium derivatives such as **21c** would not give rise to coordination of the heteroatom of the H-bonding moiety to the metal (as observed for **21a-b**) because of its positive charge.

4.3.1.3 Complexation studies for 21c.

The poor solubility of **21c** in common organic solvents did not enable us to check a wide range of complexes formation. As previously described with **20b** and **21a-b**, experiments with Zn(II), Pybox derivatives and **21b-c** were performed. When compounds **21c (Cl^-)** and **Ph-Cl-Pybox** were mixed in the presence of a stoichiometric amount of zinc(II) tetrafluoroborate in dry methanol, some crystals of **$Zn(Ph\text{-}Cl\text{-}Pybox)_2(BF_4)_2$** developed, as shown below (Fig. 4.37a). This shows that carboxyguanidinium **21c** is not a good enough ligand to overcome formation of this undesired side complex, which could be attributed to the electron withdrawing nature of the carboxyguanidinium group that lowers the donating ability of the pyridine ring of **21c**. A similar experiment was then performed with $CoCl_2$ as metal salt, and a dimer of the Pybox derivative was then crystallized, which confirmed that **21c** is a poor ligand (Fig. 4.37). Under the same conditions, complexation with CuI was studied by ^1H NMR and signals of **21c** did not suffer significant chemical shifts, suggesting that no coordination took place, and therefore **CuI(Ph-Cl-Pybox)** was formed.

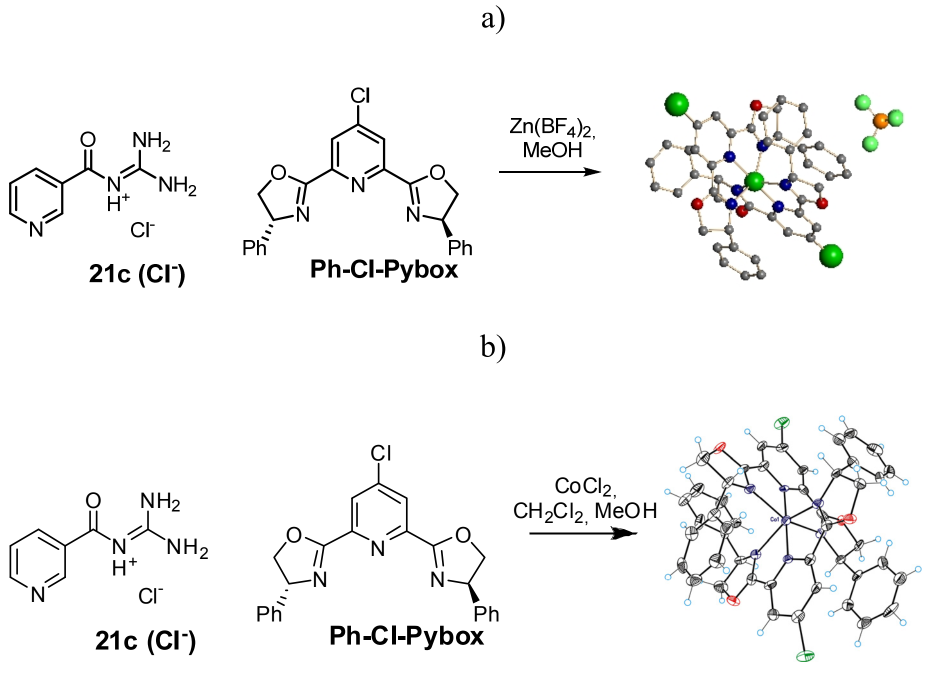
a)
O
NH2
N
H+
NH2
N
Cl-
21c (Cl-)
Cl
O
N
O
N
N
Ph
Ph
Ph-Cl-Pybox
Zn(BF4)2,
MeOH
b)
O
NH2
N
H+
NH2
N
Cl-
21c (Cl-)
Cl
O
N
O
N
N
Ph
Ph
Ph-Cl-Pybox
CoCl2,
CH2Cl2, MeOH

Fig. 4.37: Complexation experiments of **21c (Cl⁻)** and **Ph-Cl-Pybox** and X-ray structure of a) **Zn(Ph-Cl-Pybox)$_2$(BF$_4$)$_2$** ; b) **CoCl$_2$(Ph-Cl-Pybox)$_2$**.

Complexation experiments with Ru(II) were then investigated, as for **21a-b**. Different guanidinium counterions were studied and the crude mixtures were analyzed by HPLC-MS. When the reaction was performed with **21c** (Cl^-), up to 56% of **[RuCl$_2$(21c)(Ph-Cl-Pybox)]Cl$^-$** was formed (Fig. 4.38), whereas in the case of **21c** (PF_6^-), 48% of the crude mixture was made of the desired complex. However, purification of the complex by column chromatography proved difficult and could only be achieved once. The complex was characterized by ^{1}H NMR and mass spectrometry.

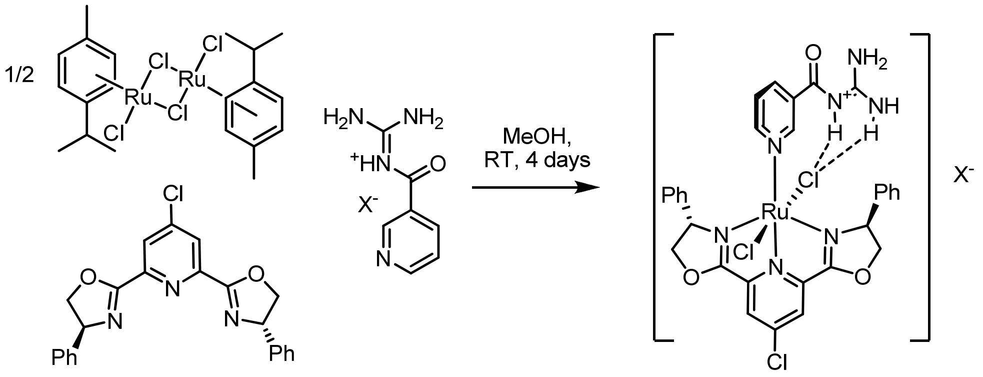

Fig. 4.38: Preparation of of **[RuCl$_2$(21c)(Ph-Cl-Pybox)]Cl$^-$**.

In order to simplify the procedure and the purification, preparation of the complex from **[RuCl$_2$(Ph-Pybox)(CO)]** was investigated, under the same conditions as for **21a-b**. MS-MALDI analysis of the crude reaction mixture showed that compound did form along with **RuCl$_2$(Ph-Pybox)$_2$**. The results observed with **21c** reveal that no guanidinium coordination of the guanidine to the metal was detected.

The formation of this side product was in every case a real drawback since separation of the formed complexes could hardly be achieved. This side complex could arise from the binding of the heteroatom of the H-bonding subunit (for **21a-b**), the poor electron donating nature of **21c** and thermodynamic factors: formation of **RuCl$_2$(Ph-Pybox)$_2$** is favoured over the heteroleptic complex since **Ph-Pybox** is a tridentate ligand. For these reasons, it was decided to study bidentate ligands, which were expected to overcome some of the encountered difficulties.

4.3.2 Bidentate functionalized ligands 24a-d.

For these bidentate ligands, formation of Zn(II) and Ru(II) complexes was only studied. In a first series of experiments, complexation of **24b(Cl$^-$)** with Zn(II) salts in THF was studied by UV-Vis titrations. This bidentate ligand was highly soluble in common organic solvents, unlike with **24a**, **24c**, and **24d**. Job Plot experiments for the complexation of **24b(Cl$^-$)** with Zn(BF_4)$_2$ and Zn(OAc)$_2$ nicely showed a 1:1 stoichiometry, though other stoichiometries were also expected. UV-Vis titrations were then performed in THF with different metal salts (Fig. 4.39).

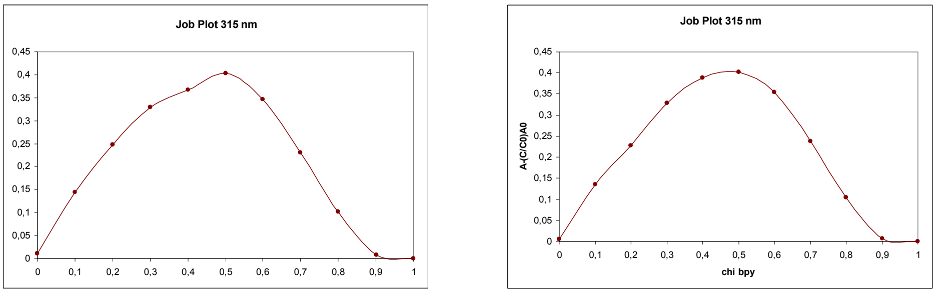

a) Zn(BF_4)$_2$ b) Zn(OAc)$_2$

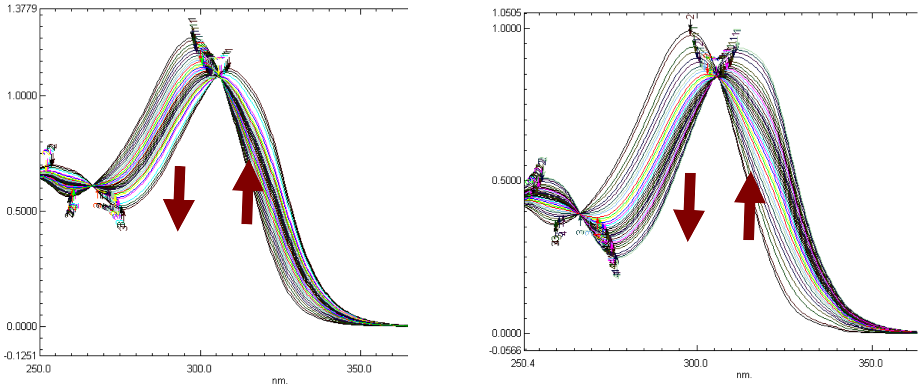

c) Zn(BF_4)$_2$ d) Zn(OAc)$_2$

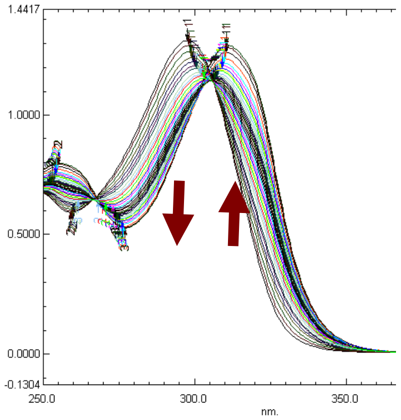

ZnX_2	K (M^{-1})
$Zn(BF_4)_2$	$4.04.10^4$
$Zn(OAc)_2$	$2.4.10^5$
$ZnCl_2$	$2.52.10^5$

e) $ZnCl_2$

f) Binding constants

Fig. 4.39: UV-Vis titrations of **24b(Cl$^-$)** with Zn(II) salts: a), b) Job Plots; c-f) Titration curves and binding constants for a 1:1 stoichiometry (fitting performed with SPECFIT®).

As shown above, the binding constant for the 1:1 complex depends on the counterion associated to the metal. For chloride and acetate, the constant is one order of magnitude higher than with non coordinating anions, such as tetrafluoroborate. With both acetate and chloride, binding constants were similar, likely by formation of a bridged dimer: **$Zn_2(Cl)_2(24b)_2(X)_2$** (X = Cl or OAc). In the case of zinc tetrafluoroborate, this bridged dimer could also be formed, since **24b(Cl$^-$)** was also a source of chloride anions. In that case, however, a competitive binding of chloride between the guanidinium and the metal is favored (H-bonding), which might be at the origin of the observed differences in binding constants (Fig. 4.40a). This was confirmed in the X-ray crystal structure of the 2:1 complex formed by **24b(Cl$^-$)** and $Zn(BF_4)_2$, for which such a bridged structure was observed (Fig. 4.40b).[24]

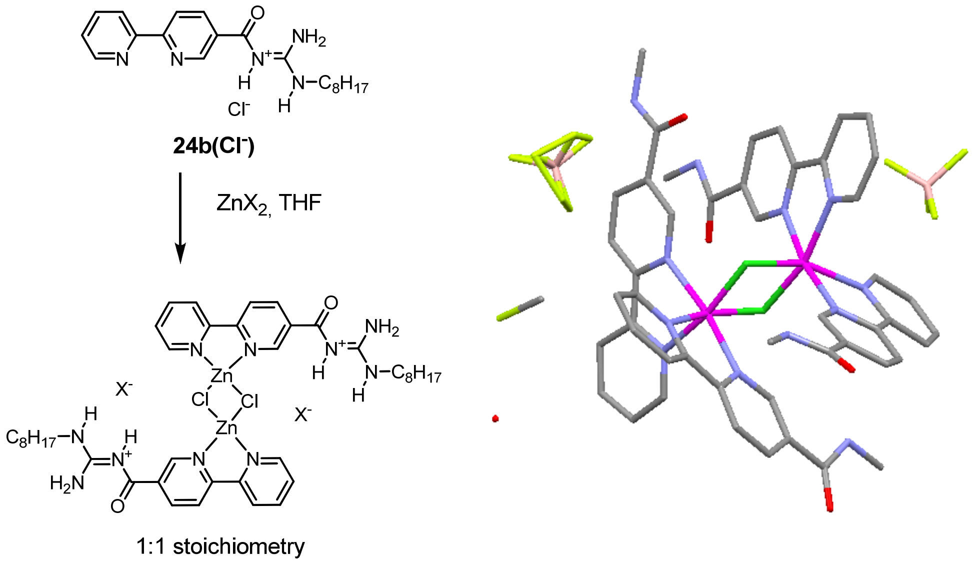

a) b)

Fig. 4.40: a) Possible complex between **24b(Cl$^-$)** and ZnX$_2$; b) Poorly resolved X-ray structure of **Zn$_2$Cl$_2$(24b)$_4$(BF$_4$)$_2$**.

Complexation experiments with Zn(II) were not pursued, since formation of the heteroleptic complex with a chiral ligand would also compete with the bridged dimer formation and the dimer of the chiral ligand, as previously observed with monodentate ligands.

---

[24] Versatility of the coordination sphere of Zn(II) enables to construct complexes of various stoichiometries. This complex was obtained by mixing two equivalents of **24b(Cl$^-$)** with one equivalent of Zn(BF$_4$)$_2$. Crystals were grown in MeOD. Structure could not be fully resolved due to the high disorder brought by the octyl chain.

As for monodentate ligands in the case of Ru(II), a control experiment was performed with 2,2'-bipyridine (**bpy**). After treatment of **Ph-Pybox** with [$RuCl_2$(*p*-cymene)]$_2$ in dichloromethane, a solution of **bpy** in ethanol was added and mixture was refluxed overnight, which afforded **[RuCl(bpy)(Ph-Pybox)]PF_6** in 69% yield after column chromatography, following a previously described procedure.[22] The compound was fully characterized by ^{1}H NMR and cyclic voltammetry. The Ru(III)/Ru(II) reduction potential was 0.71V in CH_2Cl_2. This compound was then treated with silver(I) trifluoromethanesulfonate in presence of water in order to replace the chloride by a water ligand, affording **[Ru(H_2O)(bpy)(Ph-Pybox)](PF_6)$_2$** in 57% yield after recrystallization (Fig. 4.41).

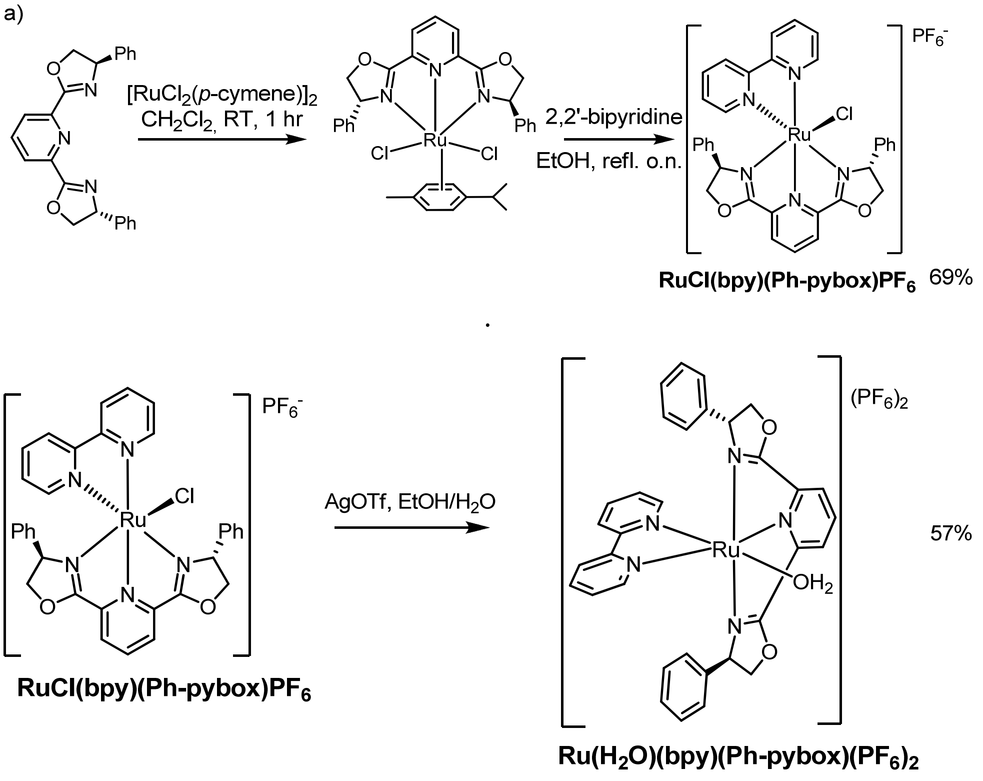
a)
Ph
O
N
N
N
O
Ph
[RuCl2(p-cymene)]2
CH2Cl2, RT, 1 hr
O
N
N
O
N
Ph
Ph
Ru
Cl
Cl
2,2'-bipyridine
EtOH, refl. o.n.
PF6-
N
N
Cl
Ru
Ph
Ph
N
N
N
O
O
RuCl(bpy)(Ph-pybox)PF6 69%
PF6-
RuCl(bpy)(Ph-pybox)PF6
AgOTf, EtOH/H2O
(PF6)2
57%
OH2
Ru(H2O)(bpy)(Ph-pybox)(PF6)2

b)

$$[Ru(Ph\text{-}Pybox)(bpy)(O)]^{2+} + n\ H^+ + 2\ e^- \rightleftharpoons [Ru(Ph\text{-}pybox)(bpy)(OH_n)]^{2+}$$

Value of n is pH dependent: n = 1 or n = 2

Fig. 4.41: a) Synthesis of **$[Ru(H_2O)(bpy)(Ph\text{-}Pybox)](PF_6)_2$**; b) Redox equation for **$[Ru(H_2O)(bpy)(Ph\text{-}Pybox)](PF_6)_2$**.

This complex was used as a pre-catalyst in epoxidation reactions (see Section 4.4), and its redox behaviour was therefore studied, since this process involves a Ru(IV) oxo species. A study by cyclic voltammetry of the reduction potential for Ru(IV) to Ru(II) at neutral pH of the prepared complex surprisingly showed that the transitory Ru(III) species could not be detected, indicating that the process goes directly from Ru(II) to Ru(IV). The measured potential for that oxidation was 0.46V.

$$[Ru(Ph\text{-}Pybox)(bpy)(H_2O)]^{2+} + OH^- \rightleftharpoons [Ru(Ph\text{-}Pybox)(bpy)(OH)]^+ + H_2O$$

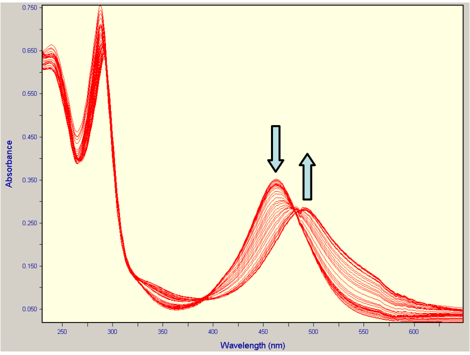

pK_A = 9.65 ± 0.06

Fig. 4.42: UV-Vis pK_A determination of **$[Ru(H_2O)(bpy)(Ph\text{-}Pybox)](PF_6)_2$**

The pK_A of the water proton was then measured by UV-Vis spectroscopy by dissolving first the **[Ru(H_2O)(bpy)(Ph-pybox)](PF_6)$_2$** in a trifluoromethanesulfonic acid solution, followed by a slow addition of aqueous NaOH. The optical properties of the hydroxo complex differ from those of the aquo ones. This enables an accurate determination of the pK_A of these protons (Fig. 4.42). With guanidinium functionalized ligands, intramolecular H-bonding between the guanidinium group and the water molecule is expected to modify significantly the value of this pK_A.

Given the efficiency of this procedure for the control experiment, similar reaction conditions were investigated for the formation of the heteroleptic complex of **24a-d**. However, as was observed for **21c**, reactions with the functionalized ligands were not as clean as for the model experiments. Furthermore, with **24a-b** (monofunctionalized bipyridyl derivatives), a mixture of stereoisomers was expected, since the guanidinium group could either face the Ru-coordinated chloride atom or be located at the other side of the complex, in a non-productive manner (in terms of a potential catalyst), as shown below (Fig. 4.43).[25] For this reason, difunctionalized bipyridyl derivatives **24c-d** were prepared and investigated, since only one (productive) configuration can result. Unfortunately, difunctionalized compounds **24c** and **24d** were insoluble in the studied solvents, resulting in complex mixtures that could not be purified, probably due to product degradation. The ^{1}H NMR spectra of the crude reaction mixtures were too complex to allow identification of the formed species. Similarly, experiments performed with **24a-b** (either protonated or not) gave rise to mixtures of products (as seen by TLC), which could not be separated by column chromatography. The desired complex could however be detected by mass spectrometry in the case of **24b**. Its isolation was unsuccessful.

---

[25] Slow ligand exchange rate around Ru(II) center was expected to prevent the reorganization of the ligands and isolation of the thermodynamically most stable isomer.

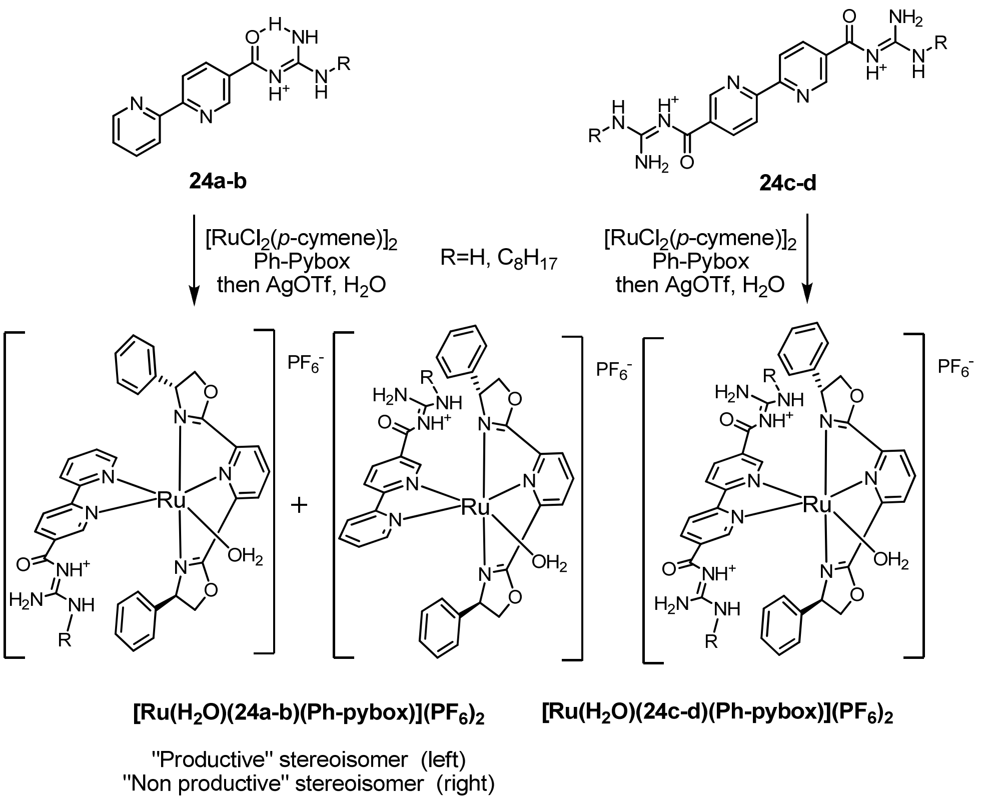
24a-b
24c-d
[RuCl2(p-cymene)]2
Ph-Pybox
then AgOTf, H2O
R=H, C8H17
[RuCl2(p-cymene)]2
Ph-Pybox
then AgOTf, H2O
PF6-
PF6-
PF6-
[Ru(H2O)(24a-b)(Ph-pybox)](PF6)2
[Ru(H2O)(24c-d)(Ph-pybox)](PF6)2
"Productive" stereoisomer (left)
"Non productive" stereoisomer (right)

Fig. 4.43: Heteroleptic complexes and their possible stereoisomers.

4.4 Catalysis experiments (preliminary results).

4.4.1 Monodentate ligands.

Though structures of the formed complexes could hardly be determined by spectroscopic methods, model catalysis experiments were performed in order to test the efficiency of these systems. Given the high efficiency of thiourea derivatives in terms of catalytic activity, emphasis was first laid on thiourea **1b**, since transition state stabilization was expected.[26] In a first attempt, inspired by the results described in the previous chapter, 1,4-addition of pyrrolidine to 2-5*H*-furanone was investigated, in the presence of tin (IV), **1b** and **(R)-BINOL**. H-bonding ligand and Lewis acid were chosen for cooperative transition state stabilization and substrate activation, whereas **(R)-BINOL** was used for asymmetry induction. Catalytic system was formed *in situ*. Results suggest that catalytic system does not take part in the reaction, since low yields and no *ee* are obtained.[27]

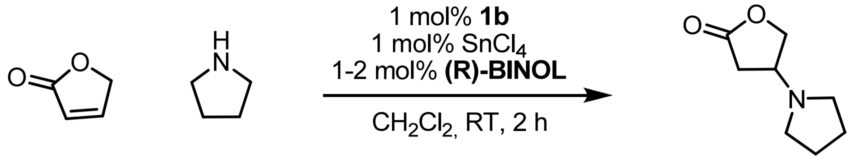

---

[26] Example for the aza-Henry reaction: Xu, X.; Furukawa, T.; Okino, T.; Miyabe, H.; Takemoto, Y. *Chem. Eur. J.* **2006**, *12*, 466.

[27] Reactions were stopped after 2 hours, at less than 100% conversion and product was isolated by column chromatography, which accounts for the low yields.

(*R*)-BINOL	**1b**	$SnCl_4$	yield (%)	optical rotation[a]
10 mol%	10 mol%	10 mol%	25	-
20 mol%	10 mol%	10 mol%	20	-
20 mol%	-	10 mol%	35	-
-	-	-	n.m.	-

[a] measured by polarimetry in $CHCl_3$ ($c = 5$) after column chromatography.

Fig. 4.44: Towards asymmetric hetero-Michael reactions.

This non catalyst activity might be due to some poisoning of the metal by **1b** (sulfur coordination, as discussed previously), that deactivates both metal and H-bonding moiety, thus rendering the activation inefficient, which lead to no asymmetry induction. Formation of the desired heteroleptic complex therefore did not take place. This catalytic process was therefore not further investigated. Acidity of used tin(IV) chloride solution might also be in cause.

Baylis-Hillman reaction of benzaldehyde with methyl vinyl ketone was also investigated in presence of 10 mol% ***i*-Pr-Pybox**, **1b** and a metal salt (Cu(I) or Zn(II)) and 20 mol% of a base (DMAP or DABCO). However, the process proved not to take place under the studied conditions for the same reasons (sulfur coordination to the metal is likely to take place and to poison the metal). Furthermore, catalytic base is also likely to bind the metal, which prevents the reaction from occurring. However with CuI and DMAP as a base, up to 10% yield could be obtained, though no *ee* could be detected by polarimetric measurements after product purification by column chromatography, which suggests that this conversion has to be attributed to the sole action of the base (DMAP) as a background reaction.

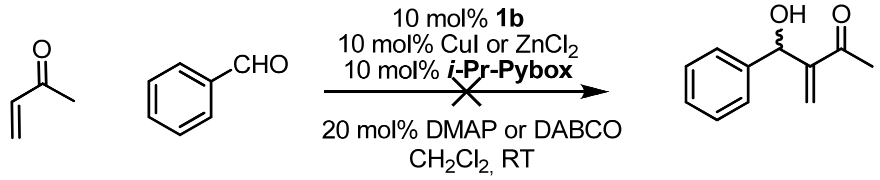

Fig. 4.45: Baylis-Hillman reaction.

These preliminary experiments performed with monodentate ligands suggest that some heteroatom coordination to the metal from the H-bonding moiety tended to poison the metal and to deactivate the catalytic system, which resulted in the non formation of the expected heteroleptic complex. For this reason, it was decided to investigate preorganized functionalized bidentate ligands in order to avoid this undesired heteroatom coordination (guanidinium is also expected not to bind the metal, as observed for thiourea derivatives).

4.4.2 Bidentate ligands.

For solubility reasons, **24b** was the only bidentate functionalized ligand suitable for catalysis experiments. Emphasis was concentrated on reactions on olefins (epoxidation,[28] cyclopropanation,[29] and aziridination[30]).

---

[28] a) Tse, M. K.; Bhor, S.; Klawonn, M.; Anilkumar, G.; Jiao, H.; Doebler, C.; Spannenberg, A.; Maegerlein, W.; Hugl, H.; Beller, M. *Chem. Eur. J.* **2006**, *12,* 1855. b) Tse, M. K.; Bhor, S.; Klawonn, M.; Anilkumar, G.; Jiao, H.; Spannenberg, A.; Doebler, C.; Maegerlein, W.; Hugl, H.; Beller, M. *Chem. Eur. J.* **2006**, *12,* 1875.

Molecular recognition of carboxylic acids through the guanidinium group of the ligand might therefore enable to functionalize unsaturated fatty acids regioselectively, or even stereoselectively, which leads to interesting targets, such as chiral hydroxyacids, aminoacids and functionalized cyclopropanes.

In collaboration with Prof. A Llobet's group (ICIQ),[31] epoxidation of olefins catalyzed by **[Ru(H$_2$O)(bpy)(Ph-Pybox)](PF$_6$)$_2$** was first studied. Initially, the efficiency of the catalyst was tested in a model reaction, namely the epoxidation of *cis*-*β*-methylstyrene in the presence of iodosobenzene diacetate (stoichiometric amount of PhI(OAc)$_2$) as oxidizing agent to transform the Ru(II)(H$_2$O) species into the catalytically active Ru(IV)(O). Cyclic voltammetry showed that this transformation does not go through a Ru(III)(OH) state (not observed), or that this state has a very short lifetime, which is quite unusual for this kind of complexes (Fig. 4.46).

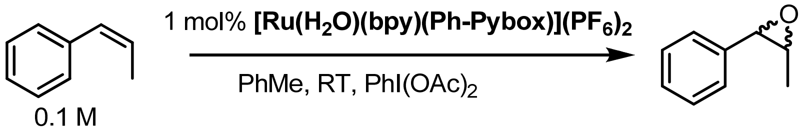

---

[29] a) Lyle, M. P. A.; Draper, N. D.; Wilson, P. D. *Org. Biomol. Chem.* **2006**, *4*, 877. b) Bouet, A.; Heller, B.; Papamicael, C.; Dupas, G.; Oudeyer, S.; Marsais, F.; Levacher, V. *Org. Biomol. Chem.* **2007**, *5*, 1397.

[30] Mohr, F.; Binfield, S. A.; Fettinger, J. C.; Vedernikov, A. N. *J. Org. Chem.* **2005**, *70*, 4833.

[31] Dr. F. Bozoglian, Institut Català d'Investigació Química (ICIQ), Tarragona.

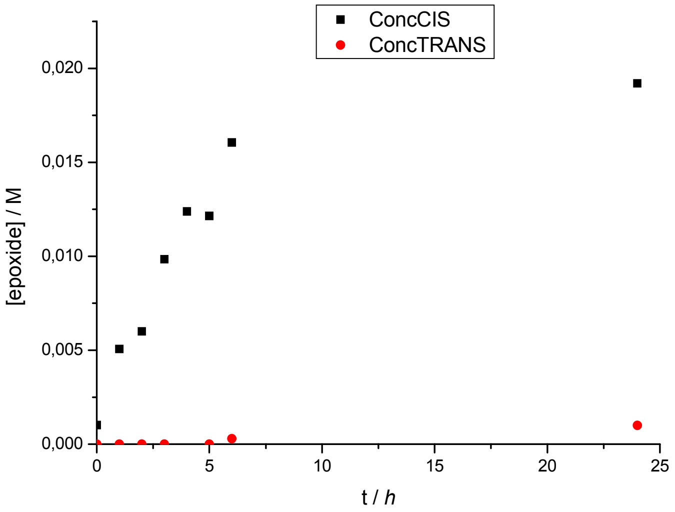

Fig. 4.46: GC-monitored model epoxidation of *cis-β*-methylstyrene catalyzed by **[Ru(H$_2$O)(bpy)(Ph-Pybox)](PF$_6$)$_2$**.

This catalyst should lead to retention of the olefin configuration. Ru(III) complexes indeed present a d^5 electron configuration and therefore have a non-filled orbital, giving rise to free rotation of the ligands in the metal coordination sphere, whereas Ru(II) (d^6) and Ru(IV) (d^4) present filled orbitals, thus preventing such rotation. However, after 24 hours, little conversion was achieved and a low turnover number (TON) of 15 could be obtained, which indicates that the catalyst is poorly active, though selective. Encouraged by these results, further model reactions were performed with guanidinium carboxylates of unsaturated acids, in order to check that the guanidinium group could resist the reaction conditions. For this purpose, compounds **88-90** were prepared, following a similar procedure as for **21c** and **24a-d**. Anion was exchanged through Dowex resins equilibrated for the studied carboxylates (Fig. 4.47).

The substrates were then submitted to epoxidation, as for the model reaction. After 24 hours, reaction mixtures were acidified with TFA and analyzed by GC-MS. As expected, no reaction took place (not detected by GC) in the case of butyrate **88** (negative control). In the cases of crotonate **89** and vinyl acetate **90**, small new peaks appear on the GC chromatograms (at 5.58 min and 5.98 min respectively), identified as the corresponding epoxides. TONs were not calculated (peaks quantification and calibration were not performed). Further experiments, currently ongoing, are required to check the results and to obtain more accurate data.

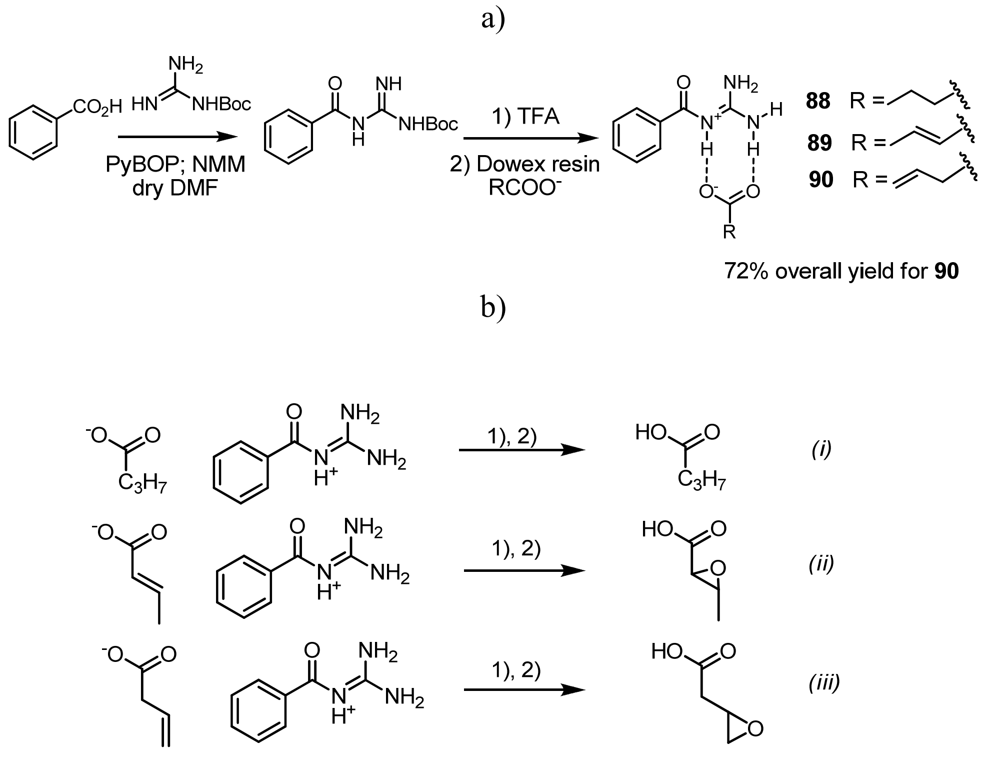
a)
CO2H
NH2
HN
NHBoc
PyBOP; NMM
dry DMF
O
NH
N
H
NHBoc
1) TFA
2) Dowex resin
RCOO-
O
NH2
N+
N
H
H
H
O-
O
R
88 R =
89 R =
90 R =
72% overall yield for 90
b)
-O
O
C3H7
NH2
NH2
N
H+
1), 2)
HO
O
C3H7
(i)
(ii)
(iii)

1) $[Ru(H_2O)(bpy)(Ph\text{-}pybox)](PF_6)_2$ 1 mol%, $PhI(OAc)_2$; CH_2Cl_2, RT, 24 h; 2) TFA

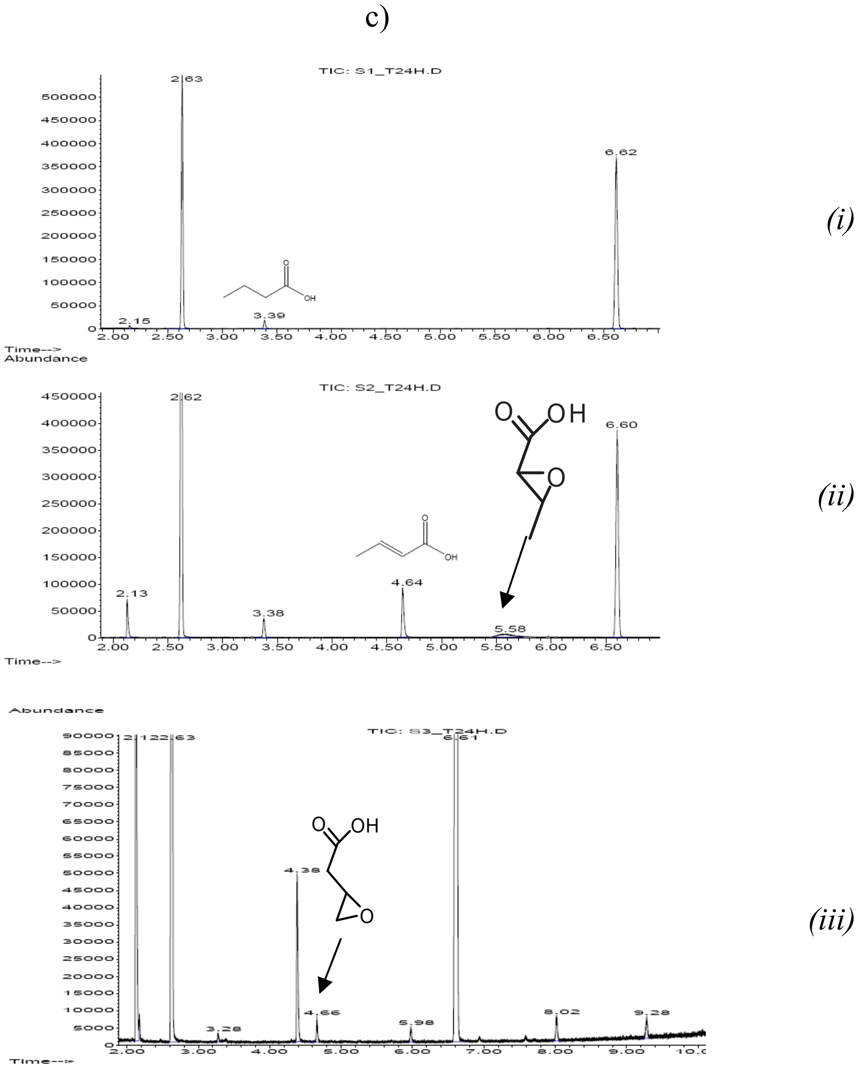

Fig. 4.47: a) Synthesis of **88-90**; b) Catalysis experiments performed on **88-90**; c) Chromatograms after acidification.

However, these preliminary results show that process is likely to work with functionalized ligands such as **24b**, since the guanidinium group did not affect the reactivity (the corresponding complex could unfortunately not be prepared so far).

Another reaction investigated was the copper(I) catalyzed cyclopropanation of unsaturated carboxylic acids. In the presence of Cu(I), ethyl diazoacetate forms a copper carbene complex, that is prompt to add to a double bond, giving rise to the corresponding cyclopropane. However, a side reaction of the metallocarbene with ethyl diazoacetate yields diethyl fumarate. This can be often prevented by slow addition (*via* syringe pump) of ethyl diazoacetate to a solution of the copper complex and the olefin substrate. *cis-β*-Methylstyrene was selected to optimize the conditions of reaction (Fig. 4.48).

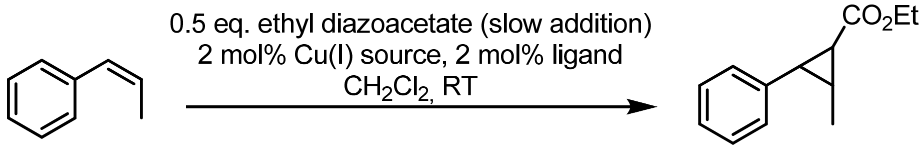
0.5 eq. ethyl diazoacetate (slow addition)
2 mol% Cu(I) source, 2 mol% ligand
CH_2Cl_2, RT
CO_2Et

Ligand	Cu(I) source	yield (%)
bpy	$Cu(OTf)_2$, 2,4-dinitrophenylhydrazine	n.m. [a]
bpy	$[Cu(MeCN)_4]PF_6$	46 [b]
24b	$[Cu(MeCN)_4]PF_6$, phenylhydrazine	n.m. [c]
24b (PF_6^-)	$[Cu(MeCN)_4]PF_6$	n.m. [d]
24b (Cl^-)	$Cu(OTf)_2$, 2,4-dinitrophenylhydrazine	16 [b]

[a] Product seen on the NMR and MS spectra of crude, [b] After isolation by column chromatography, [c] Product/starting material ratio = 0.05 in crude (NMR basis), [d] Product/starting material ratio = 0.22 in crude (NMR basis).

Fig. 4.48: Optimization of the conditions of the cyclopropanation reaction of *cis-β*-methylstyrene with ethyldiazoacetate catalyzed by Cu(I) complexes.

Though some control experiments were missing, our results showed that the carboxyguanidinium group of **24b** does not interfere to a great extent the outcome of the reaction, since the product was detected in each case. This series of experiments proved actually that the choice of the Cu(I) source was essential. Indeed, use of Cu(II) and a reducing agent such as a phenylhydrazine derivative afforded poorly reproducible results. In all cases, oxidation of Cu(I) to Cu(II) was observed and the reaction proved sensitive to air and moisture. Unfortunately, overlapping of relevant signals on the ^{1}H NMR spectra (entry 2) precluded to accurately determine the diastereoselectivity of the reaction, though the overall spectrum does not show splitted signals (which suggests at least a 95% diastereoselective process: retention of olefin configuration is likely). Thus, the process was investigated with unsaturated carboxylic acid salts (vinylacetic and crotonic acids) (Fig. 4.49).

a)

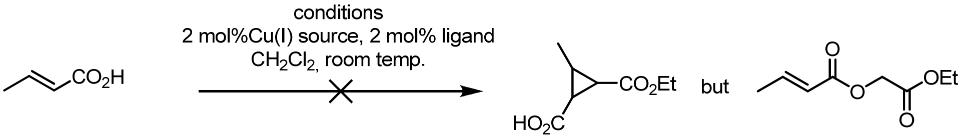

Ligand	conditions	yield
24b (Cl$^-$)	$Cu(OTf)_2$, 2,4-dinitrophenylhydrazine, slow addition of crotonic acid and ethyl diazoacetate (2/1 ratio)	n.m.
24b	$[Cu(MeCN)_4]PF_6$, slow addition of crotonic acid and ethyl diazoacetate (2/1 ratio)	56
24b	slow addition of crotonic acid and ethyl diazoacetate (1/1 ratio)	No reaction
bpy	$[Cu(MeCN)_4]PF_6$, slow addition of ethyl diazoacetate (2/1 ratio crotonic acid/ethyl diazoacetate)	60
24b	$[Cu(MeCN)_4]PF_6$, slow addition of 1 eq. crotonic acid to 1 eq. ethyl diazoacetate	diethyl fumarate[a]

[a] result of the self-reaction of ethyl diazoacetate with Cu(I).

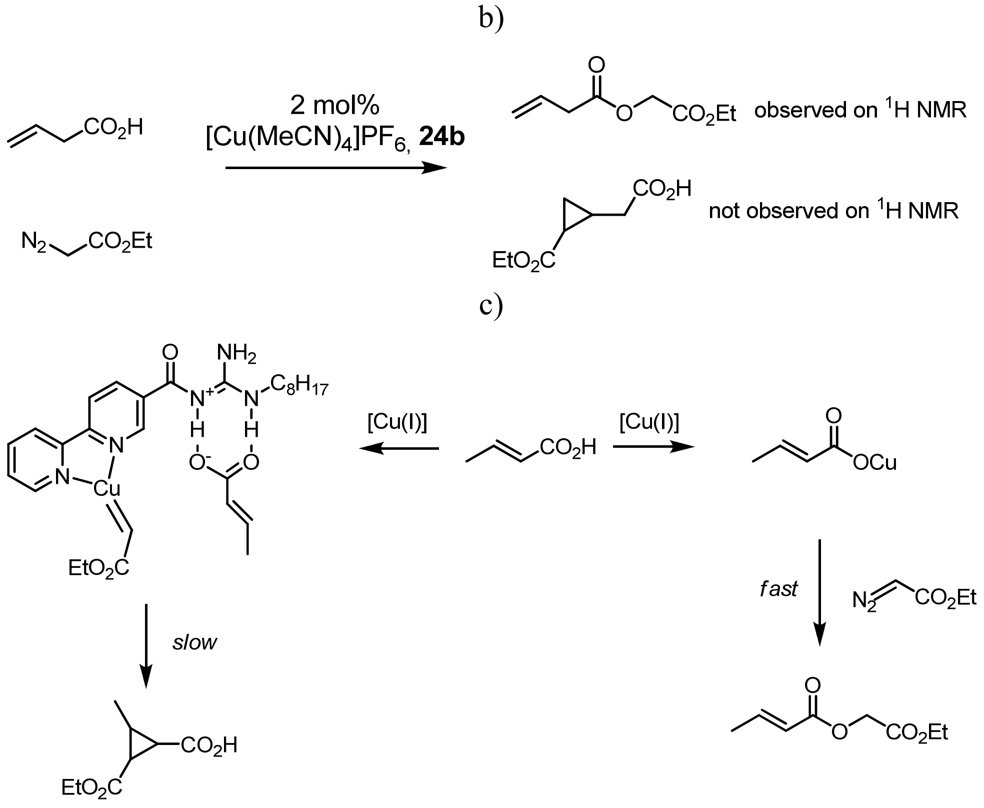
b)
CO2H
N2 CO2Et
2 mol%
[Cu(MeCN)4]PF6, 24b
O
O
CO2Et
observed on 1H NMR
CO2H
EtO2C
not observed on 1H NMR
c)
O
NH2
N+
N
C8H17
H
H
N
N
Cu
O-
O
EtO2C
[Cu(I)]
[Cu(I)]
CO2H
O
OCu
fast
N2 CO2Et
slow
CO2H
EtO2C
O
O
CO2Et

Fig. 4.49: Results for the cyclopropanation reaction of a) crotonic acid; b) vinylacetic acid; c) Proposed path for the observed esterification process.

Since a strong interaction between the carboxylic acid substrates and the metal was expected, unsaturated carboxylates were also added *via* syringe pump in order not to destroy the [Cu(**24b**)] complex. It was however surprising to observe that, in the presence of Cu(I) and any 2,2'-bipyridyl ligand (whether functionalized or not), cyclopropanation did not take place and an esterification reaction was occurring instead. Likely, formation of copper carboxylate is faster than the metallocarbene complex formation (Fig. 4.49c). Up to 60% yield for the isolated ester could be obtained after column chromatography. Similar results were obtained with vinylacetate.

In order to avoid these side-reactions (esterification and formation of diethyl fumarate), it was then decided to study the related Cu(I) catalyzed aziridination of unsaturated acids. Following a similar approach, reactivity of *cis-β*-methylstyrene was first studied, as shown in Fig. 4.50.

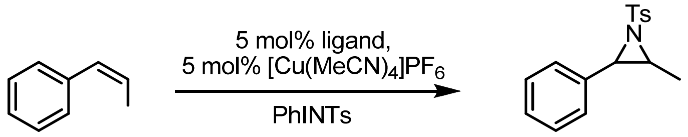

Ligand	Outcome
bpy	Oxidation to Cu(II)
24b	Product isolated by column chromatography but still impure (yield not measured)
24b (PF_6^-)	Product isolated by column chromatography but still impure (yield not measured)

Fig. 4.50: Aziridination of *cis-β*-methylstyrene catalyzed by Cu(I).

Although the yield of the reaction was not measured, the product could be successfully isolated and identified by ^{1}H NMR when the reaction was performed in the presence of 2 mol% of **24b**. The procedure was then investigated with crotonic acid with and without slow addition of the substrate. In both cases, the starting material was recovered. When the acid was added slowly, a complex reaction mixture was obtained. Unfortunately, the products could not be identified by mass spectrometry, although the amidation product was detected (also seen on the ^{1}H NMR spectrum of the crude) (Fig. 4.51).

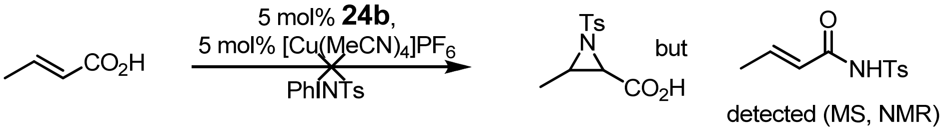

Fig. 4.51: Aziridination of unsaturated carboxylic acids catalyzed by Cu(I).

This amide formation was attributed again to the presence of copper carboxylate prior to the formation of the nitrene, which leads to the formation of the amide bond by nucleophilic attack on PhINTs.

A possible way to tackle this issue would be to investigate less oxophilic metals such as ruthenium, which was shown to catalyze the cyclopropanation of olefins.[32] More sterically hindered substrates might as well be investigated to slow down the esterification/amidification processes.

---

[32] For cyclopropanation, see: a) Nishiyama, H. *Topics in Organometallic Chemistry* **2004**, *11*, 81. For aziridination, see: b) Che, C.-M.; Yu, W.-Y. *Pure & Appl. Chem* **1999**, *71*, 281.

4.5 Conclusions.

Monodentate ligands for this combinatorial approach to supramolecular catalysis could be prepared in a rather straightforward way from cheap starting materials in good to moderate yields, although the molecular complexity of some of the designed ligands prevented their preparation. Functionalized 2,2'-bipyridines were the only bidentate ligands that could be prepared, since the synthesis of **22a-c** and **23a-b** did not work and require further investigation. In general, such a combinatorial approach requires the use of readily accessible ligands, which could be modulated after the screening of the catalysis experiments. Among the various transition metals that were investigated for the formation of the heteroleptic complexes, emphasis was laid on Cu(I), Zn(II) and Ru(II) due to their known ability to bind *N*-heterocyclic ligands in a suitable geometrical environment. However, our initial design was based exclusively on nitrogen-based ligands, which was in part responsible for the observed mixture of complexes. Use of other metal binding atoms (such as phosphorus or sulfur) should be evaluated to this aim. Finally, use of a wider diversity of ligands might also extend the scope of transition metals to be tested, as well as the scope of catalytic applications.

4.6 Experimental part.

a) General procedures.

General procedures for synthesis, chromatography and analysis were the same as in Chapters 2 and 3. HPLC-MS analysis was run on a Waters LCT Premier liquid chromatograph coupled to a time-of-flight mass spectrometer (HPLC/MS-TOF) with electrospray ionization (ESI) and atmospheric pressure chemical ionization (APCI) options.

b) Synthesis.

Dimethyl 4-chloropyridine-2,6-dicarboxylate (25a).

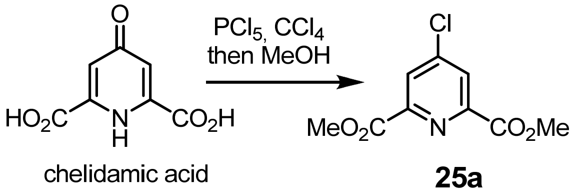

Procedure

A mixture of chelidamic acid (2.50 g, 12.43 mmol) and phosphorus pentachloride (10.35 g, 49.72 mmol) in carbon tetrachloride (12 mL) was stirred at reflux (78 ºC) for 4 hours. Methanol (dry, 8 mL) was added dropwise at room temperature and the mixture was further heated at reflux for one hour. The solvent was then eliminated *in vacuo* and the residue was placed in water (50 mL) and neutralized with sodium carbonate until pH 7. The resulting white solid was filtered and dried. The solid was then dissolved in chloroform and the resulting organic phase was washed with saturated sodium carbonate twice, followed by brine. After drying the organic phase and elimination of the solvents, **25a** was obtained as a white solid (2.4 g, 87%). **^{1}H NMR** ($CDCl_3$, 400 MHz): δ ppm 8.31 (s, 2H, H_{Ar}), 4.03 (s, 6H, CH$_3$); ^{13}**C NMR** (CDCl$_3$, 100 MHz): δ ppm 164.2, 149.4, 146.8, 128.3, 93.5.

25b was obtained in a similar way replacing chelidamic acid by pyridine 2,6-dicarboxylic acid (70% yield). ^{1}**H NMR** (CDCl$_3$, 400 MHz) δ ppm 8.25 (d, 2H, J = 7.8 Hz), 7.98 (t, 1H, J = 7.8 Hz), 3.96 (s, 6H); ^{13}**C NMR** (CDCl$_3$, 100 MHz) δ ppm 165.1, 148.1, 138.5, 128.2, 53.2.

4-Chloro-*N*^{2},*N*^{6}-bis(2-hydroxy-1-phenylethyl)pyridine-2,6-dicarboxamide (26).

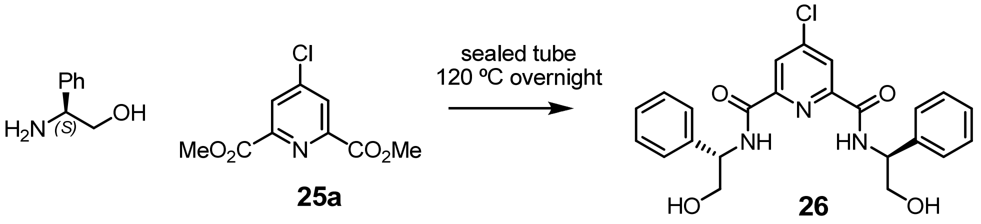

Procedure

A mixture of L-phenylglycinol (1.15 g, 8.42 mmol) and **25a** (0.97 g, 4.21 mmol) was stirred overnight at 120 ºC without any solvent. After cooling down, the resulting solid was dissolved in 8 mL AcOEt and the solution was poured dropwise in hexane (150 mL). The precipitated white solid was then filtered and operation was repeated to yield **26** as a white solid (2.00 g, quantitative).^{1}**H NMR** (CDCl$_3$, 400 MHz): δ ppm 8.81 (s, 1H, NH), 8.79 (s, 1H, NH), 8.14 (s, 2H, H$_{Ar}$), 7.37-7.21 (m, 10 H, Phenyl), 4.21 (ABX system, 2H, J = 12.7, 5.4 Hz, CH), 3.94 (d, 4H, J = 4.5 Hz, CH$_2$); ^{13}**C NMR** (CDCl$_3$, 100 MHz): δ ppm 162.9, 150.3, 147.8, 138.8, 129, 128.1, 126.7, 125.6, 65.6, 55.8.

The diamide precursor for the synthesis of **Ph-Pybox** was obtained following a similar route from **25b** (quantitative). **^{1}H NMR** ($CDCl_3$, 400 MHz) δ ppm 8.80 (s, 1H), 8.79 (s, 1H), 8.14 (d, 2H, J = 7.8 Hz), 7.82 (t, 1H, J = 7.8 Hz), 7.40-7.20 (m, 10H), 5.24-5.19 (m, 2H), 3.93 (d, 4H, J = 5.0 Hz); **^{13}C NMR** ($CDCl_3$, 100 MHz) δ ppm 163.8, 148.6, 139.0, 128.8, 127.8, 126.7, 125, 65.8, 55.8.

2,2'-(4-Chloropyridine-2,6-diyl)bis(4-phenyl-4,5-dihydrooxazole) (Ph-Cl-Pybox).

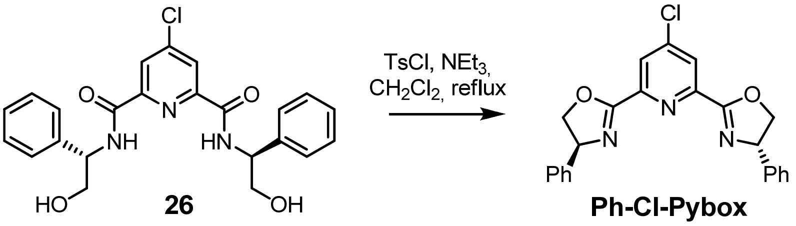

Procedure

A mixture of **26** (2.04 g, 4.65 mmol), *p*-toluenesulfonyl chloride (1.92 g, 10.1 mmol) and triethylamine (6 mL) in dry CH_2Cl_2 (15 mL) was refluxed at 42 ºC during 24 h. The mixture was then diluted with CH_2Cl_2 and the resulting organic phase was washed with NaOH 1N. Aqueous phase was extracted 3 times with CH_2Cl_2 and the gathered organic phases were dried with sodium sulfate, filtered and evaporated *in vacuo*. The resulting brown solid was then recrystallized in ethanol to yield **Ph-Cl-Pybox** as a white solid that was filtered and washed with cold ethanol (951 mg, 51% yield). **^{1}H NMR** ($CDCl_3$, 400 MHz): δ ppm 8.38 (s, 2H, H_{Ar}), 7.43-7.29 (m, 10H, Ph), 5.48 (t, 2H, J = 8.0 Hz), 4.96 (t, 2H, J = 8.6 Hz), 4.46 (t, 2H, J = 9.3

Hz); **^{13}C NMR** (CDCl$_3$, 100 MHz): δ ppm 162.7, 148.0, 145.6, 141.4, 128.9, 127.9, 126.9, 126.5, 75.7, 70.4.

Ph-Pybox was obtained following a similar treatment of the corresponding diamide precursor (54% yield). **^{1}H NMR** (CDCl$_3$, 400 MHz) δ ppm 8.36 (d, 2H, J = 7.8 Hz), 7.93 (t, 1H, J = 7.8 Hz), 7.45-7.25 (m, 10H), 5.48 (t, 2H, J = 9.4 Hz), 4.94 (t, 2H, J = 9.2 Hz), 4.44 (t, 2H, J = 8.6 Hz); **^{13}C NMR** (CDCl$_3$, 100 MHz) δ ppm 163.5, 146.8, 141.7, 137.4, 128.8, 127.8, 126.9, 126.4, 75.7, 70.4.

2,2-Diethyl-*N*^{1},*N*^{3}-bis((R)-2-hydroxy-1-phenylethyl)malonamide (27).

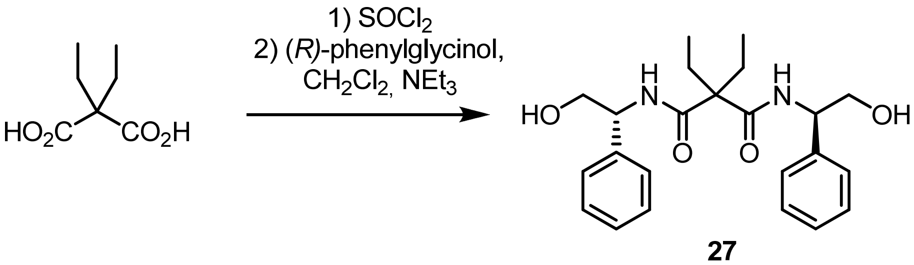

27

Procedure

A suspension of diethyl malonic acid (915 mg, 5.71 mmol) in thionyl chloride (4 mL) was heated at reflux for 3 hours. Solvent was then eliminated under vacuum. Into a flask placed under argon and at 0 ºC was dissolved triethylamine (3.97 mL) and (*R*)-phenylglycinol in dichloromethane (12 mL). A solution of the acid chloride in CH$_2$Cl$_2$ (5 mL) was then added dropwise while cold. The mixture was then left one hour at this temperature, time after which it was diluted with more dichloromethane. Organic phase was washed with HCl 1N followed by saturated aqueous NaHCO$_3$ and brine. Each aqueous phase was then further extracted with dichloromethane. Gathered organic phases were dried over sodium sulfate and solvent was eliminated under vacuum to yield 1.27 g of a white solid (56 % yield). The product was pure enough to be used in the further step.

(4*R*,4'*R*)-2,2'-(Pentane-3,3-diyl)bis(4-phenyl-4,5-dihydrooxazole) (Ph-box).

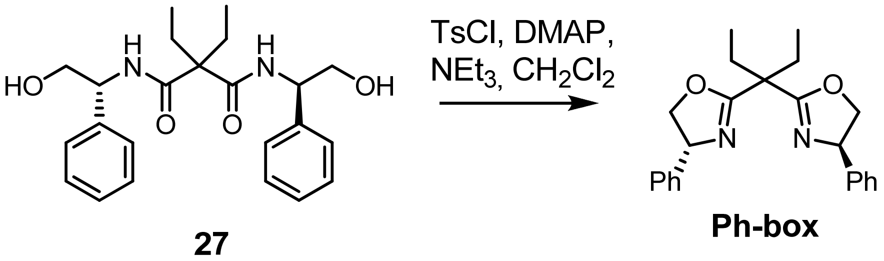

Procedure

To a suspension of the bis amide **27** (1.00 g, 2.5 mmol) in CH_2Cl_2 (10 mL) was added 4-dimethylaminopyridine (31 mg, 0.25 mmol) and the triethylamine (2 mL, 14.3 mmol). A solution of *p*-toluenesulfonylchloride (957 mg, 5 mmol) in CH_2Cl_2 was then added dropwise at room temperature under argon and the resulting solution was stirred one day at RT. The mixture was diluted with CH_2Cl_2 and washed with saturated aqueous NH_4Cl followed by 10% $NaHCO_3$. After drying and elimination of the solvents, a thick yellow oil was obtained. Column chromatography was performed using neat CH_2Cl_2 to 20% Et_2O/CH_2Cl_2. 579 mg of a translucid oil were obtained this way (**Ph-box**, 64% yield). **^{1}H NMR** ($CDCl_3$, 400 MHz): δ ppm 7.40-7.20 (m, 10 H), 5.30-5.25 (m, 2H), 4.71-4.64 (m, 2H), 4.14 (t, 2H, J = 8.2 Hz), 2.30-2.10 (m, 4H), 1.00 (t, 6H, J = 7.5 Hz); **^{13}C NMR** ($CDCl_3$, 100 MHz): δ ppm 168.9, 142.2, 128.7, 127.5, 126.8, 75.0, 69.6, 47.0, 25.7, 8.6.

N^2,*N*^{6}-Bis((*S*)-1-chloro-3-methylbutan-2-yl)pyridine-2,6-dicarboxamide (28).

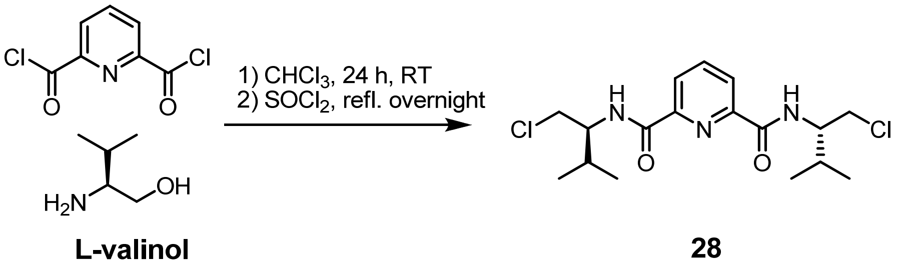

Procedure

To a solution of L-valinol (200 mg, 1.94 mmol) in dry CH_2Cl_2 (4 mL) placed at 0 ºC was added triethylamine (835 μL, 6 mmol) followed by a solution of the acid chloride (165 mg, 0.81 mmol) in 4 mL CH_2Cl_2. The resulting reaction mixture was then stirred at room temperature for three days. Thionyl chloride (3 mL) was added and resulting mixture was stirred at reflux overnight. The reaction mixture was then poured dropwise into ice-water and the organic phase was collected, washed with water, brine and dried with sodium sulfate. The solvent was then eliminated under vacuum after filtration to yield a black oil that was purified by column chromatography using CH_2Cl_2/Et_2O 5% as elution system to yield **28** after evaporation of the fractions (275 mg, 91% yield). **^{1}H NMR** ($CDCl_3$, 400 MHz): δ ppm 8.37 (d, 2 H, J = 7.8 Hz), 8.08 (t, 1H, J = 7.8 Hz), 8.04 (s,

1H), 8.02 (s, 1H), 4.25-4.15 (m, 2H), 3.84 (qd, 4H, J = 11.4, 3.3 Hz), 2.10-2.00 (m, 2H), 1.06 (dd, 12H, J = 11.6, 6.7 Hz); **^{13}C NMR** ($CDCl_3$, 100 MHz): δ ppm 163.0, 148.4, 139.3, 125.3, 54.9, 46.9, 29.6, 19.4, 18.8. **MS** (ESI$^+$): *m/z* calcd. 396.1, obt. 396.1 $[M+Na]^+$

2,6-Bis((*S*)-4-isopropyl-4,5-dihydrooxazol-2-yl)pyridine (*i*Pr-Pybox).

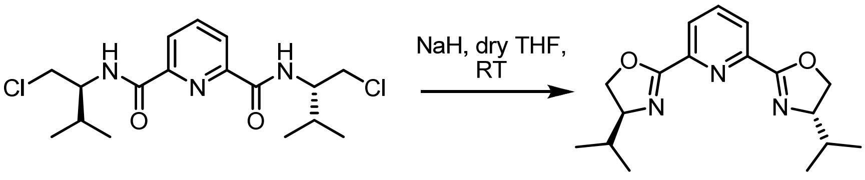

28

***i*Pr-Pybox**

Procedure

To a suspension of sodium hydride (53 mg, 2.2 mmol) in dry THF (2 mL) was added at room temperature and under argon a solution of the diamidopyridine derivative **28** (275 mg, 0.74 mmol)) in THF (3 mL). The resulting reaction mixture was stirred overnight at room temperature. The mixture was then filtered and concentrated on vacuum. The residue was extracted with diethyl ether, filtered and solvent was evaporated to yield a yellow solid (138 mg 63% yield). NMR data were found identical to the ones reported in the literature.[33]

---

[33] Nishiyama, H.; Yamaguchi, S.; Kondo, M.; Itoh, K. *J. Org. Chem.* **1992**, *57*, 4306.

1-(1*H*-Benzo[*d*]imidazol-2-yl)-3-butylurea (20a).

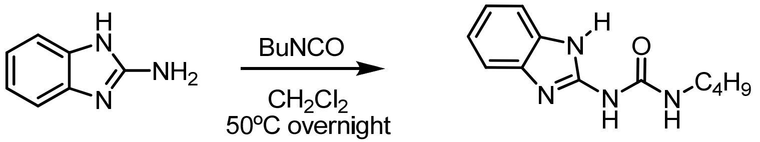

20a

Procedure

To a solution of 2-aminobenzimidazole (500 mg, 3.75 mmol) in CH_2Cl_2 (5 mL) placed in a sealed tube was added butyl isocyanate (1.27 mL, 11.27 mmol) and the resulting reaction mixture was stirred overnight at 50 ºC. The solvent was then eliminated *in vacuo* until the obtention of a solid residue. This white solid was triturated in hexane and filtered. After further drying under high vacuum, **20a** was isolated as a white solid (759 mg, 87% yield). **^{1}H NMR** (MeOD, 400 MHz): δ ppm (NHs are seen as various signals accounting for the existence of conformers and are omitted here): 7.54-7.46 (m, 2H, H_{Ar}), 7.16-7.08 (m, 2H, H_{Ar}), 3.38-3.30 (m, 2H, CH_2), 1.63-1.53 (m, 2H, CH_2), 1.49-1.36 (m, 2H, CH_2), 0.97 (t, 3H, J = 9 Hz, CH_3).

1-Butyl-3-(pyridin-2-yl)thiourea (20b).

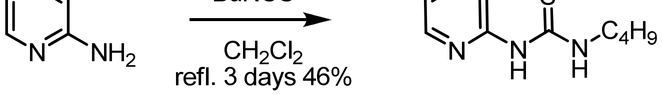

20b

Procedure

To a solution of 2-aminopyridine (1.00 g, 10.6 mmol) in CH_2Cl_2 (2 mL) was added dropwise the butylisothiocyanate (1.36 mL, 11.16 mmol). The resulting mixture was stirred at room temperature for 3 days. Reaction was stopped and solvent eliminated under vacuum. Residue was dissolved in diethyl ether and the organic phase was washed intensively with NH_4Cl 1N and brine. The organic phase was then dried with anhydrous sodium sulfate, filtered and solvent was eliminated under vacuum. **20b** was obtained as a white solid (1.03 g, 46% yield, uncomplete reaction). **^{1}H NMR** ($CDCl_3$, 400 MHz): δppm: 11.74 (t, 1H, NH), 9.57 (s, 1H, NH), 8.09 (ddd, 1H, J = 5.0, 1.8, 0.7 Hz), 7.56 (ddd, 1H, J = 9.1 , 7.3, 1.8 Hz), 6.93 (d, 1H, J = 8.5 Hz), 6.88 (ddd, 1H, J = 7.1, 5.2, 1 Hz), 3.73-3.67 (m, 2H, CH_2), 1.70-1.55 (m, 2H, CH_2), 1.45-1.35 (m, 2H, CH_2), 0.92 (t, 3H, J = 7.9 Hz, CH_3).

N-(Pyrimidin-2-yl-thiocarbamoyl)benzamide

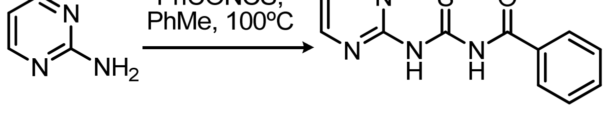

Procedure

To a refluxing solution of benzoylisothiocyanate (1.94 g, 11.9 mmol) in acetone (100 mL) was added dropwise an acetone solution of 2-aminopyrimidine (1.13 g, 11.9 mmol) and the resulting reaction mixture was stirred at reflux during 90 mn. After cooling, reaction mixture was poured into crushed ice and precipitated solid was filtered, washed with cold acetone and dried on the vacuum line (28% yield). **M.p.** 177-178 ºC; **^{1}H NMR** (MeOD, 400 MHz): δppm 13.60 (s, 1H, NH-CO), 12.10 (s, 1H, NH-CS), 8.78 (d, 2H, J = 5.4 Hz, H_{Ar}), 8.06-7.94 (m, 2H, H_{Ar}), 7.70 (t, 1H, J = 7.2 Hz, H_{Ar}), 7.63-7.59 (m, 2H, H_{Ar}), 7.30 (t, 1H, J = 5.2 Hz, H_{Ar}); **MS** (ESI$^+$): *m/z:* calc. 259.1, obt. 259.1 [(M+H)$^+$], calc. 281.0, obt. 281.0 [(M+Na)$^+$].

1-(Pyrimidin-2-yl)thiourea (29).

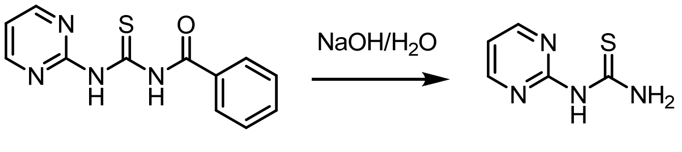

29

Procedure

To a preheated stirred solution of NaOH/H_2O 10% (12 mL) to 80 ºC was added in one portion the *N*-(pyrimidin-2-thiocarbamoyl)benzamide and resulting mixture was stirred 5 minutes. Reaction mixture was then poured into a mixture of ice and HCl 1N; resulting aqueous phase was then basified with $NaHCO_3$ until pH 8-9. Product was then collected by gravity filtration, and resulting **29** (white solid, 48% yield) was washed with water and H_2O/MeOH 1/1. **M.p.** 260-265 ºC; **^{1}H NMR** (MeOD, 400 MHz): δppm 10.65 (wide s, 1H, NH, H-bounded), 10.28 (wide s, 1H, NH), 9.21 (wide s, 1H, NH), 8.72 (d, 2H, J = 5.5 Hz, H_{Ar}), 7.22 (t, 1H, J = 5.5 Hz, H_{Ar}).

2-Methyl-1-(pyrimidin-2-yl)isothiouronium iodide (30).

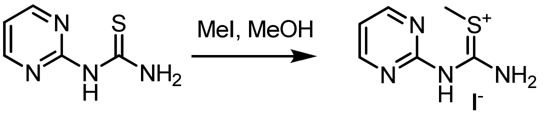

29 **30**

Procedure

In a round bottom flask was placed a solution of **29** (479 mg, 3.1 mmol) in dry methanol (100 mL) and methyl iodide (290 μl, 4.7 mmol) was added carefully at room temperature. The reaction mixture was then heated to 80 ºC overnight. The solvent was then eliminated under vacuum. Crude compound was used in the next step as obtained. **M.p.** 174-176 ºC.

Preparation of **20c** from **30** was investigated and afforded **20c** in poor yield due to non optimized procedures not described here.

5-Bromo-8-nitroisoquinoline (31).

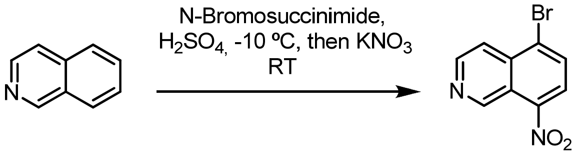

31

Procedure

To a solution of isoquinoline (11.0 g, 85 mmol) in sulfuric acid (100 mL) was added at -10 ºC the *N*-bromosuccinimide (17.8 g, 100 mmol), and resulting mixture was stirred at this temperature for 24 h. Potassium nitrate (11.0 g, 100 mmol) was then added and resulting mixture was stirred at room temperature for one hour. The mixture was then poured into crushed ice and neutralized with aqueous ammonia. The obtained precipitate was filtered off and washed with water. Solid was then dried and recrystallized with MeOH to yield **31** as a yellow-brown solid (8.12 g, 38% yield). **^{1}H NMR** (DMSO, 400 MHz): δ ppm 9.77 (s, 1H), 8.84 (d, 1H, *J* = 5.7 Hz), 8.35 (m, 2H), 8.12 (d, 1H, *J* = 5.8 Hz); **MS** (ESI$^+$): *m/z* 253.0 [(M+H)$^+$].

8-Aminoisoquinoline (32).

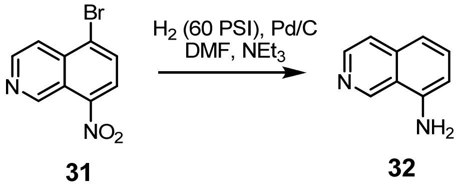

Procedure

In a hydrogenation Parr apparatus was placed 5-bromo-8-nitroisoquinoline **31** (4.0 g, 15.8 mmol) in dry DMF (90 mL) and triethylamine (2.4 mL) was added, followed by 10% palladium over activated carbon (272 mg). A hydrogen atmosphere (60 psi) was then applied to the reactor and reaction mixture was left one hour stirring at room temperature under hydrogen pressure. Reaction mixture was then filtered over celite and the solvent was eliminated under vacuum. Obtained residue was dissolved in water and resulting aqueous phase was extracted with diethyl ether. The gathered organic phases were dried over sodium sufate, filtered and solvent eliminated under vacuum to yield **32** as a white solid (1.8 g, 78% yield). **^{1}H NMR** ($CDCl_3$, 400 MHz): δ ppm 9.31 (s, 1H), 8.45 (d, 1H, J = 5.8 Hz), 7.54 (d, 1H, J = 5.6 Hz), 7.45 (t, 1H, J = 7.9 Hz), 7.19 (d, 1H, J = 8.2 Hz), 6.79 (dd, 1H, J = 7.6, 0.7 Hz), 4.24 (s, 2H).

1-(3,5-Bis(trifluoromethyl)phenyl)-3-(isoquinolin-8-yl)thiourea (21b3).

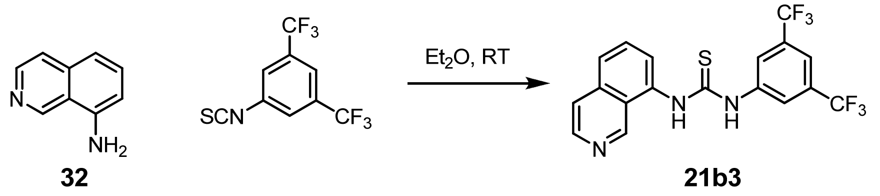

Procedure

To a solution of 8-aminoisoquinoline **32** (55.5 mg, 0.385 mmol) in diethyl ether (12 mL) was added some 3,5-bis(trifluoromethyl)-phenylisothiocyanate (70 μL, 0.385 mmol) and resulting mixture was stirred at room temperature for 2 days. **21b3** directly precipitated in the reaction mixture and was collected by filtration and washed with diethyl ether (38% yield, not optimized). **^{1}H NMR** (DMSO, 400 MHz): δ ppm 10.56 (s, 1H, NH), 10.41 (s, 1H, NH), 9.39 (s, 1H), 8.55 (s, 1H), 8.31 (m, 2H), 7.95-7.92 (m, 1H), 7.9-7.6 (m, 1H), 7.74-7.66 (m, 1H); **HR-MS** (ESI^+): *m/z* calc. for $C_{18}H_{12}N_3SF_6$ 416.0656, obt. 416.0668 $[(M+H)^+]$.

8-Isothiocyanatoisoquinoline (33).

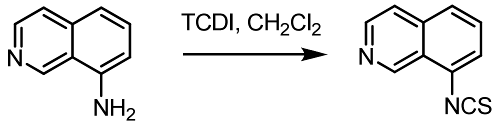

32 **33**

Procedure

To a solution of 1,1'-thiocarbonyldiimidazole (322 mg, 1.80 mmol) in dry dichloromethane (20 mL) was added the 8-aminoisoquinoline **32** (217 mg, 1.50 mmol) and the resulting mixture was stirred one day at room temperature. After elimination of solvent under reduced pressure, the crude compound was purified by silica gel column chromatography (25% AcOEt/DCM) to yield the 8-isothiocyanatoisoquinoline **33** in 68% yield. **^{1}H NMR** ($CDCl_3$, 400 MHz) δ ppm: 9.42 (s, 1H), 8.54 (d, 1H, J = 5.7 Hz), 7.65 (d, 1H, J = 7.8 Hz), 7.60-7.50 (m, 2H), 7.38 (d, 1H, J = 7.8 Hz); **^{13}C NMR** ($CDCl_3$, 100 MHz): δ ppm 147.9, 144.4, 138.5, 136.5, 130.2, 128.5, 125.9, 124.8, 123.8, 120.3; **MS** (TOF-ESI$^+$): *m/z* 187.1 [(M+H)$^+$]; **IR**: ν(NCS)=2069 cm^{-1}.

1-Butyl-3-(isoquinolin-8-yl)thiourea (21b1) and (21b2).

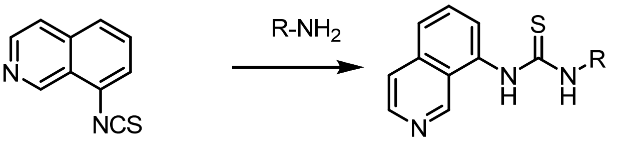

33

21b1 R = C_4H_9 69% yield (2 steps)
21b2 R = *tert*-butyl 68% yield (2 steps)

Procedure

A solution of 8-isothiocyanatoisoquinoline **33** was stirred at room temperature under argon atmosphere in butylamine (respectively *tert*-butylamine, 0.6 M concentration) for 30 minutes. The solvent was then eliminated under reduced pressure and the crude compound was purified by silica gel column chromatography (1/1 AcOEt/DCM) to yield the corresponding thioureidoisoquinoline derivative in close to quantitative yield.

1-Butyl-3-(isoquinolin-8-yl)thiourea (21b1).

^{1}H NMR (CDCl$_3$, 400 MHz) δ ppm 9.37 (s, 1H), 8.89 (s, 1H, NH), 8.49 (d, 1H, J = 5.6 Hz), 7.77 (d, 1H, J = 8.2 Hz), 7.68 (t, 1H, J = 7.8 Hz), 7.60 (d, 1H, J = 5.7 Hz), 7.53 (d, 1H, J = 7.2 Hz), 6.10 (s, 1H, NH), 3.56-3.50 (m, 2H), 1.45-1.41 (m, 2H), 1.22-1.17 (m, 2H), 0.80 (t, 3H, J = 7.4 Hz); **^{13}C NMR** (CDCl$_3$, 100 MHz) δ ppm 181.8, 148.0, 143.8, 137.0, 133.4, 130.6, 126.8, 126.1, 124.8, 120.5, 45.3, 30.9, 19.9, 13.7; **MS** (ESI$^+$): *m/z* calc. for $C_{14}H_{17}N_3NaS$ 282.1041; obt. 282.1031 [(M+Na)$^+$].

1-*tert*-Butyl-3-(isoquinolin-8-yl)thiourea (21b2).

^{1}H NMR (CDCl$_3$, 400 MHz) δ ppm 9.45 (s, 1H), 8.89 (s, 1H, NH), 7.79 (d, 1H, J = 8.2 Hz), 7.72 (t, 1H, J = 7.5 Hz), 7.68 (d, 1H, J = 5.8 Hz), 7.54 (d, 1H, J = 7.2 Hz), 5.95 (s, 1H, NH), 1.45 (s, 9H); **^{13}C NMR** (CDCl$_3$, 100 MHz) δ ppm 180.7, 148.1, 144.0, 137.1, 133.9, 130.7, 126.6, 125.9, 124.7, 120.6, 54.3, 28.9.

1-Butyl-3-(isoquinolin-8-yl)urea (21a).

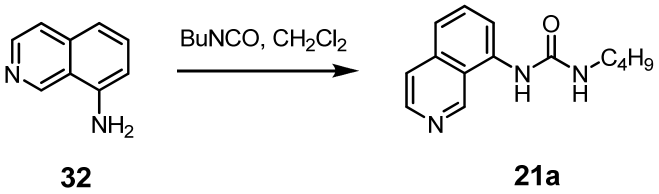

Procedure

A solution of 8-aminoisoquinoline **32** (0.50 g, 3.47 mmol) and butylisocyanate (1.93 mL, 17.34 mmol) in dry dichloromethane (20 mL) was stirred at room temperature for 5 days under argon. Hexane (200 mL) was then added dropwise to this mixture to allow the precipitation of **21a** as a yellow solid that was isolated by filtration (577 mg, 68% yield). **^{1}H NMR** ($CDCl_3$, 400 MHz) δ ppm 9.62 (s, 1H), 8.40 (d, 1H, *J* = 4.8 Hz, 1H), 8.28 (s, 1H, NH), 7.98 (d, 1H, *J* = 7.6 Hz), 7.58 (t, 1H, *J* = 7.7 Hz), 7.43 (d, 1H, *J* = 8.2 Hz), 5.89 (s, 1H, NH), 3.30-3.20 (m, 2H), 1.51-1.43 (m, 2H), 1.34-1.28 (m, 2H), 0.87 (t, 3H, *J* = 7.3 Hz).

1,3-Di(isoquinolin-8-yl)urea (34).

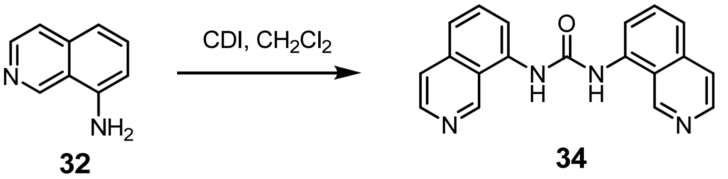

Procedure

To a solution of 1,1'-carbonyldiimidazole (506 mg, 3.51 mmol) in dry dichloromethane (20 mL) was added the 8-amino-isoquinoline **32** (217 mg, 1.50 mmol) and the resulting mixture was stirred one day at room temperature under argon. The precipitate was then filtered to yield **34** in 18% yield (202 mg). **^{1}H NMR** ([D6]-DMF, 400 MHz) δ ppm: 10.00 (s, 2H), 9.89 (s, 2H), 8.59-8.57 (m, 2H), 8.36 (d, 2H, *J* = 7.2 Hz), 7.90-7.85 (m, 2H), 7.84-7.77 (m, 2H), 7.75-7.7 (m, 2H); **MS** (TOF-ESI$^+$): *m/z* 315.1 $[M+H]^+$; 337.1 $[M+Na]^+$.

4-(2-(Dimethylamino)vinyl)nicotinonitrile (38).

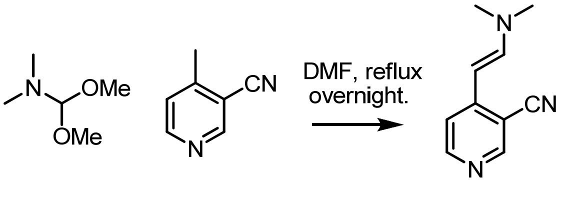

38

Procedure

A solution of 3-cyano-4-methylpyridine (2.00 g, 17.0 mmol) and *N,N*-dimethylformamide dimethylacetal (2.37 mL, 17.7 mmol) in dry DMF (60 mL) was stirred at reflux overnight. After the night, the reaction mixture was concentrated *in vacuo* and the residue was reparted between ethyl acetate and water. The organic phase was washed with water, brine and dried with sodium sulfate. After filtration, solvent was eliminated to yield **38** (2.86 g., 98% yield) as a red solid. **^{1}H NMR** ($CDCl_3$, 400 MHz): δ ppm 8.48 (s, 1H, H_{Ar}), 8.23 (d, 1H, *J* = 6.0 Hz, H_{Ar}), 7.28 (d, 1H, *J* = 14.0 Hz, ArCH=C), 7.09 (d, 1H, *J* = 6.0 Hz, H_{Ar}), 5.23 (d, 1H, *J* = 14.0 Hz, C=CHN), 2.98 (s, 6H, NMe); **MS** (ESI$^+$): *m/z* 173 [M$^+$], 158 [(M-Me)$^+$], 129 [(M-NMe$_2$)$^+$].

1-Hydroxy-2,7-naphthyridine (39).

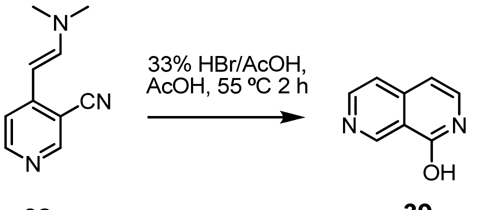

38 **39**

Procedure

A stirred solution of **38** (2.13 g, 12.27 mmol) in 20 mL acetic acid was treated dropwise at 40 ºC with 40 mL 33% HBr in AcOH. The mixture was stirred at 57 ºC for two hours and the solvent was eliminated thanks to reduced pressure. The residue was diluted with ice cold water and basified with sodium carbonate. The resulting aqueous solution was extracted overnight with chloroform in a continuous liquid-liquid extractor. The organic phase was dried with anhydrous sodium sulfate, filtered and solvent was eliminated in vacuum. Crude residue was then purified by silica gel column chromatography (CH_2Cl_2/MeOH/NH_3 95:5:1.25) to give product **39** after trituration with isopropanol (285.6 mg, 16% yield). **^{1}H NMR** (MeOD, 400 MHz): δppm 11.60 (s, 1H, OH), 9.30 (s, 1H), 8.67 (d, 1H, J = 4.9 Hz), 7.56 (d, 1H, J = 4.3 Hz), 7.42 (d, 1H, J = 4.7 Hz); **^{13}C NMR** (MeOD, 100 MHz): δppm 161.8, 151.2, 150.3, 143.6, 134.9, 119.8, 103.4; **HR-MS** (ESI$^+$): *m/z* calc. for $C_8H_6N_2O$ 147.0558, obt. 147.0559 [(M+H)$^+$].

1-Chloro-2,7-naphthyridine (36).

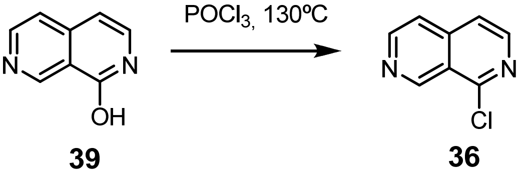

Procedure

A sealed tube, equipped with a magnetic stirrer, was charged with 1-hydroxy-2,7-naphtyridine **39** (285 mg, 1.95 mmol) and phosphorus oxychloride was added (10 mL). The mixture was stirred overnight at 130 ºC and the tube was opened after cooling. The solvent was then eliminated under reduced pressure and the residue was dissolved in saturated aqueous sodium carbonate. The resulting aqueous phase was extracted twice with chloroform and the resulting organic phase was washed with brine, dried with anhydrous Na_2SO_4, filtered and solvent was finally eliminated under vacuum to yield **36** (321 mg, quantitative). **^{1}H NMR** ($CDCl_3$, 400 MHz): δ ppm 9.60 (s, 1H), 8.71 (d, 1H, J = 6.2 Hz), 8.35 (d, 1H, J = 6.2 Hz), 7.57 (dd, 1H, J = 6.2, 1.0 Hz), 7.51 (dd, 1H, J = 6.2, 1.0 Hz); **MS** (ESI$^+$): *m/z* 164 [M$^+$], 129 [M-Cl]$^+$.

Tetrazolo[5,1-*a*][2,7]naphthyridine (41).

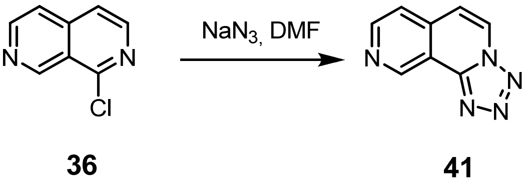

Procedure

To a mixture of naphthyridine chloride **36** (106 mg, 0.64 mmol) in dry DMF (5 mL) was added the sodium azide (167 mg, 2.57 mmol) at room temperature and under argon; the resulting mixture was then heated at 80 ºC overnight. Excess water (100 mL) was then added to the mixture. Aqueous phase was extracted with dichloromethane three times. The organic phase was then dried with anhydrous sodium sulfate, filtered and solvent was eliminated under vacuum to yield compound **41** in 67% yield. **^{1}H NMR** ($CDCl_3$, 400 MHz): δ ppm 10.11 (s, 1H), 9.03 (d, 1H, J = 5.5 Hz), 8.77 (d, 1H, J = 7.4 Hz), 7.82 (d, 1H, J = 5.2 Hz), 7.46 (d, 1H, J = 7.4 Hz); **^{13}C NMR** ($CDCl_3$, 400 MHz): δ ppm 150.7, 148.4, 146.8, 136.4, 125.5, 120.2, 115.9, 115.1.

N,N-Dimethyl-2,7-naphthyridin-1-amine (40).

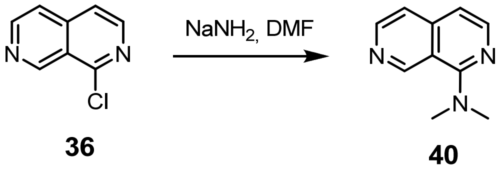

Procedure

A solution of 1-chloro-2,7-naphthyridin **36** (263 mg, 1.60 mmol) in dry DMF was added via canula to a flask containing sodium amide from the dry box (69 mg, 1.76 mmol), the mixture was then stirred at room temperature overnight . The solvent was then eliminated under vacuum and the residue was purified by column chromatography using DCM/MeOH 2% as elution system to yield **40** after evaporation of the fractions (148.1 mg, 54% yield).

^{1}H NMR ($CDCl_3$, 400 MHz): δ ppm 9.37 (s, 1H), 8.48 (d, 1H, J = 5.7 Hz), 8.11 (d, 1H, J = 5.7 Hz), 7.38 (d, 1H, J = 5.7 Hz), 6.90 (d, 1H, J = 5.7 Hz), 3.17 (s, 6H); **^{13}C NMR** ($CDCl_3$, 400 MHz): δ ppm 161.0, 150.7, 146.1, 144.9, 141.9, 119.2, 115.5, 111.2, 42.9.

2-Amino-4,5-dihydro-1*H*-imidazol-3-ine hydrate (42).

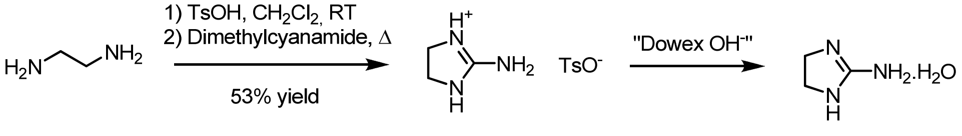

42 (TsO⁻) **42**

Procedure

To a solution of 1,2-diaminoethane (3.0 mL, 44.43 mmol) in methanol (50 mL) was added at room temperature the *p*-toluenesulfonic acid (8.45 g, 44.43 mmol) and the mixture was stirred for 15 min., time after which solvent was eliminated under reduced pressure to yield a white solid. A sample of 2-aminoethanaminium tosylate (2.29 g, 8.89 mmol) was then placed in a sealed tube containing dimethylcyanamide (724 μL, 8.89 mmol). Resulting mixture was then heated with a heat gun in order to initiate the reaction for a few seconds and then at 100 ºC for 3 hours. When left standing at room temperature, a crystalline residue was obtained; boiling ethanol (3 mL) was then added and the mixture was left crystallizing at room temperature to yield 1.20 g of **42** as a white solid (53% yield). An aliquot of 580 mg was passed through Dowex® resin for hydroxide with a water/methanol mixture (2:1) and solvent was eliminated under vacuum to yield a translucid oil that crystallised as a white solid.

2-Aminoethanaminium tosylate: white solid; **^{1}H NMR** (MeOD, 400 MHz) δ ppm 6.13 (d, 2H, J = 8.2 Hz), 5.65 (d, 2H, J = 8.2 Hz), 1.33 (s, 4H), 0.78 (s, 3H); **^{13}C NMR** (MeOD, 100 MHz) δ ppm 140.5, 138.9, 127.0, 123.9, 99.9, 38.5, 18.4.

2-Amino-4,5-dihydro-1*H*-imidazol-3-ium tosylate (**42**): white solid; **^{1}H NMR** (MeOD, 400 MHz) δ ppm 7.72 (d, 2H, J = 8.1 Hz), 7.25 (d, 2H, J = 8.1 Hz), 3.68 (s, 4H), 2.40 (s, 3H); **^{13}C NMR** (MeOD, 100 MHz) δ ppm 160.5, 142.0, 140.4, 128.5, 125.5, 42.6, 19.9.

2-Amino-4,5-dihydro-1*H*-imidazol-3-ium hydroxide (**42**): white solid; **^{1}H NMR** (MeOD, 400 MHz) δ ppm: 3.49 (s, 4H); **^{13}C NMR** (MeOD, 100 MHz) δ ppm: 163.9, 46.3.

1'*H*-Spiro[imidazolidine-2,2'-pyrrolo[2,3,4-*ij*][2,7]naphthyridine] (43).

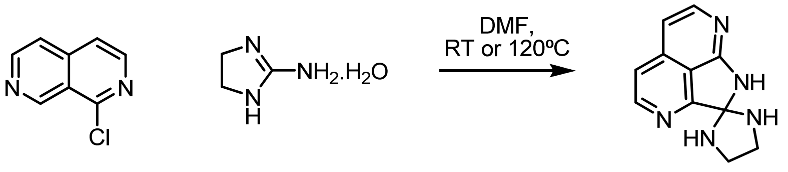

36 **42** **43**

Procedure

A solution of 1-chloro-2,7-naphthyridine **36** (100 mg, 0.6 mmol) and **23** (75 mg, 0.73 mmol) in dry DMF (3 mL) was stirred at 120 ºC during 2 days in a sealed tube. The formed white precipitate was then filtered and dried under vacuum to yield compound **43** (yield not measured). A similar result was obtained at room temperature. **^{1}H NMR** (D_2O, 400 MHz) δ ppm: 7.60 (d, 1H, *J* = 6.9 Hz), 7.47 (d, 1H, *J* = 6.9 Hz), 6.59 (d, 1H, *J* = 4.9 Hz), 6.49 (d, 1H, *J* = 5.9 Hz), 3.67 (m, 4H); **^{13}C NMR** (D_2O, 100 MHz) δ ppm: 156.5, 156.4, 148.3, 148.0, 141.9, 141.8, 112.3, 110.0, 105.2, 43.4; **MS** (TOF-ESI$^+$): *m/z* 212.1 [M+H]$^+$.

1-Amino-2-naphthonitrile (48).

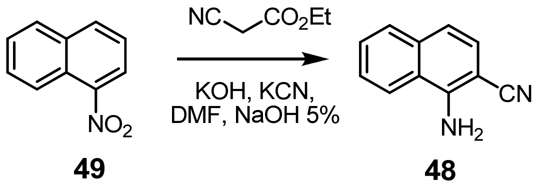

Procedure

To a solution of ethyl cyanoacetate (1.85 mL, 17.33 mmol), potassium hydroxide (0.65 g, 11.55 mmol) and potassium cyanide (0.38 g, 5.77 mmol) in dry DMF (17 mL) was added at room temperature the 1-nitronaphthalene (1.0 g, 5.77 mmol). The resulting red mixture was stirred at 50 ºC during 24 h. After this time, the reaction mixture was evaporated under vacuum and residue was refluxed in NaOH 5% for half an hour. The resulting aqueous phase was then extracted with CH_2Cl_2 and the organic phase was dried over sodium sulfate, filtered and the solvent was eliminated under vacuum to yield a black solid. Column chromatography was then performed with 20% ethyl acetate in hexane. A white solid could be obtained by evaporation of the fractions: 665 mg (69% yield). **^{1}H NMR** ($CDCl_3$, 400 MHz): δ ppm 7.81 (d, 1H, *J* = 8.3 Hz), 7.76 (d, 1H, *J* = 8 Hz), 7.59 (t, 1H, *J* = 6.9 Hz), 7.52 (t, 1H, *J* = 7.2 Hz), 7.31 (d, 1H, *J* = 8.6 Hz), 7.17 (d, 1H, *J* = 8.6 Hz), 5.19 (s, 2H, NH_2); **^{13}C NMR** ($CDCl_3$, 400 MHz): δ ppm 148.5, 135.8, 128.9, 128.9, 126.3, 126.2, 121.8, 121.3, 118.9, 118.4, 89.3; **IR**: ν (CN)=2204.63 cm^{-1}; ν (NH_2)=3440.35; 3357.07; 3251.1 cm^{-1}.

2-(Aminomethyl)naphthalen-1-amine (47).

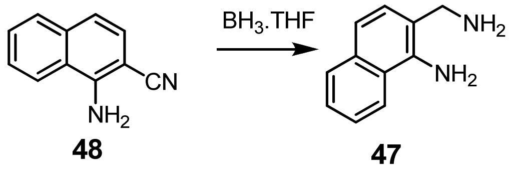

Procedure

To a solution of 1-amino-2-naphthonitrile **48** (546 mg, 3.25 mmol) in dry THF (250 mL) was added at 0 ºC and under argon BH_3.THF solution in a dropwise manner (11.4 mL, 11.4 mmol). The reaction mixture then turned yellow and was brought back at room temperature and then heated to reflux for 24 hours. Methanol was then added dropwise to the mixture at room temperature followed by HCl 1N. The mixture was then refluxed for 30 minutes. Solvent was finally eliminated under vacuum until the obtention of an aqueous phase. The aqueous phase was washed with CH_2Cl_2 and then basified with aqueous ammonia. Further extractions with CH_2Cl_2 were then performed and the gathered organic phases were dried with sodium sulfate, filtered and evaporated under vacuum to yield **47** (543 mg, 97% yield). **^{1}H NMR** ($CDCl_3$, 400 MHz): δ ppm 7.89-7.86 (m, 2H), 7.54-7.48 (m, 2H), 7.34 (d, 1H, $J = 8.3$ Hz), 7.27 (d, 1H, $J = 8.3$ Hz), 5.25 (wide s, NH_2), 4.06 (s, 2H), 1.51 (wide s, NH_2); **^{13}C NMR** ($CDCl_3$, 400 MHz): δ ppm 141.7, 133.9, 128.5, 128.0, 125.5, 124.8, 123.7, 120.6, 119.7, 117.5.

(*R*)-1-((1-Aminonaphthalen-2-yl)methyl)-3-(1-(*tert*-butyldiphenylsilyloxy)-4-(methylthio)butan-2-yl)thiourea (50).

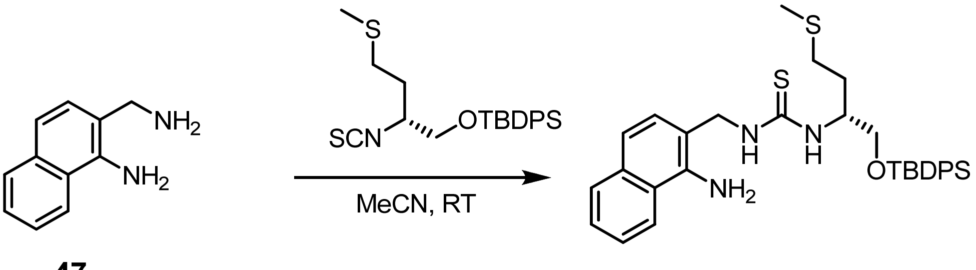

47 **50**

Procedure

To a solution of the O-silylated isothiocyanate derived from methioninol **23** (1.18 g, 2.84 mmol) in acetonitrile (10 mL) and under argon was added the 2-(aminomethyl)naphthalen-1-amine **47** (543 mg, 3.15 mmol) and the resulting mixture was left at room temperature for two days. The solvent was then eliminated thanks to vacuum and crude compound was purified by column chromatography using 10 to 35% Et_2O/Hexane to yield the desired thiourea as a brown oil after evaporation of the fractions: 1.08 g (65% yield). **^{1}H NMR** ($CDCl_3$, 400 MHz): δ ppm 7.75 (d, 2H, $J = 7.4$ Hz), 7.68 (m, 4H), 7.5-7.35 (m, 6H), 7.22-7.13 (m, 2H), 6.80 (s, 1H), 6.39 (s, 1H), 4.81 (m, 3H), 3.80-3.60 (m, 2H), 2.37 (m, 2H), 1.85 (m, 5H), 1.16 (s, 9H); **^{13}C NMR** ($CDCl_3$, 400 MHz): δ ppm 181.3, 135.7, 135.7, 134.2, 132.9, 130.1, 124.5, 128.0, 126.0, 125.1, 123.4, 120.9, 117.7, 114.8, 65.6, 53.7, 46.7, 30.7, 27.1, 19.3, 15.2.

(*R*)-11-((*tert*-Butyldiphenylsilyloxy)methyl)-13-methyl-9,10,11,12-tetrahydro-7*H*-benzo[*h*]pyrimido[2,1-*b*]quinazolin-13-ium chloride (51).

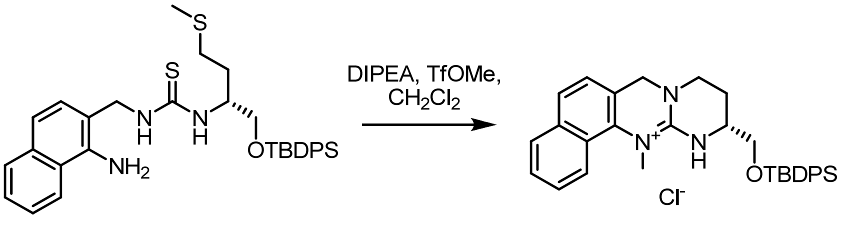
DIPEA, TfOMe,
CH2Cl2
S
N
H
NH2
OTBDPS
N+
Cl-

50 **51**

Procedure

Following the same protocol described for the synthesis of the benzoguanidinium derivative reported in the second chapter of this manuscript on the scale of 1 g of thiourea **50** (1.84 mmol), compound **51** could not be isolated, neither by column chromatography. Compound was however detected on ^{1}H NMR and mass spectra of the reaction crude. **MS** (TOF-ESI$^+$): *m/z* 520.3 [M-Cl]$^+$.

8-Nitroisoquinoline (54).

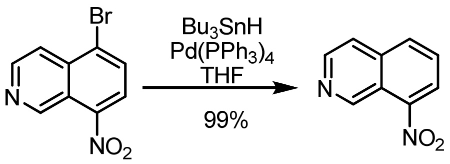
Br
Bu3SnH
Pd(PPh3)4
THF
99%
N
NO2

31 **54**

Procedure

In anhydrous conditions was introduced the Pd(PPh$_3$)$_4$ (40 mg, 35 μmol) catalyst via canula (in 3 mL THF) into a flask containing the 5-bromo-8-nitroisoquinoline **31** (250 mg, 0.99 mmol). Tributyltin hydride (322 μL, 1.2 eq.) was then added and mixture was stirred at 50 ºC for 3 h. The reaction mixture was then poured into water and extraction with diethyl ether was performed. The organic phase was dried with anhydrous sodium sulphate, filtered and solvent eliminated under vacuum. Column chromatography was then performed using 1:1 Hexane/Et$_2$O as elution system, which afforded **54** as a colourless solid (170.2 mg, 99%). **^{1}H NMR** (CDCl$_3$, 400 MHz): δ ppm 9.96 (s, 1H), 8.68 (d, 1H, J = 5.7 Hz), 8.31 (dd, 1H, J = 7.6, 0.8 Hz), 8.10 (d, 1H, J = 8.3 Hz), 7.79-7.72 (m, 2H); **^{13}C NMR** (CDCl$_3$, 100 MHz): δ ppm 148.2, 146.12, 144.4, 136.6, 133.6, 128.8, 125.1, 120.3, 120.1; **HR-MS** (ESI$^+$): *m/z* calc. for $C_9H_7N_2O_2$ 175.0508, obt. 175.0504 [M$^+$].

General procedure for the cyanoamination of nitroisoquinoline derivatives 52 and 45.

To a solution of ethylcyanoacetate (3 eq.) in DMF (0.2 mM in nitroisoquinoline derivative) were successively added potassium hydroxide (2 eq.) and potassium cyanide (1 eq.). The resulting mixture was left at room temperature until complete dissolution of potassium hydroxide. Nitroisoquinoline derivative (1 eq.) was then added and resulting reaction mixture was stirred at room temperature for 24 h. The solvent was then eliminated under vacuum and residue was treated with HCl 1N at reflux for

3 hours. The aqueous phase was then brought back at room temperature and basified with aqueous ammonia to be extracted with dichloromethane. Gathered organic phases were then washed with brine, dried over anhydrous sodium sulfate, filtered and solvent was eliminated under reduced pressure. The crude compound was then purified by column chromatography (Al_2O_3, neutral, $CHCl_3$) which enabled to isolate the following compounds:

2-(8-Nitroisoquinolin-5-yl)acetonitrile (**52** from **31**): 46% yield, **^{1}H NMR** ($CDCl_3$, 400 MHz): δ ppm 10.06 (s, 1H), 8.87 (d, 1H, J = 5.9 Hz), 8.34 (d, 1H, J = 7.8 Hz), 8.00 (d, 1H, J = 7.8 Hz), 7.78 (d, 1H, J = 5.9 Hz), 4.25 (s, 2H); **HR-MS** (ESI$^+$): calc. 214.0572, obt. for $C_{11}H_7N_3O_2$ 214.0612 [$(M+H)^+$].

8-Aminoisoquinoline-7-carbonitrile (45): yield not measured, **^{1}H NMR** ($CDCl_3$, 400 MHz): δ ppm 9.33 (s, 1H), 8.64 (d, 1H, J = 5.6 Hz), 7.60 (d, 1H, J = 5.6 Hz), 7.55 (d, 1H, J = 8.6 Hz), 7.17 (d, 1H, J = 8.6 Hz), 5.40 (s, 2H, NHs).

***N-tert*-Butylcarboxyguanidine (55).**

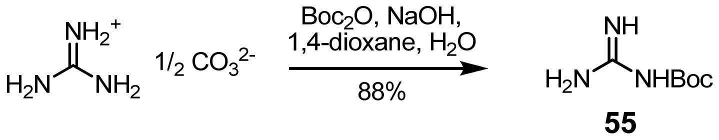

Procedure

To a suspension of guanidinium carbonate (7.10 g, 39.4 mmol) in 1,4 dioxane (80 mL) was added at room temperature a solution of sodium hydroxide 4M (40 mL) and mixture was left till complete dissolution. Di-*tert*-butyl dicarbonate (6.89 g, 31.5 mmol) was then added to the reaction mixture and resulting translucid reaction mixture was stirred at room temperature for 21 hours. The mixture was then evaporated under vacuum at 60 ºC and residue was triturated with water, unsoluble white solid was then filtered and dried under vacuum to yield the desired protected guanidine (4,43 g, 88% yield). **^{1}H NMR** (MeOD, 400 MHz): δ ppm 1.44 (s, 9H, *tert*-butyl), **^{13}C NMR** (DMSO, 75.5 MHz): δ ppm 163.2, 162.7, 75.5, 28.2; **MS** (ESI^{+}): *m/z* 160 [M+H]$^{+}$.

N-(Amino(*tert*-butoxycarbonylamino)methylene)nicotinamide (56).

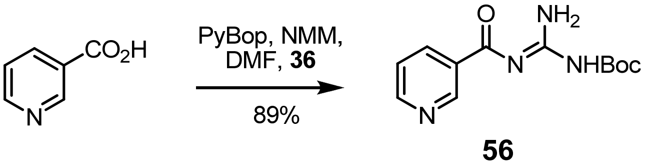

56

Procedure

To a solution of nicotinic acid (150 mg, 1.22 mmol), *N*-methylmorpholine (147 µL, 1.34 mmol, 1.1 eq) and Boc-guanidine **55** (194 mg, 1.22 mmol) in dry DMF (3 mL) was added at room temperature a solution of PyBop® (634 mg, 1.22 mmol) and *N*-methylmorpholine (147 µL, 1.34 mmol, 1.1 eq) in dry DMF (3 mL). After one day of reaction, water was added dropwise to the mixture (18 mL) and a white solid precipitated. Solid was filtered and dried *in vacuo* to yield the desired protected carboxyguanidine **56** (279 mg, 89% yield). **^{1}H NMR** (DMSO, 400 MHz): δ ppm 10.95 (s, 1H, NH), 9.67 (s, 1H, NH), 9.24 (s, 1H, NH), 8.68 (broad s, 2H), 8.35 (s, 1H), 7.48 (s, 1H), 1.5 (s, 9H, CH_3); **HR-MS** (ESI$^+$): *m/z* calc. for $C_{12}H_{17}N_4O_3$ 265.1301, obt. 265.1310 $[M+H]^+$.

3-(Guanidiniocarbonyl)-pyridine chloride (21c (Cl$^-$)).

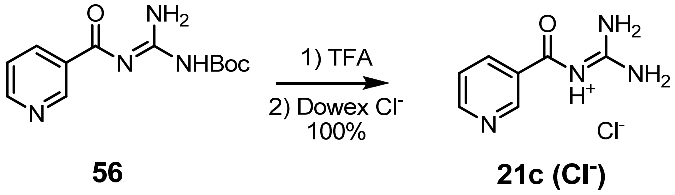

Procedure

A solution of **56** (150 mg, 0.57 mmol) in trifluoroacetic acid (11 mL) was stirred 20 minutes at room temperature, time after which excess TFA was removed by evaporation under vacuum. The residue was then triturated in THF and resulting white solid was isolated by filtration. The solid was dissolved in methanol and passed through an anion exchange resin for chloride (1:1 H_2O:MeOH was used for elution). Elimination of the solvents *in vacuo* enabled to isolate quantitatively **21c (Cl$^-$)** as a white solid. **21c (PF$_6^-$)** could be isolated by addition of stoichiometric amount of silver hexafluorophosphate to a methanol solution of **21c (Cl$^-$)** and filtration of precipitated silver chloride. Alternatively, **21c (picrate)$_2$** could be isolated by addition of a 1% picric acid solution to a 1:1 H_2O:MeOH solution of the white solid obtained after trituration in THF, which enabled the obtention of crystals (Fig. 4.16). **^{1}H NMR** (DMSO, 400 MHz): δ ppm 11.42 (s, 1H, NH), 9.10 (d, 1H, *J* = 1.9 Hz), 8.90 (dd, 1H, *J* = 4.9, 1.5 Hz), 8.60 (s, 4H, picrate), 8.37 (wide s, NH_2), 8.32 (td, 1H, *J* = 8.1, 1.9 Hz), 8.24 (wide s, NH_2), 7.72 (dd, 1H, *J* = 8, 5.2 Hz). This set of signals was similar for each studied anion except for the picrate peaks.

General procedure for the preparation of dipyrromethanes: example for 2,2'-((2-nitrophenyl)methylene)bis(1*H*-pyrrole) (57).

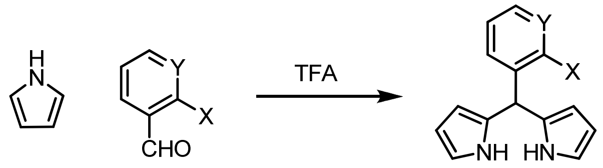

$X = NO_2$, Y = CH
X = Cl, Y = CH
X = Cl, Y = N

57 $X = NO_2$, Y = CH
58 X = Cl, Y = CH
59 X = Cl, Y = N

Procedure

Under argon and at room temperature was first degased a solution of *o*-nitrobenzaldehyde (3.0 g, 19.85 mmol) in pyrrole (35 mL) and trifluoroacetic acid (0.196 mL, 1.98 mmol) was then added. The resulting mixture was then protected from light and stirred under argon for 5 minutes. Then NaOH 0.1 N (50 mL) was added to quench the reaction followed by AcOEt. The organic layer was then washed with water and then dried with anhydrous sodium sulfate, filtered and solvent was eliminated under vacuum. The crude compound was then purified by column chromatography using hexane/ether as elution system (from 0% to 30%; gradient may vary depending on the used aldehyde) to isolate the desired compound (3.84 g, 72% yield, red oil).

2,2'-[(2-Nitrophenyl)methylene]bis(1*H*-pyrrole) (57).

Yield: 72%. ^{1}**H NMR** ($CDCl_3$, 400 MHz): δ ppm 8.13 (wide s, 2H, NH), 7.91 (dd, 1H, *J* = 8.1, 1.4 Hz), 7.54 (td, 1H, *J* = 7.6, 1.4 Hz), 7.41 (td, 1H, *J* = 8.1, 1.4 Hz), 7.30 (dd, 1H, *J* = 7.9, 1.4 Hz), 6.73-6.70 (m, 2H), 6.22 (s, 1H), 6.19 (dd, 2H, *J* = 5.9, 2.8 Hz), 5.91-5.89 (m, 2H); ^{13}**C NMR** ($CDCl_3$, 100 MHz): δ ppm 148.8, 137.3, 133.1, 131.0, 130.9, 127.9, 124.6, 117.8, 108.62, 107.5, 39.0; **MS** (ESI$^+$): *m/z* 290.1 [M+Na]$^+$.

2,2'-[(2-Chlorophenyl)methylene]bis(1*H*-pyrrole) (58).

Yield: 94%. ^{1}**H NMR** ($CDCl_3$, 400 MHz): δ ppm 7.96 (wide s, 2H, NH), 7.45-7.42 (m, 1H), 7.26-7.22 (m, 2H), 7.15-7.12 (m, 1H), 6.72 (dd, 2H, *J* = 3.9, 2.4 Hz), 6.23-6.19 (m, 2H), 5.94-5.92 (m, 3H); ^{13}**C NMR** ($CDCl_3$, 100 MHz): δ ppm 140.1, 133.7, 131.3, 129.8, 129.7, 128.2, 127.1, 117.4, 108.6, 107.5, 40.8; **HR-MS** (ESI$^+$): *m/z* calc. for $C_{15}H_{14}N_2Cl$ 257.0846, obt. 257.0857 [M+H]$^+$.

2-Chloro-3-[di(1*H*-pyrrol-2-yl)methyl]pyridine (59).

Yield: 84%. ^{1}**H NMR** ($CDCl_3$, 400 MHz): δ ppm 8.29 (dd, 1H, *J* = 4.8, 1.9 Hz), 8.20 (broad s, 2H, NH), 7.44 (dd, 1H, *J* = 7.6, 1.8 Hz), 7.20 (dd, 1H, *J* = 7.9, 5.1 Hz), 6.80-6.70 (m, 2H, pyrrolic H), 6.19 (dd, 2H, *J* = 6.1, 2.9 Hz), 5.88-5.84 (m, 3H); ^{13}**C NMR** ($CDCl_3$, 100 MHz): δ ppm 150.6, 147.7, 139.2, 137.6, 130.5, 123.3, 118.1, 108.2, 107.9, 40.7; **MS** (ESI$^+$): *m/z* calc. 258.1, obt. 258.1 [M+H]$^+$, calc. 280.1, obt. 280.1 [M+Na]$^+$, calc. 296.0, obt. 296.1 [M+K]$^+$.

General procedure for the oxidation of dipyrromethanes to dipyrromethenes: example for 2-[(2-nitrophenyl)(2*H*-pyrrol-2-ylidene)methyl]-1*H*-pyrrole (60).

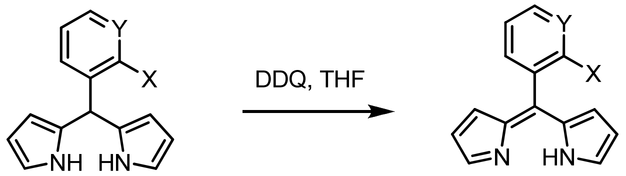

57 X = NO_2, Y = CH
58 X = Cl, Y = CH
59 X = Cl, Y = N

60 X = NO_2, Y = CH
61 X = Cl, Y = CH
62 X = Cl, Y = N

Procedure

To a solution of dipyrromethane **57** (2.45 g, 9.19 mmol) in dry THF (30 mL) was added in a dropwise fashion a solution of DDQ (2.09 g, 9.19 mmol) in dry THF (30 mL). The reaction mixture was then stirred one hour at room temperature and was then poured into water. Extraction was then performed with CH_2Cl_2. The organic phase was dried with anhydrous sodium sulfate, filtered and solvent was eliminated under vacuum. Column chromatography was then performed using neat CH_2Cl_2 as elution system to isolate the dipyrromethene **60** (1.48 g, 61% yield).

2-[(2-Nitrophenyl)(2*H*-pyrrol-2-ylidene)methyl]-1*H*-pyrrole (60).

Yield: 61%. **^{1}H NMR** ($CDCl_3$, 400 MHz): δ ppm 12.13 (wide s, 1H), 8.15 (dd, 1H, J = 7.9, 1.3 Hz), 7.73-7.62 (m, 4H), 7.55 (dd, 1H, J = 7.4, 1.6 Hz), 6.42-6.37 (m, 4H); **^{13}C NMR** ($CDCl_3$, 100 MHz): δ ppm 149.5, 144.3, 140.1, 136.7, 133.0, 132.5, 132.0, 129.9, 126.8, 124.5, 118.4; **HR-MS** (ESI$^+$): *m/z* calc. for $C_{15}H_{12}N_3O_2$ 266.093, obt. 266.0922 [(M+H)$^+$].

2-[(2-Chlorophenyl)(2H-pyrrol-2-ylidene)methyl]-1*H*-pyrrole (61).
Yield: 23%. ^{1}**H NMR** ($CDCl_3$, 400 MHz): δ ppm 7.66 (t, 2H, *J* = 1.1 Hz), 7.54-7.50 (m, 1H), 7.46-7.40 (m, 2H), 7.39-7.34 (m, 1H), 6.44 (dd, 2H, *J* = 4.2, 1.0 Hz), 6.39 (dd, 2H, *J* = 4.2, 1.4 Hz); ^{13}**C NMR** ($CDCl_3$, 100 MHz): δ ppm 141.1, 140.7, 137.8, 136.0, 133.9, 131.8, 129.8, 129.5, 127.9, 118.0.

3-[(1*H*-Pyrrol-2-yl)(2*H*-pyrrol-2-ylidene)methyl]-2-chloropyridine (62).
Yield: 30%. ^{1}**H NMR** ($CDCl_3$, 400 MHz): δ ppm 8.53 (dd, 1H, *J* = 4.8, 1.9 Hz), 7.74 (dd, 1H, *J* = 7.5, 1.9 Hz), 7.66 (s, 2H), 7.37 (dd, 1H, *J* = 7.4, 4.8 Hz), 6.41-6.38 (m, 4H), ^{13}**C NMR** ($CDCl_3$, 100 MHz): δ ppm 149.9, 144.7, 140.4, 135.1, 132.5, 127.5,121.7, 118.5, 117.8.

5,5-Difluoro-10-(2-nitrophenyl)-5*H*-dipyrrolo[1,2-*c*:1',2'-*f*][1,3,2] diazaborinin-4-ium-5-uide (64).

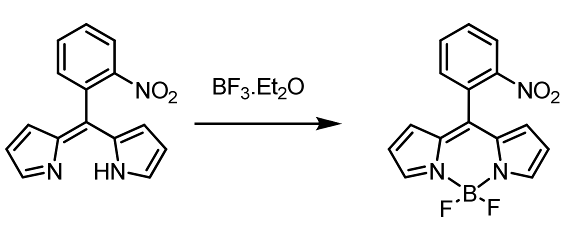

Procedure

To a solution of the dipyrromethene **60** (871 mg, 3.28 mmol) in dry CH_2Cl_2

(20 mL) was first added the triethylamine (2.74 mL, 19.70 mmol) followed by the 1.0 M solution of boron trifluoride etherate (26.26 mL, 26.26 mmol). The reaction mixture was then stirred 1 day at room temperature and under argon. The organic phase was then washed three times with saturated sodium hydrogen carbonate after neutralization with $NaHCO_3$ sat. in an erlenmeyer. The solvent was then eliminated under vacuum and the residue was adsorbed on silica. Compound was purified by silica gel column chormatography using 80% DCM/Hexane as elution system. Compound **64** was obtained as red crystals (882 mg, 86% yield). **^{1}H NMR** ($CDCl_3$, 400 MHz): δ ppm 8.23 (d, 1H, *J* = 6.0 Hz), 7.96 (s, 2H), 7.82-7.75 (m, 2H), 7.58 (dd, 1H, *J* = 5.9, 1.0 Hz), 6.68 (d, 2H, *J* = 3.1 Hz), 6.52 (d, 2H, *J* = 2.9 Hz); **^{13}C NMR** ($CDCl_3$, 100 MHz): δ ppm 145.2, 142.6, 134.6, 133.1, 132.3, 132.2, 131.2, 129.7, 128.3, 125.1, 119.2; **MS** (ESI$^+$): *m/z* calc. for $C_{15}H_{10}N_3O_2NaBF_2$ 336.0732, obt. 336.0723 [$(M+Na)^+$]; **X-ray** Crystals were grown in $CDCl_3$ (see Fig. 4.18).

Sodium 2,2-diethoxyacetate (70).

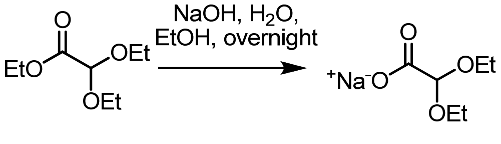

70

Procedure

To a solution of ethyl diethoxyacetate (20.3 mL, 114 mmol) in ethanol (50 mL) was added a solution of sodium hydroxide (4.56 g, 114 mmol) in water

(25 mL), and the resulting mixture was heated at reflux for 5 hours. The mixture was evaporated to dryness, and the residue dried in vacuum to give a white solid (quantitative yield). Compound **70** was stored in the dry box. ^{1}**H NMR** (D_2O, 400 MHz): δ ppm 3.62-3.52 (m, 4H), 1.15 (t, 6H, J = 8.0 Hz) (one proton missing, probably overlapping with solvent signal), ^{13}**C NMR** (D_2O, 100 MHz): δ ppm 174.5, 99.2, 62.6, 14.3.

***N*-Benzyl-2,2-diethoxyacetamide derivatives (71) and (73).**

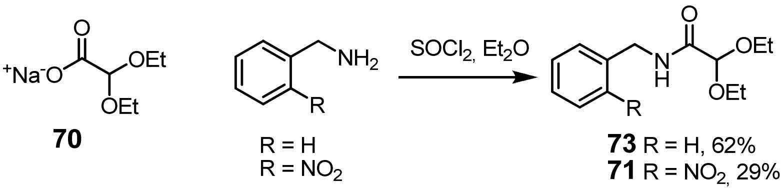

Procedure

To a suspension of sodium diethoxyacetate (1 eq.) in dry diethyl ether (1.2 M solution) placed at 0 ºC was added some thionyl chloride (1 eq.) and mixture was brought to reflux for 30 min under argon. Once back at room temperature, a solution of the benzylamine derivative (1 eq.) in dry toluene and distilled pyridine (3 parts of toluene for 2 parts of pyridine, 1.2 M solution of benzylamine in the mixture of solvents) was added via canula under argon and with vigorous stirring. The reaction mixture was then further refluxed for 30 minutes under argon. The crude mixture was then poured into crushed ice and aqueous phase was further extracted with toluene. The gathered organic phases were then washed with HCl 2% and brine. The solvent was then eliminated under vacuum and resulting yellow oil was purified by column chromatography using from 10% AcOEt/Hexane to 25% AcOEt/Hexane as elution system.

***N*-Benzyl-2,2-diethoxyacetamide (73):** yield: 62%. **^{1}H NMR** (CDCl$_3$, 400 MHz): δ ppm 7.41-7.25 (m, 5H), 6.92 (s, 1H, NH), 4.50 (d, 2H, *J* = 5.2 Hz), 3.77-3.57 (m, 4H), 1.25-1.05 (m, 6H); **^{13}C NMR** (CDCl$_3$, 100 MHz): δ ppm 167.8, 137.9, 128.7, 127.8, 127.5, 98.5, 62.6, 43.0, 15.1; **HR-MS** (TOF-ESI$^+$): *m/z* calc. for $C_{13}H_{20}NO_3$ 238.1443, obt. 238.1445 [(M+H)$^+$].

2,2-Diethoxy-*N*-(2-nitrobenzyl)acetamide (71): yield: 29%. **^{1}H NMR** (CDCl$_3$, 400 MHz): δ ppm 8.05-7.90 (m, 1H), 7.65-7.50 (m, 2H), 7.45-7.30 (m, 2H), 4.70-4.60 (m, 2H), 3.65-3.45 (m, 4H), 1.25-1.05 (m, 6H); **^{13}C NMR** (CDCl$_3$, 100 MHz) δ ppm: 168.2, 134.0, 133.3, 128.7, 125.0, 98.5, 62.6, 40.5, 15.0; **HR-MS** (ESI$^+$): *m/z* calc. for $C_{13}H_{18}N_2O_5Na$ 305.113, obt. 305.1109 [M$^+$].

3-Hydroxyisoquinoline (74).

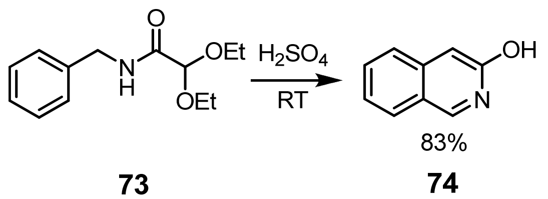

Procedure

Sulfuric acid (10 mL) was cautiously added at 0 ºC to **73** (2.69 g, 11.36 mmol) while stirring. The resulting mixture was stirred overnight at room temperature. It was then poured into cracked ice and resulting aqueous phase was filtered, then basified with ammonium hydroxide and extracted with dichloromethane. The gathered organic phases were washed with brine, dried over sodium sulfate and the solvent was eliminated under vacuum. A yellow solid was isolated (1.37 g, 83% yield). **^{1}H NMR** ($CDCl_3$, 400 MHz): δ ppm 8.70 (s, 1H), 7.77 (d, 1H, J = 8.2 Hz), 7.60 (d, 1H, J = 8.2 Hz), 7.55-7.50 (m, 1H), 7.26 (d, 1H, J = 7.6 Hz), 7.00 (s, 1H); **^{13}C NMR** ($CDCl_3$, 100 MHz): δ ppm 161.8, 146.1, 141.4, 131.4, 128.0, 125.4, 123.7, 122.6, 104.3; **HR-MS** (TOF-ESI$^+$): *m/z* calc. for C_9H_8NO 146.0606, obt. 146.0604 [$(M+H)^+$].

Isoquinolin-3-yl trifluoromethanesulfonate (75).

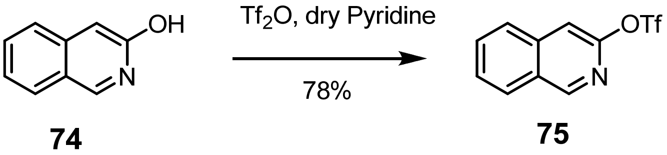

Procedure

To a solution of the 3-hydroxyisoquinoline **74** (1.37 g, 9.44 mmol) in dry pyridine (65 mL) cooled at 0 ºC was added trifluoromethane sulfonic anhydride (2.04 mL, 12.28 mmol). The mixture was then brought back at room temperature and stirred overnight. The solvent was then eliminated thanks to vacuum and residue adsorbed on silica gel. Column chromatography was then performed with 0-5% diethyl ether/hexane to yield **75** as a translucid oil (2.05 g, 78% yield). **^{1}H NMR** ($CDCl_3$, 400 MHz): δ ppm 9.10 (s, 1H), 8.08 (d, 1H, J = 8.2 Hz), 7.93 (d, 1H, J = 8.2

Hz), 7.82 (td, 1H, *J* = 5.0, 1.0 Hz), 7.72 (td, 1H, *J* = 7.5, 0.9 Hz), 7.60 (s, 1H); **^{13}C NMR** (CDCl$_3$, 100 MHz): δ ppm 152.3, 153.1, 138.4, 131.9, 128.6, 128.4, 127.9, 126.9, 110.9; **HR-MS** (TOF-ESI$^+$): *m/z* calc. for $C_{10}H_7NO_3SF_3$ 278.099, obt. 278.012 [M$^+$].

3-(Pyridin-2-yl)isoquinoline (76).

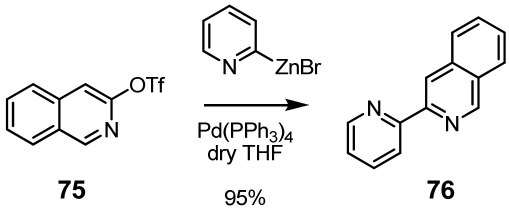

Procedure

A solution of the triflate isoquinoline derivative **75** (1.23 g, 4.45 mmol) in dry THF (20 mL) was degased with argon at room temperature. 2-Pyridylzinc bromide derivative (13.36 mL of 0.5 M THF commercial solution, 6.68 mmol) was then added via syringe followed by a THF (5 mL) solution of Pd(PPh$_3$)$_4$ (257 mg, 0.22 mmol) via canula. The reaction mixture was further bubbled with argon and then heated to reflux overnight. The resulting precipitate was then filtered, dried and dissolved in sulfuric acid with addition of crushed ice. The obtained solution was poured into more crushed ice and basified with ammonium hydroxide. The resulting aqueous phase was then extracted with dichloromethane and the gathered organic phases were washed with brine, dried over sodium sulfate, filtered and the solvent was eliminated under vacuum to yield **76** as a reddish solid (874 mg, 95% yield). **^{1}H NMR** (CDCl$_3$, 400 MHz): δ ppm 9.22 (s, 1H),

8.70 (s, 1H), 8.66 (d, 1H, *J* = 4.2 Hz), 8.44 (d, 1H, *J* = 8.0 Hz), 7.84 (dd, 2H, *J* = 8.0, 4.6 Hz), 7.73 (td, 1H, *J* = 7.7, 1.7 Hz), 7.56 (t, 1H, *J* = 6.9 Hz), 7.45 (t, 1H, *J* = 7.4 Hz), 7.18 (dd, 1H, *J* = 6.6, 4.8 Hz); **^{13}C NMR** ($CDCl_3$, 100 MHz): δ ppm 156.3, 152.0, 146.9, 149.3, 137.0, 136.5, 130.5, 128.7, 127.6, 127.6, 127.4, 123.4, 121.3, 117.8; **HR-MS** (TOF-ESI$^+$): *m/z* calc. for $C_{14}H_{11}N_2$ 207.0922, obt. 207.0915 $[M+H]^+$.

_N_-CbZ-Guanidine (83).

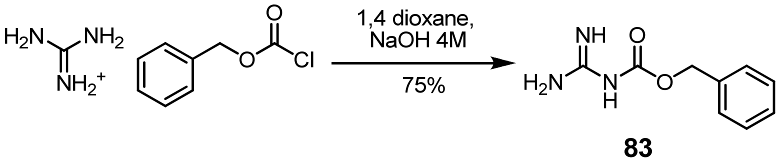

83

Procedure

To a suspension of guanidinium carbonate (7.89 g, 43.8 mmol) in 1,4 dioxane (90 mL) was added at room temperature a solution of sodium hydroxide 4 M (60 mL) and mixture was left until complete dissolution. Benzyl chloroformate (5 mL, 35 mmol) was then added to the reaction mixture and resulting reaction mixture was stirred at room temperature for 21 hours. The mixture was then evaporated under vacuum at 60 ºC and the residue was triturated with water, unsoluble white solid was then filtered and dried under vacuum (5.10 g, 75% yield). **^{1}H NMR** (MeOD, 400 MHz): δ ppm 7.50-7.28 (m, 5H), 5.44-5.17 (m, 4H), 5.13 (s, 2H); **^{13}C NMR** (MeOD, 100 MHz): δ ppm 163.6, 163.3, 137.5, 128.1, 127.4, 65.9.

N-Boc-*N'*-Cbz-Guanidine (84).

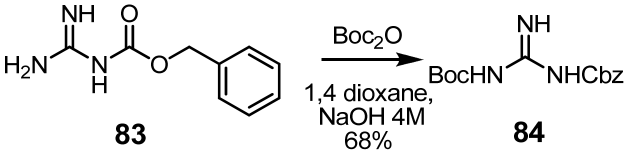

Procedure

A solution of di-*tert*-butyl dicarbonate (2.93 g, 13.42 mmol) in acetone (10 mL) was added at room temperature to a solution of *N*-Cbz-guanidine **83** (2.88 g, 14.91 mmol) and triethylamine (2.07 mL, 14.91 mmol) in acetone (30 mL). The resulting mixture was stirred at room temperature for 48 hours. The solvent was then eliminated under vacuum and residue was reparted between AcOEt (200 mL) and water. The organic layer was washed with 2 M $NaHSO_4$, water and brine. The solvent was then eliminated under vacuum after drying with anhydrous sodium sulfate and filtration (2.66 g, 68% yield). **^{1}H NMR** ($CDCl_3$, 400 MHz): δ ppm 8.86 (wide s, 3H, NHs), 7.37-7.25 (m, 5H, H_{Ar}), 5.10 (s, 2H, CH_2Ph), 1.44 (s, 9H); **^{13}C NMR** ($CDCl_3$, 100 MHz): δ ppm 161.9, 159.1, 154.4, 136.4, 128.4, 127.9, 127.8, 82.8, 66.9, 27.9.

N-Boc-*N'*-Cbz-*N"*-Triflylguanidine (85).

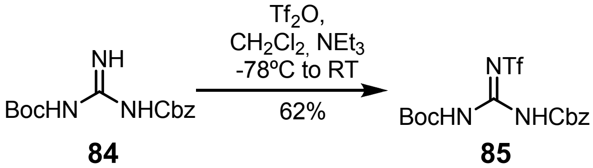

Procedure

A solution of *N*-Cbz-*N*'-Boc-guanidine **84** (1.51 g, 5.14 mmol) and triethylamine (1.07 mL) in dry DCM (50 mL) was placed under argon and cooled at -78 ºC. Triflic anhydride (1.08 mL, 6.42 mmol) was then added in such a way that cold temperature could be maintained. The reaction mixture was then brought back slowly to room temperature along 4 hours. After this time, the mixture was poured into a separation funnel and washed with 2 M $NaHSO_4$, water, and was finally dried with Na_2SO_4. The solvent was eliminated under vacuum. Column chromatography was then performed on silica gel using 75% DCM/Hexane as elution system to yield a white solid after fractions evaporation (1.36 g, 62% yield). **^{1}H NMR** ($CDCl_3$, 400 MHz): δ ppm 10.60 (s, 1H, NH), 9.89 (s, 1H, NH), 7.41 (s, 5H, H_{Ar}), 5.27 (s, 2H, CH_2Ph), 1.55 (s, 9H), **^{13}C NMR** ($CDCl_3$, 100 MHz): δ ppm 151.3, 149.5, 134.0, 129.1, 128.8, 120.9, 117.7, 86.8, 69.4, 27.9.

N-Boc-*N'*-Cbz-*N"*-Octylguanidine (86).

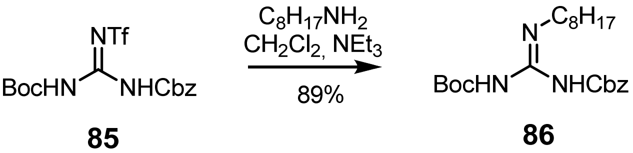

Procedure

Octylamine (0.34 mL, 2.07 mmol) was added to a solution of guanydilating agent **85** (0.80 g, 1.88 mmol) and triethylamine (0.29 mL, 2.07 mmol) in dry DCM (8 mL). The resulting mixture was stirred at room temperature. After one hour, mixture was diluted with DCM and washed with sodium bisulfate 2 M, saturated sodium carbonate and brine. The organic layer was dried with anhydrous sodium sulfate, filtered and evaporated under vacuum. Residue was then purified by column chromatography (silica gel, DCM) to yield a translucid oil (676 mg, 89% yield). **^{1}H NMR** ($CDCl_3$, 400 MHz): δ ppm 8.40 (s, 1H, NH), 7.41 (t, 2H, J = 7.2 Hz), 7.36 (t, 2H, J = 7 Hz), 7.29 (d, 1H, J = 7.1 Hz), 5.16 (s, 2H, CH_2Ph), 3.43 (dd, 2H, J = 12.6, 7.1 Hz),1.68-1.54 (m, 2H), 1.50 (s, 9H), 1.40-1.20 (m, 10H), 0.93-0.86 (m, 3H); **^{13}C NMR** ($CDCl_3$, 100 MHz): δ ppm 163.7, 156.4, 153.2, 137.1, 128.7, 128.5, 128.4, 128.0, 127.8, 83.2, 67.0, 41.1, 31.8, 29.2, 29.1, 28.9, 28.3, 28.0, 26.8, 14.1.

***N*-Boc-*N'*-Octylguanidine (87).**

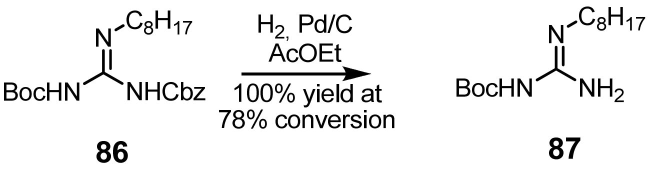

Procedure

A solution of *N*-octyl-*N'*-Boc-*N''*-Cbz-guanidine **86** (658 mg, 1.62 mmol) and 10% palladium over carbon (17 mg, 0.016 mmol) in ethyl acetate (20 mL) was placed at room temperature under an atmosphere of hydrogen by the mean of vacuum/hydrogen cycles. The resulting mixture was stirred at room temperature for 40 hours (75% conversion as seen on NMR spectrum of the crude). Column chromatography was then performed using CH_2Cl_2 to 2% MeOH/AcOEt as elution systems. After evaporation of the fractions, a translucid oil that crystallized with time was obtained (344 mg, 78%

yield). ^{1}**H NMR** ($CDCl_3$, 400 MHz): δ ppm 3.11 (t, 2H, J = 7.1 Hz), 1.65-1.54 (m, 2H), 1.47 (s, 9H), 1.40-1.20 (m, 10H), 0.93-0.83 (m, 3H); ^{13}**C NMR** ($CDCl_3$, 100 MHz): δ ppm 163.7, 161.4, 78.0, 41.3, 31.7, 29.0, 28.4, 26.8, 22.6, 14.0.

5-Methyl-2,2'-bipyridine (82).

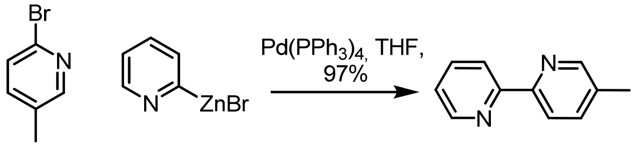

82

Procedure

To a solution of 2-bromo-5-methyl pyridine (1.05 g, 6.10 mmol) in dry THF (25 mL) placed under argon was added at room temperature the $Pd(PPh_3)_4$ (352 mg, 0.30 mmol) followed by the commercial 0.5M 2-pyridylzinc bromide solution (18.3 mL, 9.10 mmol). The reaction mixture was then refluxed for 24 hours. Once back at room temperature, obtained precipitate was filtered and dissolved in H_2SO_4 and crushed ice. The resulting aqueous phase (after dilution) was then basified with ammonia and extracted with dichloromethane (4 times). The organic layers were washed with brine, dried over sodium sulfate, filtered and solvent was eliminated thanks to vacuum to yield **82** as a red oil (996 mg, 96% yield). ^{1}**H NMR** ($CDCl_3$, 400 MHz): δ ppm 8.70-8.65 (m, 1H), 8.54-8.50 (m, 1H), 8.37 (d, 1H, J = 8.0 Hz), 8.30 (d, 1H, J = 8.0 Hz), 7.80 (td, 1H, J = 7.7, 1.8 Hz), 7.64 (dd, 1H, J = 8.0, 1.6 Hz), 7.29 (ddd, 1H, J = 7.4, 4.8, 1.1 Hz), 2.40 (s, 3H); ^{13}**C NMR** ($CDCl_3$, 100 MHz): δ ppm 156.2, 153.6, 149.6, 149.1, 137.5, 136.9, 133.5, 123.4, 120.9, 120.7, 18.4.

5-Carboxylic acid-2,2’-bipyridine (81).

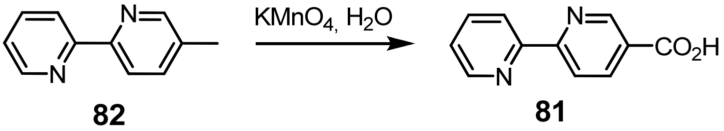

Procedure

A suspension of 5-methyl-2,2’-bipyridine (869 mg, 5.10 mmol) in water (10 mL) was heated to 70 ºC and potassium permanganate (1.61 g, 10.21 mmol) was added in portions during 2 hours. A second portion of $KMnO_4$ (1.61 g, 10.21 mmol) was then added the same way at 90 ºC during 3 hours. The reaction mixture was left one further hour at 90 ºC and precipitated MnO_2 was removed by filtration. The filtered solid was washed with hot water and the resulting gathered filtrates were concentrated *in vacuo* and slowly acidified to pH 4 with HCl 25% (dropwise addition at 0 ºC). The resulting suspension was finally placed in the freezer overnight. The white solid was then filtered and dried to yield the carboxylic acid derivative (573 mg, 56% yield). **^{1}H NMR** (DMSO, 400 MHz): δ ppm 13.44 (s, 1H, CO_2H), 9.16 (d, 1H, J = 1.4 Hz), 8.73 (dd, 1H, J =4.7, 0.7 Hz), 8.50 (dd, 1H, J = 8.3, 0.4 Hz), 8.45 (d, 1H, J = 7.9 Hz), 8.40 (dd, 1H, J = 8.2, 2.1 Hz), 7.98 (td, 1H, J = 7.7, 1.7 Hz), 7.50 (ddd, 1H, J = 7.4, 4.8, 1.0 Hz); **^{13}C NMR** (DMSO, 100 MHz): δ ppm 166.6, 158.6, 154.5, 150.6, 149.8, 138.7, 127.1, 125.7, 125.4, 121.9, 120.8.

General procedure for peptidic coupling between carboxylic acid bipyridine derivative and Boc protected guanidines (example for Boc 24a)

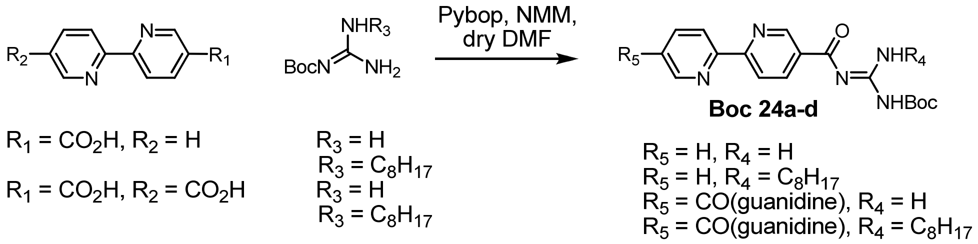
R2
R1
N
NHR3
BocN
NH2
Pybop, NMM, dry DMF
R5
O
NHR4
NHBoc
Boc 24a-d
R1 = CO2H, R2 = H
R1 = CO2H, R2 = CO2H
R3 = H
R3 = C8H17
R3 = H
R3 = C8H17
R5 = H, R4 = H
R5 = H, R4 = C8H17
R5 = CO(guanidine), R4 = H
R5 = CO(guanidine), R4 = C8H17

Procedure

To a solution of 5-carboxylic acid-2,2'-bipyridine **81** (214 mg, 1.07 mmol), Boc guanidine (170 mg, 1.07 mmol) and *N*-methylmorpholine (129 μL, 1.18 mmol) in dry DMF (2.5 mL) was added another solution of PyBOP® (556 mg, 1.07 mmol) and *N*-methylmorpholine (129 μL, 1.18 mmol) in dry DMF (2.5 mL). Resulting mixture was then stirred at room temperature for one day. After one day at room temperature, mixture was poured dropwise into 80 mL of water and a white precipitate formed. It was then filtered and dried under vacuum to yield **Boc 24a** as a white solid (310 mg, 85% yield). **^{1}H NMR** ($CDCl_3$, 400 MHz): δ ppm 9.72 (broad s, 2H), 9.43 (s, 1H), 8.70 (m, 2H), 8.57-8.37 (m, 3H), 7.88-7.76 (m, 1H), 7.39-7.29 (m, 1H), 1.36 (s, 9H); **^{13}C NMR** ($CDCl_3$, 100 MHz): δ ppm 177.1, 159.7, 158.4, 155.5, 153.3, 150.5, 149.4, 137.6, 137.0, 132.6, 124.2, 121.8, 120.5, 83.7, 28.0; **HR-MS** (TOF-ESI$^+$): *m/z* calc. for $C_{17}H_{20}N_5O_3$ 342.1566, obt. 342.155 $[M^+]$.

Boc 24b.

At the end of the reaction, the solvent was eliminated under vacuum and residue was reparted between water and 1:2 Et_2O/CH_2Cl_2. Organic phase was extensively washed with water, dried with anhydrous sodium sulfate and solvents were eliminated *in vacuo*. Column chromatography was then performed with AcOEt as elution system to yield **Boc 24b** as an oil that solidified upon standing (76% yield). **^{1}H NMR** ($CDCl_3$, 400 MHz): δ ppm 12.38 (s, 1H), 9.49 (t, 1H, J = 1.4 Hz), 8.70 (d, 1H, J = 4.7 Hz), 8.64 (t, 1H, J = 4.6 Hz), 8.55 (dd, 1H, J = 8.3, 2.1 Hz), 8.47 (d, 1H, J = 3.7 Hz), 8.45 (d, 1H, J = 4.0 Hz), 7.83 (td, 1H, J = 7.8, 1.8 Hz), 7.33 (ddd, 1H, J = 7.4, 4.8, 1.1 Hz), 3.61 (dd, 2H, J = 12.9, 7.1 Hz), 1.75-1.83 (m, 2H), 1.53 (s, 9H), 1.44-1.22 (m, 10H), 0.92-0.86 (m, 3H).

Boc 24c.

Yield: 67%; **^{1}H NMR** (DMSO, 400 MHz): δ ppm 10.99 (s, 2H, NH), 9.71 (s, 2H, NH), 9.34 (s, 2H), 8.69 (s, 2H, NH), 8.52 (s, 4H), 1.50 (s, 18H); **HR-MS** (TOF-ESI$^+$): *m/z* calc. for $C_{24}H_{30}N_8O_6Na$ 549.2186, obt. 549.2188 [M$^+$].

Boc 24d.

Yield: 78%. **^{1}H NMR** ($CDCl_3$, 400 MHz): δ ppm 9.52 (d, 2H, J = 1.3 Hz), 8.66 (t, 2H, J = 5.2 Hz), 8.58 (dd, 2H, J = 8.2, 1.9 Hz), 8.53 (d, 2H, J = 8.2 Hz), 3.63 (dd, 4H, J = 12.9, 7.0 Hz), 1.76-1.65 (m, 4H), 1.53 (s, 18H), 1.48-1.23 (m, 20 H), 0.96-0.83 (m, 6H), **^{13}C NMR** ($CDCl_3$, 100 MHz): δ ppm 175.8, 157.6, 156.7, 153.5, 151.0, 137.7, 133.4, 120.9, 83.4, 41.5, 31.8, 29.3, 29.2, 28.1, 27.0, 22.6, 14.1.

General procedure for the preparation of 24a-d (example for the preparation of 24a).

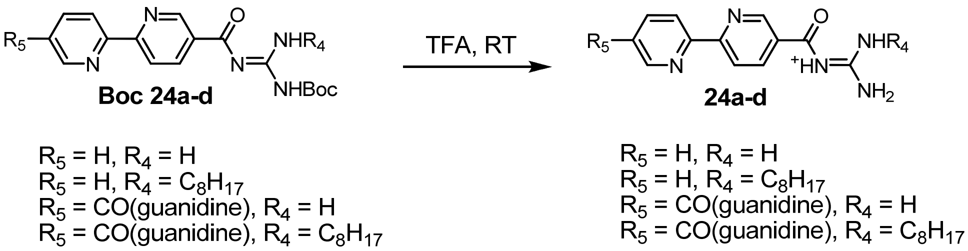
R5
N
O
NHR4
N
N
Boc 24a-d
NHBoc
TFA, RT
R5
N
O
NHR4
N
+HN
24a-d
NH2
R5 = H, R4 = H
R5 = H, R4 = C8H17
R5 = CO(guanidine), R4 = H
R5 = CO(guanidine), R4 = C8H17
R5 = H, R4 = H
R5 = H, R4 = C8H17
R5 = CO(guanidine), R4 = H
R5 = CO(guanidine), R4 = C8H17

Procedure

A solution of the Boc protected carboxyguanidine **Boc 24a** (101 mg, 0.30 mmol) in trifluoroacetic acid (5 mL) was stirred at room temperature for 15 mn. The solvent was then eliminated under reduced pressure. The obtained residue was then dissolved in MeOH/H_2O and passed through an anion exchange resin for chloride. Water was then eliminated under vacuum to yield **24a** as a white solid (61 mg, 74% yield). **^{1}H NMR** (DMSO, 400 MHz): δ ppm 12.49 (s, 1H, NH), 9.44 (d, 1H, J = 1.6 Hz), 8.84-8.74 (m, 3H), 8.74-8.64 (m, 3H), 8.58 (d, 1H, J = 8.4 Hz), 8.53 (d, 1H, J = 7.9 Hz), 8.10 (td, 1H, J = 7.8, 1.4 Hz), 7.60 (dd, 1H, J = 6.9, 5.8 Hz).

24b.

In this case, after elimination of solvents, residue was taken into CH_2Cl_2 and organic phase was washed with KOH 2N, followed by brine. After drying and elimination of the solvents, free base **24b** was obtained. Additional washing with acidic solution of suitable pH (e.g. NH_4Cl 1 N) enabled to isolate the protonated carboxyguanidinium form (white solid,

84% yield). **^{1}H NMR** ($CDCl_3$, 400 MHz): δ ppm 9.43 (s, 1H), 8.71 (d, 1H, *J* = 3.9 Hz), 8.54 (dd, 1H, *J* = 8.2, 2.0 Hz), 8.45 (d, 1H, *J* = 8.0 Hz), 8.43 (d, 1H, *J* = 8.2 Hz), 7.83 (td, 1H, *J* = 7.8, 1.8 Hz), 7.33 (ddd, 1H, *J* = 7.4, 4.8, 1.0 Hz), 3.2 (m, 2H), 1.71-1.55 (m, 2H), 1.44-1.15 (m, 10H), 0.93-0.80 (m, 3H).

24c.

A suspension of the diBoc protected diguanidine **Boc 24c** (596 mg, 1.13 mmol) derivative was stirred in HCl 4 N (60 mL) at reflux for 30 min and mixture was stirred at room temperature overnight, time after which a white precipitate is observed. This suspension was then poured slowly into NaOH 5N (60 mL). The suspension was then centrifuged and aqueous phase was removed. Water was then added and centrifugation was repeated. Water washing was then repeated twice. Resulting white solid was then dried on the vacuum line to yield **24c** (107 mg, 40% yield). **^{1}H NMR** (DMSO, 400 MHz) δ ppm: 9.28 (m, 2H), 8.47 (m, 4H), 8.20-7.60 (m, 4H), 7.60-6.77 (m, 4H); **^{13}C NMR** (DMSO, 100 MHz): δ ppm 174.3, 163.6, 156.6, 150.3, 137.5, 134.8, 120.6.

24d (poor solubility)

yield not measured; **^{1}H NMR** ($CDCl_3$, 400 MHz): δ ppm 9.33 (s, 2H), 8.46 (s, 4H), 3.46-3.20 (m, 4H), 1.84-1.65 (m, 4H), 1.45-1.18 (m, 20H), 1.00-0.79 (m, 6H).

RuCl(bpy)(Ph-pybox)]PF$_6$.

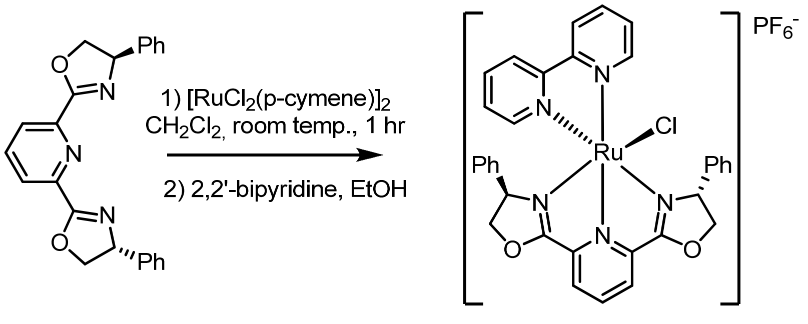

RuCl(bpy)(Ph-pybox)PF$_6$

Procedure

To a solution of [RuCl$_2$(p-cymene)]$_2$ (97 mg, 0.16 mmol) in dry CH$_2$Cl$_2$ (18 mL) was added the Ph-pybox (118 mg, 0.32 mmol) and resulting solution was stirred at room temperature for one hour, time after which solvent was eliminated under vacuum. A solution of 2,2'-bipyridine (50 mg, 0.32 mmol) in absolute ethanol (21 mL) was then added to the residue and mixture was refluxed overnight. NH$_4$PF$_6$ sat. was then added (about 3 mL) and the solvent was eliminated under reduced pressure. The residue was reparted between CH$_2$Cl$_2$ and water and organic phase was isolated, dried with anhydrous sodium sulfate, filetered and evaporated under vacuum (back extraction of aqueous phase was also performed). Column chromatography was then performed on aluminium oxide using CH$_2$Cl$_2$/MeCN (6 to 20%) as elution system to yield a red solid after evaporation of the fractions (77.3 mg, 69% yield). **^{1}H NMR** (CDCl$_3$, 400 MHz): δ ppm 9.23 (d, 1H, J = 5.3 Hz), 8.11 (d, 1H, J = 7.8 Hz), 8.06 (d, 1H, J = 7.1 Hz), 7.99 (t, 1H, J = 7.9 Hz), 7.73 (d, 1H, J = 7.8 Hz), 7.70-7.60

(m, 3H), 7.25-7.17 (m, 2H), 7.15 (d, 1H, *J* = 5.5 Hz), 7.10 (t, 2H, *J* = 7.7 Hz), 7.01 (ddd, 2H, *J* = 15.0, 7.7, 1.2 Hz), 6.90 (d, 2H, *J* = 7.2 Hz), 6.62 (t, 2H, *J* = 7.8 Hz), 6.24 (d, 2H, *J* = 7.3 Hz), 5.18 (t, 1H, *J* = 10.0 Hz), 5.14 (t, 1H, *J* = 9.9 Hz), 4.82 (t, 1H, *J* = 9.7 Hz), 4.68 (t, 1H, *J* = 9.3 Hz), 4.52 (dd, 1H, *J* = 11.6, 9.1 Hz), 4.21 (t, 1H, *J* = 10.7 Hz); **^{13}C NMR** ($CDCl_3$, 100 MHz): δ ppm 167.1, 157.7, 154.6, 152.6, 152.2, 136.6, 135.8, 135.6, 135.0, 132.3, 128.9, 128.5, 128.5, 128.5, 128.4, 126.8, 126.4, 125.6, 125.4, 124.5, 122.1, 121.6, 79.0, 78.6, 68.5, 68.4; **Cyclic voltammetry**: E [Ru(III)/Ru(II)] in 0.1 M $TBAPF_6$ in DCM: 0.71 V.; **HR-MS** (TOF-ESI$^+$): *m/z* calc. for $C_{33}H_{27}ClN_5O_2Ru$ 662.0897, obt. 662.0882 [M$^+$].

[Ru(H$_2$O)(bpy)(Ph-pybox)](PF$_6$)$_2$.

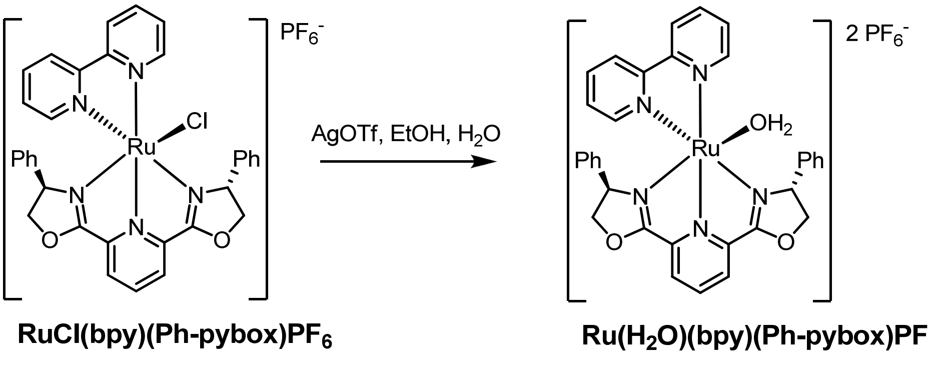

Procedure

A solution of **[RuCl(bpy)(Ph-pybox)]PF$_6$** (50 mg, 0.062 mmol) and silver trifluoromethanesulfonate (35 mg, 0.14 mmol) in a 1:3 ethanol/water mixture (15 mL) was refluxed under argon for one hour. The obtained mixture was brought back at room temperature and rested in the fridge.

Precipitated silver salts were eliminated by filtration through celite and some saturated NH_4PF_6 was then added. Solvent volume was brought to 5 mL by evaporation. The precipitated brown solid was then filtered, and recrystallized in water to yield the desired compound as a brown powder (33 mg, 57% yield). **^{1}H NMR** (D_2O, 400 MHz): δ ppm 8.33 (d, 1H, J = 5.2 Hz), 8.24 (dd, 1H, J = 8.2, 1.2 Hz), 8.21 (dd, 1H, J = 8.0, 1.1 Hz), 8.13 (t, 1H, J = 8.0 Hz), 7.92 (d, 1H, J = 8.0 Hz), 7.83 (td, 1H, J = 7.7, 1.4 Hz), 7.72 (d, 1H, J = 8.2 Hz), 7.59 (td, 1H, J = 7.6, 1.6 Hz), 7.29-7.22 (m, 2H), 7.12-6.98 (m, 4H), 6.96-6.91 (m, 1H), 6.69 (d, 2H, J = 7.4 Hz), 6.58 (t, 2H, J = 7.7 Hz), 6.29 (d, 2H, J = 7.2 Hz), 5.22 (t, 2H, J = 9.5 Hz), 5.11 (t, 2H, J = 9.8 Hz), 4.24 (t, 1H, J = 10.8 Hz); **Cyclic voltammetry:** E [Ru(IV)/Ru(II)]: 0.46 V in phosphate buffer (pH 7) and $NaClO_4$ 0.1 M

Protocol for spectrophotometric pK_a determination:

1.77 mg of the aquo complex were dissolved in 50 mL 0.1M trifluoromethanesulfonic acid, giving rise to a solution of pH 1.14. pH of the solution was brought to 12 by addition of aqueous KOH (5 M, 0.25 M and 5 mM). UV-Vis absorption was measured for each value of pH, which enables to determine the value of the pK_a (isobestic point).

General procedure for complexation studies of monodentate functionalized ligands and chiral ligands with Cu(I), Co(II) and Zn(II).

Procedure

Typically, equimolar amounts of ligands were mixed in methanol (**BINOL** was deprotonated with 2 equivalents of MeONa prior to the addition of metal salt) and one equivalent of metal salt was added. The reaction mixture was stirred one hour at room temperature under argon and solvent was eliminated under vacuum. When suitable, crude mixture was submitted to ^{1}H NMR; for paramagnetic species, mass spectrometry was the only way to characterize the compounds. This set of experiments did not enable so far to isolate and characterize a clear complex.

General procedure for complexation experiments with $\mathbf{Cu(MeCN)_4(PF_6)}$.

To a degased solution of **Ph-pybox** (1 eq.) in dry DCM and placed under argon was added the $Cu(MeCN)_4(PF_6)$ (1 eq.). The resulting mixture was stirred 30 min at room temperature. After this time, a solution of the ligand (typically isoquinoline) in dry CH_2Cl_2 was added via canula to the mixture. In the case of **21a-b**, precipitate was collected by filtration and dried under vacuum (**$\mathbf{Cu(21a\text{-}b)_2}$**); mother liquors contained **$\mathbf{Cu(Ph\text{-}Pybox)_2PF_6}$**. Compounds were analyzed by mass spectrometry and, in every case; a mixture of complexes was obtained and not separated.

$\mathbf{Zn(21b2)_2}$.

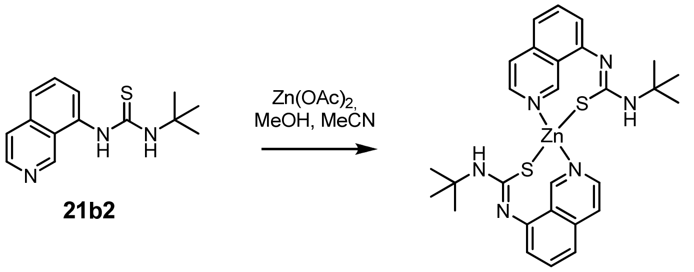

Procedure

Thioureidoisoquinoline **21b2** (30 mg, 0.12 mmol) and zinc acetate (5.3 mg, 0.03 mmol) were dissolved in a 1:1 MeOH/MeCN mixture (4 mL) and the obtained reaction mixture was stirred at room temperature for 30 min The solvent was then eliminated thanks to vacuum and residue precipitated in ether. **^{1}H NMR** ($CDCl_3$, 400 MHz): δ ppm 9.44 (s, 2H), 8.52 (s, 2H), 7.79-7.56 (m, 8H), 6.48 (s, 2H), 1.45 (s, 18H); **MS** (MALDI): *m/z* 582.2 [M$^+$].

General procedure for complexation trials with [RuCl$_2$(*p*-cymene)]$_2$ (monodentate ligands 21a-c).

Procedure

In dry CH_2Cl_2 and under argon were dissolved **Ph-Pybox** (1 eq.) and the monodentate ligand (1 eq.). To this solution was added [RuCl$_2$(p-cymene)]$_2$ (0.5 eq.) and the resulting brown mixture was left stirring at room temperature for 4 days until the obtention of a violet solution. Solvent was then eliminated thanks to vacuum and the crude compound was analyzed by mass spectrometry (MALDI in pyrene).

***trans*-RuCl$_2$(Ph-pybox)(iq):**

Compound was isolated by column chromatography in 77% yield (Al_2O_3, DCM/AcOEt 30% as elution system). **^{1}H NMR** ($CDCl_3$, 400 MHz): δ ppm 9.34 (s, 1H), 8.59 (d, 1H, *J* = 6.5 Hz), 7.78 (d, 2H, *J* = 7.7 Hz), 7.67-7.55 (m, 3H), 7.48-7.42 (m, 1H), 7.39 (d, 1H, *J* = 7.7 Hz), 7.18-7.12 (m, 4H), 7.04-6.96 (m, 6H), 6.92 (d, 1H, *J* = 6.3 Hz), 5.30-5.21 (m, 2H), 5.17 (t, 2H, *J* = 10.1 Hz), 4.60 (dd, 2H, *J* = 10.0, 8.0 Hz); **HR-MS** (TOF-ESI$^+$): *m/z* calc. for $C_{23}H_{26}N_4O_2Cl_2Ru$ 670.0476; obt. 670.0448 [M^+].

Other derivatives could not be purified in a satisfactory way and were only detected by mass spectrometry as explained in the present report.

RuCl₂(*p*-cymene)(21b2).

Procedure

A mixture of thioureidoisoquinoline **21b2** (21 mg, 0.08 mmol) and [$RuCl_2$(*p*-cymene)]$_2$ (25 mg, 0.04 mmol) in dry THF (5 mL) was heated overnight at reflux. Mixture was diluted with DCM and solvent was eliminated under vacuum. Residue was used without any further purification.

In this experiment, the metallocage **Ru_2Cl_2(*p*-cymene)$_2$(21b2)$_2$** might have formed, though mass of the obtained compound corresponds to **$RuCl_2$(*p*-cymene)(21b2)** (this metallocage was not expected at the moment of the reaction).

trans-RuCl₂(Ph-pybox)(CO).

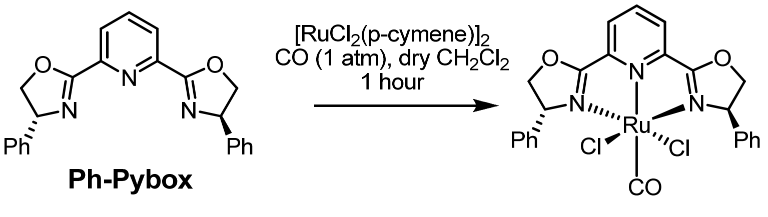

RuCl₂(Ph-Pybox)(CO)

Procedure

A solution of $[RuCl_2(p\text{-cymene})]_2$ (25 mg, 0.04 mmol) in dry CH_2Cl_2 (5 mL) was cooled at 0 ºC and placed under carbon monoxide atmosphere (balloon) over 30 minutes. **Ph-Pybox** (30 mg, 0.08 mmol) was then added via canula as a dry CH_2Cl_2 solution (5 mL). The resulting mixture was stirred at 0 ºC for one hour. Hexane was then added to the reaction mixture in order to precipitate a brown solid that was filtered and dried under vacuum (35 mg, 75% yield). Compound was purified by silica gel column chromatography using until 30% AcOEt/DCM as elution system, though some degradation was visible.**^{1}H NMR** ($CDCl_3$, 400 MHz): δ ppm 8.17 (t, 1H, J = 7.7 Hz), 7.98 (d, 2H, J = 7.9 Hz), 7.40 (s, 10H), 5.31-5.25 (m, 2H), 5.18 (t, 2H, J = 11.3 Hz), 4.69 (dd, 2H, J = 11.4, 8.5 Hz); **MS** (MALDI): *m/z* 541.8 [M-CO$^+$].

General procedure for UV-Vis monitored titration experiments with ZnX_2 (X=OAc, Cl or BF_4) and 24b(Cl^-).

Procedure (example for $Zn(OAc)_2$

Solution 1: 1.6 mg of **24b(Cl^-)** were weighed down and disolved in 10 mL THF ($4.10.10^{-4}$ M); the obtained solution was diluted 10 times.

Solution 2: 0.43 mg $Zn(OAc)_2$ were weighed down and disolved in 2 mL of solution 1; the obtained solution was diluted 10 times with solution 1 ($1.17.10^{-4}$ M).

In the cuve of UV spectrometer were introduced 1.5 mL of solution 1 and 25μL of solution 2 were added (0.05 eq.) successively. After each addition, UV-Vis absorbance spectrum was recorded. Data were gathered and fitted using the SPECFIT® software.

General procedure for catalyzed 1,4-addition of pyrrolidine to 2-5*H*-furanone.

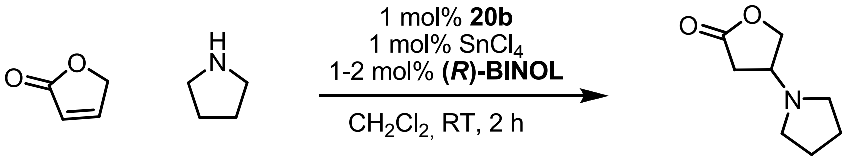

Procedure

To a solution of thiourea **20b** (2.5 mg, 12 μmol) and **(R)-BINOL** (3.4 mg, 12 μmol) in dry dichloromethane (10 mL) were added 2-5*H*-furanone (84 μL, 1.19 mmol), followed by commercial tin(IV) chloride solution (12 μL, 12 μmol) and pyrrolidine (99 μL, 1.19 mmol). The resulting reaction mixture was stirred at room temperature for two hours. The solvent was then eliminated under vacuum and the reaction crude was purified by column chromatography (SiO_2, from 75% AcOEt/Hexane to 2% MeOH/CH_2Cl_2). The Michael adduct was obtained in 20-35% yield after evaporation of the fractions.

General procedure for catalysis of Baylis-Hillman reaction of benzaldehyde with methylvinyl ketone.

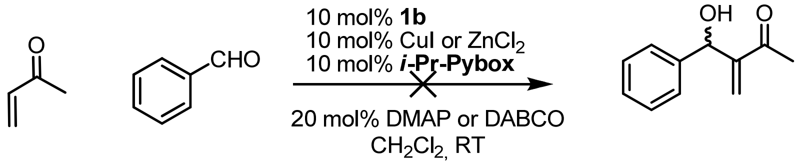
10 mol% 1b
10 mol% CuI or ZnCl2
10 mol% i-Pr-Pybox
20 mol% DMAP or DABCO
CH2Cl2, RT
O
CHO
OH
O

Procedure

A solution of the pre-formed catalytic system (complex+base, see above for complex preparation, 10 mol%) was added to a solution of benzaldehyde (26 μL, 0.25 mmol) and methylvinyl ketone (21 μL, 0.25 mmol) in dry CH_2Cl_2 (2 mL) at room temperature. The resulting reaction mixture was stirred overnight at room temperature and the solvent was eliminated under vacuum. Crude compounds were purified by silica gel column chromatography (5-35% AcOEt/Hexanes).

General procedure for the Ru(IV) catalyzed olefin epoxidation.

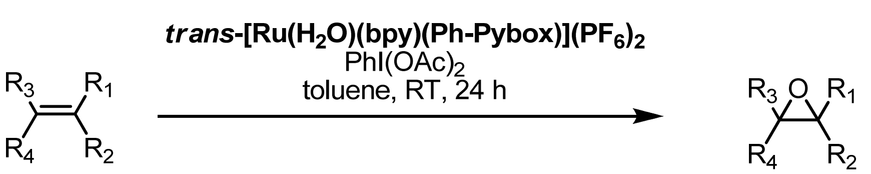
trans-[Ru(H2O)(bpy)(Ph-Pybox)](PF6)2
PhI(OAc)2
toluene, RT, 24 h
R3
R1
R4
R2
R3
O
R1
R4
R2

Procedure

To a solution of **[Ru(bpy)(Ph-pybox)H$_2$O](PF$_6$)$_2$** (0.6 mM) and substrate (60 mM) in dry dichloromethane was added the oxidant $PhI(OAc)_2$ (so that a 120 mM solution was obtained). The reaction mixture was then stirred at room temperature for 24 hours. Aliquots were taken regularly and analyzed by gas chromatography after addition of 1 eq. TFA in the case of carboxylates and quick flash chromatography in other cases.

GC (carboxylic acids): Column: Suprawax280 30m, ID 0.32mm, 0.25µm, injection volume: 0.2µL, split 100:1, $T_{inj/aux}$: 260/260 ºC, Oven: 100 ºC up to 200 ºC (10 ºC/min).

General procedure for the Cu(I) catalyzed cyclopropanation of olefins: example for the cyclopropanation of *cis*-*β*-methylstyrene.

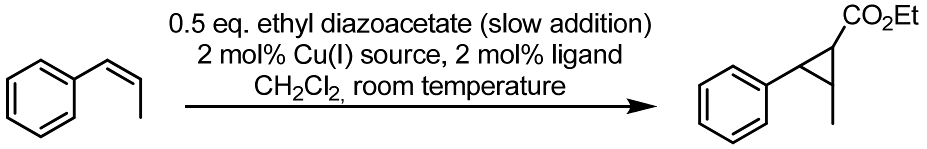
0.5 eq. ethyl diazoacetate (slow addition)
2 mol% Cu(I) source, 2 mol% ligand
CH2Cl2, room temperature
CO2Et

Procedure

To a stirred solution of **[Cu(MeCN)$_4$(PF$_6$)]** (9.4 mg, 25 µmol) in dry CH_2Cl_2 (4 mL) was added the 2,2'-bipyridine (3.9 mg, 25 µmol); *cis*-*β*-methylstyrene (250 *µ*L, 1.93 mmol) was then added. A solution of ethyl diazoacetate (102 *µ*L, 0.96 mmol) in dry DCM (3 mL) was then added over 3 hours via syringe pump and resulting mixture was then stirred overnight at room temperature. Solvent was then eliminated under vacuum and residue purified by column chromatography (SiO_2, 20% ether/hexane) to afford the corresponding product of reaction after evaporation *in vacuo* of the corresponding fractions (91 mg, 46% yield, translucid oil). **^{1}H NMR** ($CDCl_3$, 400 MHz): δ ppm 7.35-7.17 (m, 5H), 4.20 (q, 2H, J = 7.2 Hz), 2.79 (dd, 1H, *J* = 9.6, 5.0 Hz), 1.88-1.79 (m, 2H), 1.32 (t, 3H, *J* = 7.2 Hz), 0.94 (d, 3H, *J* = 6.2).

(*E*)-2-Ethoxy-2-oxoethyl but-2-enoate: translucid oil, 60% yield. **^{1}H NMR** ($CDCl_3$, 400 MHz): δ ppm 7.06 (qd, 1H, *J* = 15.5, 6.9 Hz), 5.93 (dq, 1H, *J* = 15.5, 1.6 Hz), 4.64 (s, 2H), 4.22 (q, 2H, *J* = 7.2 Hz), 1.90 (dd, 3H, *J* = 6.9, 1.7 Hz), 1.27 (t, 3H, *J* = 7.1 Hz); **^{13}C NMR** ($CDCl_3$, 100 MHz): δ ppm 167.9, 165.6, 146.5, 121.6, 61.3, 60.6, 18.1, 14.1.

General procedure for Cu(I) catalyzed olefin aziridination: example for the aziridination of *cis*-*β*-methylstyrene.

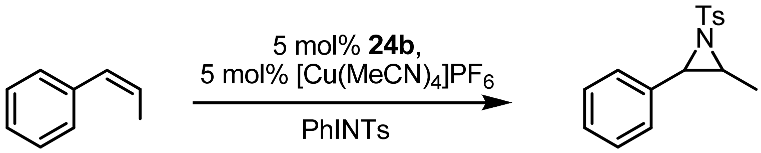

Procedure

To a flask placed under argon were added the *N*-tosylimino phenyliodinane (144 mg, 0.39 mmol) and the bipyridine derivative (6.8 mg, 19 μmol). Copper (I) complex (7.2 mg, 019 μmol) was then added via canula and cis-*β*-methylstyrene (0.1 mL, 0.77 mmol) was added. Reaction mixture was stirred overnight at room temperature. Solvent was then eliminated under vacuum and residue was purified by silica gel column chromatography using first 2% Et_2O/hexane and then 15% AcOEt/hexane. Product was isolated successfully as a translucid oil (yield not measured). **^{1}H NMR**

($CDCl_3$, 400 MHz): δ ppm 7.90 (d, 2H, J = 8.3 Hz), 7.34 (d, 2H, J = 8.1 Hz), 7.31-7.26 (m, 3H), 7.24-7.20 (m, 2H), 3.94 (d, 1H, J = 7.3 Hz), 3.20 (qd, 1H, J = 7.2, 5.8 Hz), 2.45 (s, 3H), 1.04 (d, 3H, J = 5.8 Hz).

Summary

This thesis reports on the preliminary studies of a conceptually new approach to supramolecular catalysis in which a library of *N*-heterocyclic ligands functionalized with H-bonding moieties was prepared, optimized, and complexed with transition metals and chiral ligands, aiming at forming a regioselective (substrate recognition) and enantioselective (chiral environment) catalyst for various processes (heteroleptic complex). The H-bonding moiety was initially thought to act either as an organocatalyst or as a substrate anchoring unit (depending on the catalytic activity of the used transition metal).

The first chapter of this thesis reviews some relevant examples of supramolecular approaches to catalysis, from covalent capsules to self-assembled molecular containers and their applications in catalysis. In a second part, examples where self-assembly was also used for the elaboration of ligands (evaluated in catalysis applications) are discussed.

The second chapter of this thesis aims at studying the influence of the acidity of guanidinium cations on their binding abilities with oxoanions and their catalytic activity. To this aim, three guanidinium cations were prepared, modifying their acidic character by juxtaposition of an aromatic ring to the guanidinium cation. Binding abilities of these cations with acetate were then studied by Isothermal Titration Calorimetry, NMR and IR spectroscopies. Thermodynamic cycles were then constructed for the three species. Benzoguanidinium cations presented the higher binding constant

with acetate, while dibenzoguanidinium cations were shown to be acidic enough to protonate acetate (transprotonation), resulting in lower affinity. Oxoanion binding ability of guanidinium cations therefore increases with their acidity as long as transprotonation is avoided. This trend was also reflected in the catalytic activity of guanidinium cations. Benzoguanidinium cations proved to be the optimal catalysts for the 1,4-Michael addition of pyrrolidine to 2-(*5*H)-furanone, probably due to a suitable balance of the rates of the proton exchange processes that are likely to take place, which evidenced the influence of the pK_a of guanidinium cations on their catalytic activity. Benzoguanidinium cations and related structures therefore proved to be a structure of choice for our studies.

In the third chapter, metalloporphyrin systems functionalized with H-bonding moieties are described as potential cooperative catalysts for the 1,4-Michael addition of pyrrolidine to 2-(*5*H)-furanone. Metal screening experiments proved that tin(IV) porphyrins are nice catalysts for the reaction, which enabled to iniciate cooperativity studies of the functionalized systems with model non covalent ones. Results suggested that the catalytic activity of the H-bonding moiety adds to the one of the metal in a less important manner than in non-covalent systems (non-cooperative effect), probably due to conformational issues. However, the compatibility of H-bonding and metal-substrate interactions for the catalysis of the 1,4-Michael addition of pyrrolidine to 2-(*5*H)-furanone was proven.

The last chapter of this thesis describes the preparation of a library of functionalized *N*-heterocyclic mono- and bidentate ligands (urea, thiourea, guanidinium), as well as the preparation of a library of chiral ligands. Formation of the heteroleptic complex was then investigated with Cu(I), Zn(II) and Ru(II) and results actually proved disappointing. It was found that the heteroatom of the urea or the thiourea of the functionalized ligand tended to coordinate the transition metal, leading in homoleptic complexes (bridged dimers for Cu(I) and Zn(II)). On the other hand, homoleptic complexes made of two chiral ligands were also found to be favoured. This therefore resulted in the formation of a mixture of complexes. Efforts were then addresses towards the exclusive formation of the heteroleptic complex, which could not be achieved. Preliminar catalysis experiments were also performed with carboxylic acids, without success, since coordination of the substrate to the metal was often observed.

Introducción general y resultados

Las enzimas han representado un modelo inigualable para los químicos por sus características como catalizadores. En efecto, son capaces de realizar transformaciones químicas en condiciones suaves (medio acuoso) de manera regioselectiva y/o enantioselectiva. Por esa razón, numerosas reacciones químicas son catalizadas por enzimas a la escala industrial. Dado su alto potencial catalítico, el diseño de sistemas capaces de reproducir sus características se ha estudiado intensivamente, con el objetivo de eludir sus mecanismos y expander el campo de aplicaciones catalíticas mediante el diseño de enzimas artificiales. Las enzimas son estructuras moleculares complejas, mantenidas por interacciones covalentes y supramoleculares que definen su geometría y su conformación. Por ese motivo, la catálisis supramolecular ofrece la posibilidad de aproximarse a los mecanismos enzimáticos.

Este trabajo describe estudios preliminares sobre una aproximación conceptualmente nueva de la catálisis supramolecular, para lo cual se prepararon librerías de ligandos quirales y de ligandos *N*-heterocíclicos funcionalizados por grupos dadores de enlaces hidrógeno (típicamente: urea, tiourea y guanidinio). La formación de un complejo heteroléptico entre un metal de transición y estas librerías se estudió con el objetivo de formar un catalizador capaz de inducir regioselectividad por reconocimiento molecular del sustrato de la reacción y enantioselectividad. Inicialmente, se identificaron tres situaciones, dependiendo de la actividad catalítica del metal. El grupo dador de enlaces de hidrógeno puede ejercer entonces la función de organocatalizador o de fijar el sustrato a una distancia determinada del centro activo del catalizador.

En el primer capitulo de este trabajo se revisan algunos ejemplos relevantes de aproximaciones supramoleculares a la catálisis, desde la encapsulación molecular del sustrato en cápsulas covalentes o formadas mediante procesos de auto-ensamblaje hasta la utilización de ligandos formados por auto-ensamblaje en sistemas catalíticos más clásicos, lo que permite evidenciar el potencial de la catálisis supramolecular.

En una segunda parte se estudia la influencia de la acidez de los receptores guanidinicos en su capacidad asociativa con oxoaniones mediante enlaces de hidrógeno, así como su actividad catalítica. Se llevó a cabo la síntesis de tres receptores guanidinicos, cuya acidez se modificó por yuxtaposición de un anillo aromático al grupo guanidinio. La asociación de dichos receptores con acetato mediante enlaces de hidrógeno se estudió entonces por valoración calorimétrica isotérmica, espectrometrías RMN y IR. También se construyeron ciclos termodinámicos para cada compuesto estudiado, lo cual nos permito evidenciar que la fuerza de los enlaces de hidrógeno se ve incrementada con la acidez del receptor guanidinico si se evita la transprotonación. El catión benzoguanidinico resultó ser el que formaba los enlaces de hidrógeno más fuertes con acetato, debido a su mayor acidez. En cambio, el receptor dibenzoguanidinico protona el acetato, lo cual da lugar a un par desfavorecido por perdida de las cargas electrónicas y de las interacciones dipolares favorables. Respecto a la actividad catalítica, también se observó un comportamiento óptimo para un valor determinado del pK_a del catalizador. El receptor benzoguanidico resultó ser el mejor catalizador de la adición de Michael de pirrolidona a 2-(5H)-furanona, debido probablemente a su acidez que permite acelerar los intercambios de protones entre las especies transitorias. Los receptores benzoguanidicos resultaron ser, según este estudio, los candidatos óptimos para nuestros estudios.

La tercera parte de este trabajo describe estudios de cooperatividad de sistemas catalíticos formados por una metaloporfirina equipada con grupos dadores de enlaces de hidrógeno. Se estudió la compatibilidad de la activación por ácido de Lewis y la activación por enlaces de hidrógeno en la adición de Michael de pirrolidona a 2-(5H)-furanona. Se demostró en primer lugar el potencial catalítico de las porfirinas de estaño para esta reacción y se estudió, en una segunda parte, la compatibilidad de ambas interacciones en la activación y la cooperatividad del sistema. Los resultados obtenidos demostraron que la actividad catalítica de los dadores de enlaces de hidrógeno se añade a la del ácido de Lewis, pero el sistema equivalente no covalentemente unido resultó ser más eficaz, lo cual sugiere que la conformación de las metaloporfirinas funcionalizadas no era óptima. No obstante, se demostró la compatibilidad de ambas interacciones en activación del sustrato.

El último capitulo de esta tesis describe la preparación de una librería de ligandos mono- y bidentados equipados con grupos dadores de enlaces de hidrógeno, así como una librería de ligandos quirales. La formación del complejo heteroléptico se investigó con Cu(I), Zn(II) y Ru(II). Las dificultades encontradas se basan en la formación competitiva de dos complejos homolépticos formados, por una parte, por dos ligandos quirales y, por otra parte, por dos ligandos nitrogenados funcionalizados (coordinación al metal del heteroátomo del grupo dador de enlaces de hidrógeno). El uso de bipiridinas funcionalizadas con grupos guanidinicos pareció entonces ser la mejor solución, pero el complejo heteroléptico tampoco se pudo aislar con esta familia de ligandos. Aún así se hicieron pruebas de estos sistemas en catálisis (con sistemas modelos o funcionalizados) con ácidos carboxílicos como sustratos. La coordinación competitiva del àcido carboxílico al metal no dio lugar a la catálisis esperada.